Kinetics and thermodynamics of the interaction of proteins with dyes coupled to soluble polymers

Maytum, Robin

Award date:
1997

Awarding institution:
University of Bath

Kinetics and Thermodynamics of the Interaction of Proteins with Dyes Coupled to Soluble Polymers

submitted by Robin Maytum

for the degree of PhD

to the University of Bath

1997

ProQuest LLC
789 East Eisenhower Parkway
P.O. Box 1346
Ann Arbor, MI 48106-1346

Abstract

Mayes et al. (1990,1992) examined the interaction of Cibracon Blue dye-dextran conjugates with lysozyme as a model system and showed that although equilibrium binding experiments showed a reasonable fit to a simple binding model, kinetic experiments showed a more complex curve than could be explained by such a model. From this work Hubble et. al. (1993) have then proposed a model for the binding interaction which involves dye stacking to take into account this deviation. Although the propensity for triazine dyes to 'stack' through non-covalent interactions between their planar aromatic rings has been known for some time (Subramanian, 1982) little effort has been made to quantify this interaction or to take account of its effect in spectral binding assays of proteins with this dyes.

To further the previous work investigations have been made of the interaction of a wide range of dye-dextran conjugates differing in both the size of the dextran backbone and dye loading with several different model proteins. By using both spectral and fluorescence techniques the validly of these techniques for monitoring dye binding has been shown. However kinetic measurements revealed the kinetics of the interaction to be far faster than that previously seen with lysozyme. Combining kinetic data of dye - protein interactions with measurements of the dye stacking interaction it has been shown that intermolecular dye stacking is unlikely to be a kinetically significant process for Cibracon Blue F3-GA, but may well be significant for other dyes. Attempts have been made to analyze the binding kinetics measured over an extensive range of conditions, but as yet these have failed to yield an alternative model which is consistent with all the results.

Contents

Introduction

1.1 General Background

The application of biotechnology is being used to produce an increasing number of important products, ranging from beer to therapeutic antibodies. The application of the product governs the quantity and levels of purity required ranging from the bulk quantities required for the chemical and food industries, where purity is secondary to cost, to those of the pharmaceutical industry where purity is critical but the value much higher[1]. For the *in vivo* usage of pharmaceutical products such as proteins, the final product must be free of all possible contaminants from its source[2]. For all of these the purification process is often the most important stage in the production a commercial product. Frequently it may govern the viability of production of the product. Three important factors must be weighed in any purification process :-

1. Purity of the product.
2. Yield of the product.
3. Cost of the process.

Ideally the purification should give the highest yield and desired purity of product at the lowest cost.

For products where high purity is required biospecific affinity chromatography provides one of the best methods for achieving this goal. On a research basis it is also becoming an increasingly common technique, especially for the purification of 'tagged' recombinant proteins in which engineered specific binding sites are attached to the proteins and used for their subsequent purification. An example of this is 'His-tagging' in which a poly histidine sequence is introduced which produces a high affinity metal ion binding site which can then be used with a metal-chelate affinity column. Other examples include fusion proteins where an entire protein domain with a specific binding site is introduced such as Glutathione-S-Transferase (GST) or Maltose Binding Protein (MaltBP).

Affinity chromatography depends on the specific binding that occurs between many biological macromolecules and their ligands, such as inhibitors, effectors, substrates, hormones, antigens, sugars, and nucleic acids[3,4]. These specific interactions are used in

affinity chromatography to bind the desired macromolecule to an insoluble support matrix bearing a suitable ligand. As only macromolecules with binding sites specific for the ligand should bind to the matrix it offers a simple, possibly single step purification, with a theoretically high purity and yield. Thus it fulfils at least two of the desired criteria for a purification and hopefully all three. The general principles of an affinity purification are shown in **Figure 1.1**.

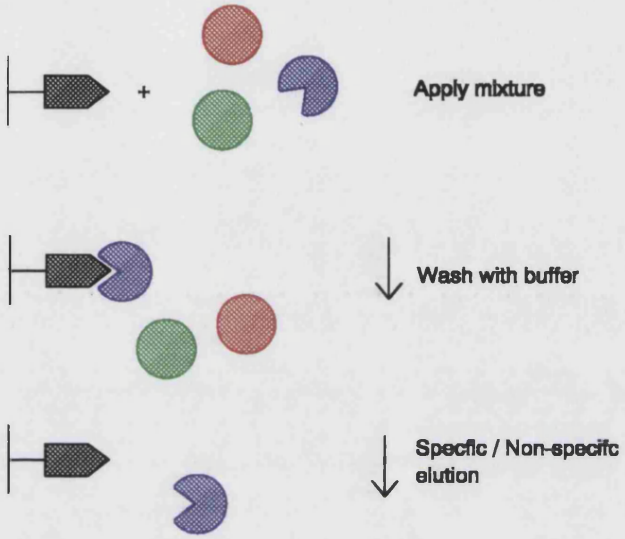

Figure 1.1: Principle of affinity chromatography. The raw mixture is applied to the affinity column. Proteins with an appropriate ligand binding site bind to the column whilst the remainder are washed from the column. The bound protein is then eluted from the column with either a specific eluant (e.g. the natural ligand) or a non-specific eluant such as a high salt concentration.

Affinity chromatography has been largely developed on an empirical basis, with little basic research into the processes involved taking place until recently. As wide scale usage of affinity chromatography on a commercial scale increases, it is becoming increasingly important that a more fundamental understanding of the processes involved are developed so that a rational approach can be used for its optimisation. On a lab scale properties such as the cycle time for a purification and the relative cost of the affinity matrix are generally not of great importance. However on a commercial basis such properties have great significance. For example it has been shown that the availability of immobilised ligand on a support matrix can be below 2% of the total ligand attached to the matrix[5]. This is obviously of concern as

low ligand availability effects both the capacity of the column, the cost and difficulty of its production, as well as increasing the possibility of non-specific interactions with 'unavailable' ligands.

The support matrix that is used for the ligand can have significant effects on the properties of the column, both in terms of effecting the interaction with the ligand and the physical properties of the column. In terms of their physical properties they can be generally classified into two types, porous and non-porous. Porous supports have generally been based upon polysaccharides and have a structure which gives a large surface area allowing a high binding capacity, but which are also mechanically weak. These supports typically have pore diffusional limitations which results in slow binding kinetics[6]. Conversely non-porous supports are physically strong and have fast binding kinetics less hampered by mass transfer limitations, but capacity is limited by the surface area of the beads[7]. This can only be increased by decreasing the bead size, which is itself ruled by pressure drop limitations as decreasing bead size increases the back pressure of a column. A compromise between these two types of matrix is what can be termed a "tentacle" support matrix. In this system ligands are attached onto large hydrophyllic polymers which are themselves attached to the surface of stable non-porous beads. The polymer "brush boarder" around the beads increases their surface area whilst retaining the mechanical advantages of a solid support. Thus such a support should show fast binding kinetics and a capacity approaching that of a non-porous support. This technique has been applied to both ion-exchange[8,9] and metal-chelate chromatography[10].

A related technique to affinity chromatography is that of affinity partitioning. This uses affinity interactions to preferentially distribute the macromolecule to one phase of an aqueous two phase system. Aqueous two phase systems have the advantages over the more familiar aqueous/organic two phase systems in that the majority component of both phases is water. This is important for biological extractions as the materials of interest, normally proteins, are sensitive to changes in their solvent environment to the extent that many of them will denature in the presence of an organic solvent. Additionally there are large forces involved in the transition of molecules across the boundary layer between the two phases which may also

act to cause denaturation and produce the secondary problem of accumulation of molecules at the boundary layer. This means that such two phase systems are normally unsuitable for biological extractions.

Aqueous two phase systems are commonly made by mixing two large molecular weight polymers of different chemical natures. The most commonly used system consists of a hydrocarbon ether polymer, polyethylene glycol (PEG) and dextran, a polysaccharide mainly consisting of α-1,6 glucose, shown in **Figure 1.2**. Systems containing reasonable quantities (5-10 % w/v) of both polymers naturally form a two phase aqueous system. Two phase systems can also be formed between a single polymer and a salt solution, an example of which is that formed between PEG and potassium sulphate. These systems have the disadvantage over the two polymer systems of having a higher interfacial surface tension which may be disadvantageous for the previously mentioned reasons.

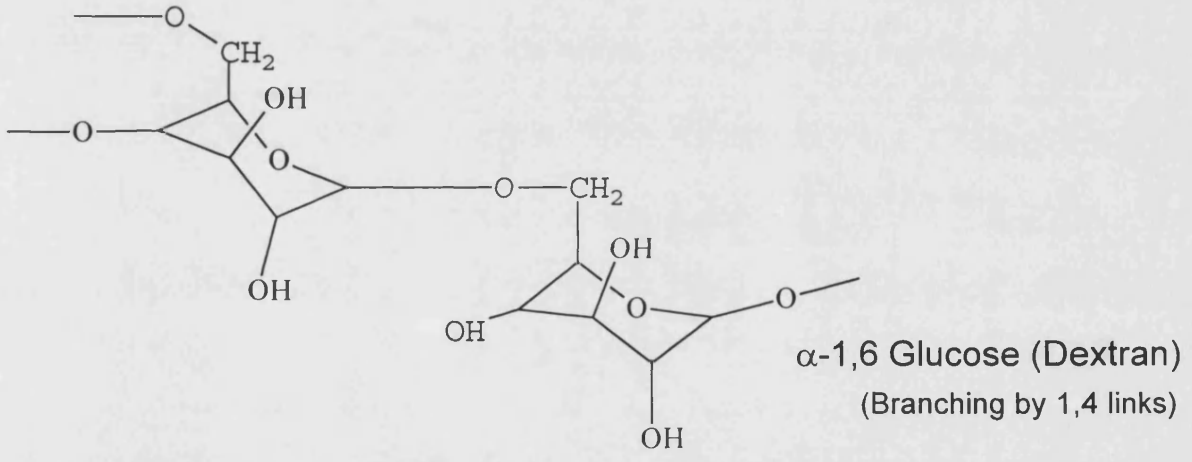

Figure 1.2: Chemical structure of dextran, poly(a-1,6 Glucose). The structure of the polymer is typically greater than 80 % α-1,6 Glucose with a small number of branches formed by α-1,4 links.

Partitioning behaviour of molecules between the two phases is governed by a wide variety of factors. It is highly dependant upon the surface properties of the molecules which govern their interactions with the bulk polymers present in either phase[11] .The behaviour of particles within a two phase system is also effected greatly by their size. Small particles tend towards an even distribution between the phases whilst larger particles such as proteins or even cells tend towards a more extreme partitioning behaviour[12] Proteins are in the middle ground and

normally undergo reasonably strong partitioning into one of the phases. However most proteins display similar properties in two phase systems so it is likely that the desired protein will partition into the same phase as the majority of the rest of the proteins in a mixture. However this problem can be turned to an advantage by using separator molecules consisting of a large molecule which undergoes relatively extreme partitioning to which the protein also binds. These can therefore be used to direct the partitioning of the desired protein into the opposite phase to that of the majority of the rest of the proteins. Originally this was achieved using the bulk polymers making up the phases as the affinity ligands[13]. This was then extended with the use of synthesised affinity ligands, usually consisting of an affinity ligand bound to one of the bulk phase polymers. This technique has been applied most widely to the most commonly used dextran and poly(ethylene glycol) (PEG) phase system using ligands bound to the PEG[14,15,16,17,18,19,20]. More recently dextran has also been used as a carrier in similar two phase systems[21,22,23].

Investigation of the binding interactions taking place with affinity adsorbents based upon an insoluble matrix is greatly complicated by diffusional limitations on mass transfer[24]. Thus it is advantageous to study these interactions in a single phase using soluble supports for the ligands[25] as used in the two phase systems previously mentioned. Providing the viscosity of the system is not high, mass transfer limitations are negligible. In this case the kinetic and equilibrium data obtained for the ligand-carrier system can then be directly compared to those for the free ligand. Therefore such a system can be used to quantify and characterise the effects of ligand immobilisation on the binding interactions between ligand and receptor and the effectiveness of the system judged.

The obvious choice for an affinity ligand would be one of the natural ligands of the macromolecule that is being purified. However the use of naturally occurring biological ligands can have many disadvantages, especially on a process scale, since the ligands tend to be both biologically and chemically labile as well as being difficult to immobilise in high yields while retaining their binding activity[26,27].

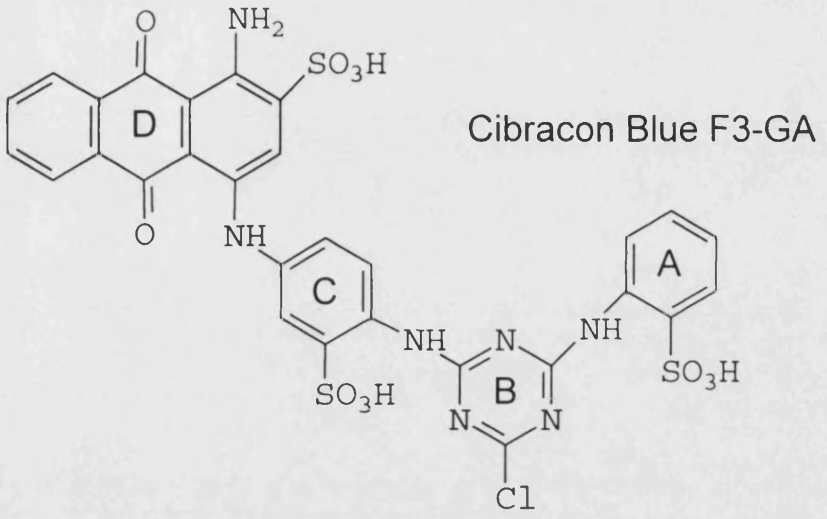

Figure 1.3: Chemical structure of Cibracon Blue F3-GA. By convention the aromatic rings are labelled A-D as shown to allow easy reference to specific portions of the structure.

These problems have been overcome in part by the use of 'pseudo-' or 'biomimetic' ligands. These are compounds which display binding characteristics similar to their biological counterparts. One of the commonest classes of these compounds is the triazine dyes. These are compounds based around the reactive centre of a triazine ring to which other groups are attached to produce a coloured, reactive compound. The serendipitous discovery of the biomimetic nature of these compounds was from noticing that pyruvate kinase co-eluted with blue dextran (Cibracon Blue F3-GA linked to a dextran carrier) during gel filtration[28]. It was initially proposed that Cibracon Blue was a conformational analogue of the nicotine adenine dinucleotide (NAD) molecule and that it could be used as a diagnostic probe for the 'dinucleotide binding fold' in proteins[26,29,30]. This however was shown to be only partially true, with some dinucleotide binding proteins not binding to Cibracon Blue affinity columns, and other proteins binding although lacking a dinucleotide binding fold[31].

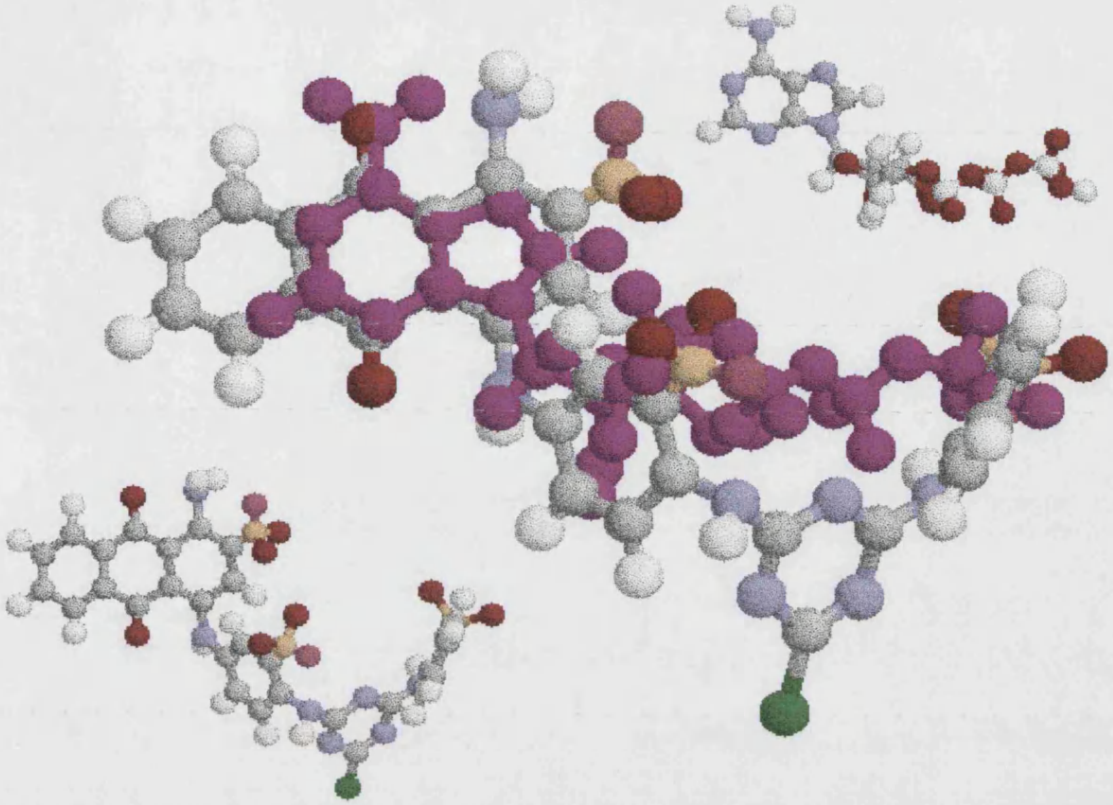

Figure 1.4: Superposition of Cibracon Blue F3-GA and ATP ball and stick molecular models showing similarities between their structures. Middle image shows ATP (magenta) superimposed over Cibracon Blue F3-GA (CPK colours). Bottom right and top left show half size CPK coloured images of the two separate molecules. Molecules were created using Alchemy III (Tripos Associates) and imaged using Rasmol v2.6 (Roger Sayle, Glaxo-Welcome) enhanced by MultiCHEM (Berkeley, USA).

The first comparison of Cibracon Blue F3-GA structure (shown in **Figure 1.3**) was in fact to that of the nucleotide co-factor ATP[32] and it was only later that this was generalised to cover the 'dinucleotide binding fold'. Specific binding to the nucleotide binding site has generally been 'proved' through the use of competitive binding assays with the natural co-factor, showing that the dye acts as a competitive inhibitor to the cofactor. Quantitative studies have also shown a stoichiometric binding of the dye to proteins again suggesting specific binding. In the case of horse liver alcohol dehydrogenase, Cibracon Blue has been co-crystallised with the protein and the electron density map shows the selective binding of the para-sulphonate isomer of the A-ring in the co-enzyme binding site[33]. It is also fortuitous that in the crystal structure the triazine ring is orientated such that it is exposed to the solvent which means that coupling of the dye to a matrix should not overly hinder binding. Although overall the

binding seems to mimic that of the co-factor there are important specific differences due to the differences between the structures, notably in the regions of the B and A rings. These differences were investigated further by Lowe et al.[34] who showed that by alterations in the substituents of the A ring the affinity of the dye could be altered by over three orders of magnitude.

Structural comparisons with nucleotides such as that with ATP shown in **Figure 1.4**, show that the D and C rings bear a close resemblance to the structure of the AMP portion of the nucleotide cofactors. It is thus understandable why the dye should interact with a wide variety of nucleotide requiring enzymes. However it is also apparent that the differences between the structures could easily account for the fact that the dye will also not bind to some nucleotide requiring enzymes. Examination of the dye structure also shows why it can also act as a specific absorbent for other proteins which do not contain a nucleotide binding site. The dye has many features with both polar and aromatic groups along with several charged sulphonates. These in combination with the flexibility of the molecule allow it to interact non-covalently with a number of sites on the surface of a protein in an array of interactions whose cumulative strength is at least equivalent of that of a biospecific ligand. These properties are common to most of the range of reactive textile dyes which have a wide variety of structures, examples of which are shown in **Figure 1.5**. Thus a whole range of the textile dyes have found uses for the purification of proteins. Attempts have been made to classify these dyes according to their binding properties and develop screening protocols for the rapid selection of an appropriate dye for use in a purification[35]. Parallel to this attempts are also being made to engineer novel affinity ligands with improved affinity, capacity and specificity using structures derived from those of the original dye molecules.

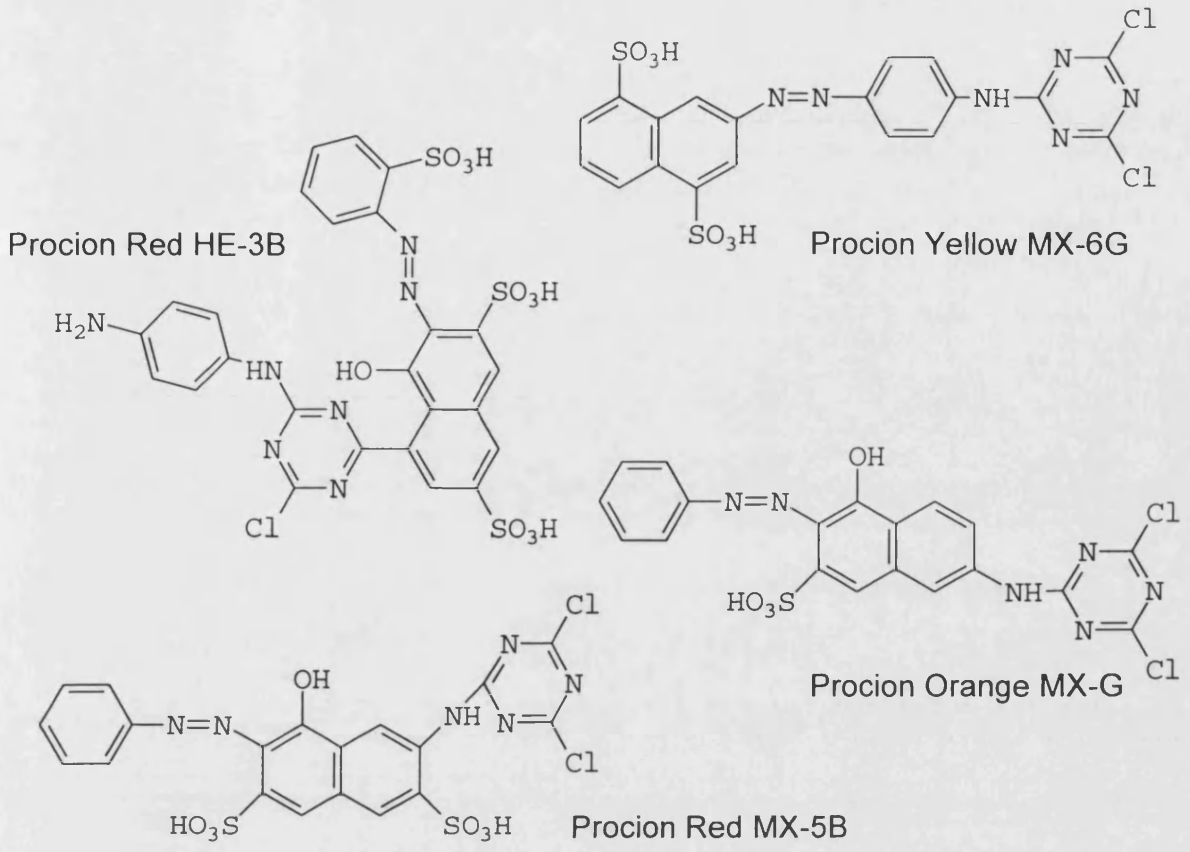

Figure 1.5: Additional members of the family of triazine dyes. Illustrated are both mono- and di-chloro triazines. Many sub-families are derived from the basis of some of the di-chloro triazines. For example Cibracon Blue F3-GA is itself derived from Procion Blue MX-3G which is a dichloro-triazine lacking the A ring of Cibracon Blue F3-GA.

There are several methods of quantifying the binding between proteins and ligands, some of which can also yield some information about the type of interactions taking place.

Spectrophotometry is a well-established technique[36,37] which can provide both quantitative and qualitative information about the binding interactions[38] and can be applied to both equilibrium and kinetic measurements[39]. In the case of the reactive dyes this is based upon changes in the environment of the chromaphoric groups of the dye molecule upon binding causing an alteration in the absorbance spectrum of the dye. In this respect these dyes benefit from their origins as textile colorants as their absorbance in the visible region is centred well away from the protein absorbance in the near UV: Thus the signal is clear from any direct interference from protein absorbance. Binding to proteins is normally characterised by a red-

shift of the dye absorbance which has been associated with a decrease in the polarity of the environment relative to that of water. The change in visible absorbance can be measured as a difference spectrum between two solutions that contain equal quantities of dye, but only one of which contains the protein. The magnitude of the difference spectrum is directly proportional to the quantity of dye bound and can be used to produce a binding curve. Examination of the profile of the difference spectrum has been used to deduce information about the mode of binding of the dye. Subramanian[38] measured the difference spectrum of the dye in a variety of polar and non-polar solvent systems. By comparison of the characteristic shapes of the difference spectra produced in the different solvent environments with those produced upon the binding of the dye to a range of proteins, information about the nature of the binding interaction with these proteins was deduced.

Fluorescence titrations have also been used to quantify binding constants and number of binding sites[40,41,42,43,44] using a variety of fluorescence methods. Fluorescence quenching has been used as an analytical method for measuring the interaction between LDH and the triazine dye Procion Yellow[45]. However the wider application of this technique is probably limited due to its dependance upon the binding of the ligand causing quenching of the intrinsic protein fluorescence, which may not occur in all cases. The actual method of quenching is not known, and has a variety of possible explanations. It could be the result of electron transfer between the protein's tryptophan and the bound molecule, or due to a complex formation between them, or a change in the environment of the tryptophan caused by a conformational change upon binding[46,47]. There are also additional problems with this technique due to the not inconsiderable absorbance of the dye in the near UV in the same region which is used to monitor protein fluorescence. This absorbance causes what is termed as an 'inner filter' effect, the absorbance reducing the effective illumination of the sample and hence the fluorescent yield. This is especially problematic in titration measurements where the concentration of dye is being altered and hence the magnitude of the effect and the correction which has to be made for it varies throughout the experiment.

Another method that has been used to quantify and qualitate the interaction of reactive dyes with proteins containing nucleotide binding sites has been through the use of competitive

assays using the natural co-factors. As previously mentioned the success of this technique depend on the dye binding specifically and reversibly at the same site as that of the co-factor. Thus it can be deduced that in systems where it has been used there is strong evidence that the dye binds at the co-factor binding site, as otherwise no effect would be seen. Application of this technique ranges from competitive elution of proteins from dye affinity columns, where specific elution at relatively low concentrations of co-factor infers competitive binding. Spectral displacement assays, where the difference spectrum of bound dye is quenched by the addition of co-factor displacing the dye from the protein. To inhibition assays of the enzymic activity of the protein by addition of dye and analysis of the resultant curves in terms of competitive inhibition.

However this technique is only of use in determining a binding constant of the dye to the protein and does not facilitate analysis of the binding kinetics of the dye to the protein. Its use is therefore limited, especially in model systems where it has been shown that spectral and fluorimetric methods provide simple methods of measuring dye affinity which can also be utilised for kinetic measurements.

1.2 Aims of the Project

Previous work has studied the interactions between dextran - Cibracon Blue F3-GA conjugates and lysozyme[25,39,48]. Lysozyme is presumed to have a single high specificity binding site for Cibracon Blue F3-GA, and thus provides a simple system for modelling. One possible criticism of this system is that the actual binding site for Cibracon Blue F3-GA on the lysozyme molecule is unknown and so it is difficult to draw unambiguous conclusions from the results. However, providing it is assumed that there is one specific binding site much useful information has been deduced from these studies. Further studies of this system using spectral kinetic techniques should help validate the conclusions of the previous studies and possibly elucidate other possible explanations for the complex binding kinetics previously seen.

Modelling of the binding of lysozyme to Cibracon Blue F3-GA has indicated that only around 30 percent of the dye bound to the backbone was actually available for binding to the enzyme from equilibrium experiments[25,39] with a slightly higher figure from kinetic studies[48]. These results are possibly complicated by the presence of a lower affinity non-specific interaction as well as the higher affinity specific interaction. The use of a system with a known binding site such as LDH should help confirm the validity of the proposed models and confirm their wider application to other dye binding systems.

The interaction between triazine dyes and lactate dehydrogenase (LDH) has been extensively studied, using both column chromatography and two phase systems, and with a variety of alternative dyes[49,50,51,52,53]. Lactate dehydrogenase is a tetrameric enzyme with each subunit having its own catalytic centre and an NAD^+ co-factor binding site. There should therefore be four dye binding sites per enzymic unit. This gives the possibility of multiple specific interactions between the enzyme and dye molecules taking place. By using a large dextran 'backbone' to which several dye molecules are attached it may be possible to get 'chelating' effects with the flexible backbone allowing more than one dye molecule on a single backbone to interact with the same enzymic unit. By synthesising a range of dye-dextran conjugates using dextrans of varying backbone size and dye loadings it should be possible to characterise the interactions taking place and successfully model the system. In this light it is interesting

to note that in the majority of the two phase studies calculation of the number of partitioning molecules bound per tetrameric unit gives values only in the region of 1-2. In one of the few studies on the effect of ligand density upon protein binding[54] it was reported that although inhibition studies showed that with increasing ligand density it appeared that increasingly co-operative binding was being seen, the extraction profiles seen in two-phase systems using the same conjugates did not reflect this apparently higher affinty.

Dye stacking, a non-covalent interaction between dye molecules in solution, has been shown to take place by experiments measuring the deviation of the absorbance of solutions of dye from that expected from Beers' Law. It has also been shown that dye solutions produce a difference spectrum when a solution of double the concentration and half the path length is compared to that of a standard[24]. Additionally measurements of the apparent size of dye-dextran conjugates in solution have shown that the apparent size of the conjugates is reduced as the dye concentration is increased. This suggests that the dye stacking interaction may be causing the conjugates to fold up on themselves in solution due to increasing intramolecular stacking taking place as the dye loading is increased.

A model involving dye stacking has been produced which improves the fit over a simple binding model to kinetic data gathered for the binding interactions of free dye and dye-dextran to lysozyme[32]. In combination these data imply that the stacking interaction may have a significant role effecting the binding of protein to affinity ligands which warrants further investigation to test the validity of the model produced for binding taking into account dye stacking interactions.

Fluorescence titration provides several advantages for quantification of the interaction between dye and LDH. The measurement of the interaction has a higher sensitivity, the interaction being able to be monitored at least an order of magnitude lower concentration. The use of fluorescence to monitor binding also simplifies the production of models taking into account stacking effects as stacking has no direct effect on the measurement of binding as it does in a spectral system. As fluorescence measurements are only sensitive to the interaction between dye and enzyme which causes quenching they provide a highly specific probe for measurement of binding. This is advantageous over spectral measurements which can

possibly be influenced by other possible interactions between dye and enzyme as well as dye-dye interactions such as stacking.

By using both spectral and fluorometric methods to measure interactions between the dye and LDH a useful comparison between the methods can be made, and the validity of any proposed binding model checked against data from both measurement systems.

The study will then be extended to cover other model proteins such as horse liver alcohol dehydrogenase, a dimeric enzyme with two co-factor binding sites and also a monomeric enzyme such as yeast saccharopine dehydrogenase or scallop octapine dehydrogenase. These should allow comparison and separation of binding phenomena which are general to all of these proteins and those which are depend upon co-operative effects specific to those possessing more than one ligand binding site.

Methods

In general all standard reagents used were of technical grade or higher obtained from Sigma (Pool, England) unless otherwise stated.

2.1 Synthesis of Dye-Dextran conjugates

The procedure used for synthesis of dye-dextran conjugates is a further modification of the method of Bohme et al.[56], previously modified by Mayes et al.[25]. Triazine dyes contain a triazine ring substituted with one or two chlorine atoms. These act as leaving groups and react readily with nucleophiles such as hydroxyl groups.

Dextran is made up of many glucose subunits, each of which has several free hydroxyls. In a suitable alkaline environment the hydroxyl groups of the glucose moieties react with the triazine ring displacing the chloride group resulting in attachment to the glucose via an ether linkage as shown in **Figure 2.1**.

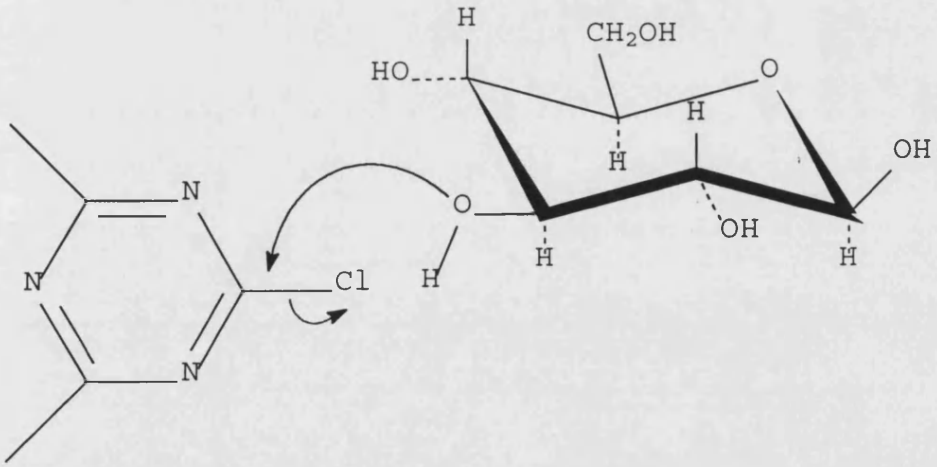

Figure 2.1 : Reaction of the triazine group with glucose

Solutions containing 2 g polymer and 2 g Na_2CO_3 in 100 mls (2 % w/v) distilled water were made to which various quantities (0.1 - 3g) of dye were added. The mixtures were then

incubated at 45 C for at least 48 hr. to allow the reaction to reach completion. Purification of the product was by successive ethanol precipitation. This consisted of addition of an equal quantity of ethanol and cooling for 30 min at -20 C. The precipitate was then spun down in a Sorval GSA rotor @ 15k rpm, 20 mins and the supernatant, containing unbound dye, discarded. After the initial precipitation the pellet was resuspended in 50 mls distilled water for the subsequent precipitations. The conjugate was purified at least twice by this method, until the supernatant appeared relatively colourless. The final resuspension was made into 40 mls distilled water to which a few crystals of sodium azide were added to inhibit microbial growth.

This method was used for the synthesis of the Cibracon Blue F3-GA - dextran conjugates; for the Cibracon Red HB conjugates the sodium carbonate in the reaction mixtures was replaced by 0.1 M sodium hydroxide, the remainder of the procedure being unaltered.

The quantities of dye added to the reaction mixtures were calculated to produce conjugates with degrees of substitution relative to the lowest molecular weight backbone used. The following assumptions were made during these calculations :-

1. The molecular weight of the smallest backbone used was 39,500 Da. (which will henceforth be referred to as T40). This is the average molecular weight of the backbone, and does not take into account the polydispersity of the sample.

2. The dye powder used contains only around 60 % by weight active dye, the remainder being a combination of preservatives, anti-microbials, residual impurities from the synthesis reactions and inactive dye. All of these are presumed not to take place in any reactions with the dextran and dye and are removed in the purification steps and hence ignored.

3. Only around 30 % of the dye reacts with the dextran. The reaction involved in the covalent coupling of the dye to the dextran backbone links the dye to hydroxyl groups on the sugar molecules making up the backbone. There is however a competing reaction with the free hydroxyls of water in solution, which inactivates the dye stopping its subsequent reaction with the dextran. Thus the amount of dye coupled to the dextran is dependent upon the relative rates of the reaction of the dye with water and the reaction with dextran.

Using these approximations the dye quantities needed to produce relative substitutions of 1,2,5,10 and 20 mol / mol dextran were calculated and used for a trial synthesis using the lowest molecular weight T40 backbone. The actual degree of substitution of the conjugates was assessed by a combination of dry weight determination and absorbance measurements.

Dry weight determinations were made using 1 ml samples of the stock solution which were dried to constant weight in an oven at 80 C.

It is known that Cibracon Blue F3-GA deviates from Beer's Law in water/buffer solutions. Therefore the concentration of dye was measured under denaturing conditions in 6 molar hydrochloric acid according to the acid hydrolysis method of Chambers[57]. Mayes et al.[25] showed that the hydrolysis spectra had an isosbestic point in its time course at 541 nm. This allows the immediate measurement of the concentration of dye without waiting for the hydrolysis reaction to run to completion. This accuracy of this assumes that under these conditions no stacking or other interactions take place which cause any deviation from Beer's Law. The extinction coefficient of dye under these conditions at 541 nm was determined by Mayes[58] to be 3,950 $M^{-1}cm^{-1}$.

After the results from the initial synthesis reaction had been determined, further conjugates were produced using Cibracon Blue F3-GA for dextran backbones of 73,000 Da. (T73) and 124,500 Da. (T124) along with previously synthesised conjugates with backbone sizes of

500,000 Da. (5D) and 2,000,000 Da. (20D). Similar conjugates were also produced with Cibracon Red HB as the dye using a similar procedure as for Cibracon Blue F3-GA and using T40 and T124 dextran backbones.

Stock solutions were stored at 4 C to prevent microbial growth.

2.2 Dye Purification

For the experiments involving free dye, pure inactive dye is required. The dye supplied was shown to be mainly in the active form. Thus to produce pure inactive dye the dye has first to be inactivated, and then purified. The dye is inactivated by taking 0.5 g dye and placing in 10 mls 0.1 M NaOH. This is then incubated in an oven for 2 hours at 80 C. The solution is neutralised by the addition of 1 ml 1 M HCl before subsequent purification.

Dye purification and analysis follows the methods used by Pearson et. al.[59]. Purification is by column chromatography using a 0.6 x 100 cm column packed with Sephadex LH-20. The column is washed and run using 1:1 methanol:water at approximately 0.5 ml/min flow rate. The column eluant is passed through a HPLC flow cell in a Unicam Series 2 spectrophotometer and the absorbance measured at 280 nm. Fractions are collected every 10 mins (approx. 5 mls) using a Frac - 100 automatic fraction collector. Fractions of the main peak containing the pure deactivated Cibracon Blue F3-GA are then analysed for purity using TLC.

Small samples (1-2 ul) were spotted onto 10 cm silica TLC plates and run in a tank pre-equilibrated with the dye TLC solvent mixture. Fractions containing only pure deactivated dye are pooled and dried using a rotary evaporator.

Dye TLC solvent mixture:

4 parts Propan-1-ol

3 parts Distilled Water

1 part Ethyl Acetate

2 parts Butan-1-ol

For larger scale purification a larger (5 x 60 cm) column of Sephadex LH-20 was used with a higher flow rate of 3 ml/min. This allowed the application of considerably larger (5-10 ml) samples without any reduction in resolution of the peaks.

2.3 Dye - Glucose Preparation

Dye glucose was prepared by a similar reaction to that used to prepare dye-dextran conjugates as shown in **Figure 2.2.** Cibracon Blue F3-GA (1g) was mixed with an equal quantity of diacetone glucose (1g) dissolved in 100 mls 2% w/v sodium carbonate solution. The mixture was incubated with stirring at 45 C overnight.

10 mls of the resulting reaction mixture was then taken and dried down in a rotary evaporator and the residue resuspended in 20 mls 60:40 methanol / water. 1 ml samples were purified using a 100 x 0.6 cm Sephadex LH 20 column. The column was run using the 60:40 methanol:water mix at a flow rate of 0.5 ml/min. The absorbance of the eluant was recorded at 280 nm using a Unicam spectrometer linked to a pen recorder and fractions were collected every 10 minutes using a Frac -100 fraction collector.

Analysis of the resulting peaks was by TLC using plastic backed silica plates with the dye TLC solvent mixture described previously. Plates 6 - 7 cm long were used with 1-5 ul of sample being applied dependant upon the concentration of the sample.

As with the previous dye purification, a preparative column (5 x 60 cm) was used for large scale preparation of pure dye glucose with a flow rate of 3 ml / min. Fractions were analysed and pooled in the same was as for the smaller column.

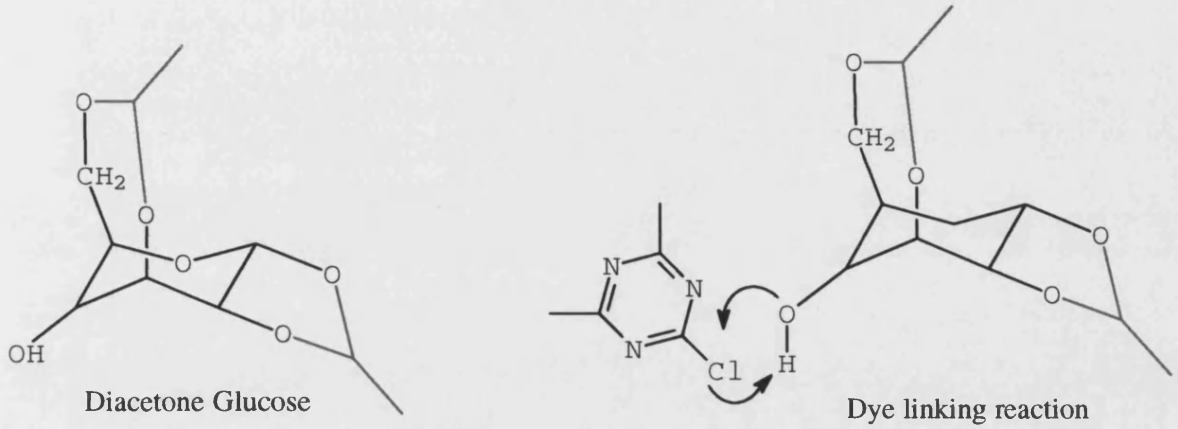

Figure 2.2 : Structure of diacetone glucose and its linking reaction to dextran

2.4 Difference Spectra

Difference spectra were measured in two ways, firstly by keeping the enzyme concentration fixed and varying the dye concentration and secondly the reverse, by keeping the dye concentration fixed and varying the enzyme concentration.

In both cases the spectra were measured using a Cecil 6000 series twin beam spectrophotometer with solutions buffered in 50 mM sodium phosphate buffer pH 7.9. A sample volume of 2 ml was used in both reference and sample paths in matched 10 x 10 mm quartz cuvettes.

In the first method the sample cuvette contained enzyme at approximately 2 uM, the actual concentration being determined by absorbance measurements at 280 nm using an extinction coefficient for the enzyme of 0.162 $mM^{-1}cm^{-1}$ [60] The reference cuvette contains buffer only. A baseline is then scanned from 420 - 800 nm. Concentrated dye or conjugate solution (1 mM

with respect to dye) is then added in equal quantities to both cuvettes, starting with an addition volume of 2.5 ul. The solutions are then mixed thoroughly using small stirrers which can be left at the sides of the cuvettes afterwards without interfering with the light path. The spectrum is then scanned again, producing a difference spectrum between the sample which contains both dye and enzyme and the reference that contains only dye. This process is repeated, with the quantity of dye being added increased as the magnitude of the increase in the difference spectrum decreases, until the end point is reached and there is no further increase in the magnitude of the difference spectrum.

The second experiment uses a very similar method. Initially the cuvettes contain equal quantities of dye, made by adding 1 ml of a stock dye solution to each cuvette and 1 ml of 2 x phosphate buffer. The exact concentration of dye in the stock solution is determined separately at 541 nm in 6 M HCl. The baseline is then measured. Then small aliquots of concentrated enzyme solution (approximately 1 mM with respect to subunits) are added to the sample cuvette, while buffer only is added to the reference. The solutions being mixed and the spectra taken as previously until the end point is again reached.

2.5 Deviation from Beer's Law

Deviation from Beer's Law in the dye absorbance was measured by taking absorbance readings of a cuvette to which successive additions of concentrated dye solution were made. From the known dye concentration of the concentrated stock solution the expected absorbance (according to Beer's Law) was calculated, taking into account the small dilution effect due to the additional volume of each addition. The actual absorbance of the dye solution was measured in 50 mM sodium phosphate buffer pH 7.9 in an initial volume of 2 mls in a 10 x 10 mm cuvette using just the sample beam of a Cecil 6000 Series twin beam

spectrophotometer. By comparing the actual value to the expected value the deviation from Beer's Law could be calculated.

2.6 Fluorescence Titrations

Measurement of binding by fluorescence titration was by the quenching of the natural fluorescence of the tryptophans within the LDH. Fluorescence measurements were taken using a Perkin Elmer LE 5B Luminescence Spectrophotometer. Samples of 0.5 mls of an approximately 0.2 mM LDH solution were excited at 280 nm in a 5 x 5 mm quartz cuvette and the fluorescence measured at 320 nm. The concentration of the solution was adjusted to an absorbance of 780 (+/- 10) units to give a reproducible start point, compensating for any pipetting errors. Titration was by successive additions of 2.5 ul of dye or conjugate stock solution (200 uM with respect to dye). The solution was mixed and the fluorescence recorded after each addition. Additions were continued until the decrease in fluorescence became constant, at which point the increasing quenching was due only to the increasing absorbance of the dye and the end point had been reached (For an explanation of the inner filter effect caused by dye absorbance and its correction see section **4.10**.)

2.7 Stop-Flow Experiments

Stop-flow experiments were made using a Hi-Tech Scientific SF 61-MX multimixing stop-flow system. This system consists of a mixing unit capable of both conventional stop-flow and multi-mixing modes of operation. All the experiments were done using only the conventional stop-flow mode of operation.

Figure 2.3 shows the principle components of a stop-flow system. In the stop-flow operating mode reactants are placed in two reservoirs. Liquid from each is then drawn down into two

drive syringes vertically below the reservoirs. Valves are then used to change the flow path from the reservoirs to the mixing path. When the machine is triggered, a pneumatic ram rapidly drives the syringes upwards forcing the reactants through a mixing cell into the observation chamber and from there into the stop syringe. The stop syringe is set at such a volume to ensure that the reaction chamber is flushed of its previous contents and filled with freshly mixed reactants. When the stop syringe is filled, flow through the system ceases and this triggers the computer controlled data acquisition system to start recording data. The system can be configured in a variety of optical modes to monitor the reaction taking place in the observation cell allowing both fluorescence and absorbance measurements of the reaction to be taken.

The mixing unit is liquid jacketed to allow thermostating of the drive syringes, resevoirs and the mixing / observation cell. For thermostating purposes an externally thermosated cirulating unit with cooling capacity was used so that termeratures below ambient could be achieved. The pipework between the circulator and the mixing unit was insulated to reduce thermal losses or gains between them. The desired temerature was set according to the internal temperature sensor in the mixing unit, there normally being a constant temperature differential between the temperature set on the circulator and the actual temerature of the mixing unit once it had been allowed to equilibrate for around half an hour.

In operation the shot volume for each run was set to 150 ul. The volume of the pipework from the drive syringes to the stop syringe including the mixing unit and obervation cell is approximately 75 ul, this being the theoretical minimum shot volume. The practical minimum shot volume has to allow for some additional flow through to ensure that the observation cell is filled with fresh reactants, which is why a shot volume of 150 ul was chosen. It is obviously desirable to set the shot volume as low as possible to reduce usage of material for

each run, without compromising the reaction by having too much residue from the previous shot. Before recording data for a set of shots it is necessary to pre-equilabrate the mixture in the obervation cell. This is due to the fact that flow through the system is not perfectly lamina, therefore there is always a few percent of the previous mixture in each run. To minimise the effects of this on the observed kinetics by ensuring that the reactants being observed are as close as possible to the desired final concentrations (half that in the syringes) it is therefore necessary to push through at least 2 shots of the reaction mixture before consistant kinetic results can be recorded.

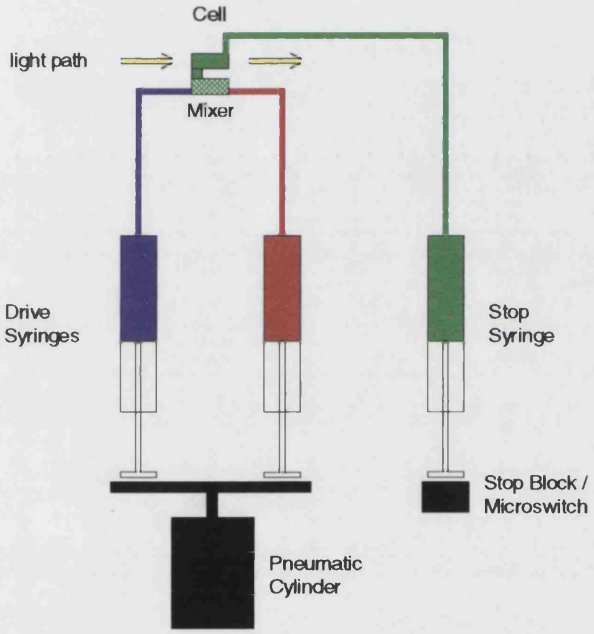

Figure 2.3 : A simplified stop-flow system

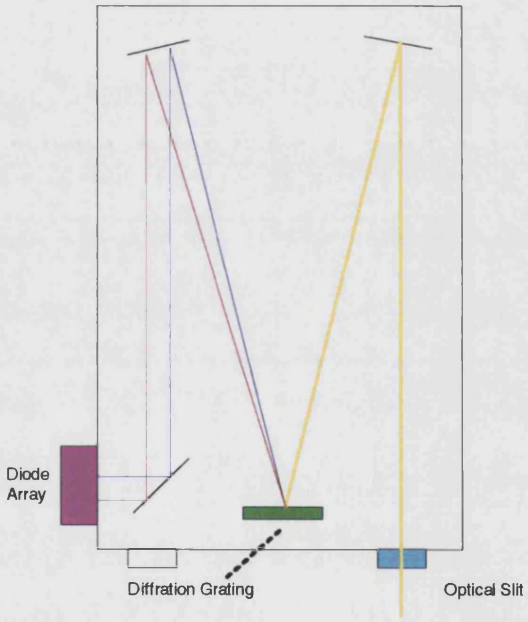

Figure 2.4 : Diode array detector

Figure 2.4 shows the diode array system used for the simultaneous measurement of absorbance at multiple wavelengths. This system works by applying white light through the observation cell. The transmitted light is then fed by a light guide into a monochromator set up as a diffraction system. This produces a spectrum of light which is then reflected across the surface of the diode array detector. The detector itself consists of a linear array of 512

individual photodiodes. The diffraction grating is set up so that the diode array receives an approximately 400 nm range of light, giving a theoretical resolution of around .8 nm per photodoide. A single scan consists of reading the voltages from each of the photodiodes which are read at 1 MHz, therefore taking approximately 0.5 ms to read the complete array. The wavelength range of useful data that can be taken from the diode array is limited by second order diffraction effects which occur at twice the wavelength of the diffracted light. Thus at shorter starting wavelengths less than a 400 nm range can be used, the upper limit being twice the lowest wavelength used e.g. 250 - 500 nm or 300 - 600 nm.

2.8 Preparation of Sepharose 4B Affinity Media

Cibracon Blue F3-GA was linked to Sepharose 4B by the following method.:
Solution A (200 mls) was preheated in a waterbath to 60 C with stirring. To this was then added solution B (50 mls). The mixture was allowed to react for 4 hrs at 60 C with continuous stirring. The reaction mixture was then filtered with a sintered glass funnel. The residue (now a dark blue colour) was then washed with 500 mls of 50 percent aqueous ethanol followed by a similar volume of distilled water. The washed Cibracon Blue Sepharose was then packed in a column and washed with a further 500 mls of 50 percent ethanol before being stored for use in 50 percent ethanol at 4 C in a brown glass vessel.

Solution A:

100 mls of Sepharose 4B

100 mls distilled water.

Solution B:

1g Cibracon Blue F3 - GA	(4 grams / litre final)
23 g sodium carbonate	(2 M final)
14 g sodium chloride	(1 M final)

Reactive Green 19 - Sepharose 4B was produced in a similar manner to Cibracon Blue F3-GA - Sepharose 4B above. However only 50 mls of Sepharose 4B was used, with an additional 50 mls of distilled water being added to keep the same final volume. The Cibracon Blue F3-GA in solution B was substituted for the same quantity of Reactive Green 19. The reaction was carried out overnight at 45 C in a waterbath with constant stirring. The reaction mix was washed in a similar manner to the Cibracon Blue - Sepharose and stored in 50 percent ethanol at 4C as before.

2.9 Purification of Saccharopine Dehydrogenase from Baker's Yeast (*Saccharomyces Cerravisiae*)

Saccharopine dehydrogenase (N6-(glutar-2-yl)-L-lysine:NAD oxidoreductase (L-lysine forming)) is a monomeric dehydrogenase catalysing the formation of Saccharopine from L-lysine and α-ketoglutarate.

$$\text{Saccharopine} + NAD^+ + H_2O \Leftrightarrow \text{lysine} + \alpha\text{-ketoglutarate} + NADH + H^+ \quad (1)$$

The enzyme was purified using a method based upon that of Ogawa et al.[61] which itself was a modification of the pervious method of Fujioka et al.[62]

The enzyme was assayed using the reverse of reaction (1) following the disappearance of NADH spectrophotimetrically at 340 nm with typically 5-20 ul of sample being assayed in a final volume of 2 mls of assay mixture.

Saccharopine dehydrogenase assay mixture:

0.2 mM NADH	10 ul of 7.1 mg / ml stock.
5 uM α-ketoglutarate	10 ul of 36.5 mg / ml stock.
12 uM L-lysine	10 ul of 110 mg / ml stock.

100 mM Potassium Phosphate buffer to 2 mls.

Sample rates were measured using a Cecil CE 6600 spectrophotometer measuring the disappearance of NADH at 340 nm with a chart speed of 3 cm / min. The spectrophotometer was blanked against phosphate buffer and the spectrophotometer set recording against assay buffer only to give a baseline. The sample was then added and rapidly mixed and the reaction recorded over a typical timecourse of around 2 minutes.

Step 1 - Autolysis of yeast and preparation of cell-free extract. The first step was to produce dried yeast powder from fresh Baker's Yeast by air drying. Fresh Baker's Yeast was split into small pieces and spread over tissue on drying racks at 37 C. After initial drying overnight the semi-dried yeast was crushed further by hand to produce fine particles. This was then allowed to dry further at 37 C for two days until totally dry.

A total of 5 Kg of yeast cake was air dried yielding 1420 g of dried yeast powder which was stored in sealed dark glass containers at room temperature for further use

An autolysate was then prepared by homogenising 120g of dried yeast in 360 mls of lysis buffer containing 67 mM potassium phosphate (3.28 g / 360 mls). This was then allowed to stand at 37 C for 6 hours and then at 4 C for at least 2 weeks. To produce a cell-free extract the autolysate was centrifuged for 30 min at 5,000 rpm, Sorval GSA rotor and the pellet discarded.

Step 2 - Ammonium sulphate fractionation. To the autolysate 28 g / 100 mls ammonium sulphate was added slowly with stirring. After leaving for 30 min the mixture was then centrifuged at 10,000g for 30 min. The precipitate was discarded and a further 12g / 100 mls (original volume) was added to the supernatant.. This was again added slowly with stirring and left for 30 min before centrifugation at 10,000 g for 30 min. The supernatant was discarded and the pellet kept for further purification.

Step 3a - Affinity chromatography. In an attempt to simplify the purification procedure an affinity chromatography step purification using Cibracon Blue Sepharose 4B prepared as described previously (q.v.) was attempted at this stage. A small quantity of the pellet from step 2 was taken and dissolved in approximately 5 mls of column buffer A. This was then further diluted to a final concentration of around 20 mg / ml. A 15 x 0.6 cm column of Cibracon Blue Sepharose 4B was equilibrated with approximately 100 mls of column buffer A at a flow rate of approximately 18 mls / hr. Diluted extract (10 mls) was then applied to the column followed by washing with buffer A until the absorbance of the outflow became close to zero. Fractions of the flow-through peak were collected every 10 minutes (approximately 3 mls). The buffer was then changed to column buffer B and fractions were again collected. As an alternative to the single step elution with buffer B a convex gradient

elution from 0 - 1 M potassium chloride using 33 ml buffer A and 66 ml buffer B in a gradient maker with reservoirs with a 1:2 ratio of diameters, followed by a further 50 mls of buffer B was also used.

Fractions were assayed for enzyme activity and for total protein using a Bio-Rad microtitre assay (q.v.).

Column Buffer A:

20 mMsodium phosphate pH 6.8

1 mM EDTA

Column buffer B:

20 mM sodium phosphate pH 6.8

1 mM EDTA

1 M potassium chloride

Step 3b - CM - Sephadex Column chromatography. The ammonium sulphate pellet from step 2 was dissolved in a minimal volume of column buffer A. This is then dialysed against buffer A to remove the majority of the ammonium sulphate before loading onto a CM - Sephadex ion exchange column previously equilibrated with buffer A. The column is then washed with buffer A until the absorbance is close to zero. Bound protein is then eluted by a convex gradient of 0 - 1 M potassium chloride (Buffer B). Fractions with a high activity were pooled and precipitated with ammonium sulphate (60g / 100 ml).

Step 4. Sephadex G-100 Column chromatography. The pooled precipitate from step 3b is resuspended in a minimal volume of buffer A and dialysed against buffer A. This is then

loaded onto a G-100 Sephadex column pre-equilibrated with buffer A. Elution is carried out using buffer B and the most active fractions pooled and precipitated with ammonium sulphate as before.

2.10 Purification of Scallop Octopine Dehydrogenase

Octopine Dehydrogenase is a monomeric NAD-dependant dehydrogenase which catalyses the reductive condensation of pyruvate and L-arginine to D-octopine

$$\text{L-arginine} + \text{pyruvate} + \text{NADH} + H^+ \Leftrightarrow \text{D-octopine} + NAD^+ + H_2O \quad (2)$$

A variety of methods have been used for the purification of Octopine dehydrogenase from Scallops[63,64,65]. These vary mainly in the exact form of the media used in the ion exchange and gel filtration steps and in the addition of a final affinity chromatography step[65]. The method used here is adapted from appropriate steps from these methods.

The enzyme activity was assayed spectrophotometrically using reaction (2) following the disappearance of NADH spectrophotometrically at 366 nm. Typical sample sizes of 5 - 20 ul were assayed in a final volume of 1 ml of assay buffer.

Octopine dehydrogenase assay mixture:

0.25 mM NADH	25 ul of 7.1 mg / ml stock.
2.5 mM Sodium Pyruvate	25 ul of 11 mg / ml stock.
5.0 mM L-arginine	25 ul of 34.8 mg / ml stock.

100 mM Sodium Phosphate buffer pH 7.0 to 1 ml.

Reaction rates were measured using a Cecil CE 6600 spectrophotometer recording the absorbance at 366 nm with a chart speed of 3 cm / min. The spectrometer was blanked against the reaction mix less NADH. Rates were recorded by starting the spectrophotometer recording with just the sample buffer in the cuvette. This gave a starting point for the reaction. Sample was then added and rapidly mixed, with a typical time course of 1-2 minutes being recorded after addition.

All the following purification steps were carried out at 4 C.

Step 1 - Preparation of Crude Extract. Frozen Scallops (obtained 'fresh' frozen from a fish wholesaler) were taken and the reproductive organs removed to leave mainly fast striated adductor muscle. The still frozen tissue was then thinly sliced by hand to aid homogenisation. For the first trial the sliced tissue (453 g) was then homogenised in a Waring blender after the addition of 1.5 l ice cold homogenising buffer. The homogenate was then stirred for 1 hour. The mixture was centrifuged at 27,600 g for 30 min (13,000 rpm, Sorval GSA rotor) and the pellet discarded.

For the large scale preparations, this procedure was modified. 1.2 kg sliced tissue was homogenised in 1.6 l homogenising buffer. This was allowed to stand for 30 min with stirring before centrifugation as before. The supernatant decanted and the pellet resuspended and homogenised again in a further 800 mls of homogenising buffer (0.1 mM EDTA, 93 mg / 2.5 litres). This mixture was then centrifuged and the supernatant pooled with that from the first extraction.

Step 2. Ammonium Sulphate Fractionation. To the pooled crude extract from the first step, 228 g / l of ground ammonium sulphate was added slowly with stirring. This was then left for a further 30 min before centrifugation at 27,600 g for 30 min. The precipitate was discarded and a further 237 g / l of the original volume of ammonium sulphate was added to the supernatant. This was again left for 30 min before centrifugation as before. The supernatant was discarded and the pellet kept.

Step 3. 50g (wet weight) of pellet from the 40 - 70 percent ammonium sulphate cut was resuspended in 100 mls of column buffer A. This was then centrifuged at 140,000 g for 3.5 hrs (Beckman Type 35 rotor, 35k rpm) to remove high molecular weight muscular proteins. The pellet was discarded and the supernatant kept for the next step.
For the smaller trials this step was omitted

Column Buffer A:

20 mM Tris-HCl pH 7.4	6.055 g
1 mM EDTA	0.93 g
0.1 mM DTT	0.045 g
	to 2.5 l with distilled water.

Step 4a. Ion-exchange chromatography. Initially a DEAE Sephacel column was packed following the protocol of Thoai et al.[63]. However it was found that the different salt concentrations used for elution produced large bed volume changes which made this medium difficult to use. It was therefore decided to use DE 52, a cellulose based ion-exchange media

with similar chemical properties, but much improved physical properties for the later purifcations.

For the trial a 1.6 x 20 cm column was packed with DEAE Sephacel and pre equilibrated with buffer B (buffer A containing 67 mM sodium chloride) at a flow rate of approximately 25 ml / hr. The precipitate from step 2 was resuspended in 100 mls of buffer A. This was then dialysed against 3 x 1 l buffer A. The dialysate was then centrifuged at 36,000 g for 30 min (20k rpm, Sorval SS-34 rotor) to remove precipitated protein. The supernatant was divided into two portions and half kept for a trial affinity chromatography step (step 4b, below). To the other half, sodium chloride was added to 67 mM before loading onto the DE52 column. The column was then washed with further buffer B until the outflow absorbance (280 nm) was close to zero. Stepwise elutions were then performed using buffer A plus 107 mM, 175 mM and then 1M sodium chloride. The flow through from the initial loading and wash was pooled for analysis and 10 min (4.2 ml) fractions were taken from the 175 mM wash. Active fractions from the 175 mM elution were pooled and precipitated by the addition of 52 g / 100 mls ammonium sulphate.

For the later preparations a DE 52 column of the same size was used in place of the DEAE Sephacel for the previously mentioned reasons. Two trials were run using approximately 5g (wet weight) of ammonium sulphate precipitate from step 2. The precipitate was redissolved in 50 mls buffer A and dialysed against 3 x 400 mls buffer A. This was then made up to 67 mM salt for the first run, washed with buffer A plus 67 mM sodium chloride and eluted using 107 mM, 175 mM, 250 mM and 1 M sodium chloride concentrations. For the second run the salt concentrations used were 50 mM sodium chloride for loading and washing then 80 mM, 130 mM, and 1 M steps for the elutions. These NaCl concentrations were also used for the large scale purification.

Peaks or fractions were collected from each step of the elution and assayed for activity and analysed by SDS - polyacrylamide gel electrophoresis. Active fractions or peaks were pooled and precipitated by the addition of 50 g / 100 mls ammonium sulphate followed by centrifugation.

Step 4b Affinity chromatography using Cibracon Blue Sepharose 4B. A small column (1.6 x 15 cm) was loaded with Cibracon Blue F3-GA Sepharose 4B synthesised as detailed previously. This column was pre equilibrated with buffer A at a flow rate of 25 ml / hr. Approximately 50 mls of dialysed ammonium sulphate precipitate was loaded onto the column and washed with buffer A until the absorbance approached zero. The column was eluted with a 0 - 1 M convex sodium chloride gradient (1:2 ratio diameter gradient maker) with samples taken every 10 min (approximately 2.5 mls). Both the flow through and the fractions were analysed for activity.

As an alternative a commercial Reactive Blue Sepharose CL 4B affinity media (Sigma) was also packed in a similar size column and loaded and eluted in the same manner.

Step 5. Size exclusion chromatography using Sephadex G-100. Sephadex G-100 was resuspended in buffer A and left overnight at room temperature to rehydrate. Initially a 1.6 x 60 cm column was then packed and equilibrated with buffer A at a flow rate of 25 ml / hr. Ammonium sulphate precipitates from the previous step were dissolved in a small volume (up to 1 ml) of buffer A and applied to the column and 4.5 ml fractions were collected. Fractions were then assayed for activity and analysed by gel electrophoresis.

For the later runs a larger 1.6 x 100 cm column was used with a flow rate of 36 ml / hour with fractions collected every 7.5 min (approx. 4.6 ml). For this column up to 2 ml of sample was

loaded at one time. Active fractions from several runs were pooled and precipitated by addition of 50 g / 100 mls ammonium sulphate.

Step 6. Affinity Chromatography. Small columns (0.6 x 8 cm) were packed with Cibracon Blue F3-GA Sepharose 4B and Reactive Green 19 Sepharose 4B which had been previously synthesised. These were pre equilibrated with buffer A at a flow rate of 15 ml / hr with fractions being taken every 10 min (approximately 2.5 ml).

The pooled G-100 fractions from the first purification were loaded onto the Cibracon Blue affinity column in approximately 2 mls of buffer A. The column was then washed with further buffer A with fractions being taken for analysis until the outflow absorbance was close to zero. The column was eluted with a 0 - 1 M convex sodium chloride gradient (total volume 90 mls). Fractions were then assayed for activity.

A similar procedure was used for the Reactive Green column, except that a stepwise elution procedure was used in place of the gradient with 150 mM, 300 mM and 1 M sodium chloride concentrations being used. Fractions were again collected at each elution step and assayed for activity.

Results

3.1 Synthesis of Dye-Dextran Conjugates

After purification of the initial set of dye-dextran conjugates, their degree of substitution was determined. This allowed an assessment of the success of the coupling reaction that could be used as a guide for the production of further conjugates.

The results of this (**Table 3.1**) showed that the assumptions made for the calculation of the dye to be added were in the correct region for the lower range of substitutions, but showed an increasing deviation for the higher theoretical substitution ratios.

This showed an effective limit on the maximum degree of substitution which could be produced in a single step reaction. The coding for the dye conjugates is based upon the relative amount of dye added in the synthesis reaction. **Table 3.1** gives details of the actual amount of dye added and the relative substitution produced. This is then shown graphically in **Figure 3.1**.

Table 3.1: Results for the synthesis of the T40 series dye-dextran conjugates

Dye-dextran Code No.	Dye added (grams)	Relative Substitution (No. dye per 39.5 kDa.)
T40.1	0.131	0.53
T40.2	0.262	1.29
T40.5	0.655	2.83
T40.10	1.310	3.51
T40.20	2.620	3.88

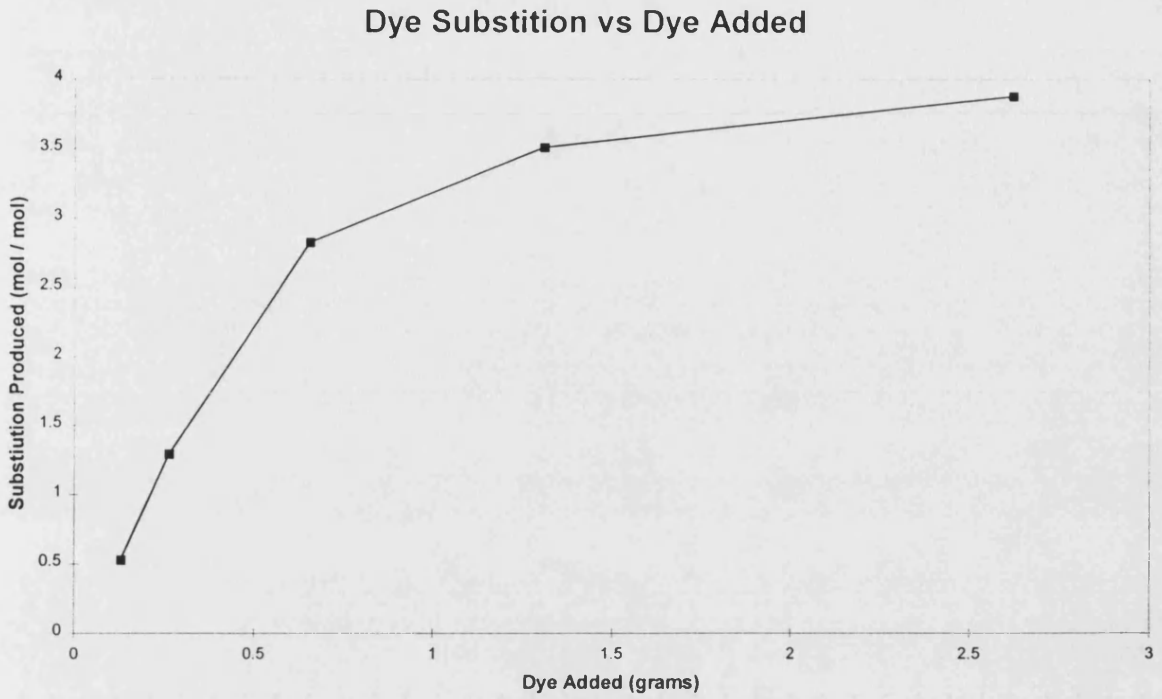

Figure 3.1 : Graph showing the average number of dye molecules bound to each dextran when increasing quantities of dye were reacted with 2g of dextran with a 39.5 kDa average size.

For the initial set of conjugates produce for the range of dextran backbones it was decided to limit the range of conjugation to that which could be achieved by a single step synthesis. The other dextran conjugates were therefore produced using the same set of dye concentrations as those used to produce the T40 series.

Relative substitution or *relative dye loading* is a term that will be used throughout the rest of the text. It is taken to mean the number of dye molecules bound to the dextran backbone per 39.5 kDa. of backbone, i.e. the loading relative to a T40 backbone.

The conjugates were coded according to the size of the dextran backbone used and the amount of dye used during their synthesis. For example T40.2 is the conjugate that has a T40 dextran backbone and had 2 relative units of dye used during its synthesis.

Table 3.2 shows the results for the synthesis of the other Cibracon Blue - dextran conjugates, with both the actual degree of substitution and the relative degree of substitution for each conjugate produced.

Table 3.2: Dye loadings of the T73 and T124 series.

Dye-Dextran Code No.	Absolute Substitution	Relative Substitution
T73.1	1.17	0.658
T73.2	3.19	1.80
T73.5	5.07	2.86
T124.1	2.38	0.758
T124.2	3.81	1.22
T124.5	7.30	2.32

Table 3.3 shows the relative and absolute loadings of the previously synthesised 5D and 20D dextran series (backbone sizes of 500 kDa and 2,000 kDa respectively) also used in this work.

Table 3.3 : Dye loadings of the 5D and 20D series.

Dye - Dextran code number	Absolute Substitution	Relative Substitution
5D2	16	1.28
5D5	53	4.24
5D8	124	9.92
20D4	54	1.08
20D9	196	3.92

A range of dye-dextran conjugates were also synthesised using the triazine dye Cibracon Red HE-3B. These were produced to allow comparison of binding data for alternative triazine dye to Cibracon Blue F3-GA which may have slightly different properties. Conjugates were synthesised with dextrans baackobone sizes at the two extremes of backbone size of 40 kDa (coded T40.xR) and 2,000 kDa. (coded T2000.xR). The results of the synthesis of the Cibracon Red HB - dextran conjugates, with both the actual and relative degrees of substitution for each conjugate produced are shown below in **Table 3.4**.

Table 3.4: Dye loadings for T40.R and T124.R series dye-dextran conjugates

Dye-Dextran Code No.	Absolute Substitution	Relative Substitution
T40.1R	1.32	1.31
T40.2R	2.42	2.42
T40.5R	5.27	5.27
T2000.1R	69.8	1.38
T2000.2R	162.1	3.20
T2000.5R	524.7	10.34

3.2 Dye Purification

Figure 3.2 shows an elution profile for dye on the 0.6 x 100 cm Sephadex LH-20 column run under the original conditions. The main elution peak is off scale and there are several other minor peaks of contaminants visible. Analysis of fractions taken across the major peak using TLC shows it to compose of a mixture of three coloured compounds (**Figure 3.3**). By comparison with the starting dye samples run on either side of the plate these are shown to correspond to the major blue coloured components present in the original source material. The top running blue component is presumed to be active (chloro-triazine) Cibracon Blue F3-GA, the middle component deactivated (hydroxy- triazine) Cibracon Blue F3-GA and the third probably a precursor from the synthesis

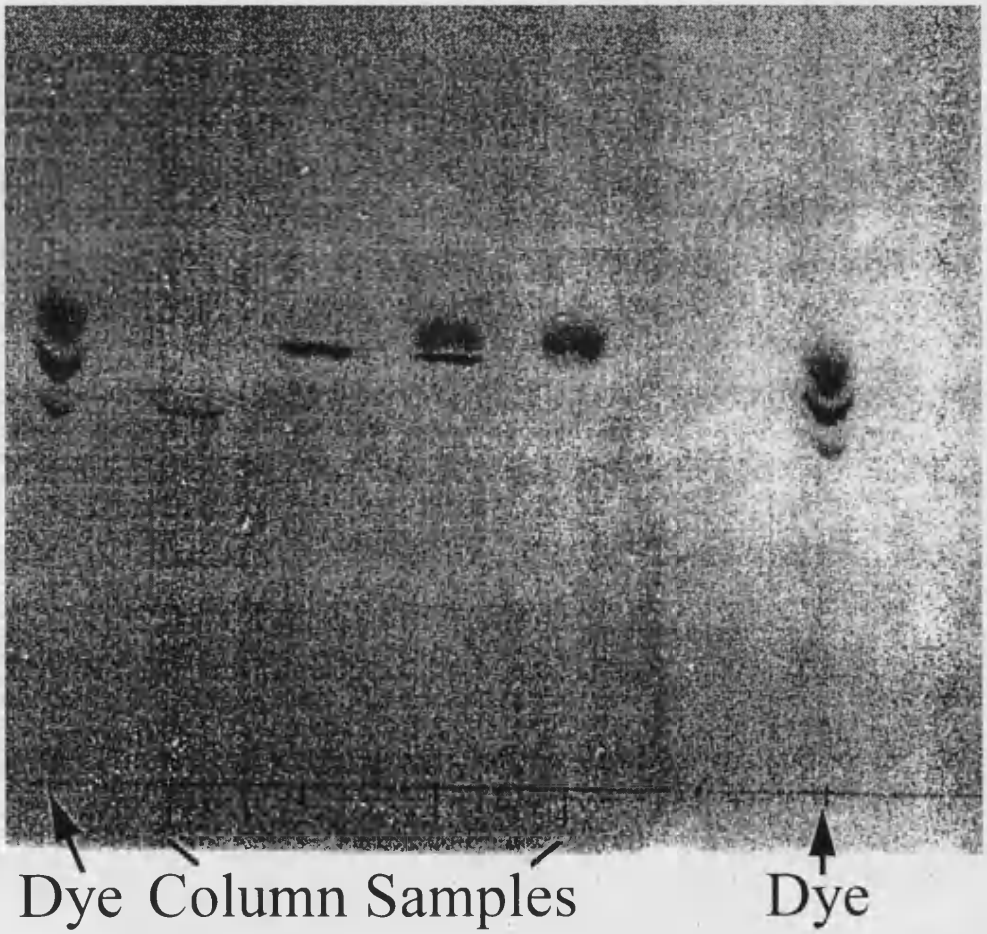

Figure 3.3 : TLC of original dye samples and fractions taken across the major peak of the separation of dye on a Sephadex LH-20 column as shown in **Figure 3.4**. Approximately 2 ul of each fraction plus the initial material was spotted on the plate and the TLC then run with a 4:3:1:2 mixture of propan-1-ol, water, ethyl acetate and butan-1-ol.

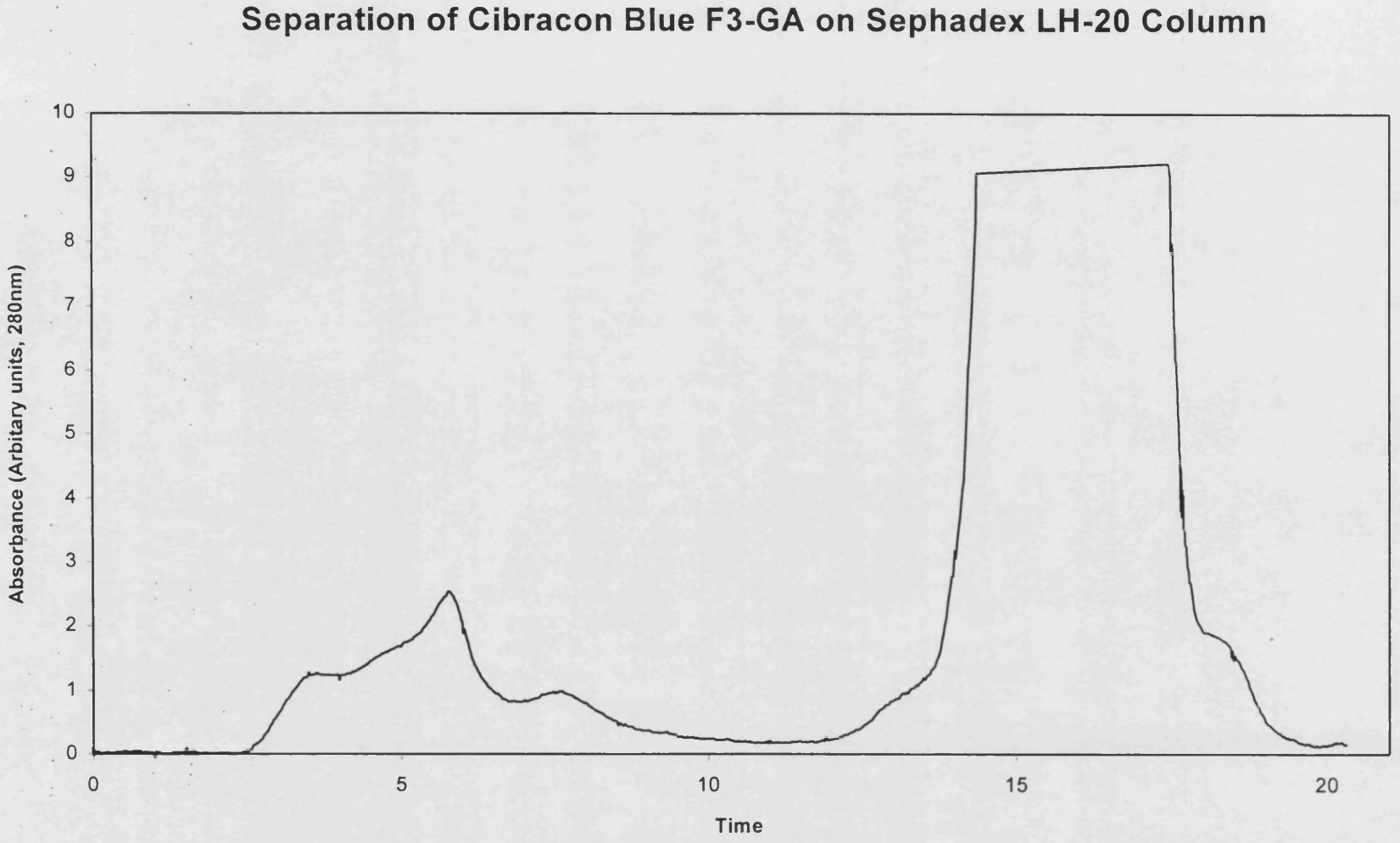

Figure 3.2 : Elution Profile of Cibracon Blue F3-GA run on a 0.6 x 100 cm Sephadex LH-20 column, non-alkalised MeOH / H_2O with a flow rate of 0.5 ml / min. Approximately 5 mgs of dye as supplied by Sigma was loaded in 1 ml solvent. Fractions were taken across the main peak and analysed by TLC.

The identification of the top two components as the active and inactive forms of the dye can be demonstrated by the interconversion of the chloro to hydroxyl forms under alkaline conditions, with the top running band disappearing with more of the middle band being produced.

Figure 3.4 shows the elution profile of the same column run with the 1:1 methanol : water mixture, but including 1 ml 1M sodium hydroxide per 500 mls solvent. It can be seen that the three major components now elute separately with much reduced cross contamination. This is due to an increased retention time on the column of all the components with the differences between them being increased. This is presumably due to an enhancement of the hydrophobic interactions between the media and the dye moieties under these conditions. The tailing peak of the highly retained material was cleared from the column by switching to a non-alkaline methanol / water solvent mixture producing the sharp peak at the end of the tail. This shows the high pH sensitivity of the interaction of these compounds with the column

This was then successfully upscaled to a 2.5 x 60 cm column allowing loading and separation of 10 - 20 ml samples of dye with little loss of resolution compared to the smaller diameter column as shown in **Figure 3.5**. In fact it can be seen that additional peaks of impurities are visible in comparison to the runs on the smaller volume column. This can be attributed to the increase in the quantity of dye loaded to the column and hence that of the impurities present. Use of the larger column allowed separation of dye up to around a hundred milligram scale in a single run.

Thus, the dye as supplied by Sigma seems to consist mainly of the 'active' chloro- triazine form with some hydroxyl and a major coloured contaminant. To produce the 'inactive' hydroxyl form the dye was allowed to react under alkaline conditions resulting with the chloride group being subnstiuted by a hydroxyl. Comparison of samples by TLC before and

after deactivation shows that the majority of the dye is converted into the hydroxyl form over the 2 hour time course (**Figure 3.6**).

A sample incubated overnight under the same conditions changed to a more purple colour than the blue normally seen. Analysis of the sample by TLC showed the production of a large number of other coloured species (results not shown), presumably breakdown products of the dye due to the extended hydrolysis period. This shows that the hydrolysis must not be allowed to run for too long; otherwise additional impurities would be introduced.

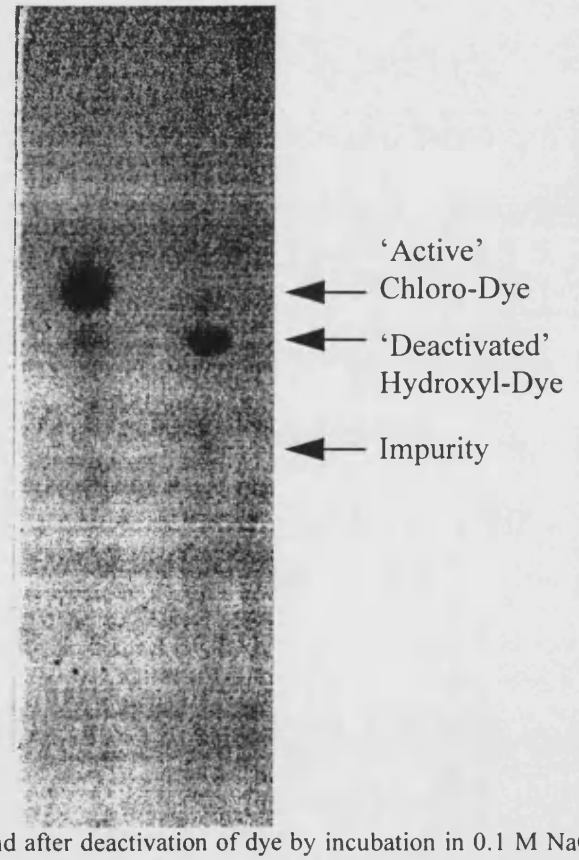

Figure 3.6 : TLC before and after deactivation of dye by incubation in 0.1 M NaOH for 2 hours at 60 C. This shows the conversion of the higher running major component of the stock (presumed to be 'active' chloro-dye) to one running with a slightly lower r.f. (presumed to be the 'deactivated' hydroxyl-dye). The r.f. of the major impurity present seems unchanged indicating it is probably not a chloro-triazine containing compound which would be expected to have reacted to form a new product under these conditions.

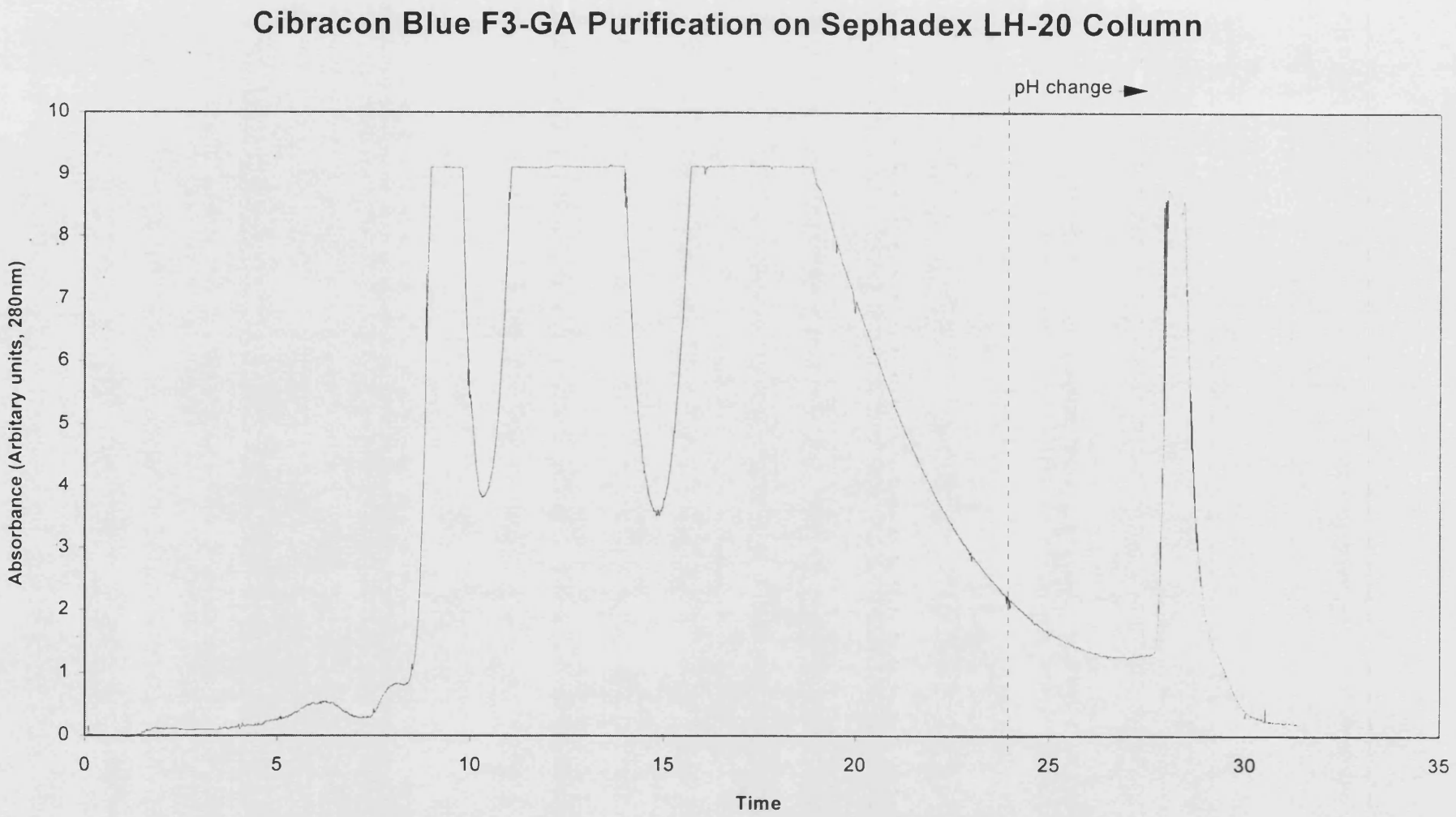

Figure 3.4 : Elution profile of Sephadex LH-20 column (0.6 x 100 cm) run with alkaline 1:1 MeOH / H_20. The column was loaded with approximately 10 mgs of dye dissolved in 0.5 ml. The column was eluted at 0.5 ml / min and fractions collected every 10 minutes.

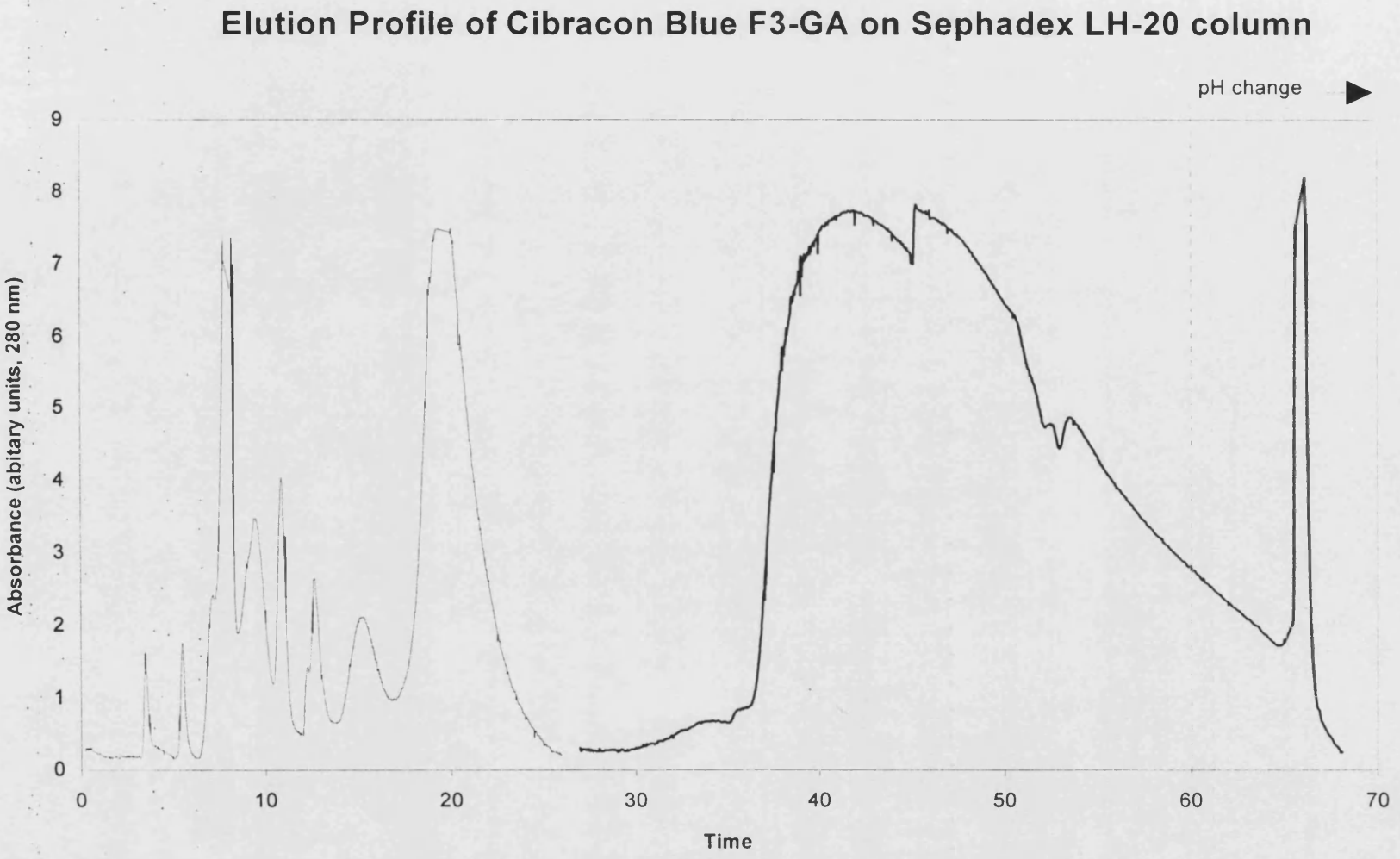

Figure 3.5 : Elution profile of dye separated on preparative (2.5 x 60 cm) Sephadex LH-20 column. 100 mgs of dye was applied in 10 mls 1:1 methanol / water and eluted with alkaline 1:1 MeOH / H_20 at 3 ml / min. The major elution peak of deactivated dye was pooled.

3.3 Dye - Glucose Preparation

Diacetone glucose has four out of the free hydroxyls protected by two acetoyl groups. This leaves only the 4' hydroxyl free to react. The bonds linking the protective acetone groups are stable under the alkaline conditions used for the linking reaction to the triazine ring of the dye. The protective groups can then be removed by hydrolysing them under mild conditions in which the dye-glucose formed is stable, producing a pure product of Cibracon Blue - 4' substituted glucose.

Figure 3.7a shows a TLC of the reaction mix following overnight reaction at 45 C. This shows the appearance of a coloured compound running with a higher r.f. than any of the reactants. This is presumed to be the 4' linked Cibracon Blue diacetone glucose expected to be formed by the reaction. However upon acid hydrolysis of the unpurified reaction mixture this compound disappears, but no new product appears. This can be explained by the product of the reaction, the more hydrophilic 4' linked Cibracon Blue glucose, having the same or similar r.f. to one of the starting compounds. The column chromatography step used for the purification of the dye compounds relies on the same sort of physical properties as the TLC. It was therefore unlikely that the hydrolysed dye-glucose could be purified from the reaction mixture after hydrolysis in the crude reaction mixture. Therefore the protected 4' diacetone glucose-dye was purified using column chromatography under similar conditions to those used for the purification of deactivated dye. The elution profile from the column is shown in **Figure 3.8** and a TLC showing fractions pooled across the peak of product in **Figure 3.9**. The purified protected diacetone-glucose was then subsequently acid hydrolysed to produce the product of dye-glucose. This was then further column purified (**Figure 3.11**) to yield the final product of pure dye-glucose. **Figure 3.10** shows a TLC of the purified diacetone glucose before hydrolysis and fractions taken from the purification after hydrolysis. This shows the appearance of a new product with a lower r.f. . As expected this runs at approximately the same, but slightly higher r.f. than the 'deactivated' hydroxyl form of Cibracon Blue F3-GA.

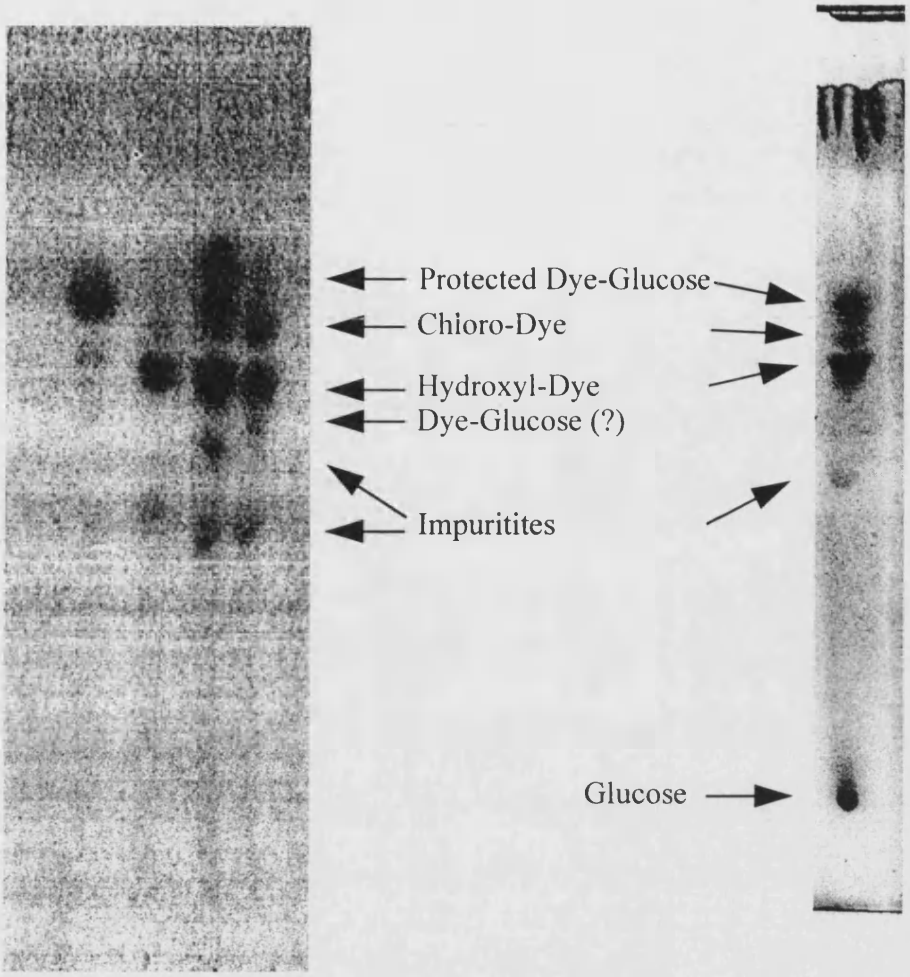

Figures 3.7a, 3.7b : 3.7a, TLC of (left to right) chloro-dye and hydroxyl-dye (references),protected dye-glucose mixture after reaction and after subsequent acid hydrolysis to produce deprotected dye-glucose. The deprotection reaction shows that the product of dye-glucose runs with a similar r.f. to previous components. **3.7b**, This TLC of the reaction mixture has been iodine stained revealing the unreacted glucose at the origin which does not migrate in the solvent mixture used. No additional products are visualised.

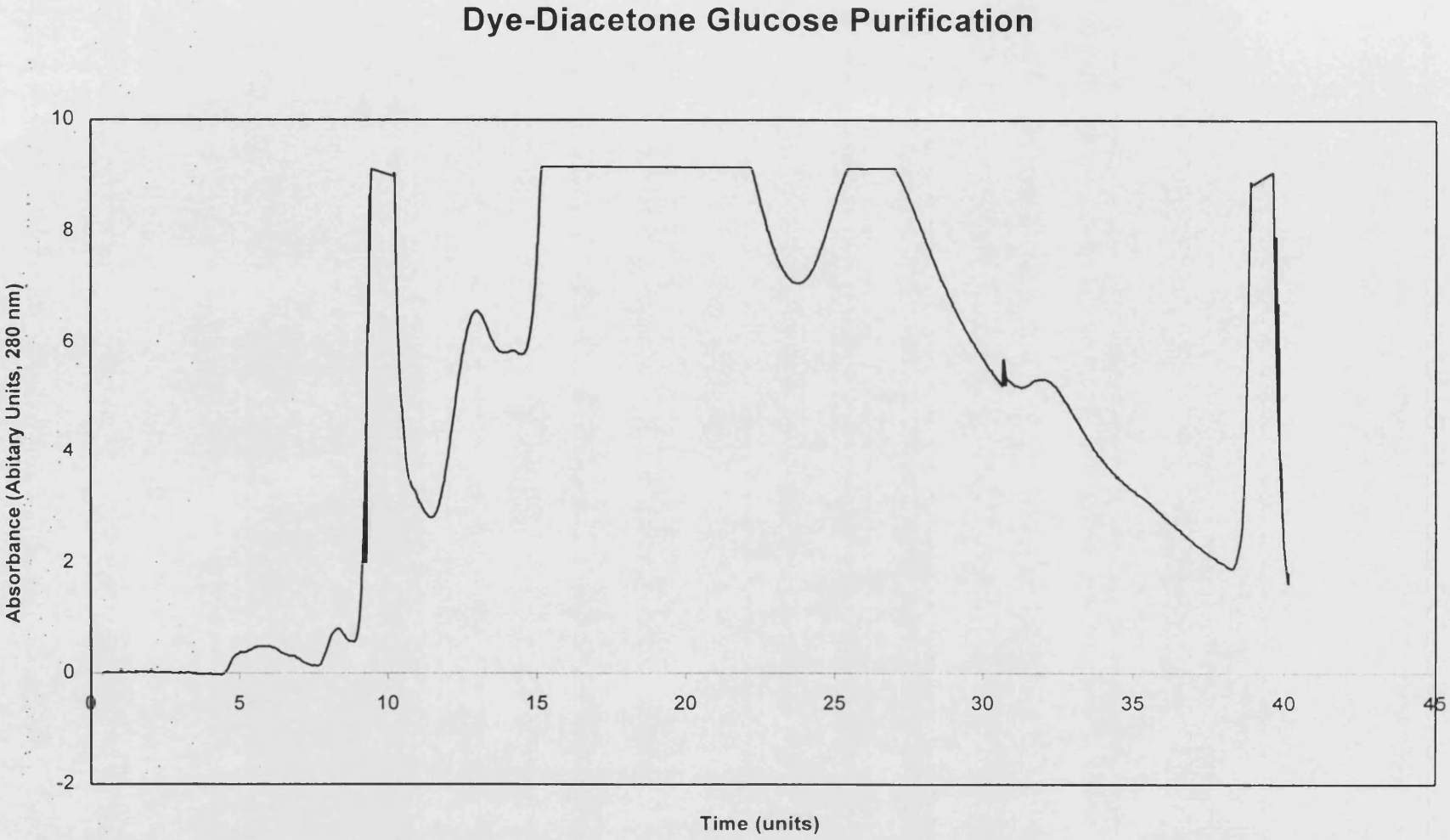

Figure 3.8 : Chromatogram of reaction mixture separated on a 2.5 x 60 cm Sephadex LH-20 column to yield pure diacetone glucose. The column was loaded with approximately 100 mgs of the reaction mixture in 10 mls MeOH / H_20 and eluted with alkaline MeOH / H_20 at 3 ml / min.

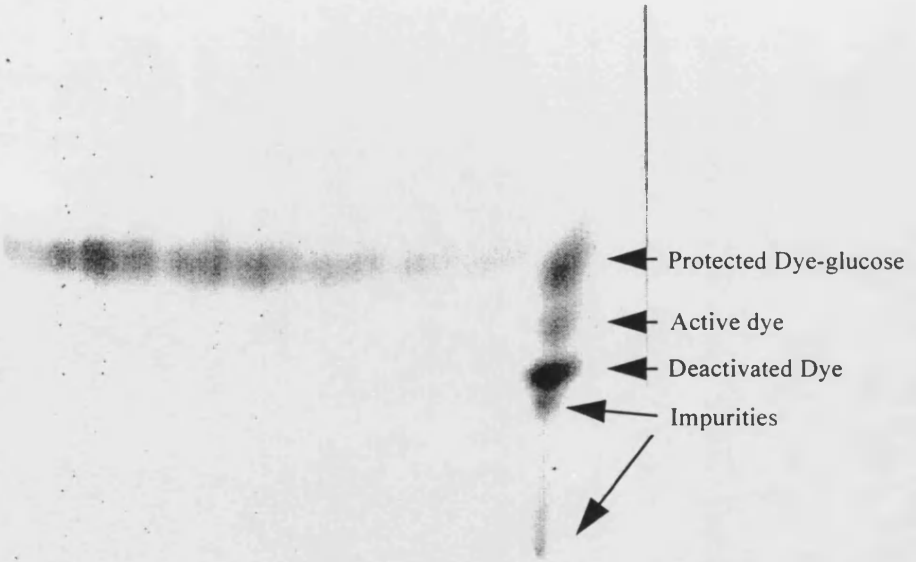

Figure 3.9 : TLC of reaction mixture before overnight incubation at 45 C and the purified protected diacetone glucose.

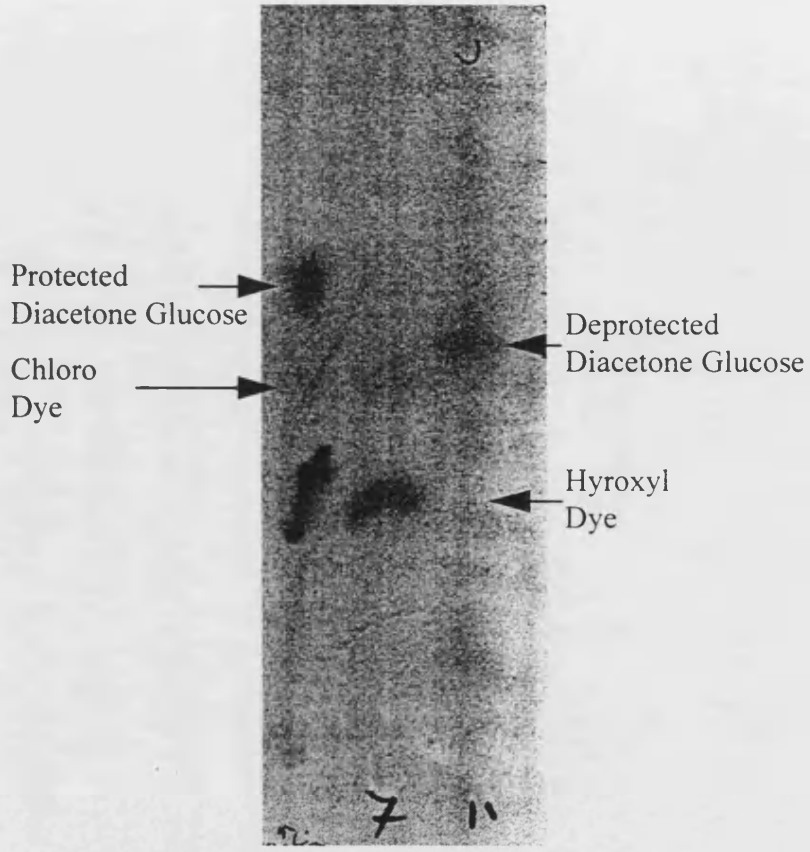

Figure 3.10 : TLC of purified diacetone glucose before and fractions taken after deprotection and purification on a Sephadex LH-20 column.

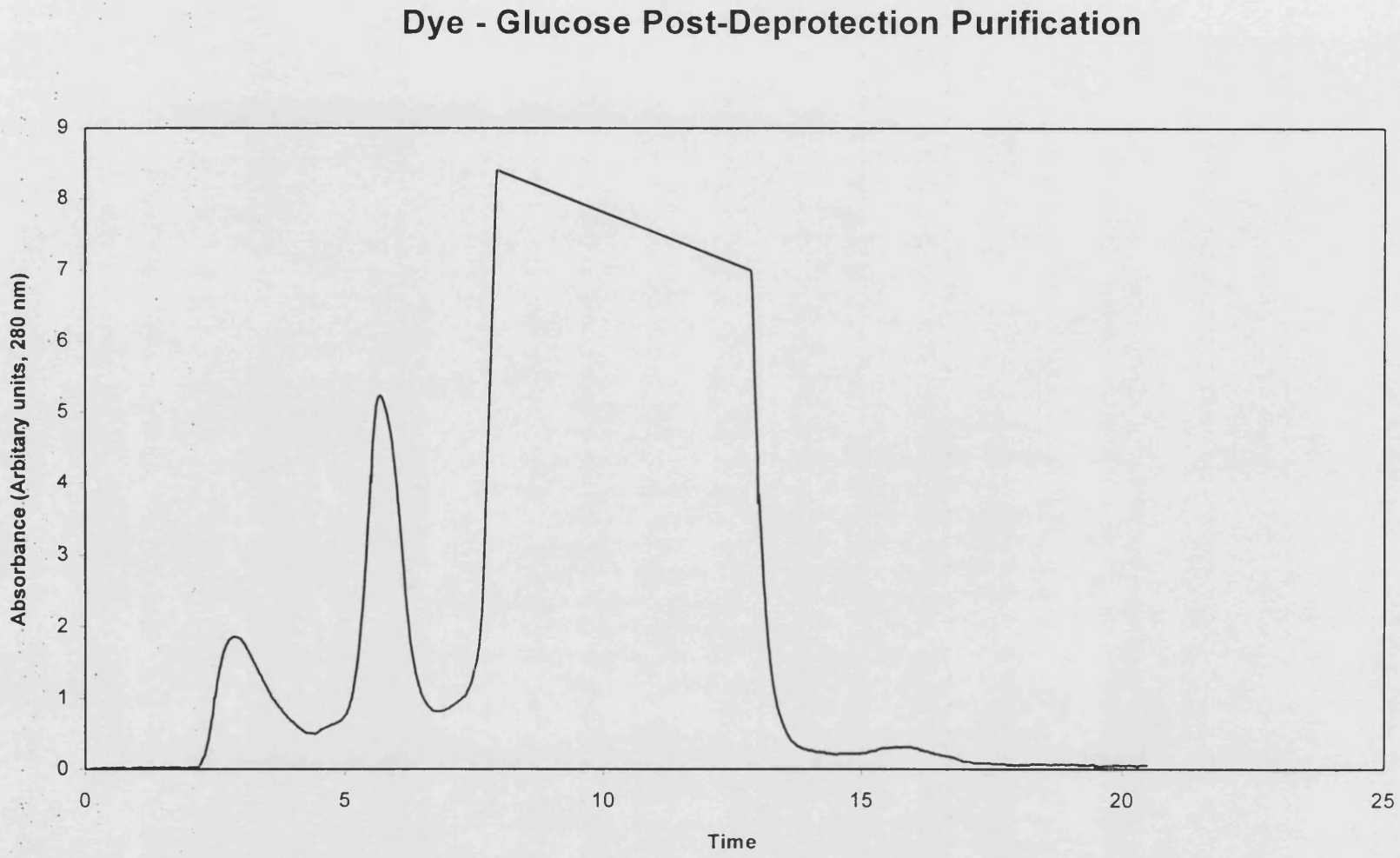

Figure 3.11: Purification of deprotected diacetone glucose on 0.6 x 100 cm Sephadex LH-20 column eluted with alkaline 1:1 MeOH / H_20 at 0.5 ml / min. 5 mls fractions were taken across the peak and analysed by TLC.

3.4 Cibacron Blue F3-GA Deviation from Beer's Law

The deviation of the absorbance of dye in solution from Beer's Law is shown in **Figure 3.12a**. The predicted absorbance line shows the expected relationship between absorbance and concentration for the dye if it conformed to Beer's Law; i.e. if measured absorbance is directly proportional to concentration. It can be seen from the meaured absorbance (corrected for dilution effects) that the dye shows a negative deviation from Beer's Law, with the measured absorbance being less than expected as the concentration of dye was increased.

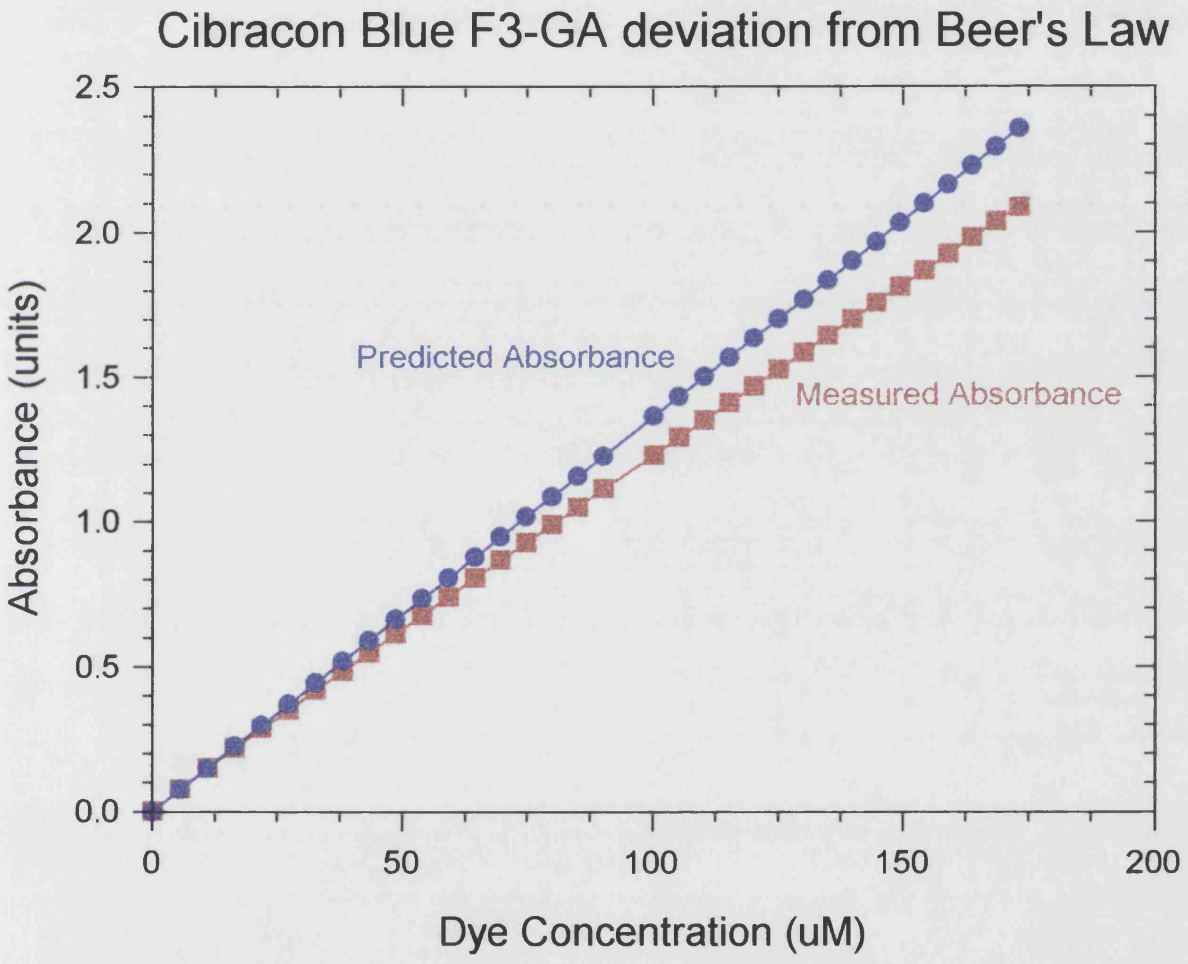

Figure 3.12a : This shows the deviation of the measured absorbance at 610 nm for a solution of increasing dye concentration from that which would be expected if the dye conformed to Beer's Law. The line through the measured points is a fit to a simple stacking model as described in the text yielding an extinction coefficient for stacked dye of 11,088 $M^{-1}cm^{-1}$ and the equilibrium constant as 8.7×10^{-5} M.

Presuming a simple model of dye stacking, in which free dye is in equilibrium with a stacked dye complex consisting of two interacting dye molecules, the absorbance of a dye containing solution can be modelled as explained in section **4.4** of the discussion. This provides an extinction coefficient for the stacked dye and an equilibrium constant for the interaction. The extinction coefficient determined for the stacked dye represents that of the complex consisting of a pair of interacting dye molecules. Thus the extinction coefficient of a single dye molecule under stacked conditions will be half this, a value of 11,070 $M^{-1}cm^{-1}$. The equilibrium constant was for the stacking interaction was determined as 5.9×10^{-6} M.

The data and fit are reploted in **Figure 3.12b** as the amplitude of the deviation from Beer's Law against dye concentration.

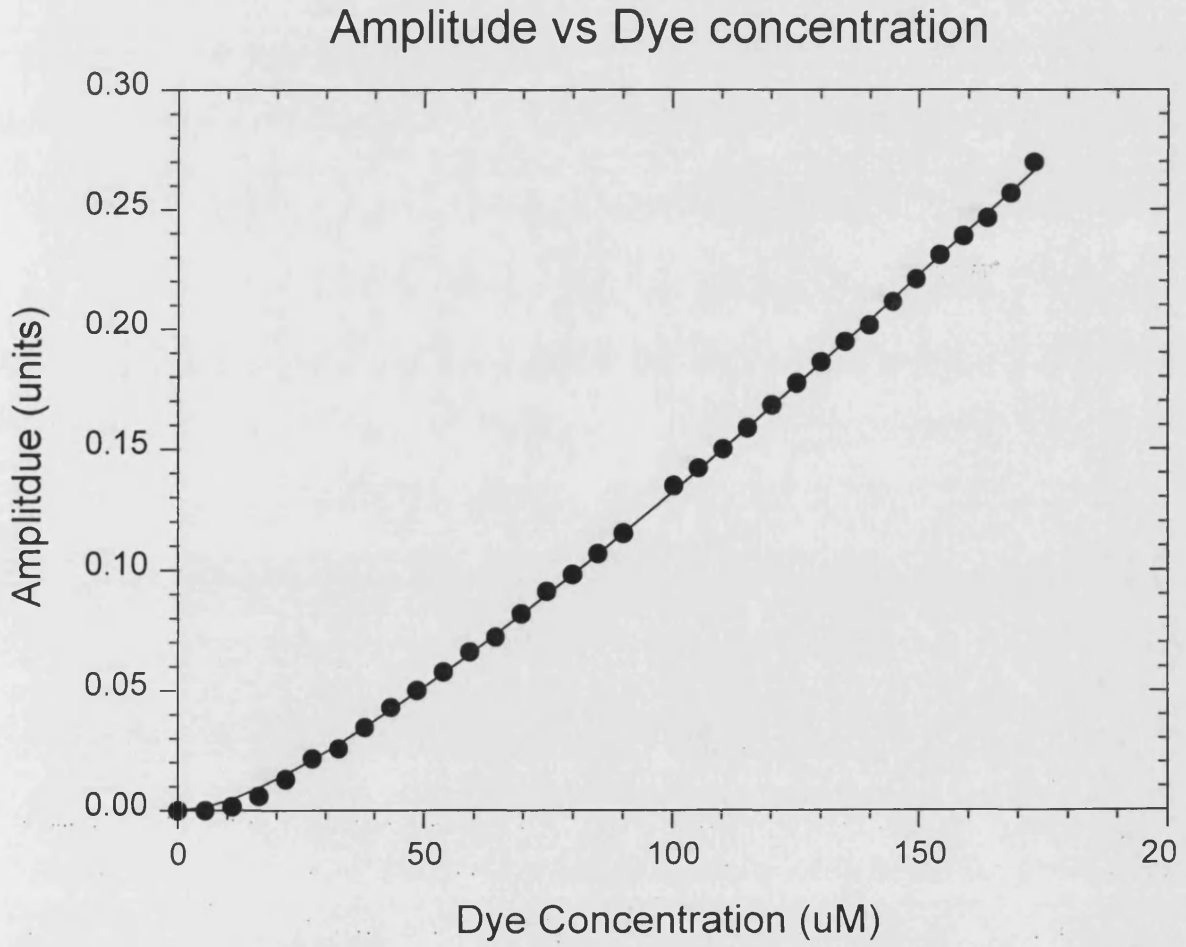

Figure 3.12b : This shows the difference of the measured absorbance (610 nm) from the predicted absorbance along with the curve fit generated using the simple stacking model.

3.5 Purification of Saccharopine Dehydrogenase from Baker's Yeast (*Saccharomyces Cerravisiae*)

The initial trial of 300 g yeast powder was autolysed and the cell-free extract prepared from it. This was split into different portions to test both the original purification procedure and a single step affinity purification using Cibracon Blue Sepharose CL-4B.

The autolysate was analysed for saccharopine dehydrogenase activity using both the full assay mixture containing NADH, α-ketoglutarate and L-lysine and one without any α-ketoglutarate or L-lysine. This allowed correction in the initial assay for NADH hydrolysis due to activity of other NADH utilising enzymes in the raw mixture. Comparison of the rates from the two reactions in **Figure 3.13** shows that there is a small, fast initial burst of NADH usage before the rate steadies for a short period before then declining due to substrate depletion. The initial burst can be ascribed to the presence of small quantities of substrates for other NADH utilising enzymes in the raw extract. These are quickly depleted in the initial burst then giving a short 'steady state'. The difference in rates of between the two reactions should be due to saccharopine dehydrogenase activity. The presence of a quite a large 'steady state' rate in the NADH only containing mixture is due to other NADH oxidase activity within the assay and shows that any rates and hence initial specific enzymic activity determinations from such complex mixtures must be viewed with some caution.

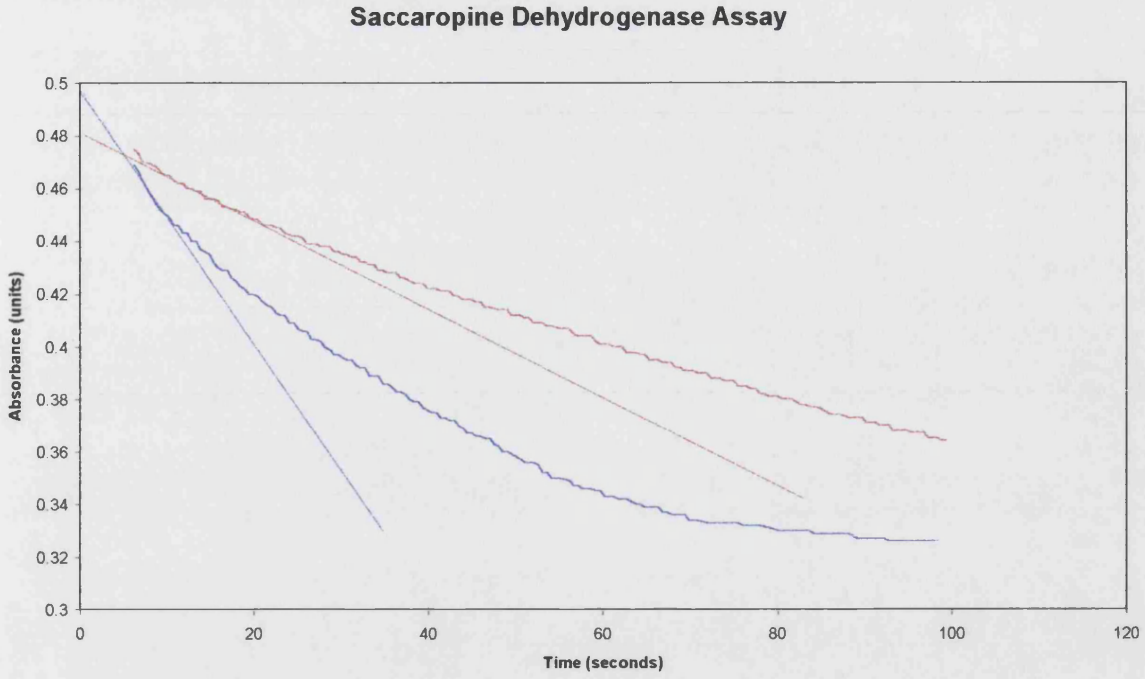

Figure 3.13 : This shows an overlay of measured rates for NADH usage followed at 340 nm in the assay mixture with and without the addition of α-ketoglutarate and L-lysine

The initial trial affinity purification elution profile is shown in **Figure 3.14**. This shows that only a small proportion of activity appears to have been retained on the column and was eluted by the 1 M KCl wash. This material is also at a lower specific activity than the flow through. This shows that proportionally less of the enzyme is present in the bound material than in that applied to the column, making this a negative step in purification. The measured rates are however not corrected for any background activity, which had been previously been shown to be up to 50 percent of the total measured rate.

To try and improve the purity and specificty of the elution from the column a gradient elution using a 0 - 1 M KCl gradient was used to attempt to determine a suitable salt concentration range for specific elution of saccharopine dehydrogenase activity. The elution profile using this gradient is shown in **Figure 3.15.** The results of this show only a single elution peak with a

a long tail with the activity eluting in proportion to the protein concentration. The activity is also low and the specific activity no better than that for the single step elution.

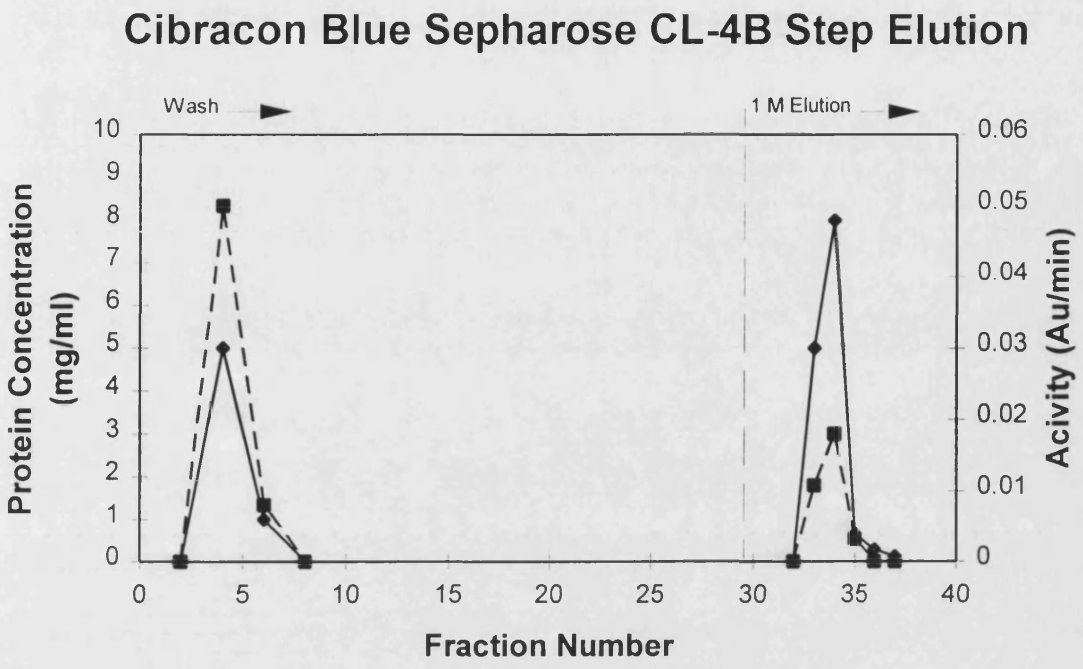

Figure 3.14 : Cibracon Blue Sepharose CL-4B column loaded with 9 mls of 8.5 mg/ml, 0.3 Ad_{340nm}/min activity yeast lysate, washed with loading buffer and eluted with 1M KCl. Protein concentration was determined by BioRad assay and enzymic activity as detailed in the methods section. 2.8 ml fractions were collected at a flow rate of 17 ml / hour. Protein concentration is shown by the solid lines with diamond markers, activity by the dashed line with square markers.

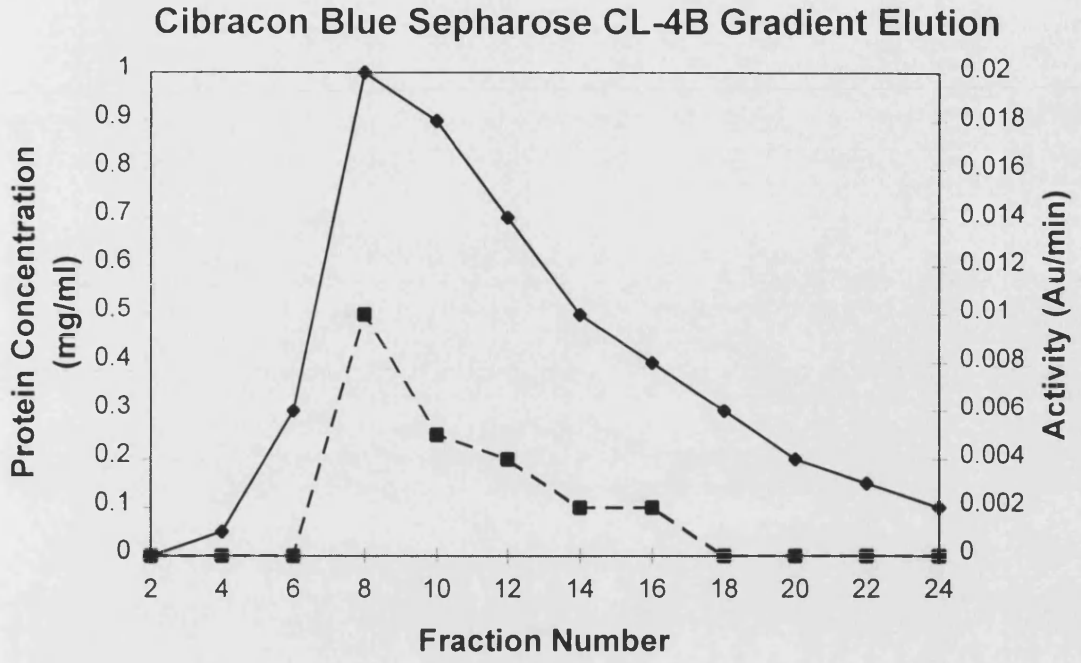

Figure 3.15 : Fraction analysis of the elution of a Cibracon Blue Sepharose CL-4B column loaded with 10 mls of yeast lysate (10 mg protein, 4.1 Ad_{340nm}/min activity per ml) and eluted with a 0 - 1 M KCl gradient. The column was eluted at a flow rate of 17 ml/hour and 2.8 ml fractions collected and analysed for protein concentration and activity as for the previous figure. Protein concentration is shown by the solid lines with diamond markers, activity by the dashed line with square markers.

Overall these two experiments show that an affinity step is unsuitable at this stage in the purification. This is probably due the large number of other proteins still present which bind to the column. These may both compete with saccharopine dehydrogenase binding, reducing the yield, and also co-elute with it reducing the purity.

The next step in the original protocol after the ammonium sulphate cut was an ion-exchange step using a CM-Sephadex column. **Figure 3.16** shows the loading and elution profile of the CM-Sephadex column loaded and eluted with a 0.1 - 1 M NaCl gradient. Fractions taken from the eluted peak of material were then run on a 12 percent SDS-PAGE gel as shown in **Figure 3.17** The gel shows the presence of a band running at approximately 40 kDa. which is what would be expected for Saccharopine Dehydrogenase. However there are still numerous other contaminating components present.

The next step in the purification would have been fractionation of pooled fractions from the CM-Sephadex column on a gel filtration (Sephadex G-100 column as described in the methods section). However a trial spectral titration using purified saccharopine dehydrogenase obtained from Sigma showed no apparent spectral change upon addition to Cibracon Blue F3-GA. This meant that saccharopine dehydrogenase was not suitable for use as a model enzyme and therefore the purification was discontinued.

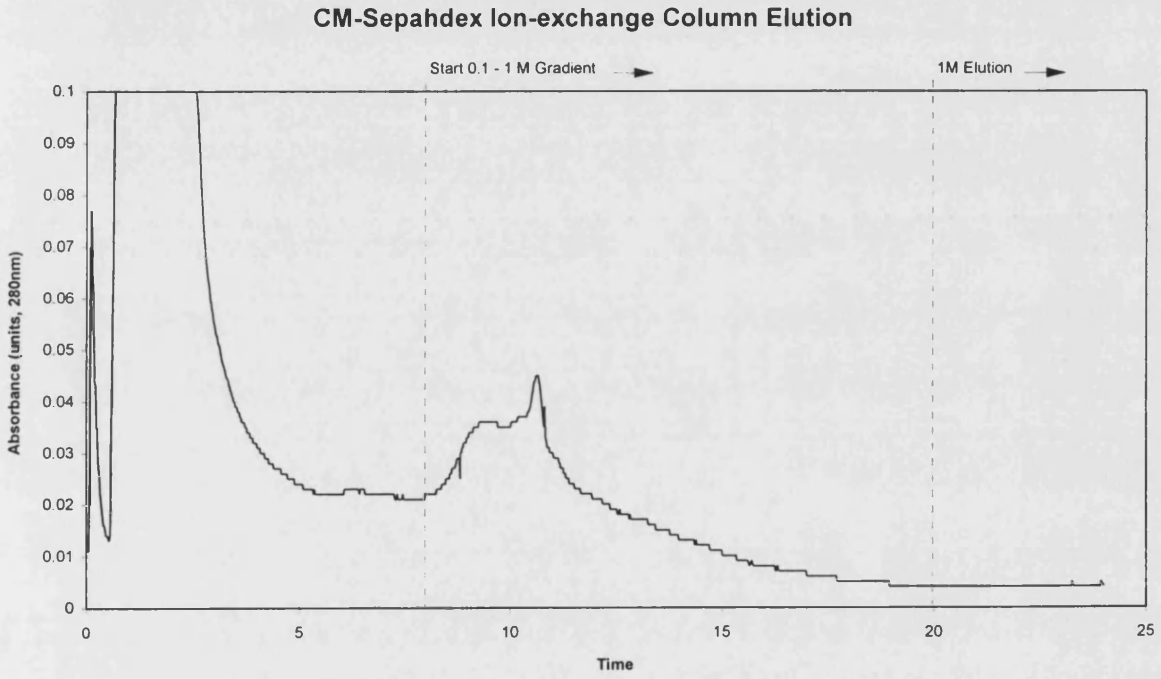

Figure 3.16: Loading and elution of dialysed 30-65 percent ammonium sulphate cut on CM-Sephadex column followed by elution with a 0.1 - 1 M NaCl gradient. Fractions were collected every 2 ml along the gradient.

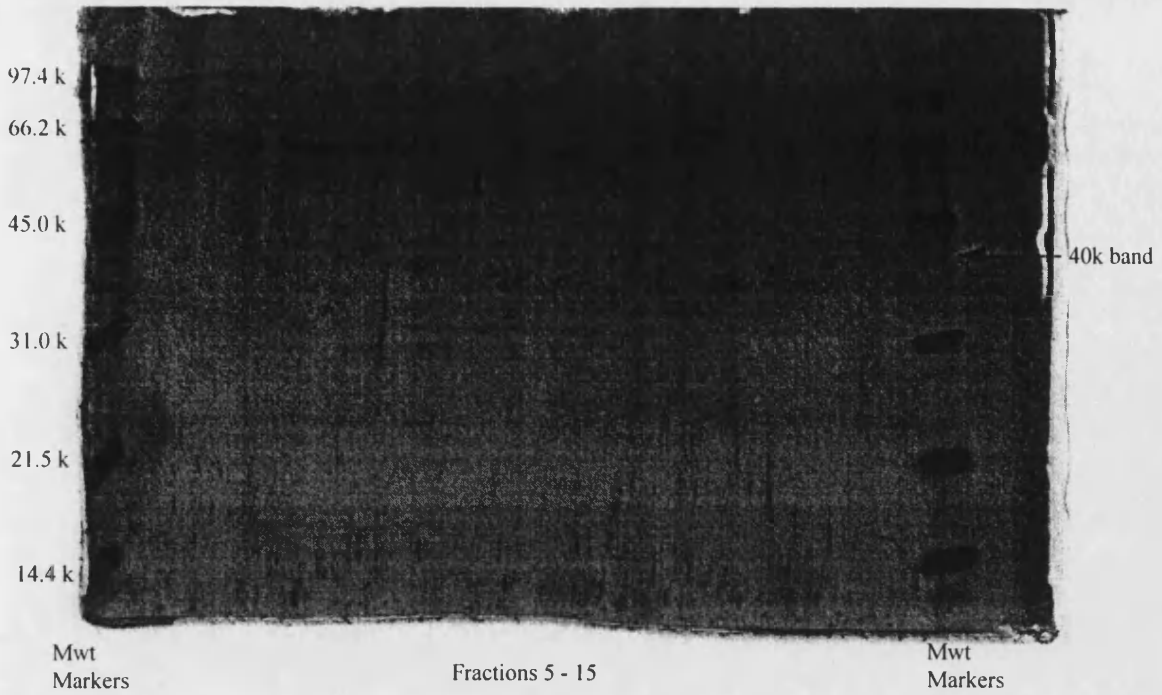

Figure 3.17: Gel of fractions 5 - 15 taken across the elution peak from the CM - Sephadex ion exchange column. 10 ul samples from each fraction were taken and heated to 95 C with 10 ul sample loading buffer before application to the gel. The gel was then conventionally stained with Coomassie Blue R-250

3.6 Purification of Scallop Octopine Dehydrogenase

The activity of the initial lysate was measured both with the full reaction mixture and in the absence of L-arginine to measure any background activity present. For the initial lysate specific activity was assayed as 6.8 units/ml with the complete assay mixture and background activity as 0.18 units/ml. As the background activity was only 2.5 percent of the total assayed activity it was considered unnecessary to correct for this. Subsequently all samples were measured without any correction for background activity, which would be expected to decline further throughout the purification.

The lysate was then fractionated by the addition of ammonium sulphate and dialysed into Column Buffer A (20 mM Tris pH 7.4, 1 mM EDTA, 0.1 mM DTT) as detailed in the methods section. The dialysate was centrifuged to remove the precipitated protein yielding 115 mls of supernatant.

	Specific Activity (units / ml)	Volume (ml)	Total Activity (units)
Initial Lysate	6.8	1500	10,200
Ammonium sulphate cut	>50	115	>5,750

The supernatant was then split into two portions; 67 mls were used for an ion exchange trial using a DEAE Sephacel anion exchange column whilst the remaining 48 mls were used for a trial affinity chromatography step using a Cibracon Blue F3-GA column.

Figure 3.18 shows the flow through and initial wash with 50 mM NaCl from the DEAE Sephacel column. The eluent was pooled and kept for subsequent analysis. The column was then washed with an 107 mM NaCl step to remove additional low affinity bound proteins. Octopine Dehydrogenase was then eluted from the column using a 175 mM NaCl elution step **(Figure 3.19)**. Fractions were taken and analysed for activity to check if the activity eluted as

a distinct peak or if it was evenly distributed within all the other proteins in the elution peak as monitored by the 280 nm absorbance of the eluent.

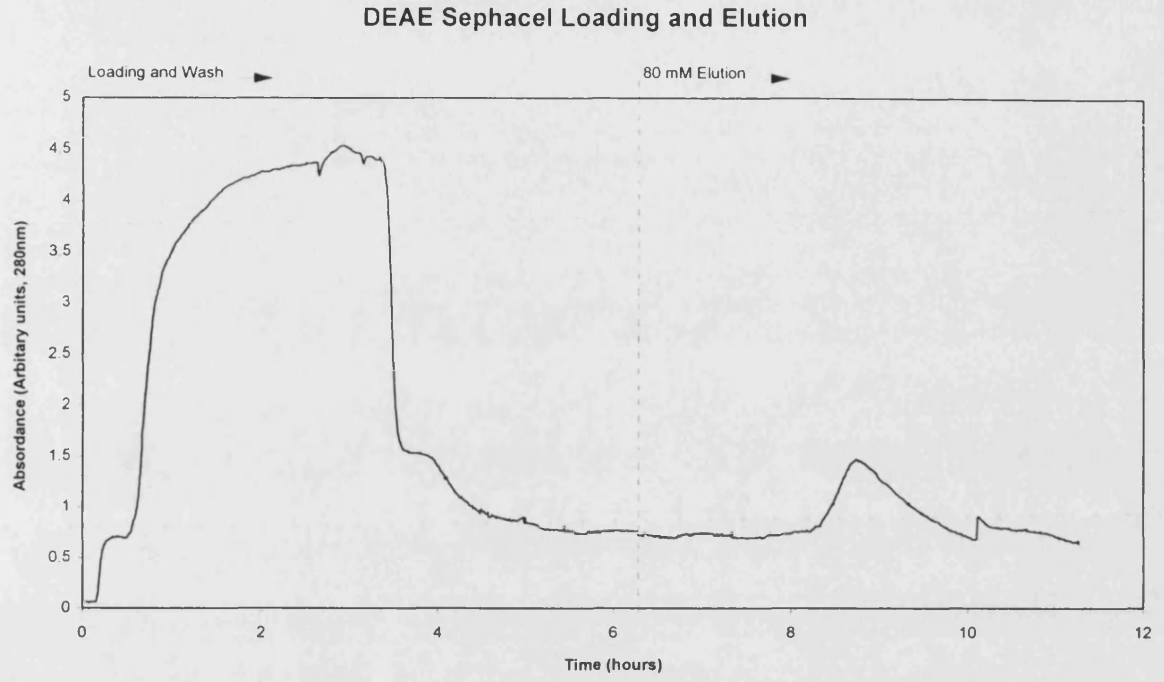

Figure 3.18: This shows the loading and washing of a 1.6 x 20 cm DEAE Sephacel column loaded with 67 mls (3,350 units activity) of dialysed ammonium sulphate cut. The column was loaded and washed at a flow rate of 25.8 ml/hour. The sample was made up to a salt concentration of 50 mM by addition of solid NaCl before loading and washed with buffer containing 50 mM NaCl

Comparison of the flow through and elution peaks shows that the majority of protein loaded onto the column does not bind to it. Assay of enzymic activity of the flow through from the column show that despite the large quantity of non-binding material no activity was present, indicating that all the Octopine Dehydrogenase bound to the column. Comparison of the activity of the fractions eluted from the column and their UV absorbance shows that there is no separate peak of activity within the elution peak; therefore all fractions from 8 - 28 were pooled.

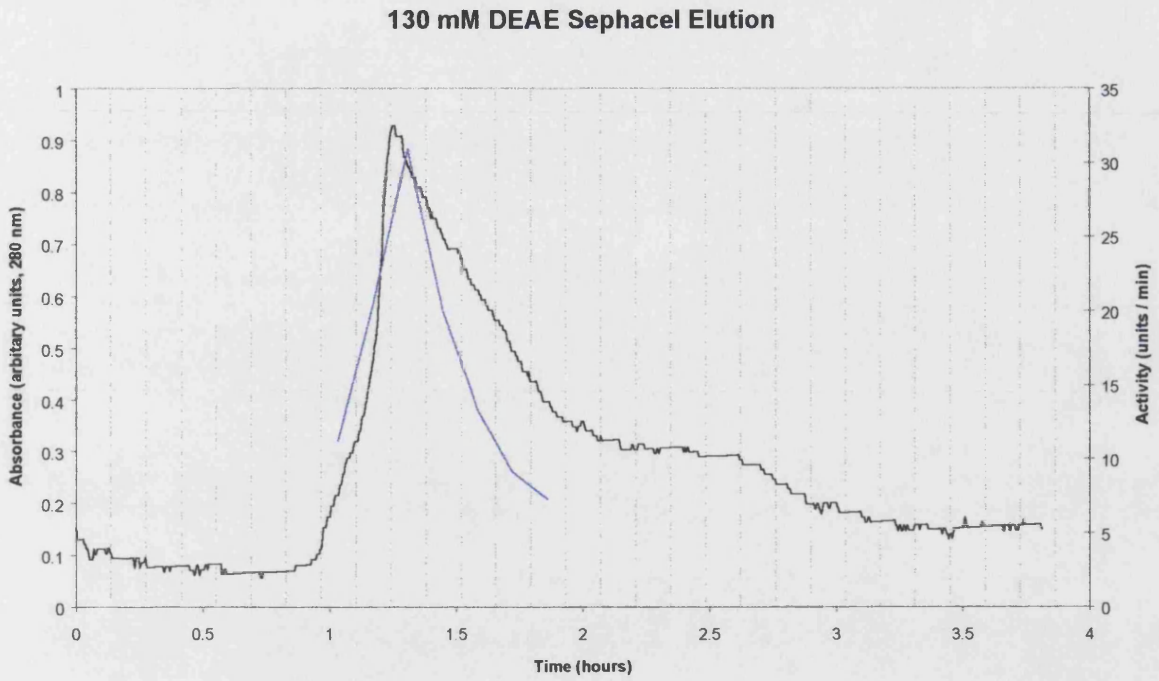

Figure 3.19: This is the elution profile of the DEAE Sephacel column loaded and eluted with a 175 mM NaCl step after previously washing with a 107 mM NaCl step to remove additional low affinity bound proteins. Flow rate was 25.8 ml/hour as before and 4.2 ml (10 min) fractions collected (shown by dotted lines). Fractions 8 - 14 were assayed for enzymic activity as shown.

Figure 3.20 shows the loading and elution profile for the trial affinity purification using a Sepharose CL-4B affinity column. The elution profile using a 0 - 1 M NaCl gradient shows only a single peak with a long tail, not the multiple peaks that might be expected if specific proteins with different affinities were being eluted. Activity assays of the flow through and the peak from the gradient elution show that most of the activity does not bind to the column and is present in the flow through. There is very little activity present in the eluted peak from the column. This shows that an affinity step is not appropriate at this stage in the purification. There are two possible explanations for this: either the Octopine Dehydrogenase does not bind to the column, or its binding is masked by other proteins binding with a higher affinity.

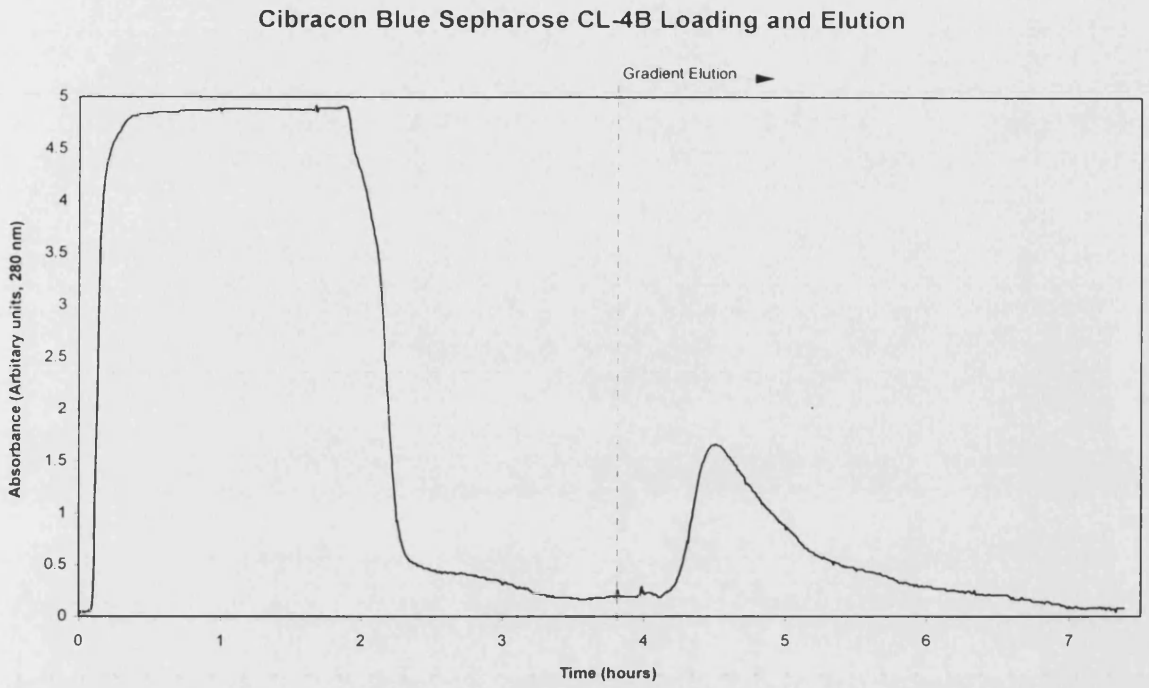

Figure 3.20 : This shows the loading and elution profile of the Cibracon Blue Sepharose CL-4B column. 48 mls (2,400 units activity) of dialysed ammonium sulphate cut was applied and then washed with 20 mM Tris pH 7.4, 1 mM EDTA, 0.1 DTT. The column was then eluted with a 0 - 1 M NaCl gradient and 4.2 ml (10 min) fractions were collected for analysis.

The pooled fractions from the DEAE Sephacel ion exchange step were then applied to a Cibracon Blue Sepharose 4B column to determine if loading a smaller quantity of less impure protein would yield better results. The column was loaded, washed and eluted in a similar manner to that used previously with 4.2 ml (10 min) fractions being collected from the gradient elution and analysed for activity. **Figure 3.21** shows the gradient elution from the column along with the activity analysis of the fractions. It can be seen that although in this case there does appear to be a peak of activity eluted from the column, the overall quantity of protein bound and more importantly the enzymic activity bound is low. From this it appears that the Cibracon Blue Sepharose 4B affinity column is still ineffective as a purification step.

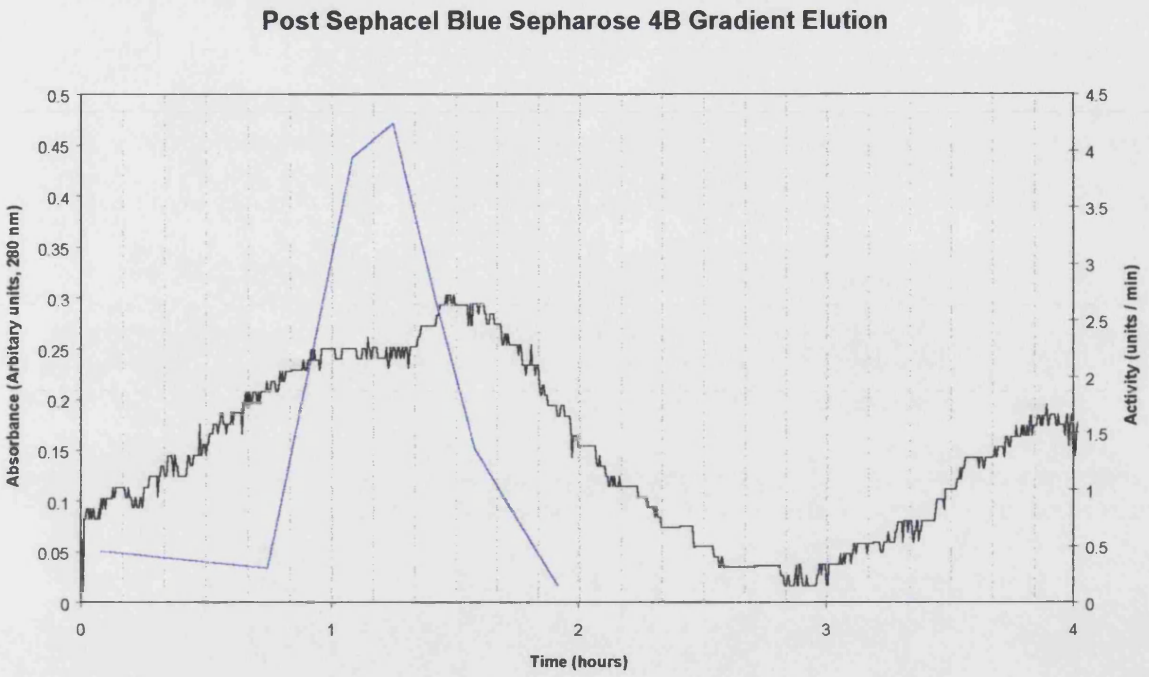

Figure 3.21 : This figure shows the UV absorbance of the 0 - 1 M NaCl elution of the Cibracon Blue Sepharose 4B column after loading with 77 mls (pooled fractions 5-21) from the Sephacel ion exchange step. Elution was at a flow rate of 25.8 ml/hour and 4.2 ml (10 min) fractions were collected. Fractions are marked by the dotted lines.

As the use of an affinity chromatography step in the initial stages of the purification had been unsucessfull in purifying the enzyme, the purification to the ammonium sulphate cut step was repeated on a large scale.

A total of 4 batches of approximately 1.2 kg of Scallop tissue to a total weight of 4.86 kg starting material were processed. After homogenisation and extraction of soluble material this yielded over 100 g of 30 - 65 % ammonium sulphate precipitate which was stored at 4 C and used as a stock for subsequent purifications.

Two trial loadings of 5g (wet weight) ammonium sulphate precipitate onto a cellulose DE-52 column showed that it bound and eluted Saccharopine dehydrogenase in a similar manner to the DEAE-Sephacel column originally used, but without the physical problems with variations in the bed volume encountered with the DEAE-Sephacel.

Having sucessfully used the DE-52 cellulose media as a replacement for the DEADE-Sephacel ion-exchange media on a small scale, it was upscaled using a large 2.5 x 60 cm column. For

this 50g (wet weight) of ammonium sulphate precipitate was taken and dialysed against 3 x 600 mls of buffer containing 50 mM NaCl. The dialysate was clarified by ultracentrifugation at 100,000 g to remove precipitated and high molecular weight muscular proteins. The supernatant (105 mls) was loaded onto the column and washed with the same buffer before stepwise elutions using buffer solutions containing 80 mM, 130 mM and 1M NaCl as shown in **Figure 3.22.**

Material from the 130 mM step was pooled (153 mls) and precipitated using ammonium sulphate (516 g/l) to concentrate it. The ammonium sulphate precipitate was then redissolved into running buffer for further purification by gel filtration.

The initial trial of gel filtration used a 1.6 x 60 cm column packed with Sephadex G-100. This was pre-equilibrated with the column running buffer at a flow rate of 25 ml / hour before loading of the pooled protein redissolved into 1 ml of the same buffer. The material loaded was pooled from the 130 mM wash step from the second trial DE 52 ion exchange step.

The activity eluted in between the excluded volume and the void volume, after the major peak of absorbing material which eluted at the excluded volume of the column. This showed that most of the contaminants consisted of higher molecular weight proteins than the Saccharopine Dehydrogenase which should be a monomer of around 40 kDa. The active fractions were pooled and precipitated by the addition of 500 g/l Ammonium Sulphate.

This procedure was then scaled up to a 1.6 x 100 cm Sephadex G - 100 column with a flow rate of 36 ml / hr. With the larger column up to 2 ml samples were loaded. A typical elution profile for the larger column loaded with 2 mls of material pooled from the large ion exchange run is shown in **Figure 2.23**.

The material from the large ion-exchange purification was redissolved into approximately 14 ml of buffer and purified in 6 runs on the gel filtration column. Fractions were collected and assayed for all of the runs with active fractions being pooled and the protein precipitated by the addition of 500 g/l ammonium sulphate.

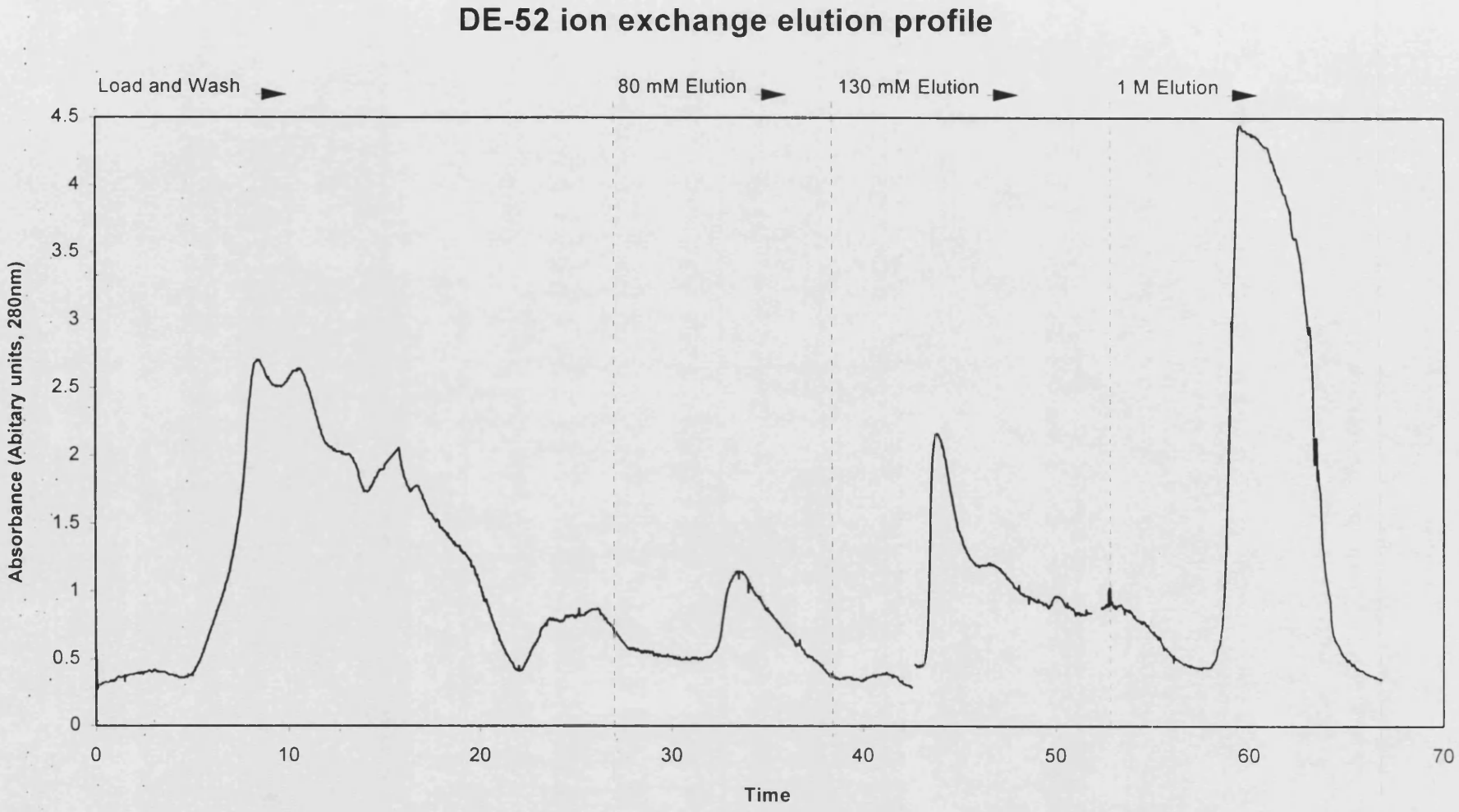

Figure 3.22 : Loading and elution of dialysed and centrifuged ammonium sulphate cut (50g wet weight) on DE-52 ion-exchange column. The sample was loaded and washed in 50 mM NaCl buffer at 50 ml/hr then eluted stepwise with 80 mM, 130 mM and 1 M NaCl. Peaks from each step were pooled for analysis.

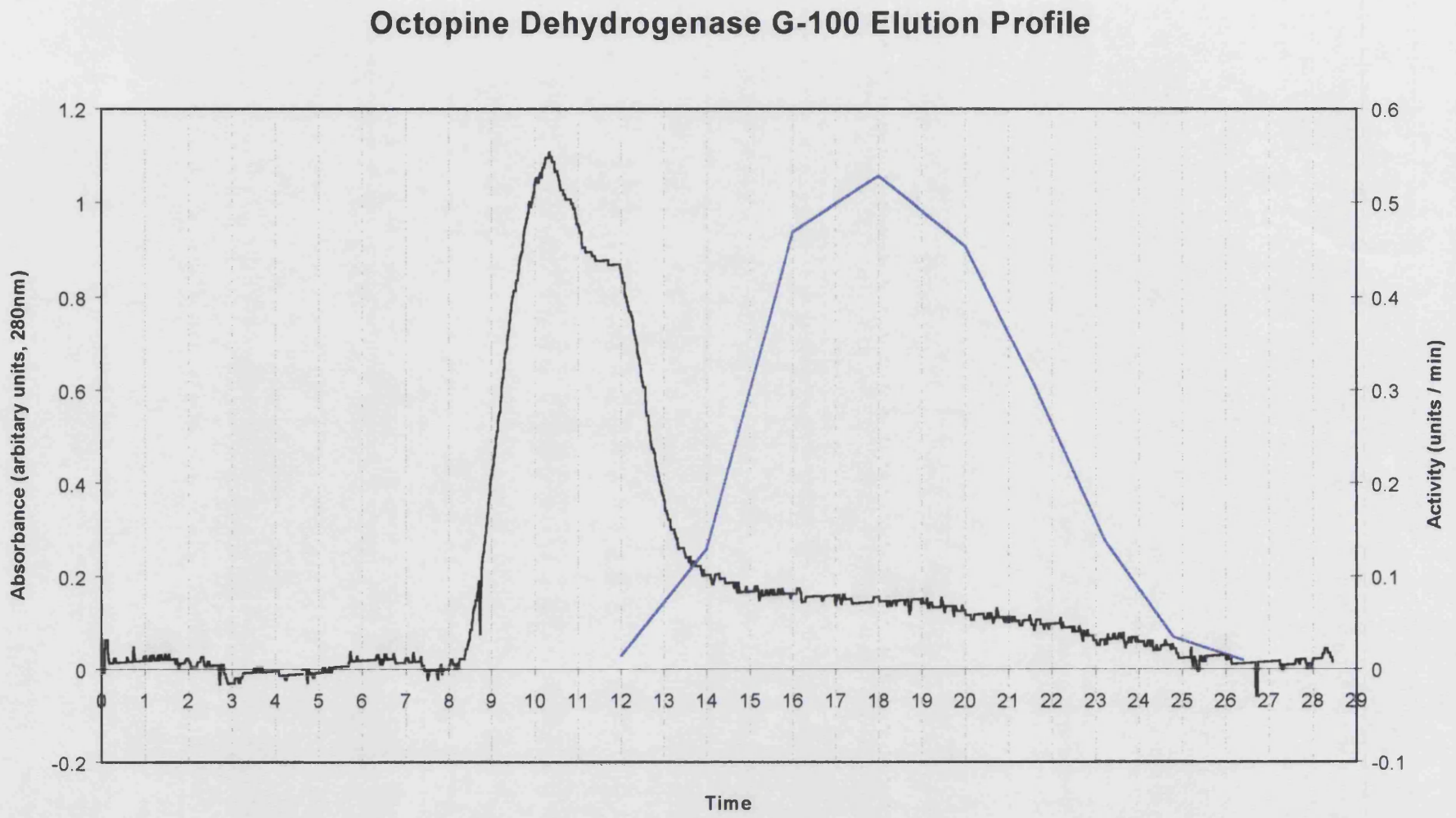

Figure 3.23 : Elution profile of 2 mls of resuspended sample from 130 mM DE-52 elution loaded on 1.6 x 100 cm G-100 column eluted at 36 ml / hour with 4.6 ml fractions collected. The enzymic activity of fractions was assayed and is shown in blue

The protein pooled from the activity peak from the trial gel filtration step and that pooled from the activity peaks from the subsequent preparative runs was stored as an ammonium sulphate precipitate. The preparative runs yielded a total of approximately 20 mgs protein which was suspended in 10 mls of 3.2 M ammonium sulphate solution.

Samples from both the initial trial run and the subsequent preparative purification were run on a 10 - 27 percent SDS-PAGE gradient gel to assess the purity. The gel was fixed in a trichloroacetic acid / sulphosalicylic solution before staining using a colloidal Coomassie Blue B-250 stain and is shown in **Figure 3.24.**

Figure 3.24 : SDS -PAGE gel of pooled sample from the first G-100 purification and from the pooled activity peaks from 6 G-100 column runs. The gel is a pre-cast 10-27 percent gradient gel (Sigma) stained with a colloidal Coomassie Blue B-250 stain. Densitometry of the gel shows the Octopine dehydrogenase in the pooled G-100 sample to be approximately 25 percent pure.

The stained gel was analysed by scanning with a Hewlett Packard ScanJet IIIc connected to a PC and densitometry performed using Quantiscan (Biosoft) gel densitometry software. This showed the Octopine Dehydrogenase to be around 25 percent pure after the gel filtration step. The purity of the pooled material from the gel filtration step was still far lower than that required for the enzyme to be used for binding measurements. An affinity purification step using a Cibracon Blue F3-GA affinity column wa therefore attempted. Approximately 2 mgs of ammonium sulphate precipitated protein from the previous gel filtration step was resuspended in 1 ml of running buffer and loaded onto the column and then eluted with a 0 - 1 M NaCl gradient.

The loading and elution profile is shown in **Figure 3.25**. From this it can be seem that most of the active material is present in the initial wash and does not bind to the column. However, the enzyme does not co-elute with the absorption peak, which suggests that it might be interacting weakly with the dye-ligand, but not strongly enough for the enzyme to actually be retained on the column. The gradient elution only shows a trace of activity eluting at the very start of the gradient with very little if any protein binding to the column at all.

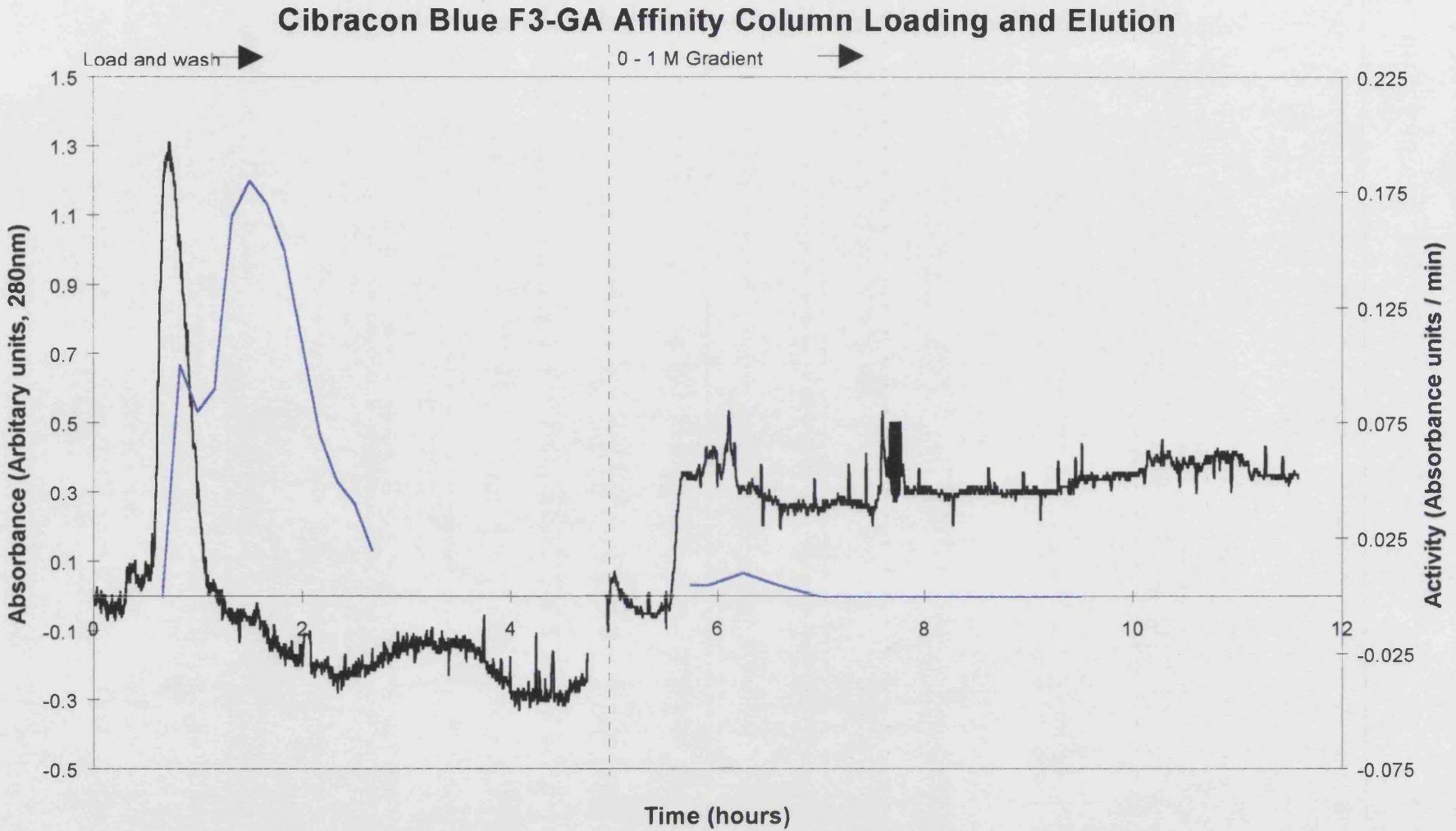

Figure 3.25: Loading and elution profile of 0.6 x 8 cm Cibracon Blue F3-GA Sephadex CL 4B column.. The column was loaded with 2 mgs of protein and washed with 20 mM Tris pH 7.4, 1 mM DTT at a flow rate of 18 ml/hr and eluted with a 0 - 1 M NaCl gradient in the same buffer. 3 ml fractions were collected and analysed for activity.

A Reactive Green 19 affinity column as had been described previously for the purification of Octopine Dehydrogenase[64] was also used for a trial purification. Reactive Green 19 Sepharose 4B was synthesised as described in the methods section. A 0.8 x 8 cm column was packed and equilibrated with the running buffer at a flow rate of 18 ml/hour. As for the previous affinity trail, approximately 2 mgs of ammonium sulphate precipitated protein was resuspended in 1 ml running buffer and loaded onto the column. The column was then washed with the same buffer before eluting using steps of 150 mM and 300 mM NaCl as described in the original paper. The loading, washing and elution profile is shown in **Figure 3.26**

Most of the activity is not retained on the column and is eluted in the washing step after the major peak of absorbing material. There is some activity eluted by the 150 mM step, but non at all by the 300 mM step.

As neither of the affinity polishing steps worked, the enzyme was not successfully purified to the level need to use it for binding experiments with our system.

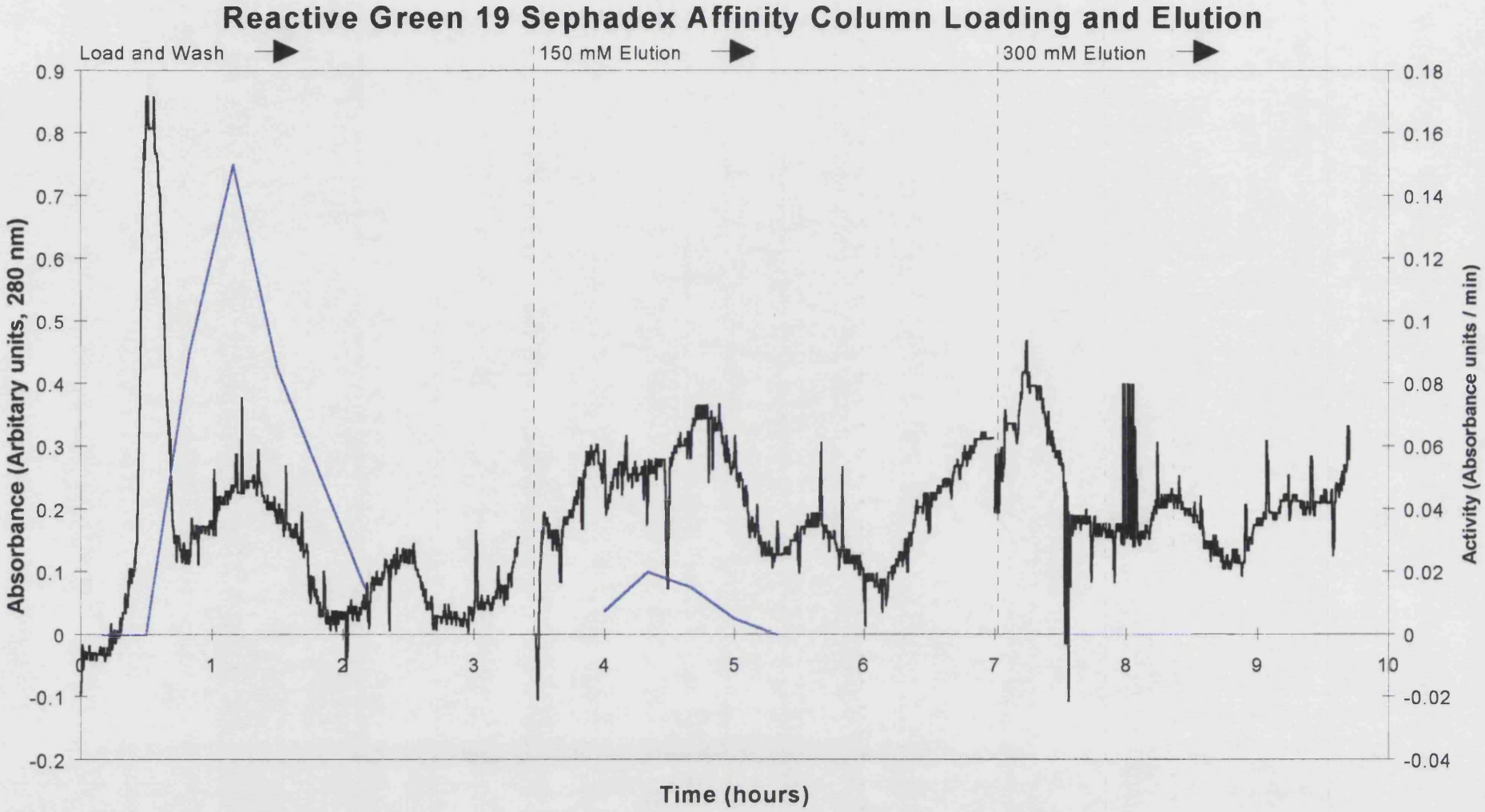

Figure 3.26 : Loading and step elutions of 0.6 x 8 cm Reactive Green 19 Sephadex CL-4B column. The column was loaded with 2 mgs of and washed with 20 mM Tris pH 7.4, 1 mM DTT at a flow rate of 18 ml/hr and eluted stepwise with 150 mM and 300 mM NaCl. 3 ml fractions were collected and analysed for enzymic activity.

3.7 Spectral Titrations using Lysozyme

The first set of dye dextran conjugates (T40 series) were titrated against lysozyme in a similar manner to that described by Mayes et al.[39] for the larger backbone conjugates previously described. A difference spectral titration of the T40.1 conjugate is shown in **Figure 3.28**. The difference is measured between the hypochromic trough and hyperchromic peak at 595 nm and 690 nm respectively. This provides a measurement of larger magnitude and independent of any small baseline shifts that might be present by purely measuring a single peak or trough. Alternatively the isosbestic point at 645 nm can be used as a reference to compensate for any baseline variation. This presumes that there are only two absorbing species present and therefore the magnitude of the difference spectrum at any point is proportional to the relative quantities of each. The presence of an isosbestic point (where there is no change in the absorption) tends to be indicative of only two differently absorbing species being present; when more absorbing species are present it is less likely that there will be points where all of them will have the same absolute absorption.

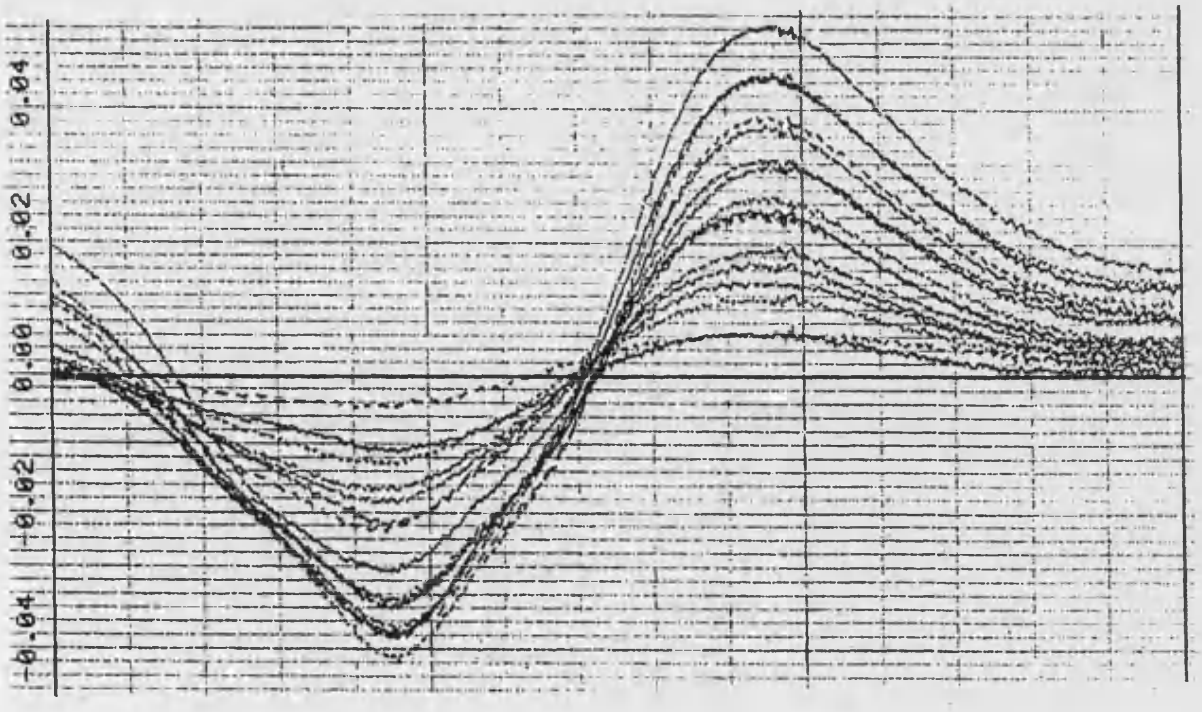

Figure 3.28 : Difference spectral titration of lysozyme with T40.1 conjugate. Sequential additions of lysozyme were made to the sample cuvette with an equal quantity of buffer to the reference. A difference spectrum was then scanned from 400 nm to 700 nm after each addition of lysozyme.

The results of the titrations for the T40 series with Lysozyme are shown in Figures **3.29 - 3.32**. The results have been fitted to a mutual depletion model (discussed in detail in **section 4.7** of the discussion) and the determined constants are displayed in the table below. The data were first fitted allowing the values of all variables to float apart from the total dye available (**Dt**) which was determined spectrophotimetrically for each sample. This allowed the determination of the average difference between the extinction coefficients of free and bound dye (**ΔE**) which was then fixed for all the samples and the fits were then re-run. Presuming specific binding is taking place, the same interaction is being measured in all cases and this value should be constant for all of the samples. Fractional dye availability (**Fa**) is simply the ratio between the total dye (**Dt**) and the available dye (**Da**) calculated from the fit.

Table 3.5: Determined constants for T40 series binding to Lysozyme

	ΔE ($M^{-1}cm^{-1}$)	**Kd** (uM)	**Da** (uM)	**Dt** (uM)	**Fa**
T40.1	0.007	48.2	15.9	58.7	27.1
T40.2	0.007	54.4	12.2	55.2	22.1
T40.5	0.007	18.2	10.8	54.7	19.7
T40.20	0.007	12.8	10.0	55.4	18.1

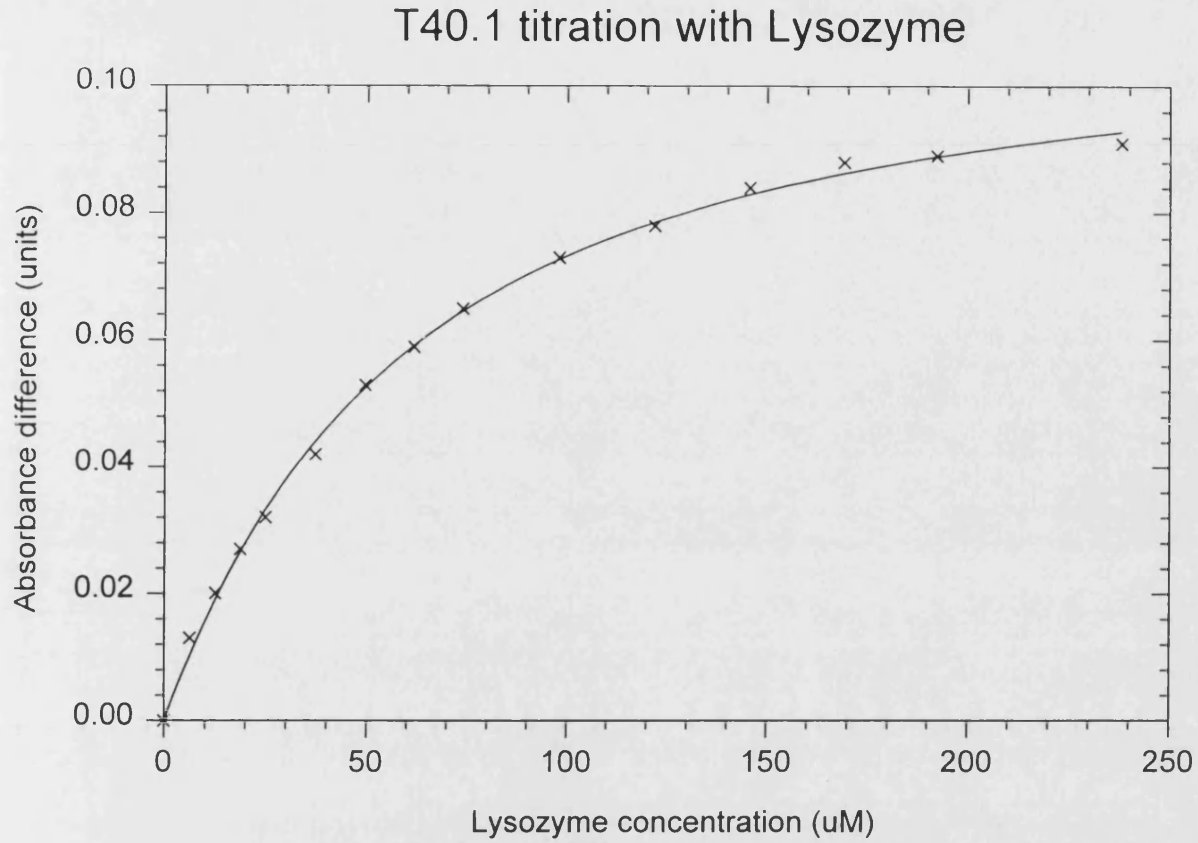

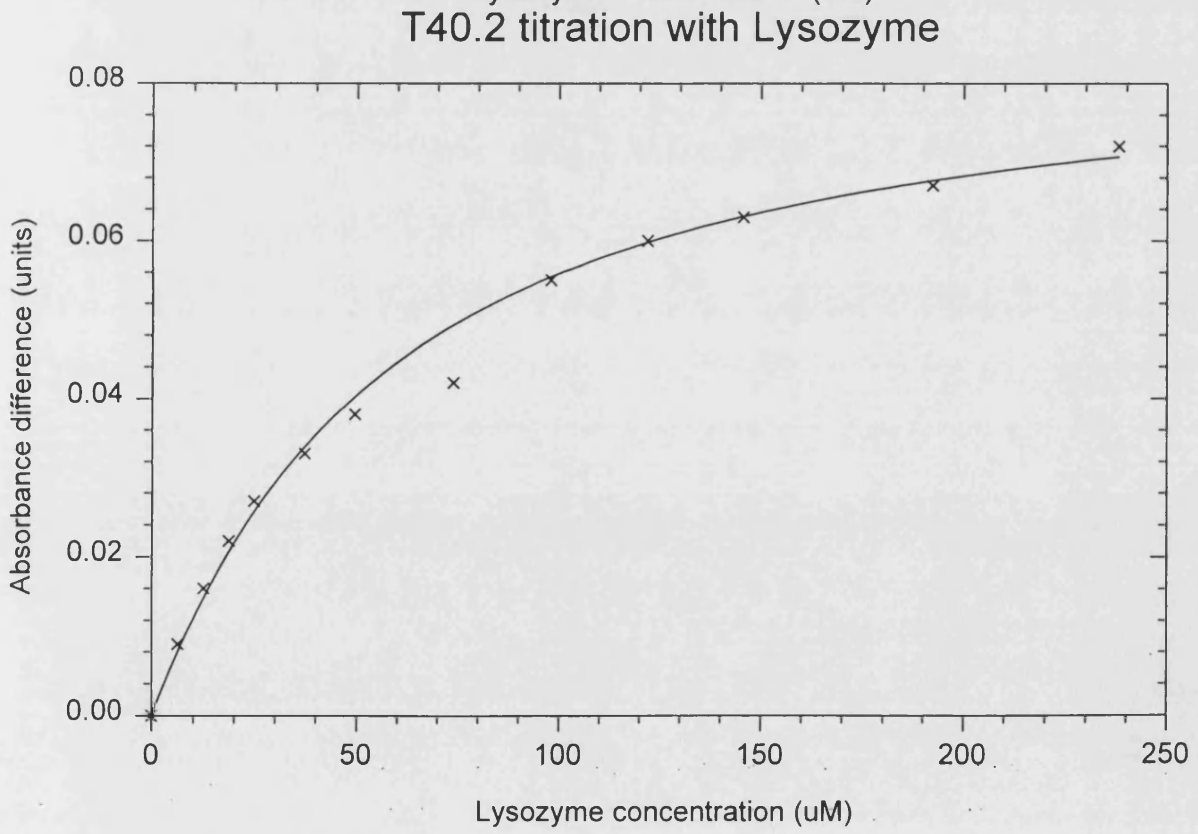

Figures 3.29, 3.30 : These figures show binding data for the T40.1 and T40.2 conjugates. The difference between the hypo and hyper-chromic peaks (595 nm and 690 nm respectively) is plotted against the concentration of lysozyme added. Values for determined variables are shown in **Table 3.5.**

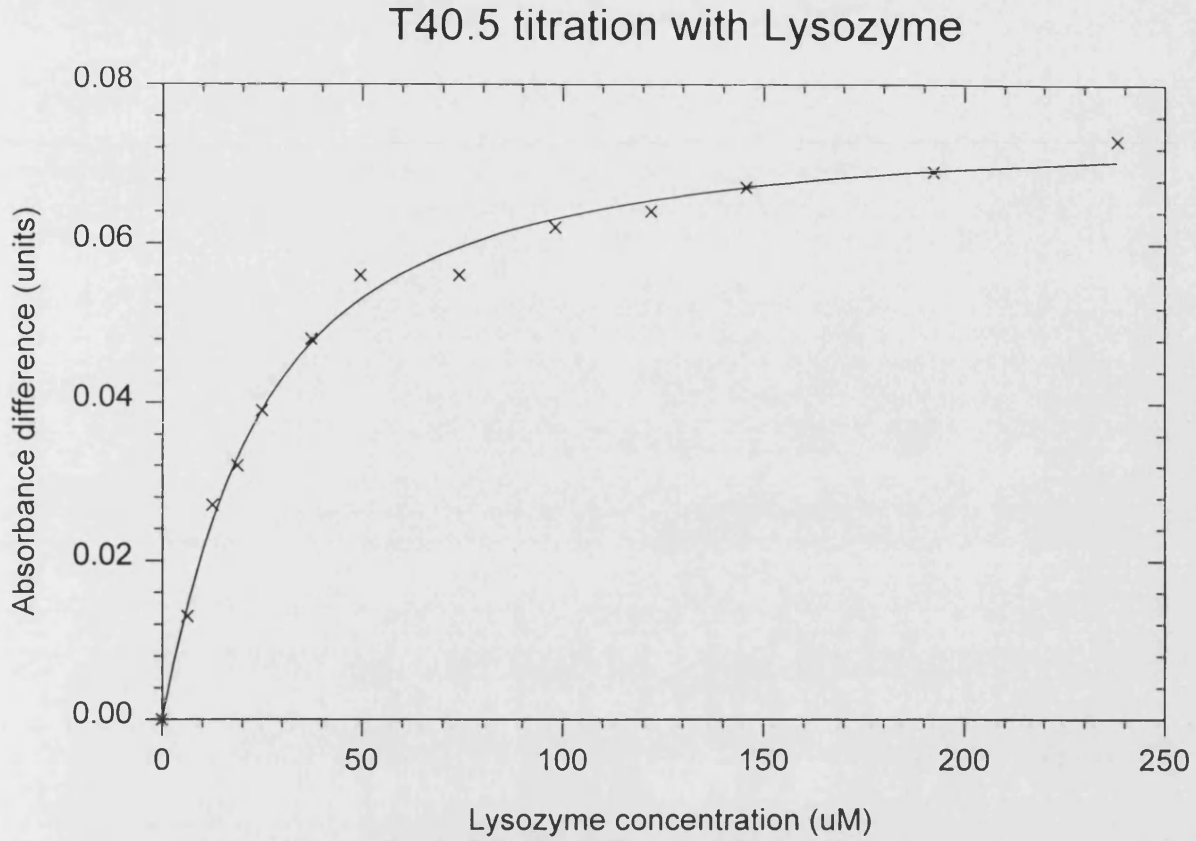

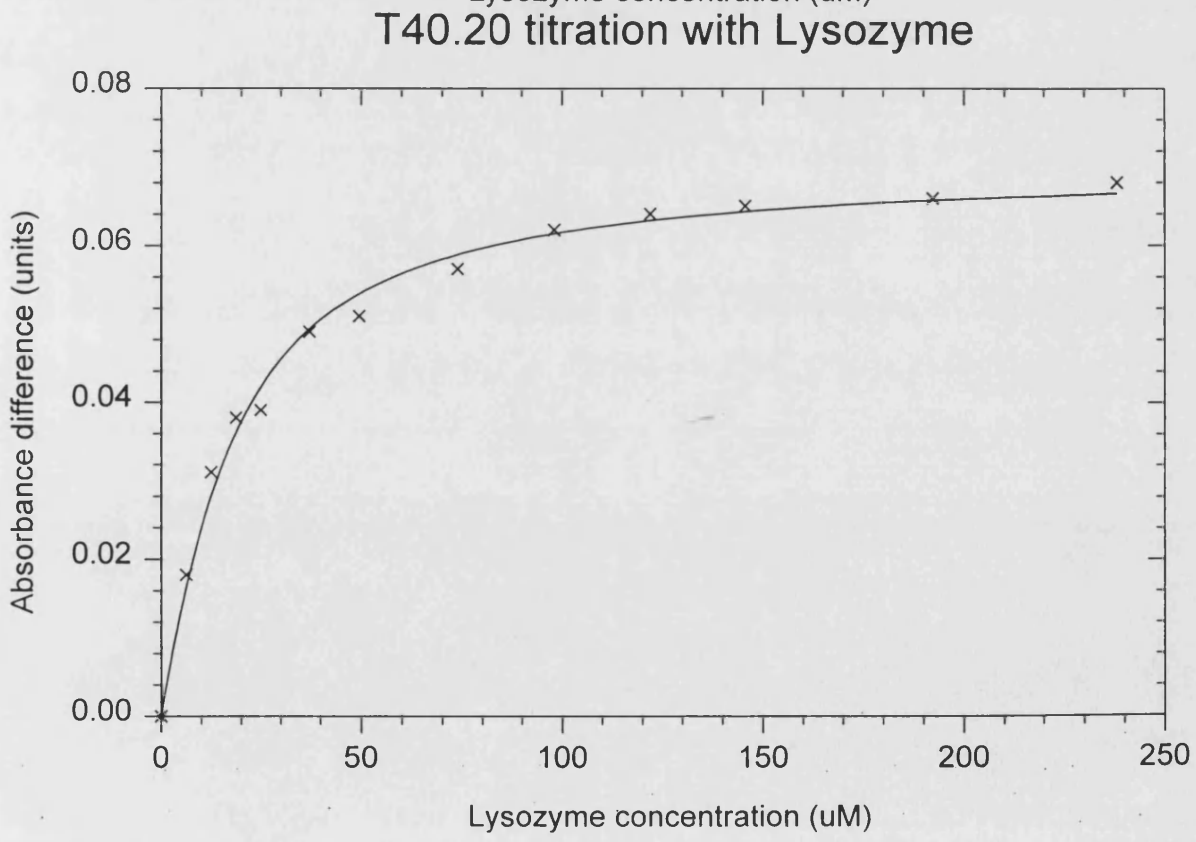

Figures 3.31, 3.32 : These figures show binding data for the T40.5 and T40.20 conjugates. The difference between the hypo and hyper-chromic peaks (595 nm and 690 nm respectively) is plotted against the concentration of lysozyme added. Values for determined variables are shown in **Table 3.5.**

3.8 Dye - Lysozyme Rapid Kinetics

Previous work done on the kinetics of binding of proteins to dye-dextrans by Mayes et. al.[39] used lysozyme as a model protein to measure binding equilibria and kinetics. This provided an obvious starting point for the set up and testing of the diode array system on the stop-flow (SF-61 MX, HiTech Scientific) which had not been used previously. Unless otherwise stated all data manipulation was carried out on a PC using the software supplied with the equipment. A outline of the basic principles of stop-flow and the use of a diode array for simultaneous measurement of multiple wavelengths is described in the methods section.

Initial experiments used a standard system containing 50 mM sodium phosphate buffer pH 7.9 with 50 uM Cibracon Blue F3-GA in one syringe and lysozyme at varying concentrations in the other. All reactions were carried out at 25 C. The time scale for this reaction and the spectral changes expected to be produced were known from the previous kinetic and spectral titrations byMayes et al.[39]. Hence it was known that the reaction occurred at a rate suitable for observation with the diode array, and an appropriate set of wavelengths for observation could be chosen to include the major hypo- and hyper-chromic shifts involved.

The following graphs show the results of a set of kinetic binding experiments of lysozyme with free dye at decreasing final concentrations (250, 125, 62.5 and 31.25 uM) against a final concentration of 25 uM free dye (50 uM syringe concentration). The spectra are results averaged from 4 or 5 individual experiments at each concentration. The first figure (**Figure 3.33**) shows the raw absorbance data from the highest concentration (250 uM). This is then shown in **Figure 3.34** as difference spectra relative to the initial spectrum. This shows the hypo- and hyper-chromic shifts in the absorbance spectrum of the dye produced on binding of the dye to lysozyme. **Figure 3.35** then shows cross sections taken through the data at the

three isosbestic points of 395 nm, 530 nm and 650 nm (black, red and cyan respectively). The difference spectra and cross sections through the isosbestic points (as determined from the first experiment) for the experiments with lower lysozyme concentrations are then shown in the following figures (**Figures 3.36 - 3.41**).

It can be seen from the difference spectra of the experiments that aggregation is beginning to occur at the lower concentrations, increasing markedly as the concentration is reduced towards equimolarity with the dye.

This effect is best illustrated by **Figures 3.35, 3.37, 3.39 & 3.41** which show the cross sections taken through the data at the isosbestic points. At these points there should be no change is the absorbance as both the free and bound dye have exactly the same extinction coefficient. However the observed drift of these isosbestics shows that additional 'absorption' (in fact light scattering) is present. Comparison of the changes in the isosbestics shows that the magnitude of the change produced increases rapidly as the wavelength is reduced. This is what would be expected due to the presence of light scattering aggregates, as the magnitude of light scattering is exponentially related to the wavelength of incident light.

This problem of aggregation when using the free dye was noted by Mayes et. al.[39] and effectively prevents an equilibrium titration of lysozyme with the dye as the initial additions of lysozyme to a dye solution cause precipitation. These experiments show that this seems to be a concentration dependent phenomenon and as the relative concentration of lysozyme is increased the rate of precipitation decreases. This suggests that binding and aggregation are two competing reactions such that as the concentration of lysozyme is raised the amount of dye available to facilitate aggregation decreases.

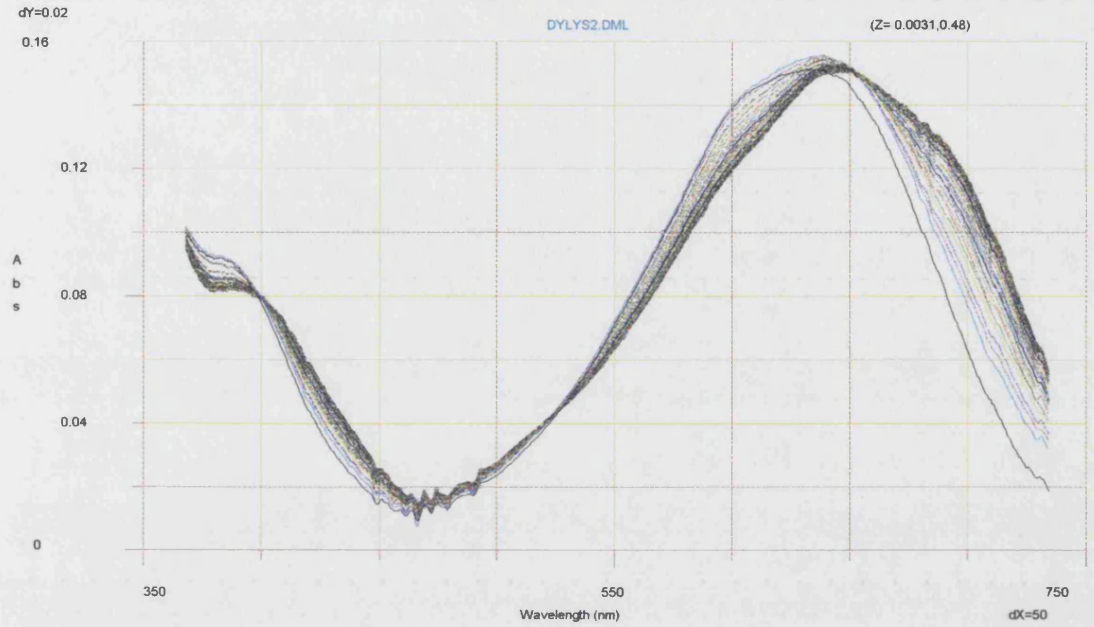

Figure 3.33 : Absolute absorption spectra taken of binding reaction between 25 uM Cibracon Blue F3-GA and 250 uM Lysozyme. The initial spectrum (black) can be seen to be displaced further from the rest at higher wavelengths. This is due to the effects of photodiode bleaching on the initial spectrum. A total of 96 spectra were recorded over a period of 0.48 seconds giving a resolution of 0.005 seconds between scans. The same timecourse was used for all of the subsequent free dye - lysozyme datasets.

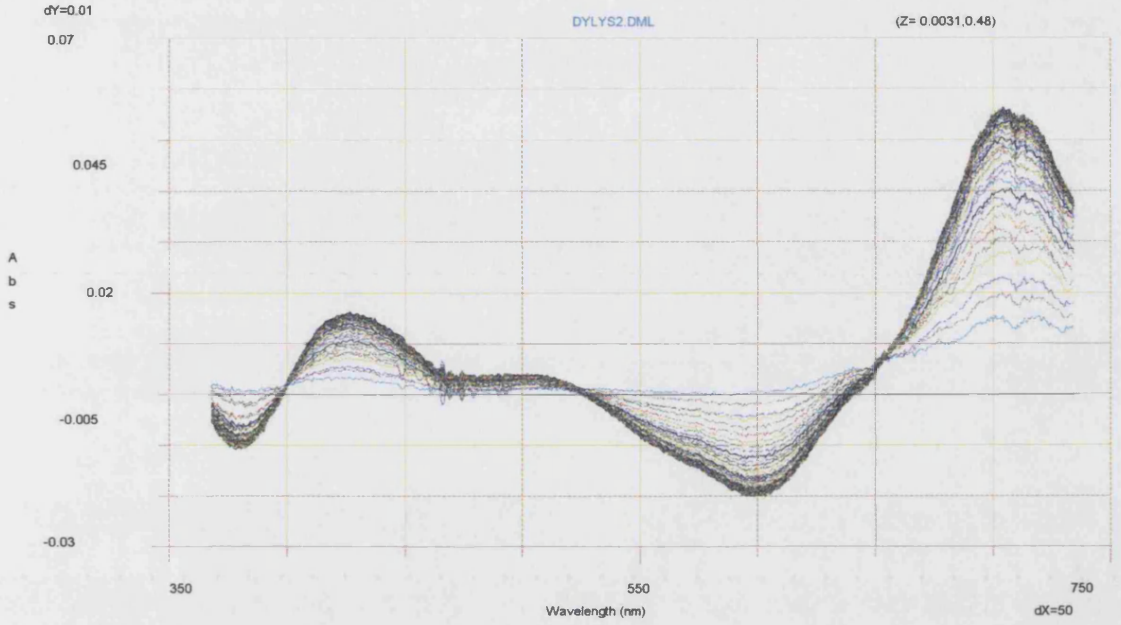

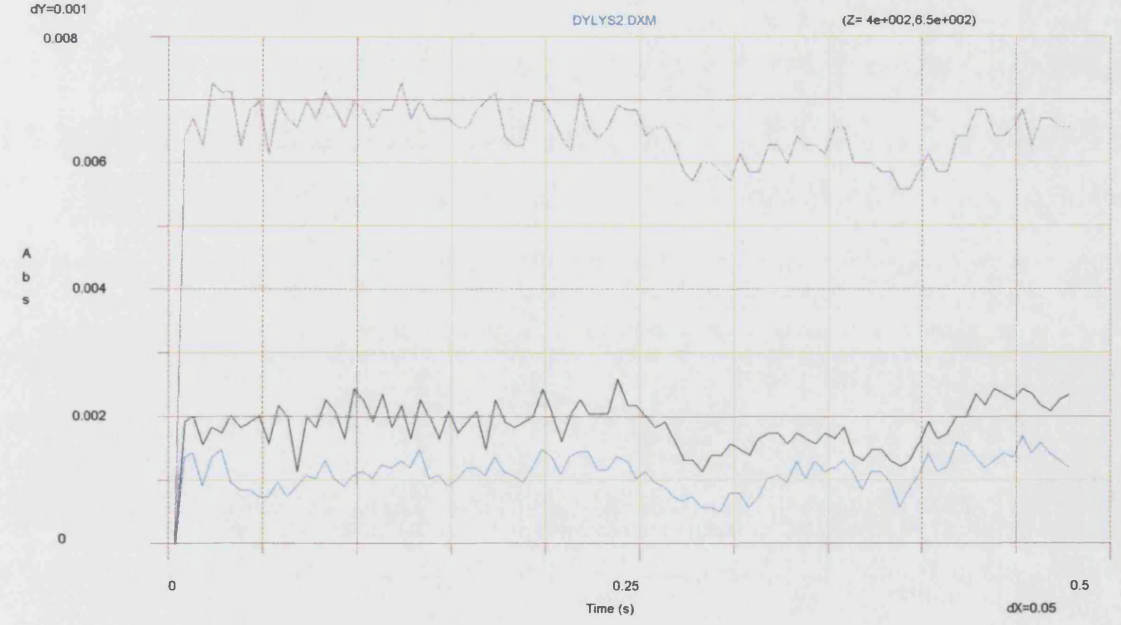

Figures 3.34, 3.35 : (Top) Difference spectrum produced by subtracting the initial spectrum in the dataset from all subsequent ones. (Bottom) Cross sections at the isosbestics of 395 (black), 530 (cyan) and 650 nm (red).

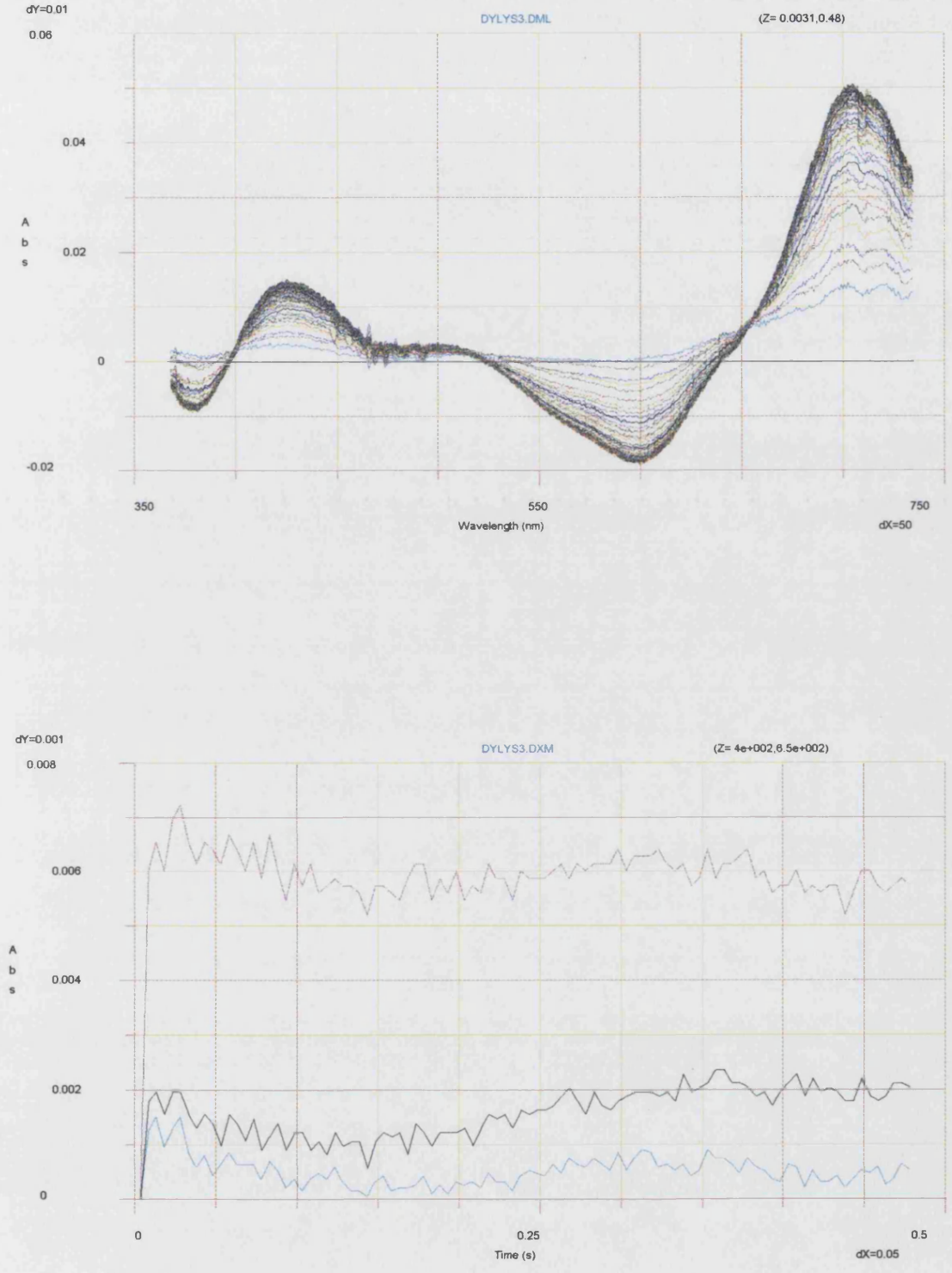

Figures 3.36, 3.37 : (Top) The difference spectrum for the reaction of 125 uM lysozyme with 25 uM Cibracon Blue F3-GA. (Bottom) Cross sections through the isosbestics at 395 (black), 530 (cyan) and 650 nm (red).

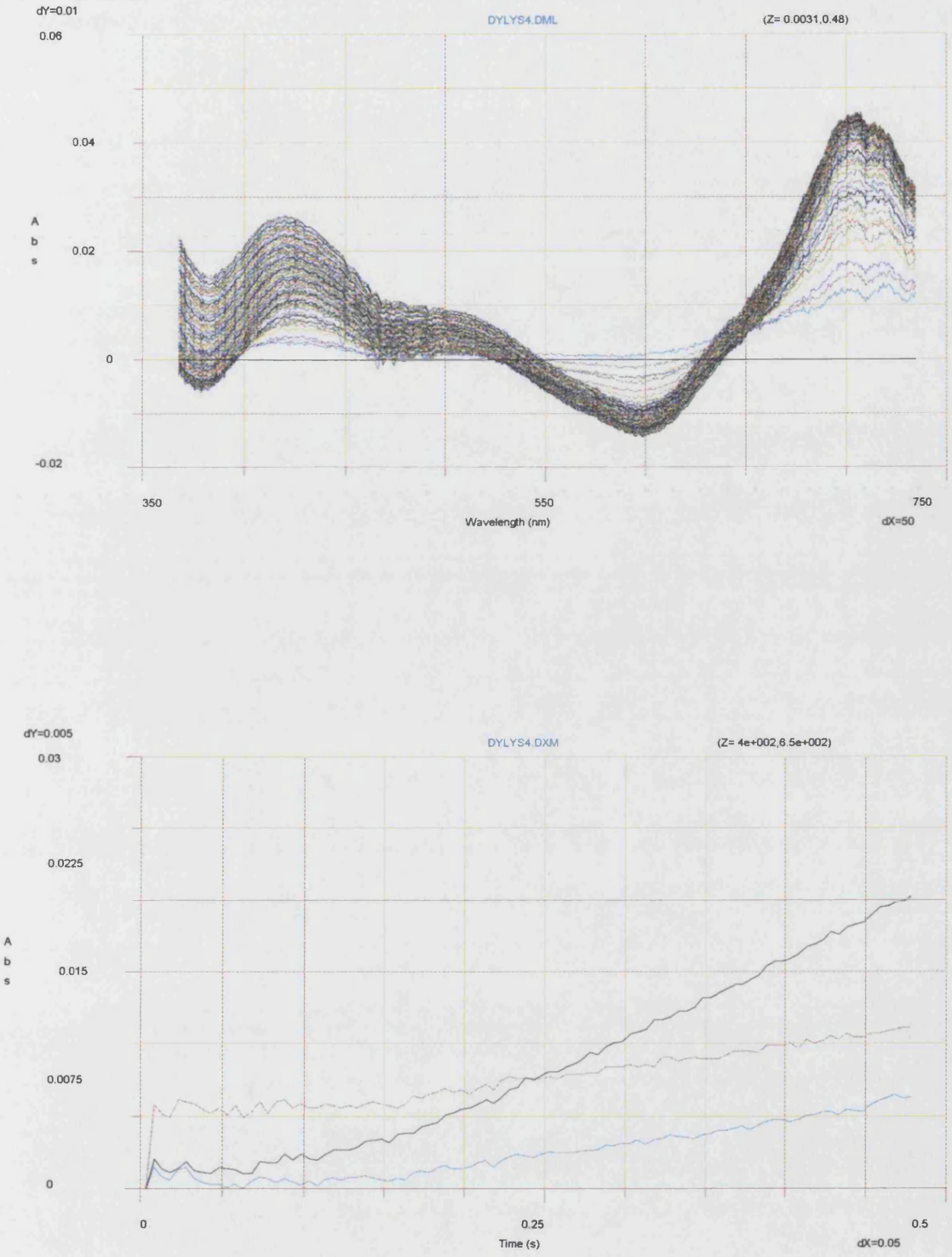

Figures 3.38, 3.39 : (Top) The difference spectrum for the reaction of 62.5 uM lysozyme with 25 uM Cibracon Blue F3-GA. (Bottom) Cross sections through the isosbestics at 395 (black), 530 (cyan) and 650 nm (red).

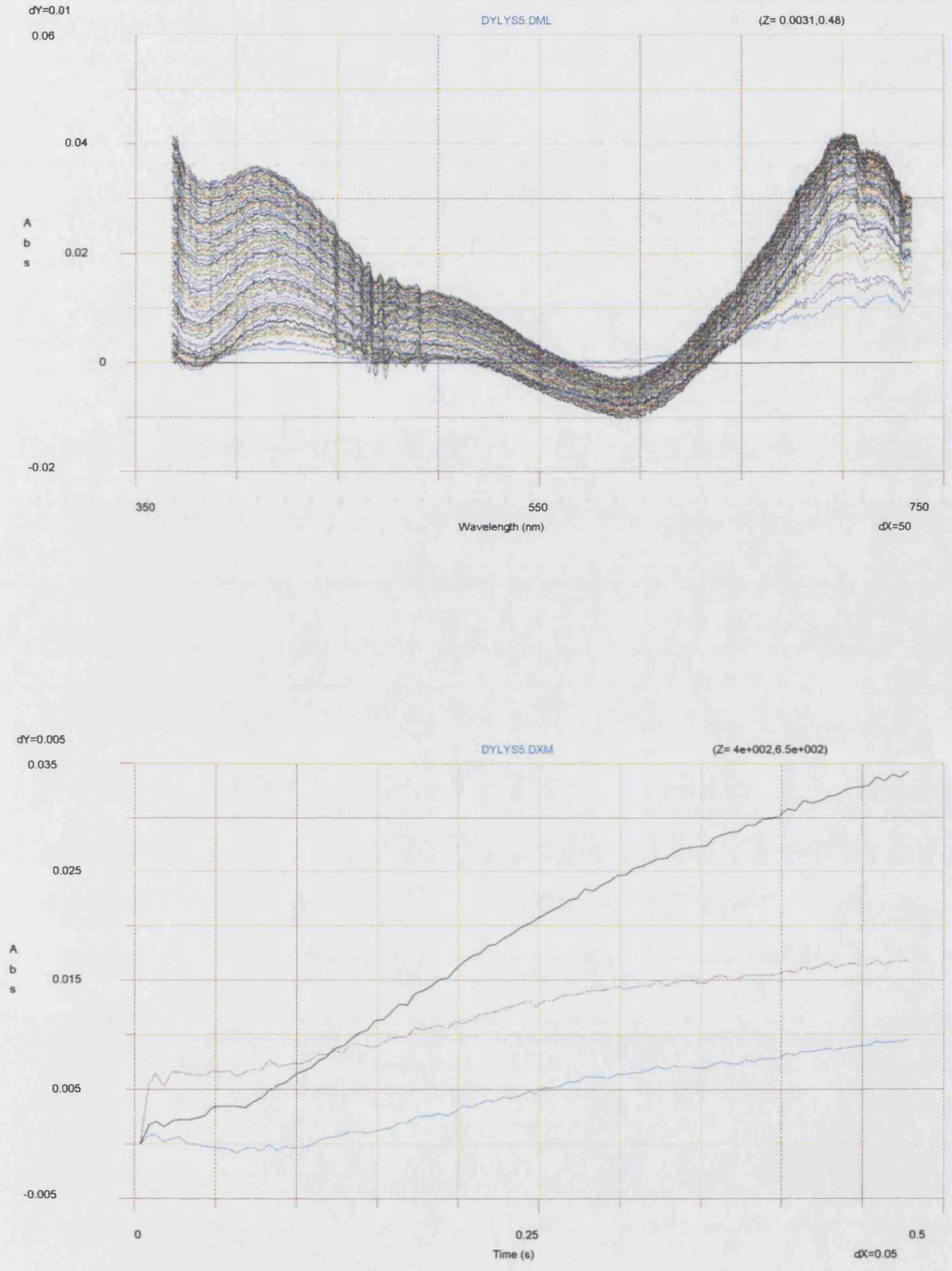

Figures 3.40, 3.41 : (Top) Difference spectrum for the reaction of 31.25 uM lysozyme with 25 uM Cibracon Blue F3-GA. (Bottom) Cross sections through the isosbestics at 395 (black), 530 (cyan) and 650 nm (red).

The Dylys2 dataset were globally fitted to a simple binding model with the Specfit software (R. Binstead), a fitting program using Singular Value Decomposition (SVD) to produce a fit to an entire 3D dataset.

Figures 3.42-3.45 show cross sections through the dataset at the maxima and minima in the spectrum, with a single minima at 600 nm and maxima at 425 nm and 705 nm. The program uses SVD to produce an approximation to the 3D surface described by the dataset using a set of eigenvectors and eigenvalues. This effectively minimises the dataset so that it can be used to fit a model. When supplied with a model the program with then attempt to evolve spectra of the components involved and values for the rate constants described in the model.

A simple irreversible binding model is applicable in this case due to the excess of lysozyme making the reaction pseudo first order in respect to lysozyme. The fit produces a single forward rate constant which is used along with the evolved spectra of the free and bound dye to produce a fit at all wavelengths. The cross sections shown are through the original dataset, rather than the decomposed data which will tend to be less noisy due to its representation as a minimal number of eigenvectors and values.

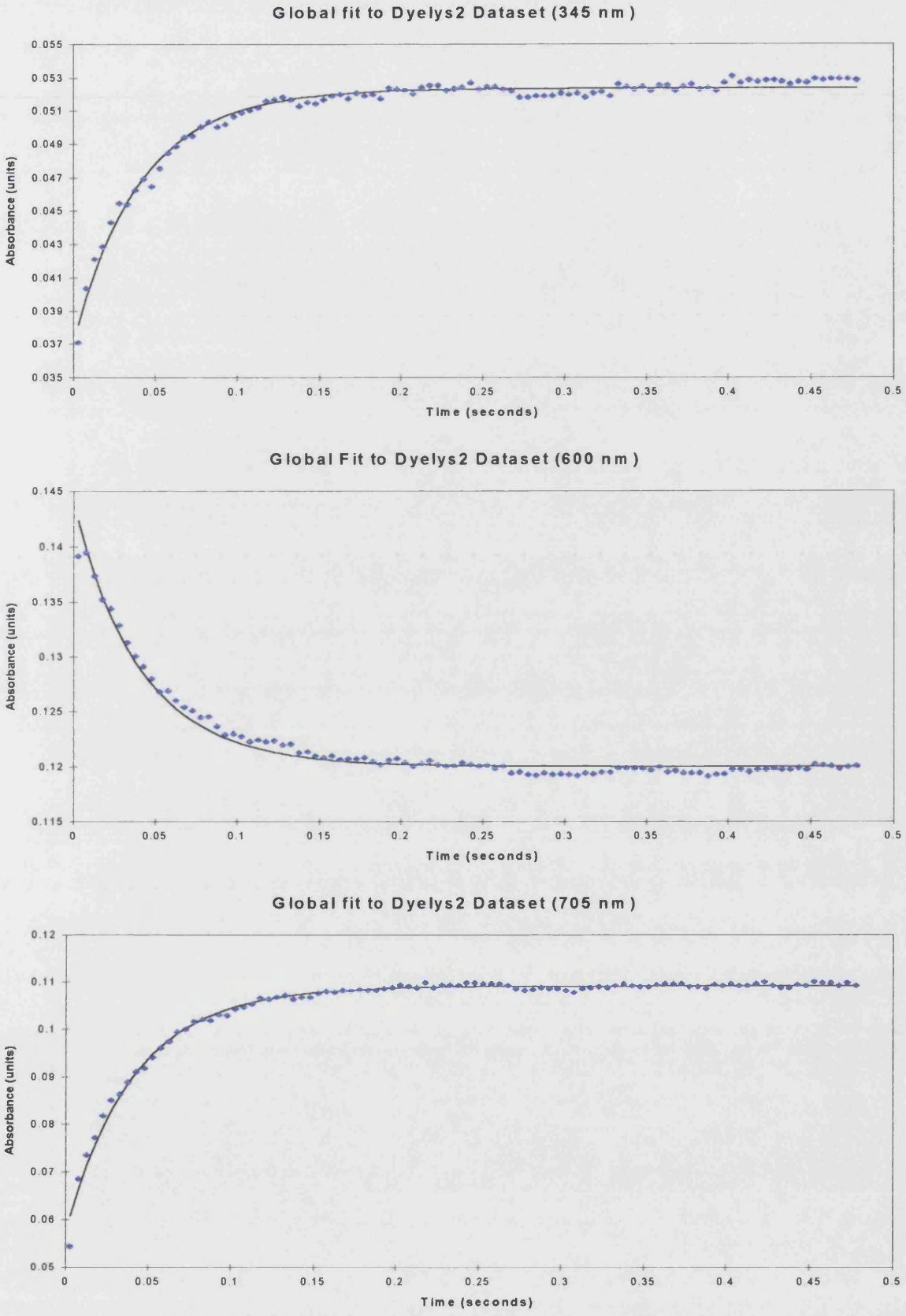

Figures 3.42-3.45 : Global fit produced to Dyelys2 dataset. The figures show cross sections through the fit at 425, 600 and 705 nm which represent the maxima and minima of the difference spectrum produced.

To allow complete comparison with the previous work by Mayes et. al.[39] a set of experiments similar to those with the free Cibracon Blue F3-GA were repeated using the dye-dextran conjugate 5d8 (500 kDa. backbone, 9.92 relative substitution - see **Table 3.3**). The difference spectrum of 25 uM 5d8 mixed with 250 uM Lysozyme (both final concentrations) is shown in **Figure 3.46**.

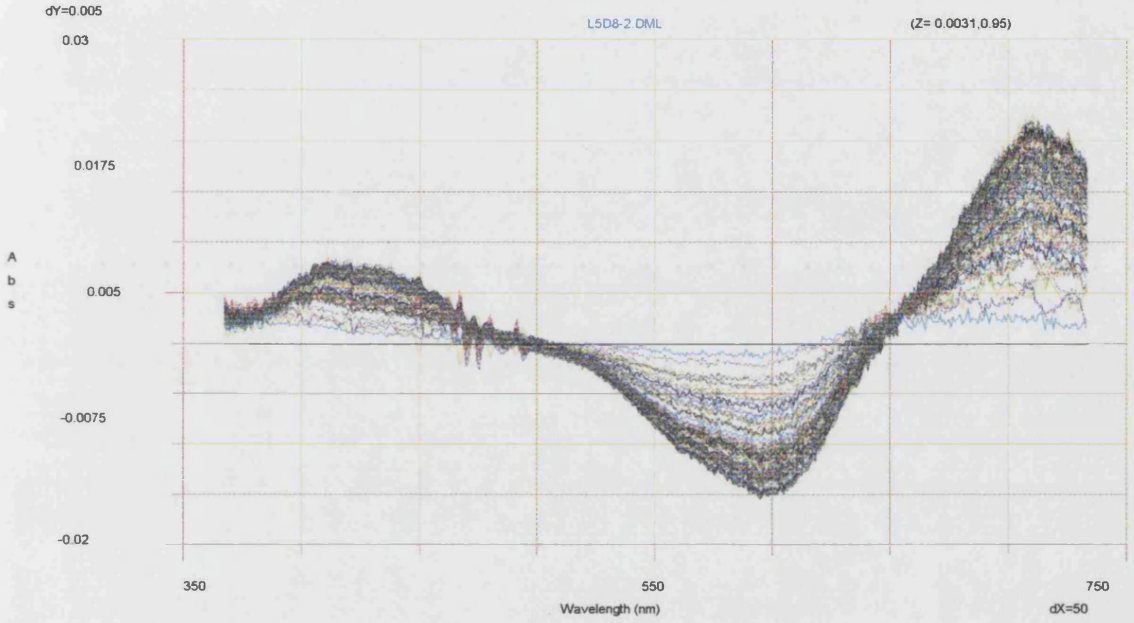

Figure 3.46 : This figure shows the difference spectrum produced on binding of 250 uM Lysozyme to 44 uM (final concentrations) of the dye-dextran conjugate 5d8. A total of 96 spectra are shown overlaid which were recorded over 0.96 seconds.

It was shown by Mayes et. al.[39] that a simple binding model is not capable of describing the binding kinetics of lysozyme to a dye-dextran conjugate. This is demonstrated in **Figure 3.47** which shows a single exponential fit, representing a simple irreversible binding model, to the 5d8-1 dataset at 595 nm. It can be clearly seen that the data deviate markedly and systematically from the fit, showing that a more complex model is needed to properly describe the binding kinetics.

Datasets were collected for lysozyme binding to 5d8 at two different final dye concentrations (44 uM and 88 uM) and four lysozyme concentrations (31.25 uM, 62.5 uM, 125 uM and 250

uM). Cross sections were taken through these datasets at the maxima and minima of the difference spectrum (425 nm, 595 nm and 705 nm) and are shown in **Figures 3.48-3.53**.

For illustrative purposes these cross sections have been corrected so that they all finish at the same point. Each figure shows a overlay of cross sections at one wavelength at all four lysozyme concentrations used for each of the dye concentrations. **Figures 3.48-3.50** show time courses for the reactions using 44 uM 5d8 whilst **Figures 3.51-3.53** show the same using a concentration of 88 uM 5d8 dye-dextran conjugate.

It can be seen that there is apparently little difference between the difference spectra produced at all the wavelengths for all the lysozyme concentrations used, with the possible exception of the highest dye-dextran (88 uM) and lowest lysozyme concentrations (31.25 uM) used (blue traces, **Figures 3.51-3.53**).

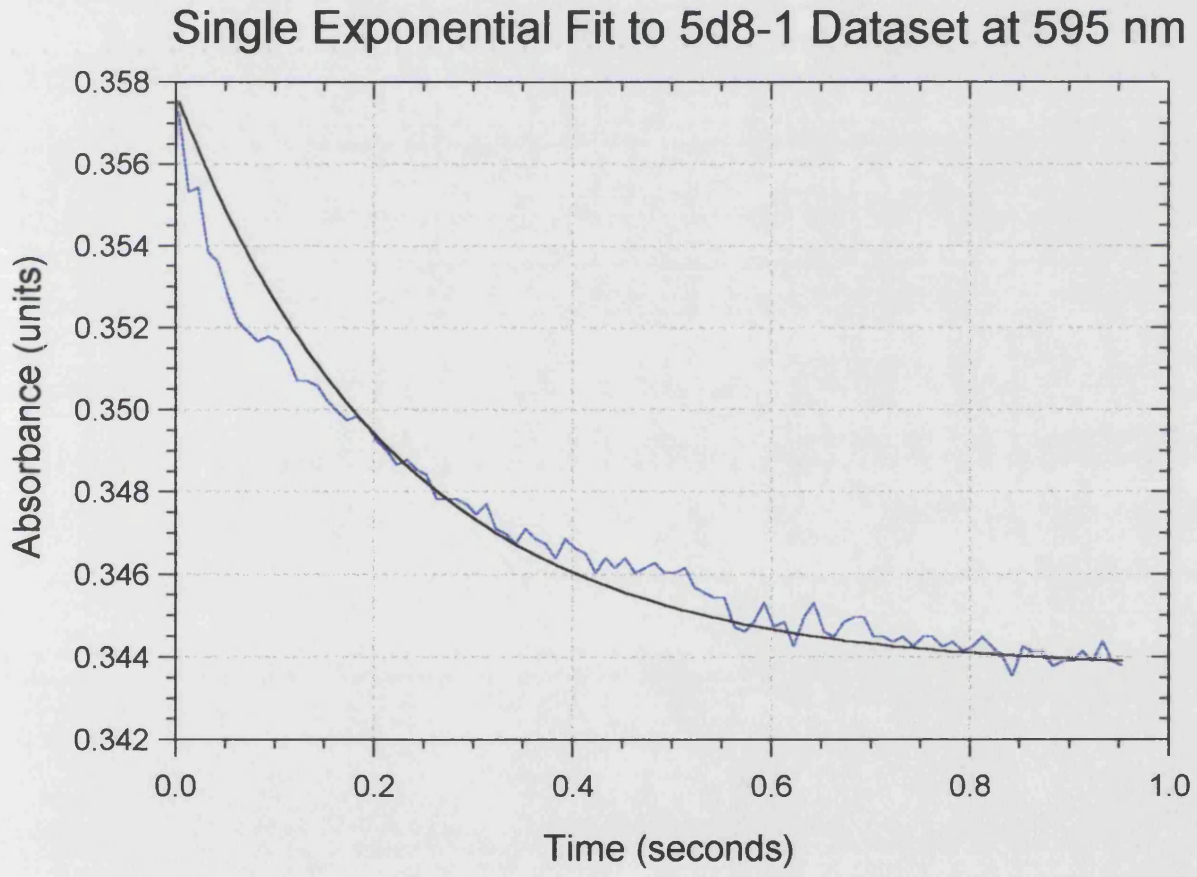

Figure 3.47 : This shows a simple binding model (single exponential) fit to a cross section through the 5d8-1 dataset (shown in previous figure) at 595 nm. The fit is shown in black and the data in blue. Parameters for the fit are K = 4.48 , $\Delta A = 0.014$.

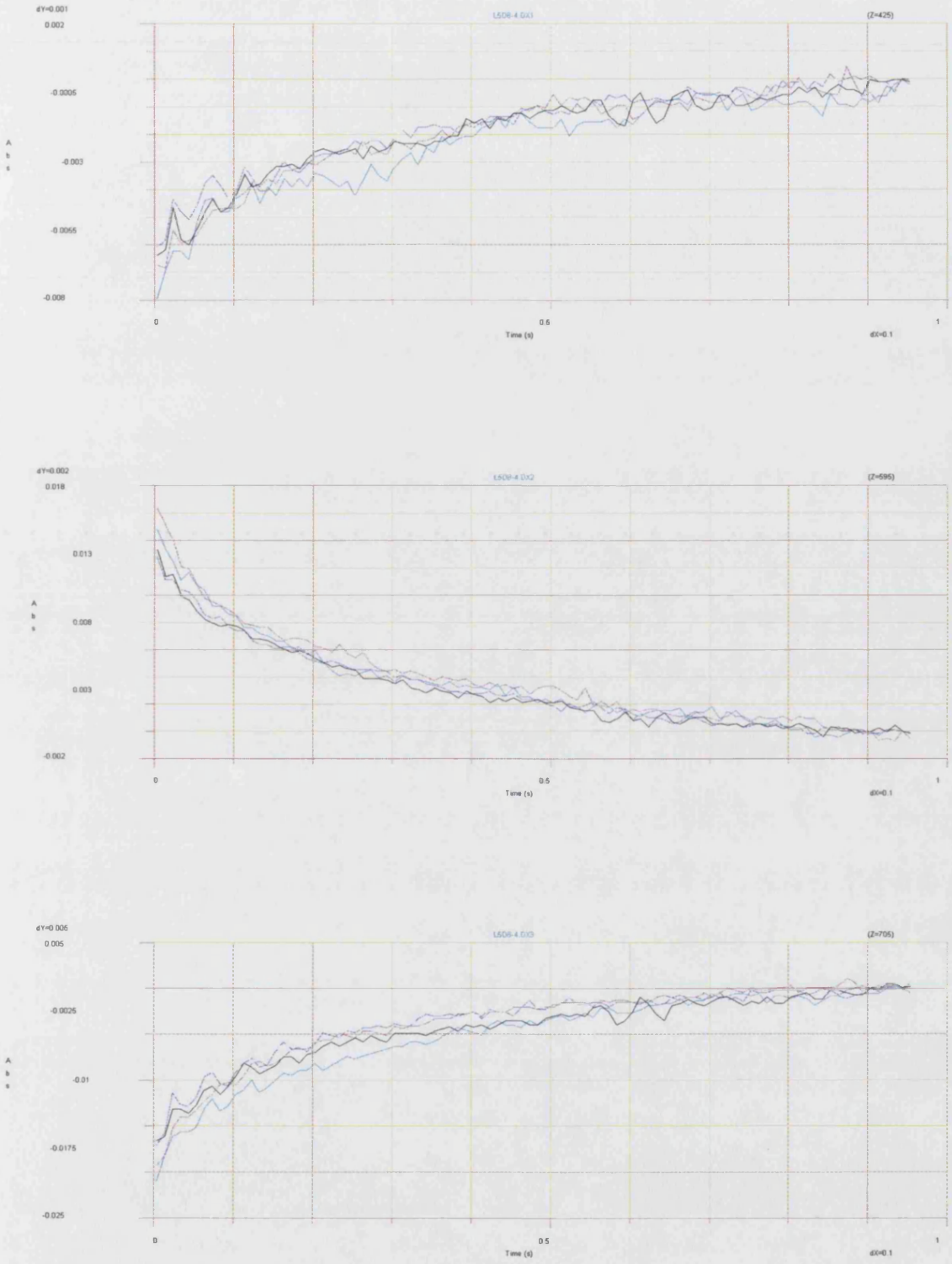

Figures 3.48-3.50 : These figures show cross sections for a set of 5d8 datasets at 425, 595 and 705 nm respectively. Dye concentration is 44 uM in all the experiments with final lysozyme concentrations of 31.25, 62.5, 125 and 250 uM shown respectively in blue, cyan, red and black

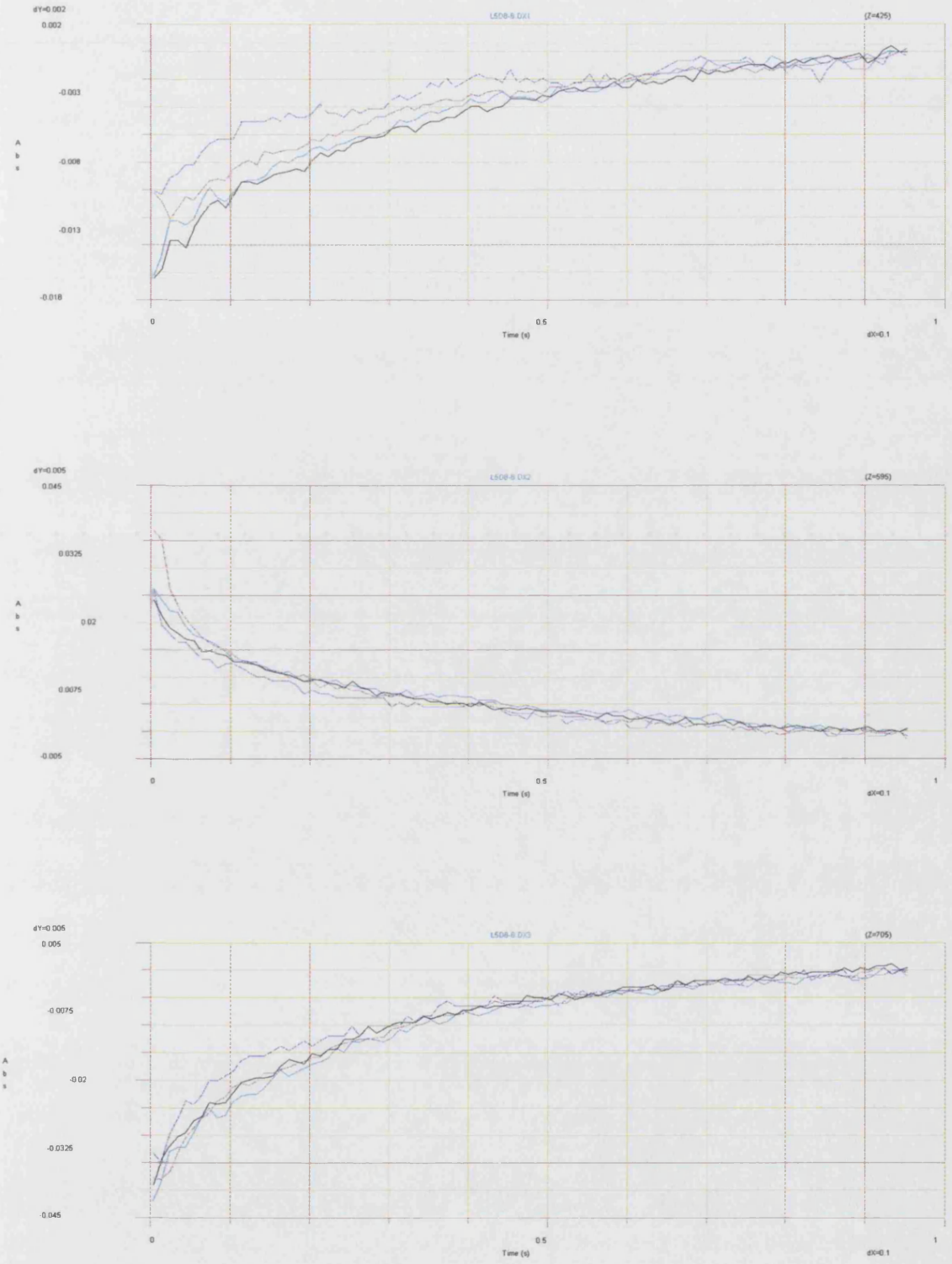

Figures 3.51 - 3.53 : These figures show cross sections for a set of 5d8 datasets at 425, 595 and 705 nm respectively. Dye concentration is 88 uM in all the experiments with final lysozyme concentrations of 31.25, 62.5, 125 and 250 uM shown respectively in blue, cyan, red and black.

3.9 Spectral Titration with LDH

Spectral titration of the dye and dye-dextran conjugates initially took place by titrating the dye or dye-dextran against a fixed concentration of LDH, as done in similar experiments by other investigators[26]. This produced reasonable difference spectra, but with an apparently unstable baseline (**Figure 3.54**). The differences between the apparent baseline for each trace made quantification of the true peak size for each addition difficult.

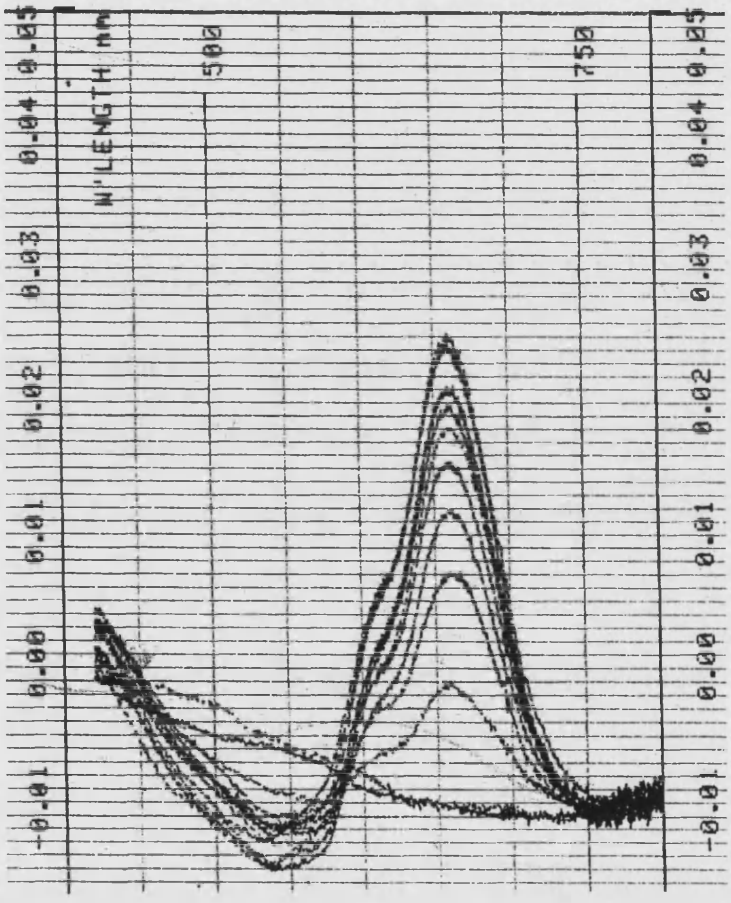

Figure 3.54 : Spectral titration of T40.20 dye-dextran conjugate against LDH. The sample cuvette contained 2 uM LDH (8 uM site concentration) and the reference buffer only. Sequential additions of small volumes of a 1 mM T40.20 solution were made to both sample and reference cuvettes and the difference spectra recorded from 420 - 800 nm after each addition. The initial spectrum is the almost flat baseline with the difference spectra progressively increasing in magnitude as more dye was added up to a final dye concentration of 50 uM

The reverse experiment, as performed by Mayes et al.[25] in which enzyme is added to dye is shown in **Figure 3.55** which shows a difference spectrum for LDH titrated against free dye. This can be seen to give a difference spectrum similar to that of the reverse experiment

(**Figure 54**) but with a better baseline stability, with the spectra producing a clearer isosbestic point.

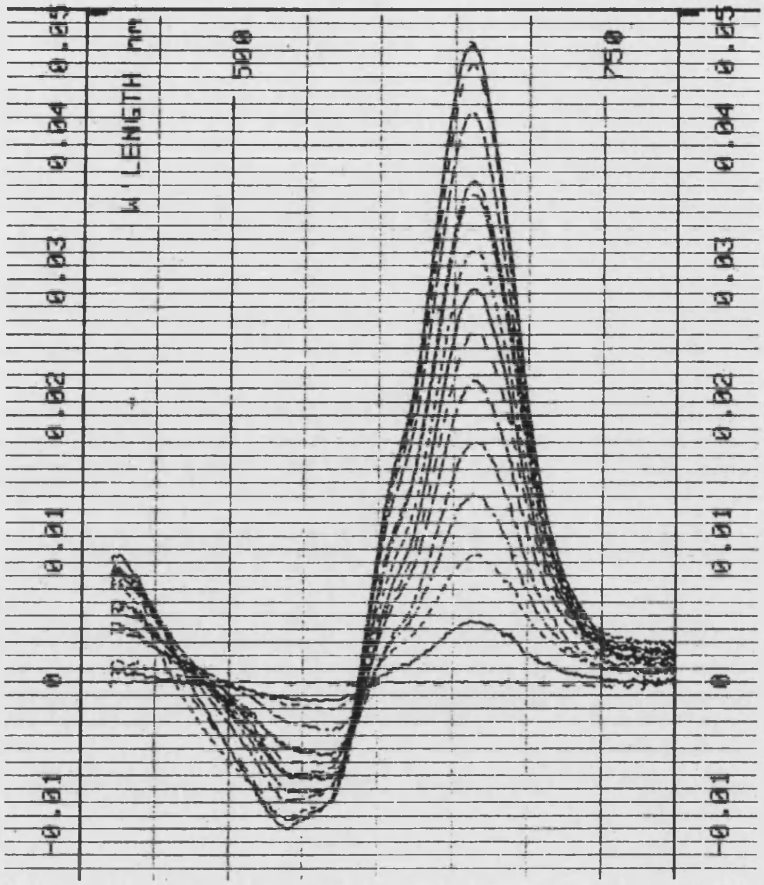

Figure 3.55 : Spectral titration of LDH against 25 uM Cibracon Blue F3-GA. Repeated additions of varying quantities of 1 mM LDH stock were made to the sample cuvette whilst buffer only was added to the reference. The difference spectrum from 420 - 800 nm was scanned after each addition.

Figure 3.56 shows the spectrum of LDH titrated against a dye dextran conjugate. It can be seen that this produces a similar difference to free dye (**Figure 3.55**) but has a less distinct hyperchromic portion at 420-500 nm. This shows that the dextran backbone does exhibit some effect upon the environment of the dye molecule, altering the difference spectrum produced. However, it is not known whether this is due to an effect on the dye-LDH binding interaction itself or just an effect due to the presence of the dextran backbone in the vicinity of the dye. It must be noted that the shape of the peak of the absorbance spectrum of free active dye, free deactivated dye and dye dextran between 600 nm and 650 nm does vary

slightly in its shape implying that the slightly different chemical natures of the three variants has some effect on the absorbance spectrum of the molecules (**Figure 3.57**).

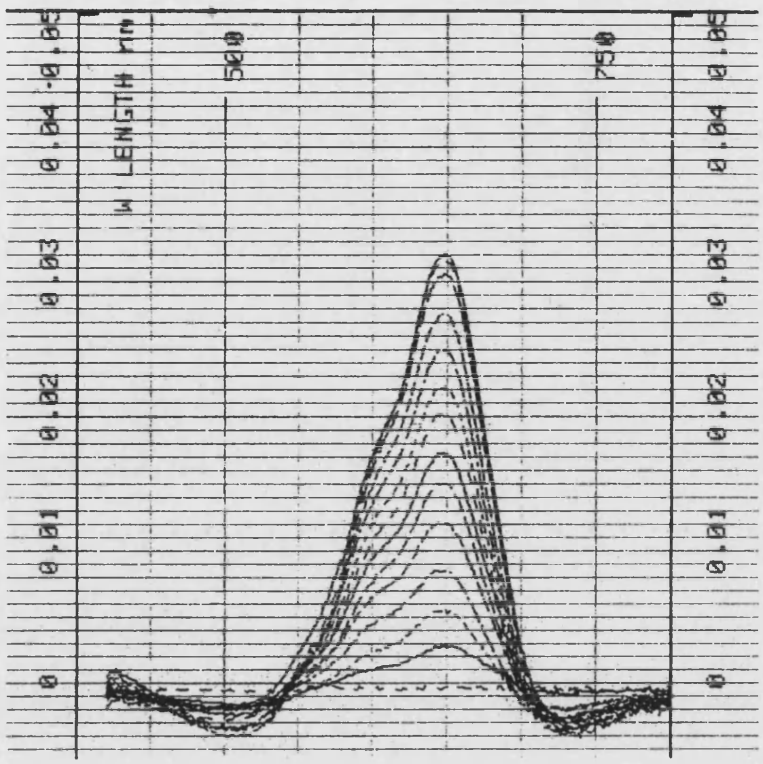

Figure 3.56 : Spectral titration of LDH against T40.20 dye-dextran conjugate. Repeated additions of varying quantities of 1 uM LDH stock were made to the sample cuvette whilst buffer only was added to the reference. The difference spectrum from 420 - 800 nm was scanned after each addition.

The data from the difference spectra are interpreted by measuring the amplitude of the hyperchromic peak for each step in the titration. The amplitude was measured at the maximum which was at 650 nm for the titrations involving free dye and 660 nm for those with the dye-dextran conjugate. This gave a set of data for each titration of the magnitude of the spectral interaction versus the amount of LDH or dye added.

The magnitude of the spectral change is presumed to be directly related to the concentration of the LDH-dye complex and hence gives a quantitative estimate of its concentration in the solution. The interaction was then modelled using either a simple mutual depletion model or by a more complex model taking into account dye stacking interactions.

The figures show the data collected from repetitions of the experiments from both the fixed dye and fixed enzyme spectral titrations. The results were initially curve fitted using the

simple mutual depletion model equation (explained in the discussion) using the equation fitting function in a computerised graph drawing program Fig P (BioSoft) which uses a Marquant Least Squares fitting procedure. Later all data were fitted using Scientist (MicroMath) which is a more advanced program capable of producing iterative fits to differential equations as well as explicit equations also using a least squres proceedure as explained in section **4.7**.

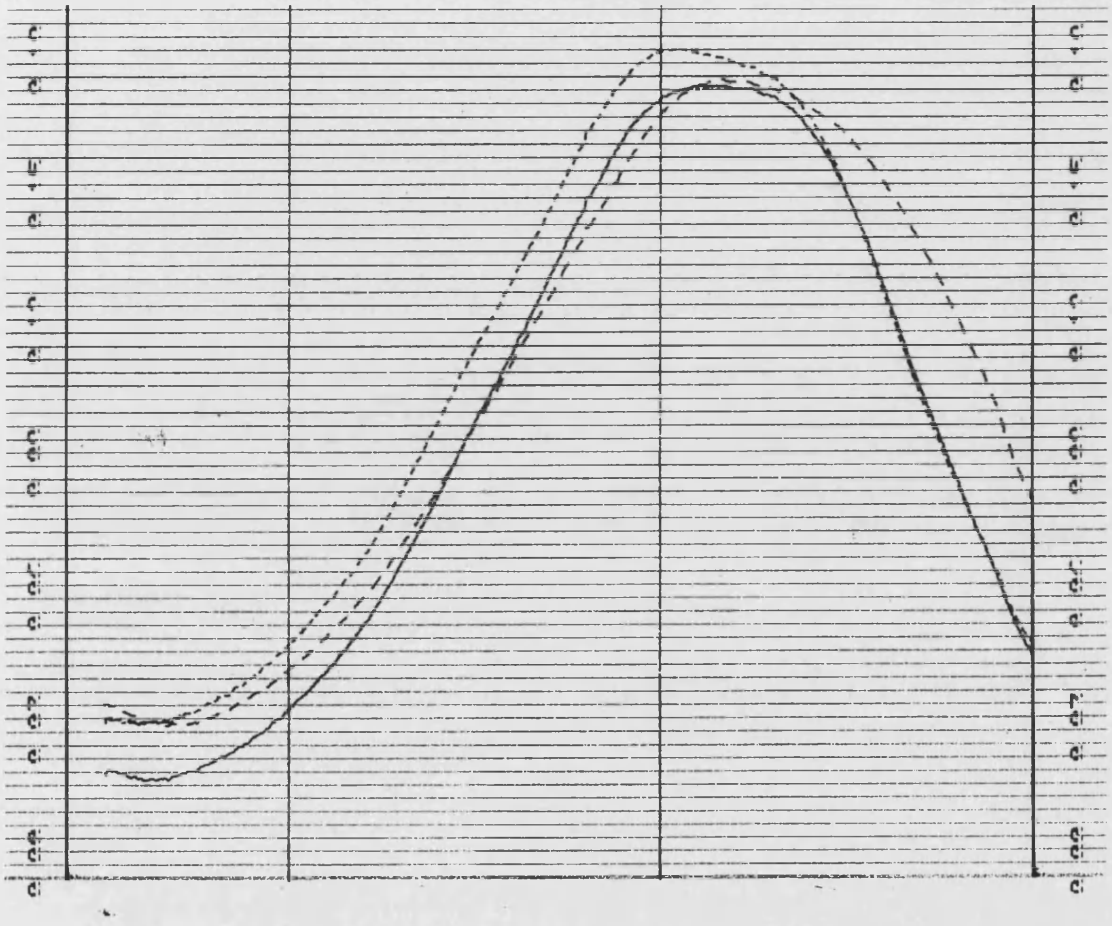

Figure 3.57 : This figure shows overlaid scans of active (chloro - triazine, dotted line) Cibracon Blue F3-GA, deactivated (hydroxy - triazine, solid line) Cibracon Blue F3-GA and Cibracon Blue F3-GA conjugated to a dextran backbone (conjugate 5d8, dashed line).

As a control, spectra of both the active (chloro-triazine) and deactivated (hydroxy triazine) forms of Cibacron Blue F3-GA as well as that of one of the dye-dextran conjugates (5d8) were scanned between 450 and 800 nm. The scans are shown overlaid in **Figure 3.57,**

showing that there are differences between the absorbance spectra of each of the species of dye.

The results for the spectral titrations of free dye and dye-conjugates against LDH are shown in **Figures 3.58 - 3.62.** All titrations were fitted using the mutual depletion model as previously described for lysozyme. The LDH concentration in all titrations was fixed at 2.5 uM LDH (10 uM subunits / binding sites). Dye concentration on the graphs is determined according to the stock solution concentration and the volume of dye solution added. For dye-dextran conjugates this does not take into account the fact that the dye concentration available for binding is probably considerably lower than this. Therefore the actual value of the dye available for binding (**Da**) should be adjusted downwards by a factor (**Fa**) to take account of this. For free dye where all dye is assumed avaialable for binding the value of **Fa** was fixed at 1.0. **Table 3.6** shows the values for the constants used for each of the fits. The available binding site concentration (**Lt**) was fixed at 10 uM and the values for the **Kd** the difference in the extinction coefficients (**ΔE**) allowed to float for each fit.

Table 3.6 : Constants used for mutual depletion fits for titrations vs LDH

	Lt (uM)	Kd (uM)	ΔE ($uM^{-1}cm^{-1}$)	Fa
Free Dye	10.0	1.68	0.0038	1.0
T40.5	10.0	1.89	0.0040	0.70
T40.10	10.0	2.57	0.0041	0.61
T40.20	10.0	0.84	0.0029	0.55
T124.5	10.0	0.83	0.0028	0.28

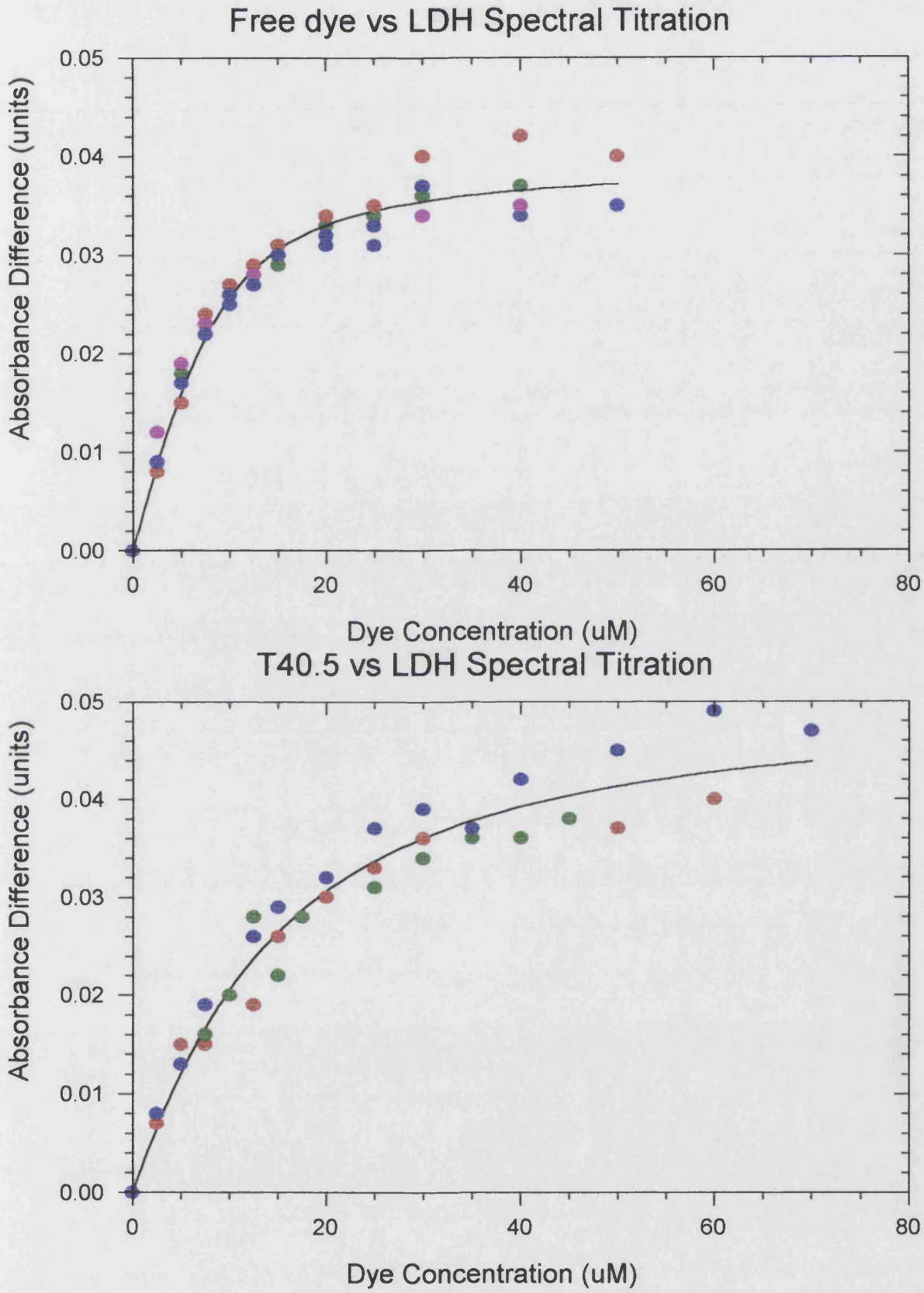

Figures 3.58, 3.59 : Difference binding curves produced by titrating dye or dye-dextran against a fixed concentration (8 uM Subunits) of LDH at 25 C. Values were taken at the maxima of 660 nm for free dye (top) and 650 nm for T40.5 (bottom). Individual datasets are shown in colour and the fitted curve in black.

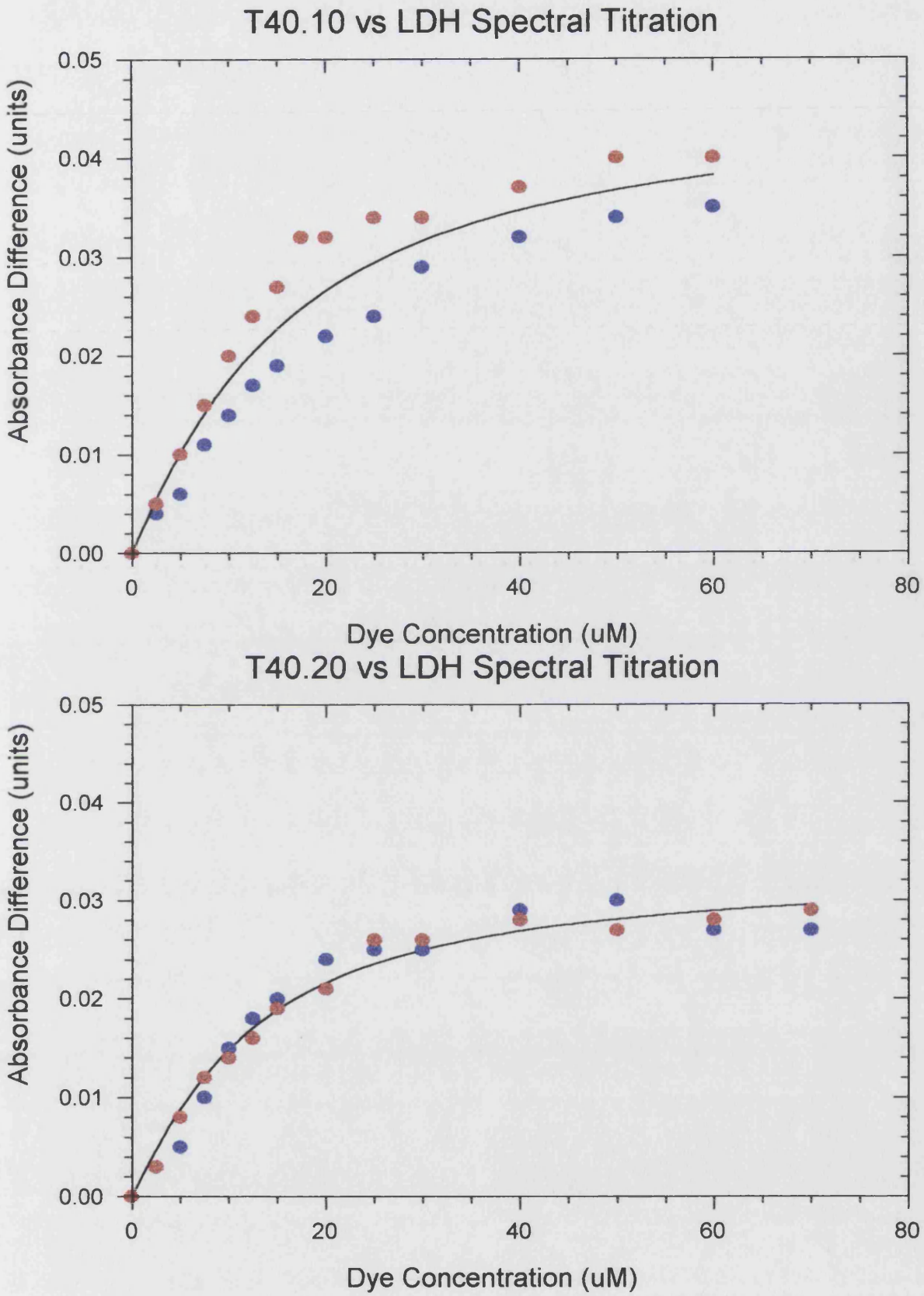

Figures 3.60, 3.61 : These figures show the difference binding curves produced by dye-dextran conjugates T40.10 (top) and T40.20 (bottom) against a fixed concentration (8 uM Subunits) of LDH at 25 C. Values were taken at the maxima of 650 nm. Individual datasets are shown in colour and the fit to the data in black.

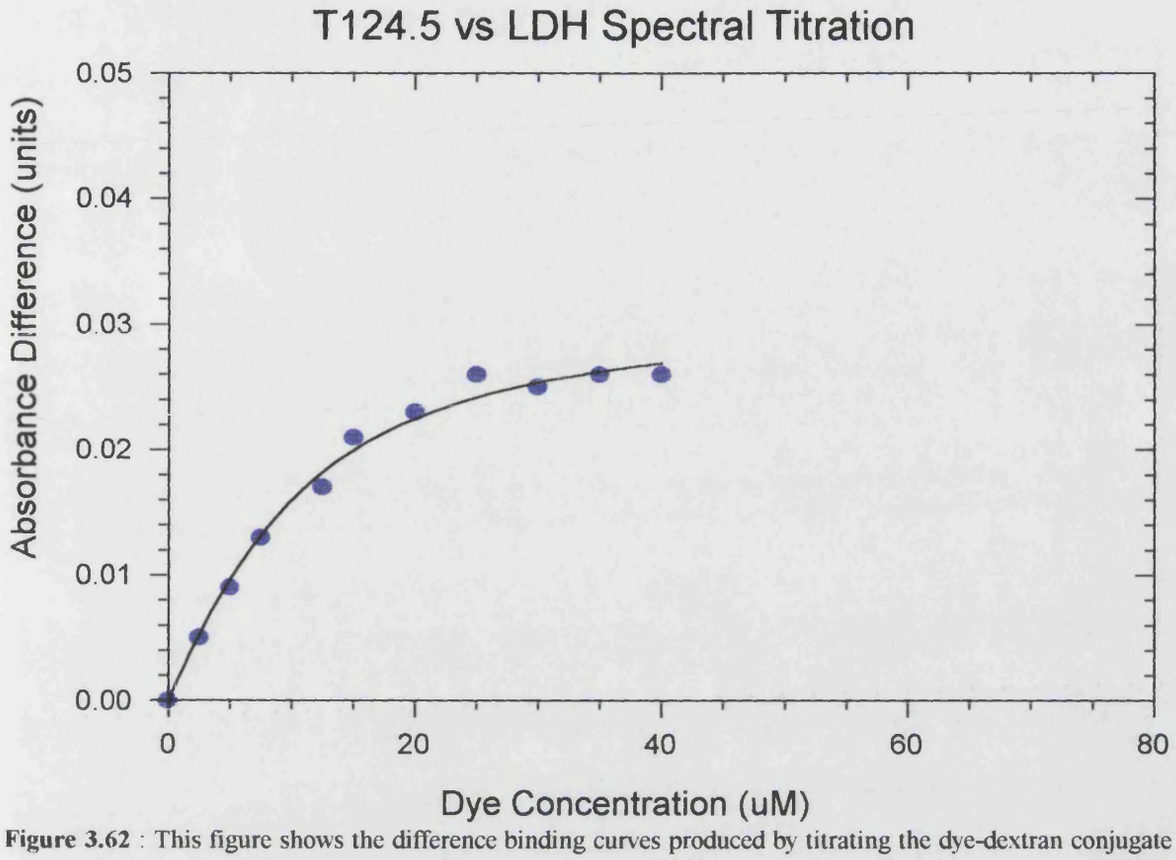

Figure 3.62 : This figure shows the difference binding curves produced by titrating the dye-dextran conjugate T124.5 against a fixed concentration (8 uM Subunits) of LDH at 25 C. Values were taken at the maxima of 650 nm. The dataset is shown in colour and the fit to the data in black.

The results for the titrations in which dye or dye-dextran were titrated against LDH are shown in **Figures 3.63 - 3.67**. As for the previous titrations these were again fitted to the mutual depletion model, the only difference being that the fixed concentration is now that of the dye and the LDH concentration is varied. For the fits **Lt** therefore now represents the available dye concentration. The constants used for the fits are shown in **Table 3.7.**

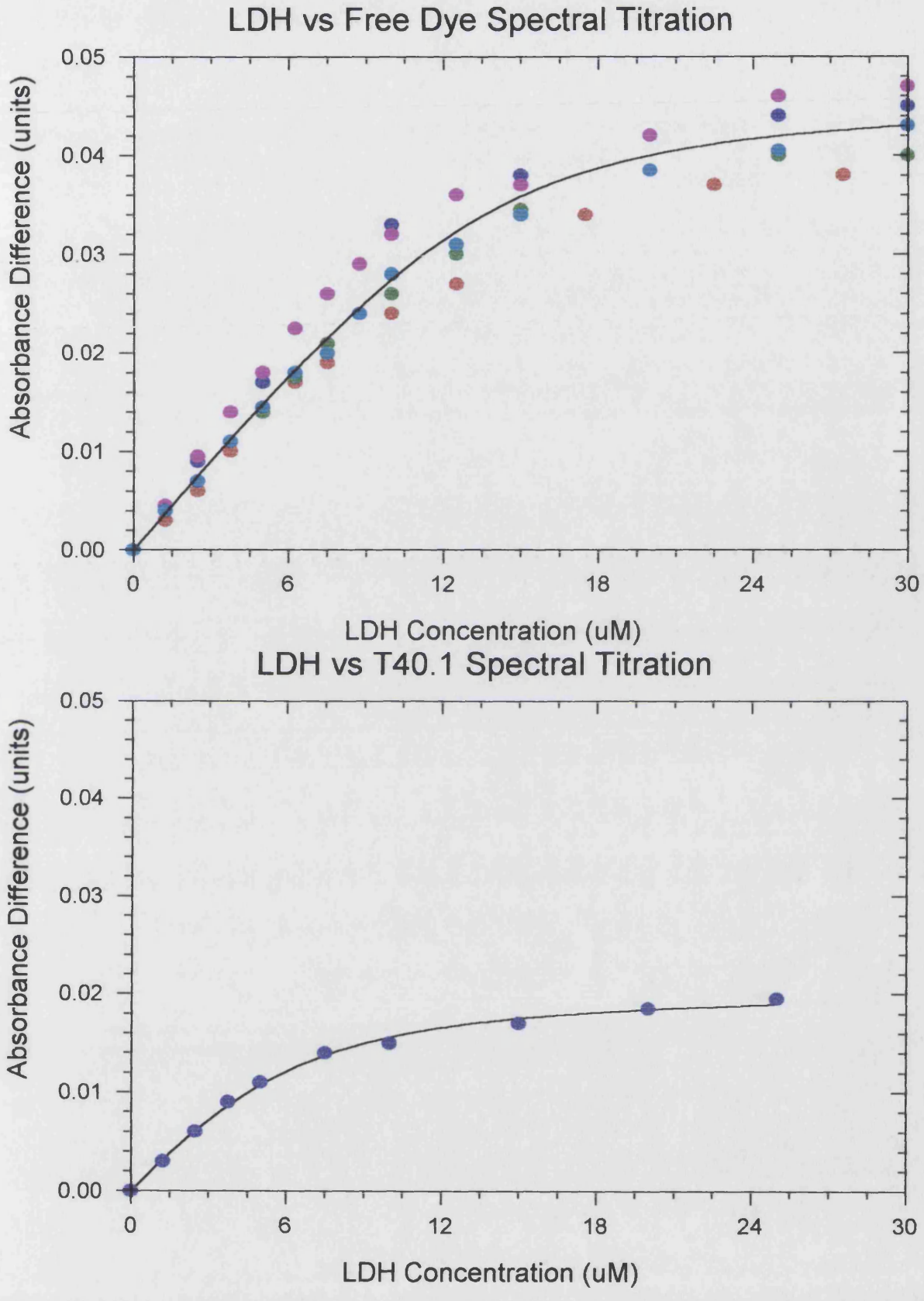

Figures 3.63,3.64 : Difference binding curves produced by titrating LDH (1mM subunits stock) against a fixed concentration (20 uM) of dye or dye-dextran at 25 C. Values were taken at the maxima of 660 nm for free dye (top) and 650 nm for T40.1 (bottom). Individual datasets are shown in colour and the fit to the data in black.

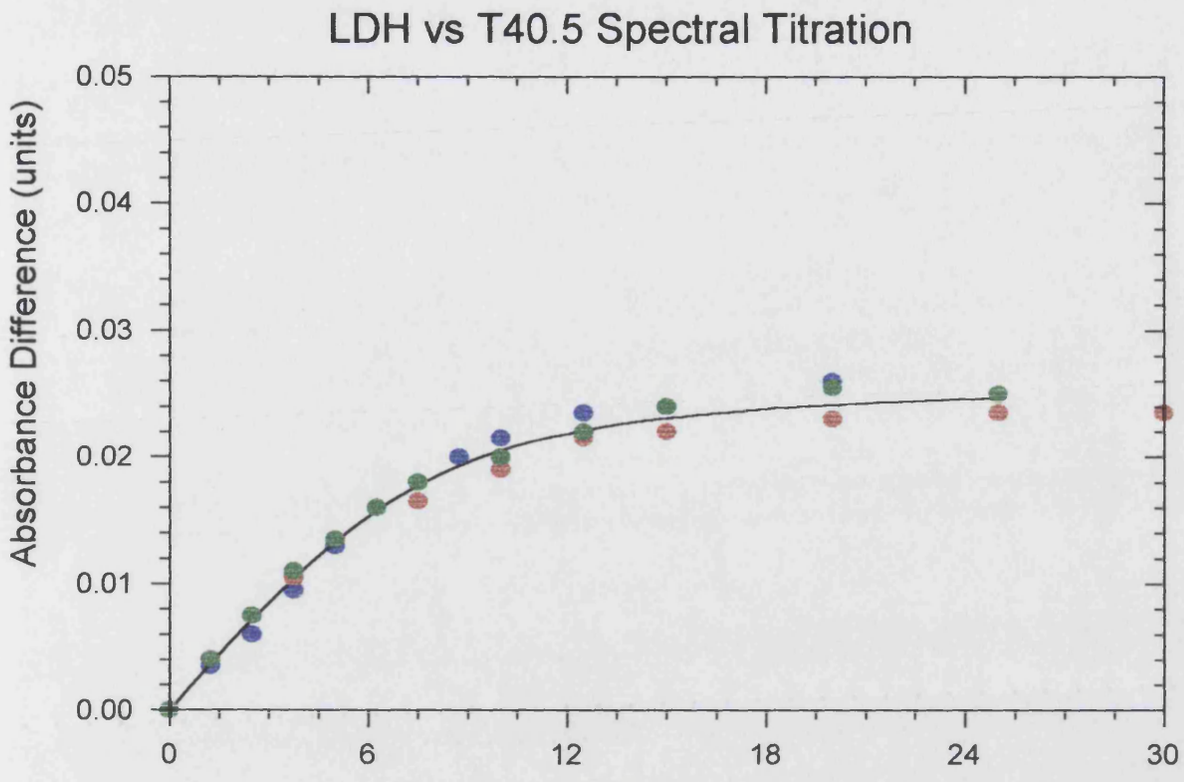

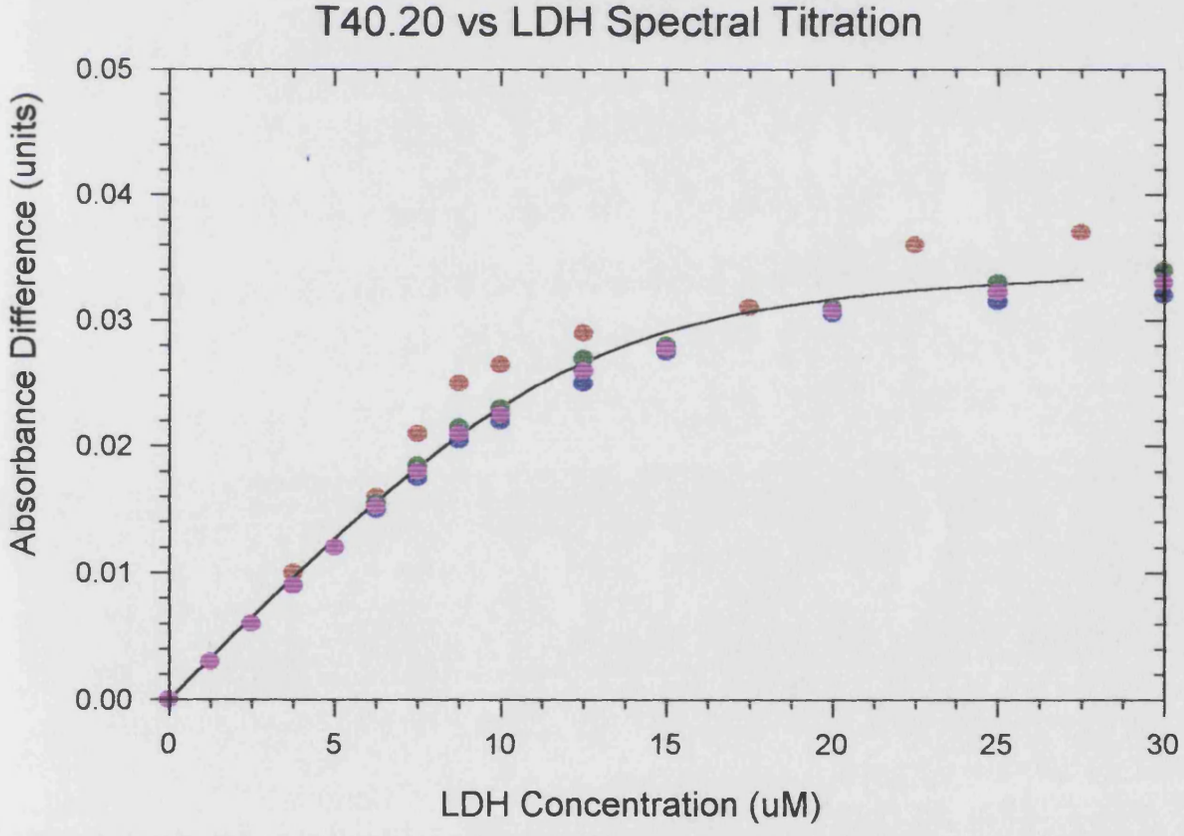

Figures 3.65,3.66 : Difference binding curves produced by titrating LDH (1mM subunits stock) against a fixed concentration (20 uM) of dye-dextrans T40.5 and T40.20 at 25 C. Values were taken at the maxima of 650 nm. Individual datasets are shown in colour and the fit to the data in black.

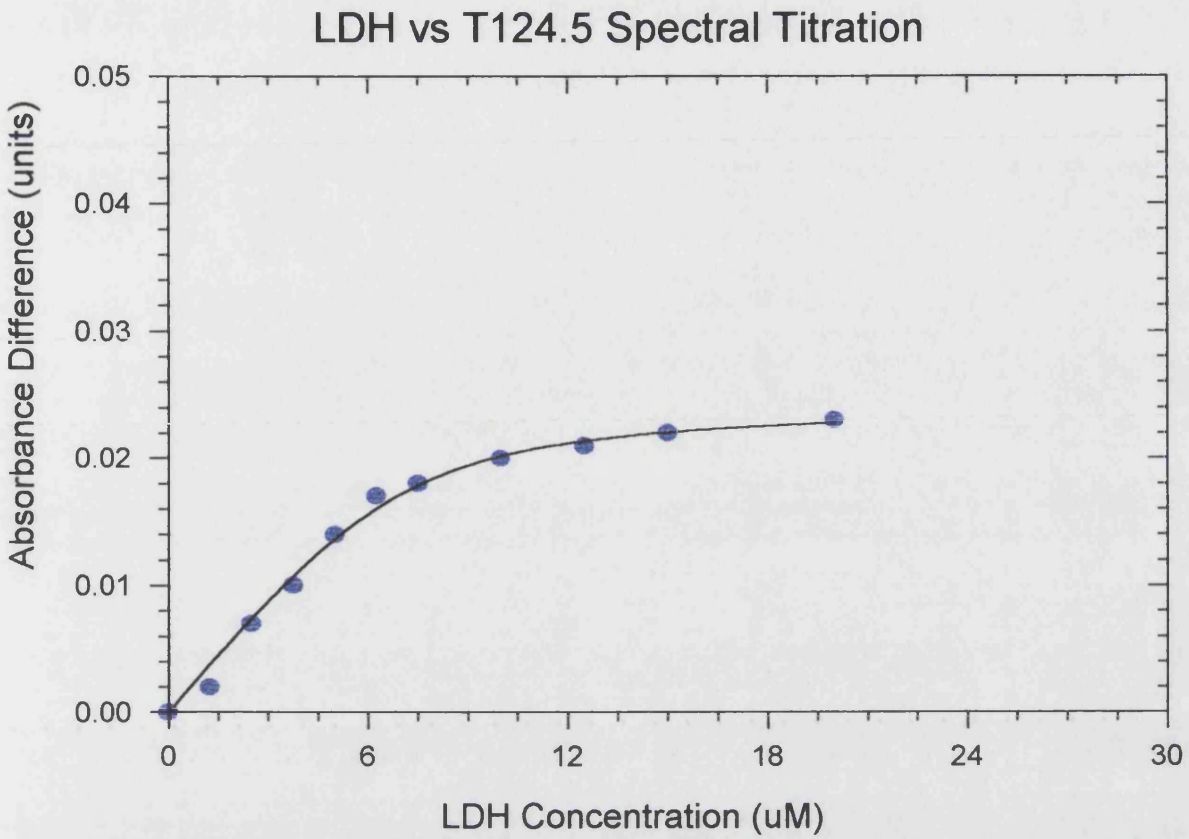

Figure 3.67 : Difference spectra produced by titrating LDH (1mM subunits stock) against a fixed concentration (20 uM) of dye-dextran T124.5 at 25 C. Values were taken at the maxima of 650 nm. Individual datasets are shown in colour and the fit to the data in black.

Table 3.7 : Constants used for mutual depletion fits for titrations vs dye

	Da (uM)	**Kd** (uM)	$\Delta E(uM^{-1}cm^{-1})$	**Fa**
Free Dye	13.7	1.23	0.0034	1
T40.1	5.92	1.81	0.0035	0.30
T40.5	7.52	1.16	0.0035	0.38
T40.20	12.2	1.10	0.0029	0.61
T124.5	6.92	0.848	0.0035	0.35

Once it had been determined that there were observable spectral kinetics of the dye-dextran protein interaction at 4 C it was therefore prudent to determine if the large decrease in rate from 25 C to 4 C also effected the equilibrium binding as measured using the spectral titration.

The results of the titrations of the two T40 series conjugates and the two 2D series conjugates used for the kinetic work are shown in **Figures 3.67 -3.70**. The titration curves were again fitted using the mutual depletion model as for the similar titrations at 25 C shown previously. The determined constants for the fits for the T40 series are shown in **Table 3.8** and those for the 2D series are shown in **Table 3.9**.

Table 3.8 : Constants used for mutual depletion fits for titrations vs T40 series at 4 C

	Da (uM)	**Kd** (uM)	ΔE ($uM^{-1}cm^{-1}$)	**Fa**
T40.1	11.5	2.33	0.0022	0.58
T40.20	13.3	1.18	0.0024	0.67

Table 3.9 : Constants used for mutual depletion fits for titrations vs 2D series at 4 C

	Da (uM)	**Kd** (uM)	ΔE ($uM^{-1}cm^{-1}$)	**Fa**
2D4	12.6	1.20	0.0030	0.63
2D9	10.45	1.06	0.0032	0.52

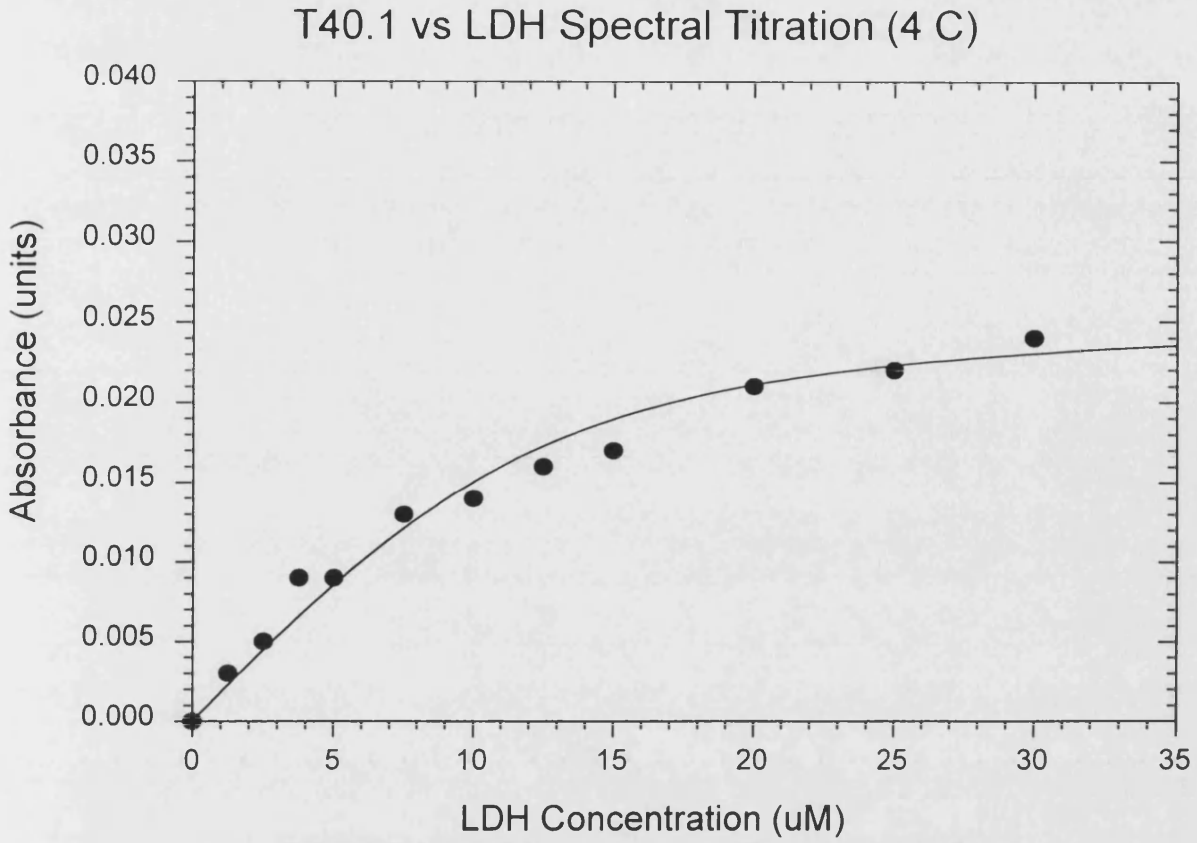

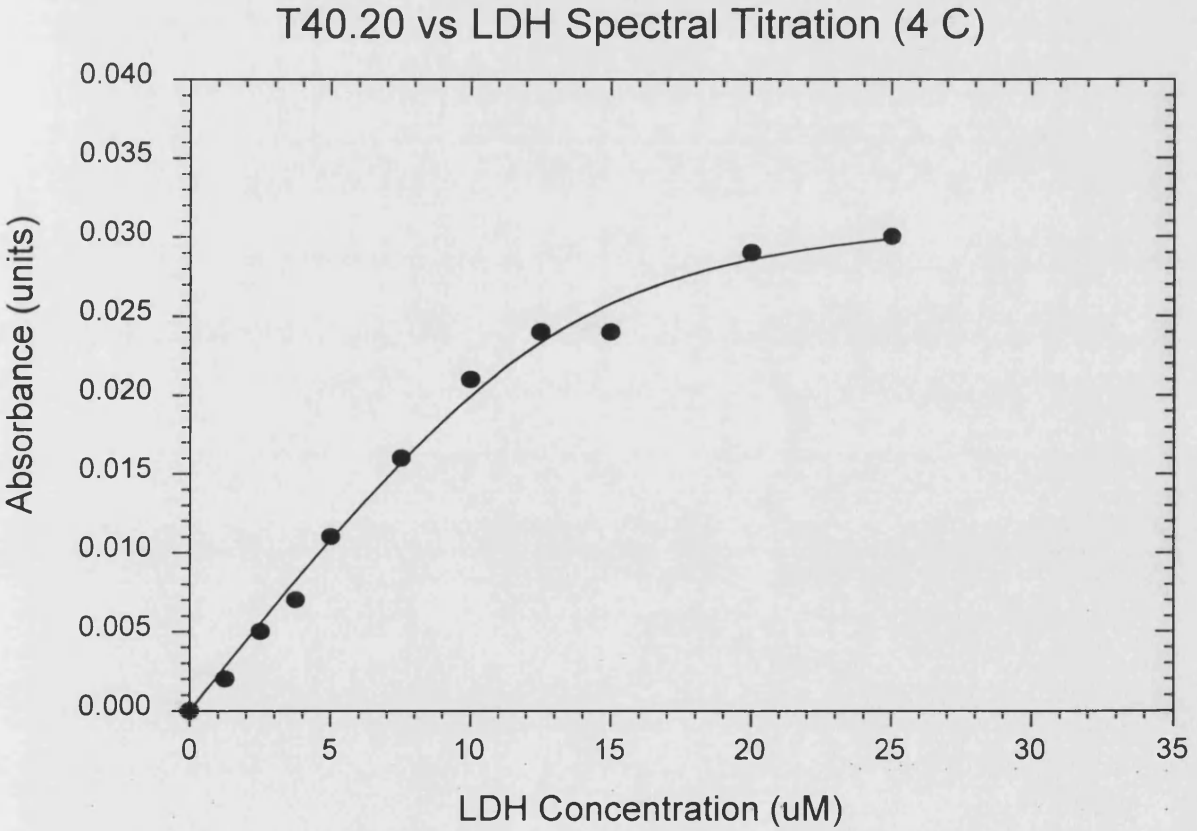

Figures 3.67, 3.68 : Difference spectra produced by titrating LDH (1mM subunits stock) against a fixed concentration (20 uM) of dye-dextrans T40.1 and T40.20 at 4 C. Values were taken at the maxima of 650 nm. Datasets are shown as points with the fit to the data as the solid line.

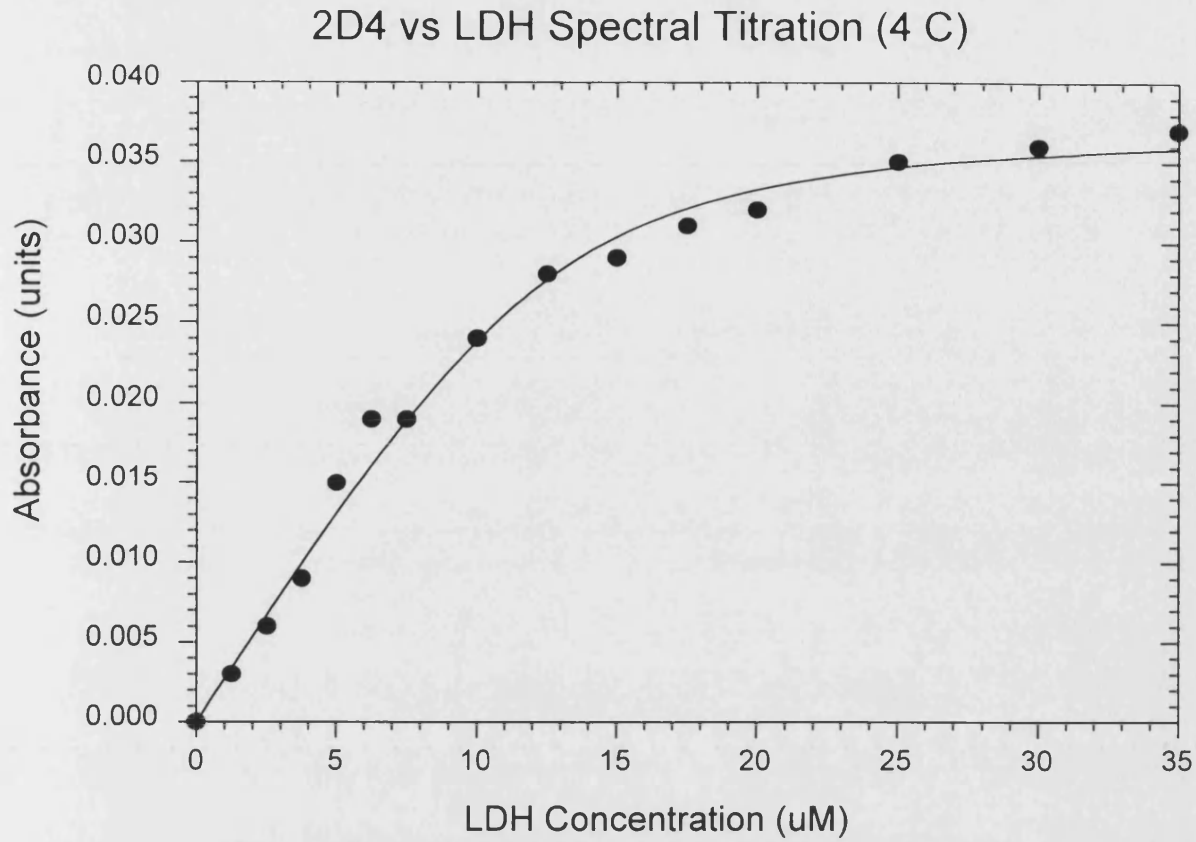

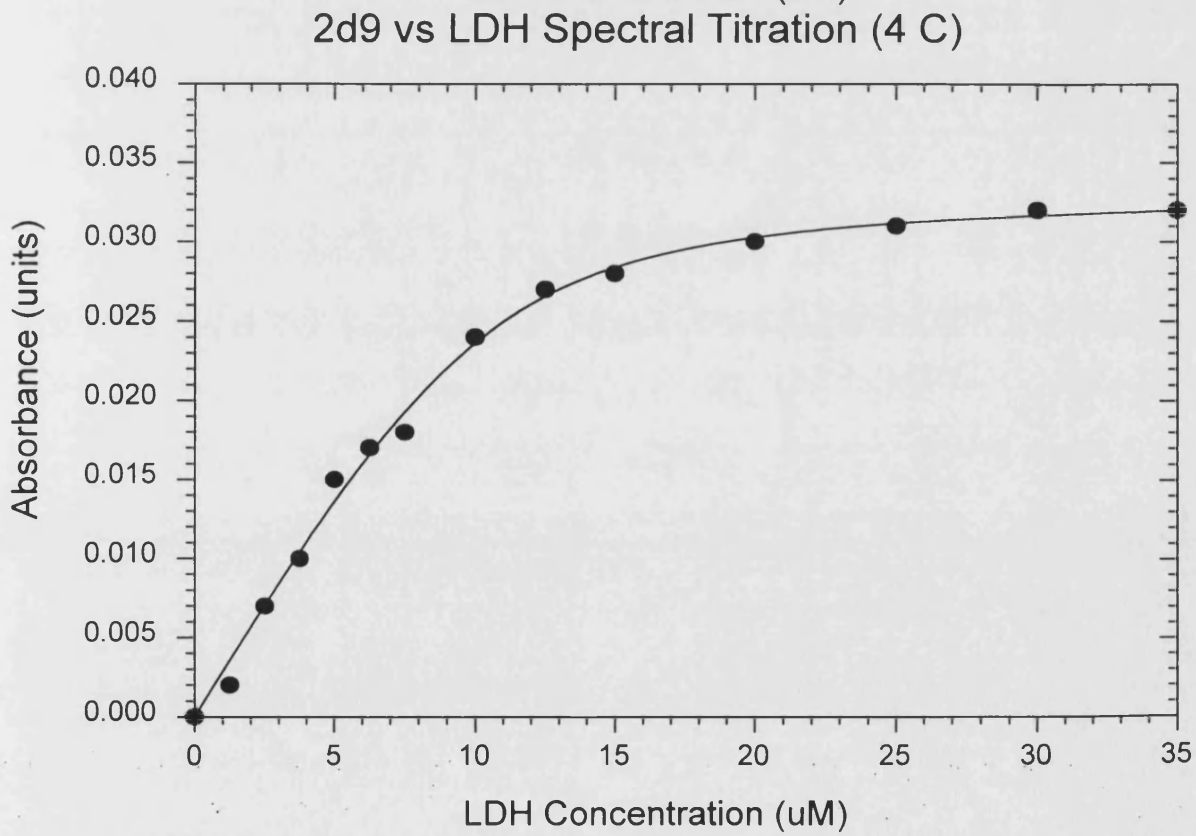

Figures 3.69,3.70 : Difference spectra produced by titrating LDH (1mM subunits stock) against a fixed concentration (20 uM) of dye-dextrans 2D4 and 2D9 at 4 C. Values were taken at the maxima of 650 nm. Datasets are shown as points with the fit to the data as the solid line.

3.10 Dye-Glucose Spectral Titration

The spectral titration of dye-glucose with LDH is shown in **Figure 3.71.** It can be seen by comparison with the spectral titration of free Cibacron Blue F3-GA shown in **Figure 3.55** that the difference spectrum produced is essentially unchanged from that observed with the free dye. The spectra still have the significant hypochromic shift centred at approximately 540 nm which is the major difference between that of the free-dye and that observed for a dye-dextran conjugate as shown in **Figure 3.56**.

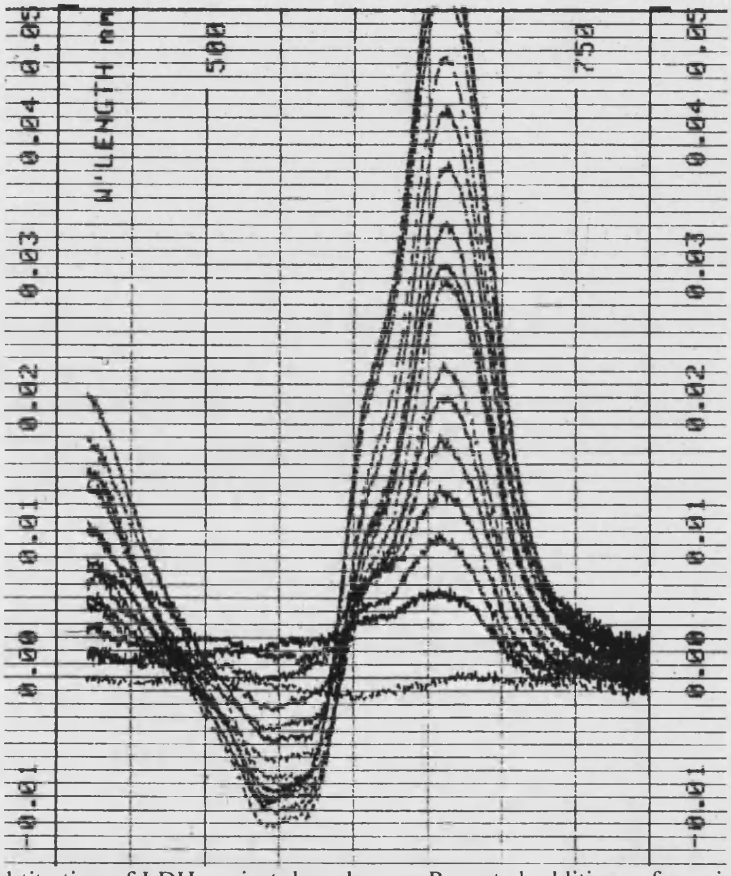

Figure 3.71 : Spectral titration of LDH against dye-glucose. Repeated additions of varying quantities of 1 uM LDH stock were made to the sample cuvette whilst buffer only was added to the reference. The difference spectrum from 420 - 800 nm was scanned after each addition.

The magnitude of the hyperchromic peak at 660 nm was used to produce a binding curve and the data fitted to the mutual depletion model as for the previous titrations. The data and curve fit produced are shown in **Figure 3.72**. The values for the constants determined for the curve fit are shown in **Table 3.10**.

Table 3.10 : Constants for mutual depletion fits for dye-glucose titration vs LDH at 25 C

	Lt (uM)	**Kd** (uM)	**ΔE** ($uM^{-1}cm^{-1}$)
Dye-Glucose	31.0	2.17	0.0017

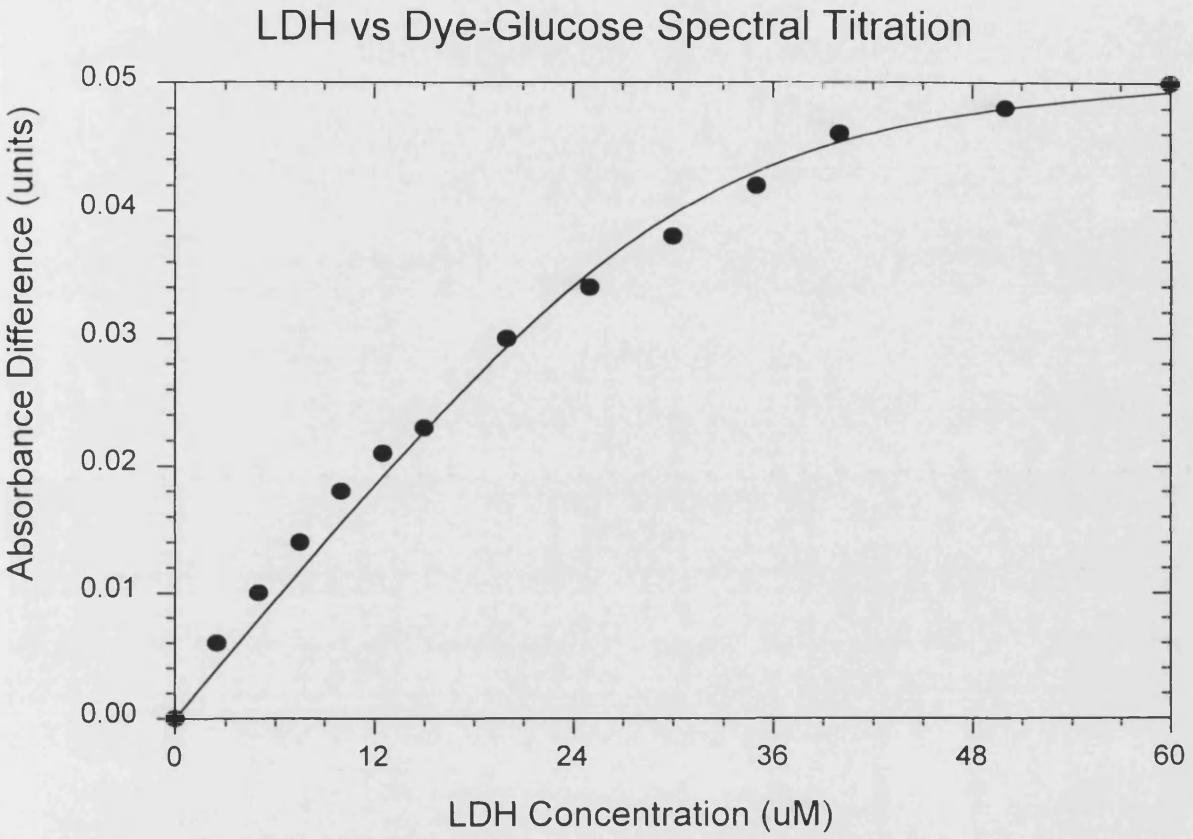

Figure 3.72 : Difference binding curve produced by titrating LDH (1mM subunits stock) against a fixed concentration (20 uM) of dye-glucose at 25 C. Values were taken at the maxima of 660 nm. Datasets are shown as points with the fit to the data as the solid line.

3.11 Fluorescence titrations

The results from the fluorescence titrations are a set of fluorescence values versus concentration of dye or dye conjugate added. These are then converted to the absolute difference in fluorescence versus dye concentration. The raw data is first corrected for both the dilution effect of the addition of the dye containing solution and the effect of dye absorbance at the excitation and emission wavelengths (inner filter effect) as explained in the discussion (**section 4.10**). The corrected data are then converted into an absolute difference from the initial value which is then used for fitting.

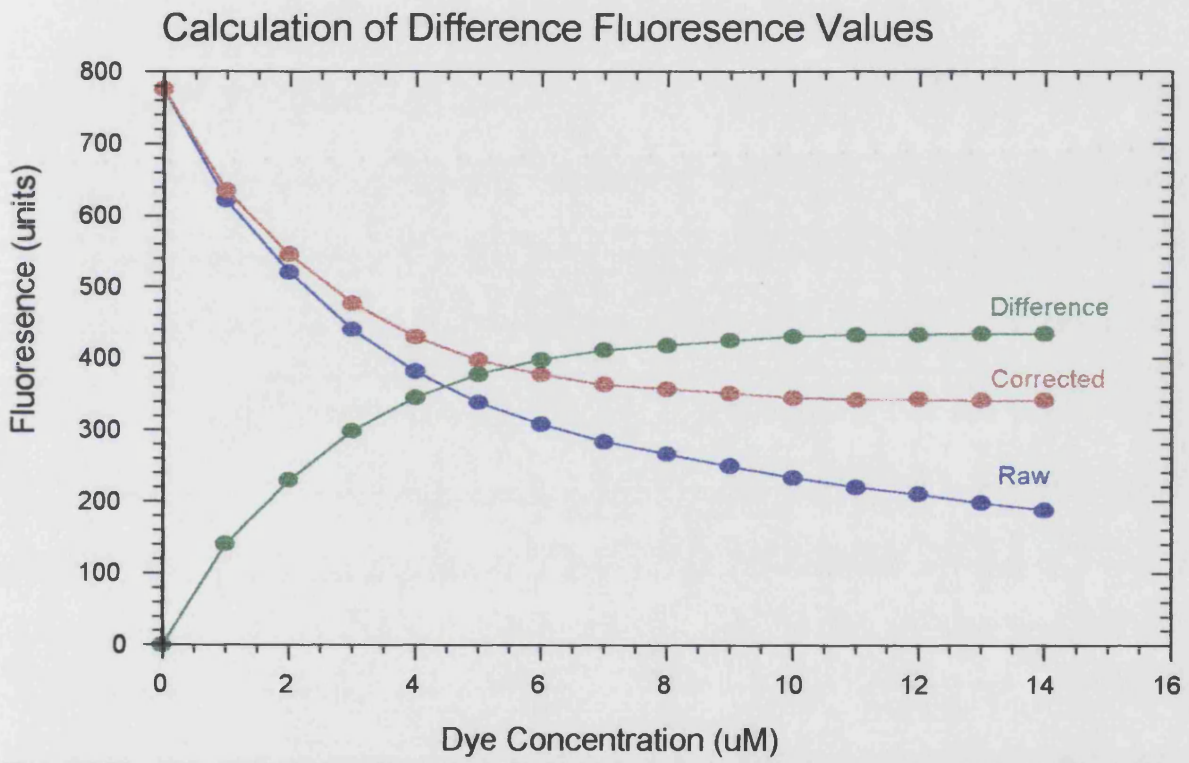

Figure 3.73 : This shows the raw data from a fluorescence titration, the data then corrected for dilution effects due to the addition of dye and the inner filter effect caused by the absorbance of the dye, and finally the absolute difference of the corrected data.

The data from these fluorescence titration experiments is shown in the following figures (**Figures 3.74 - 3.78**). Each figure shows a set of titrations of dye-dextran conjugates with different loadings of dye on a single backbone size. The datasets for each dye loading are

represented as sets of points of a single colour, with the fitted curve being shown as a solid line in the same colour.

It can be seen that the reproducibility of the experiments is good, with for the most part only minor variations between repetitions of each experiment.

The data were curve fitted to the mutual depletion model which is essentially the same as that used for the spectral titration shown previously, but in this case in place of the **ΔE** term, the term **ΔF** is used. This represents the change in fluorescence per micromole on dye binding. The constants determined for the curve fits are shown in **Tables 3.11-3.14.**

It can be seen that as the dye loading increases, the half saturation concentration decreases, indicating a stronger affinity for the higher loadings which agrees the published results from the spectral titrations of dye - dextran conjugates with lysozyme[25,39,48].

Table 3.11 : Constants for fits for free dye and T40 series fluorescence titrations vs LDH

	Lt (uM)	**Kd** (uM)	**ΔF** (uM^{-1})
Free Dye	2.05	0.39	234
T40.1	2.05	3.04	188
T40.2	2.05	4.64	204
T40.5	2.05	2.51	255
T40.10	2.05	1.25	249
T40.20	2.05	1.63	233

Table 3.12 : Constants for fits for T73 series fluorescence titrations vs LDH

	Lt (uM)	**Kd** (uM)	**ΔF** (uM^{-1})
T73.1	2.05	1.59	222
T73.2	2.05	1.16	224
T73.5	2.05	1.00	252

Table 3.13 : Constants for fits for T124 series fluorescence titrations vs LDH

	Lt(uM)	**Kd**(uM)	Δ**F**(uM^{-1})
T124.1	2.05	1.10	223
T124.2	2.05	0.77	239
T124.5	2.05	0.66	242

Table 3.14 : Constants for fits for 2D series fluorescence titrations vs LDH

	Lt(uM)	**Kd**(uM)	Δ**F**(uM^{-1})
2D4	2.05	1.74	270
2D9	2.05	0.95	307

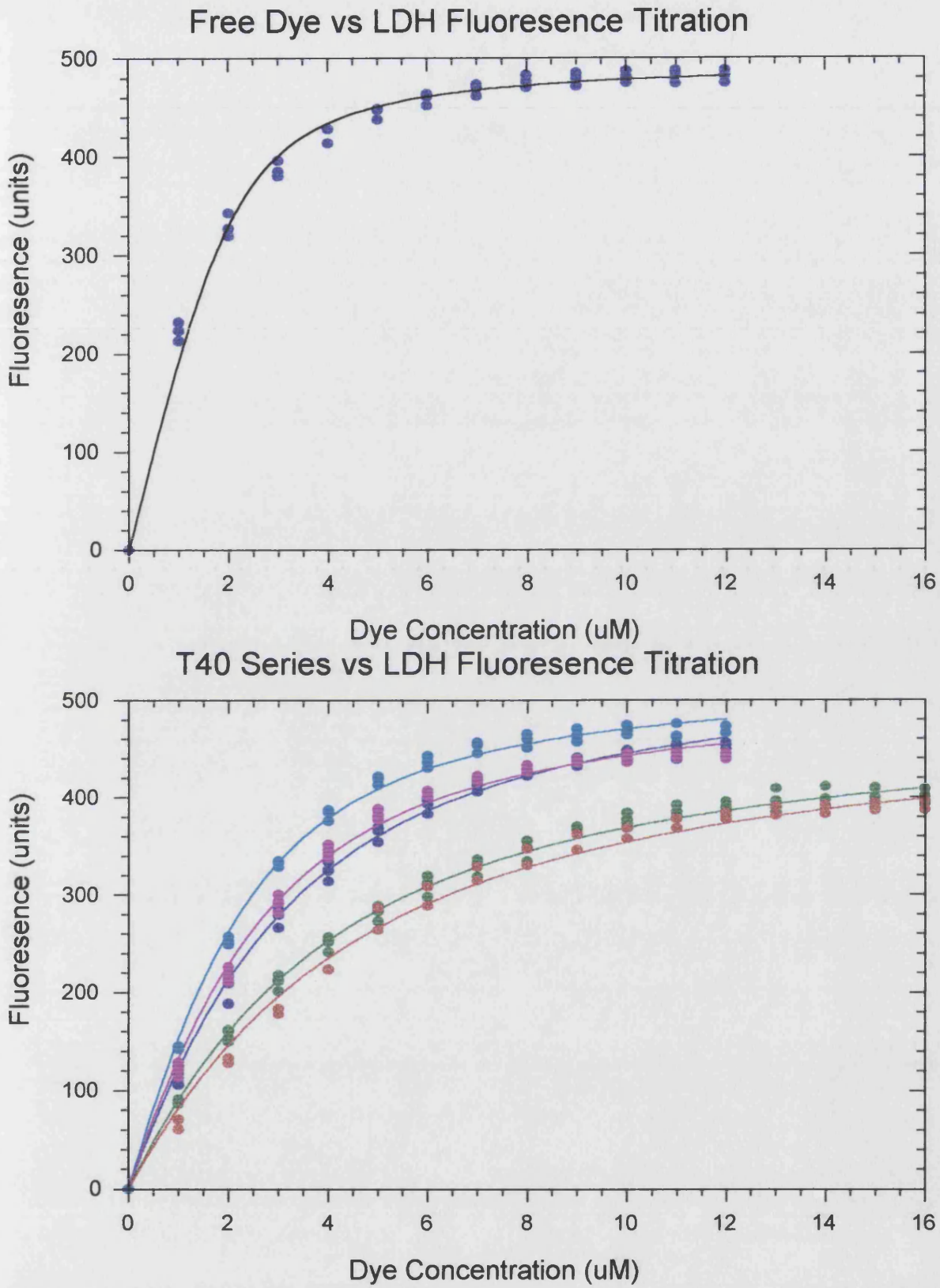

Figures 3.74, 3.75 : Fluorescence titrations for Free Dye (top) and T40 dye-dextrans (bottom). Titrations measured quenching of 2.05 uM LDH fluoresence by the addition of small volumes of 200 uM stock solutions. Quenchcing curves were corrected for the inner filter effect of the dye and shown as a difference curve. T40.1, T40.2, T40.5, T40.10 and T40.20 datasets are shown in red, green, blue, magenta and cyan respectively

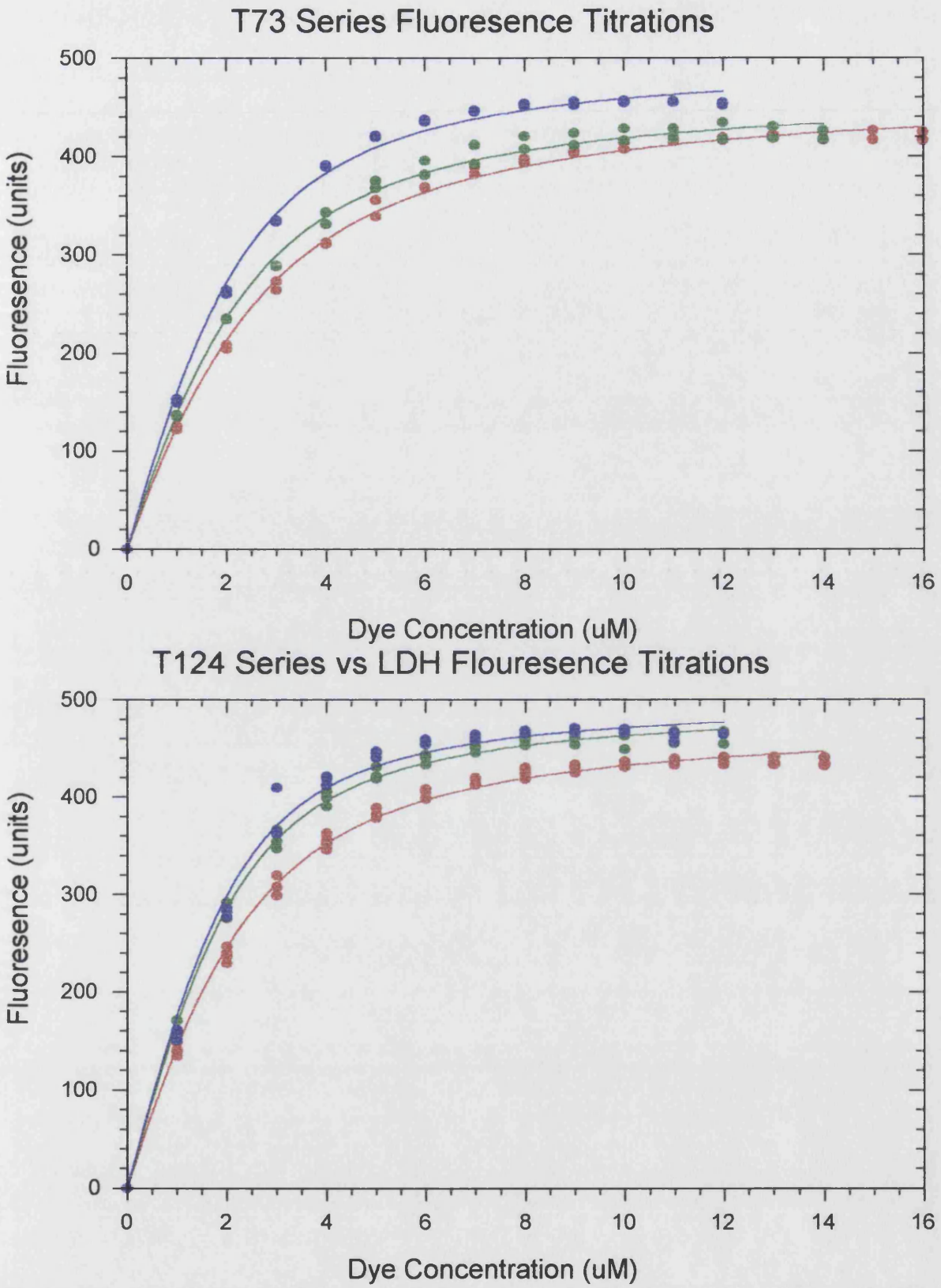

Figures 3.76, 3.77 : Fluorescence titrations for the dye-dextran series T73 (top) and T124 (bottom). Titrations measured quenching of 2.05 uM LDH by the addition of small volumes of 200 uM stock solutions. Quenching curves were corrected for the inner filter effect of the dye and shown as a difference curve from the initial value. T70.1, T70.2 and T70.5 (likewise T124.1, T124.2, T124.5) are shown in red, green, blue respectively

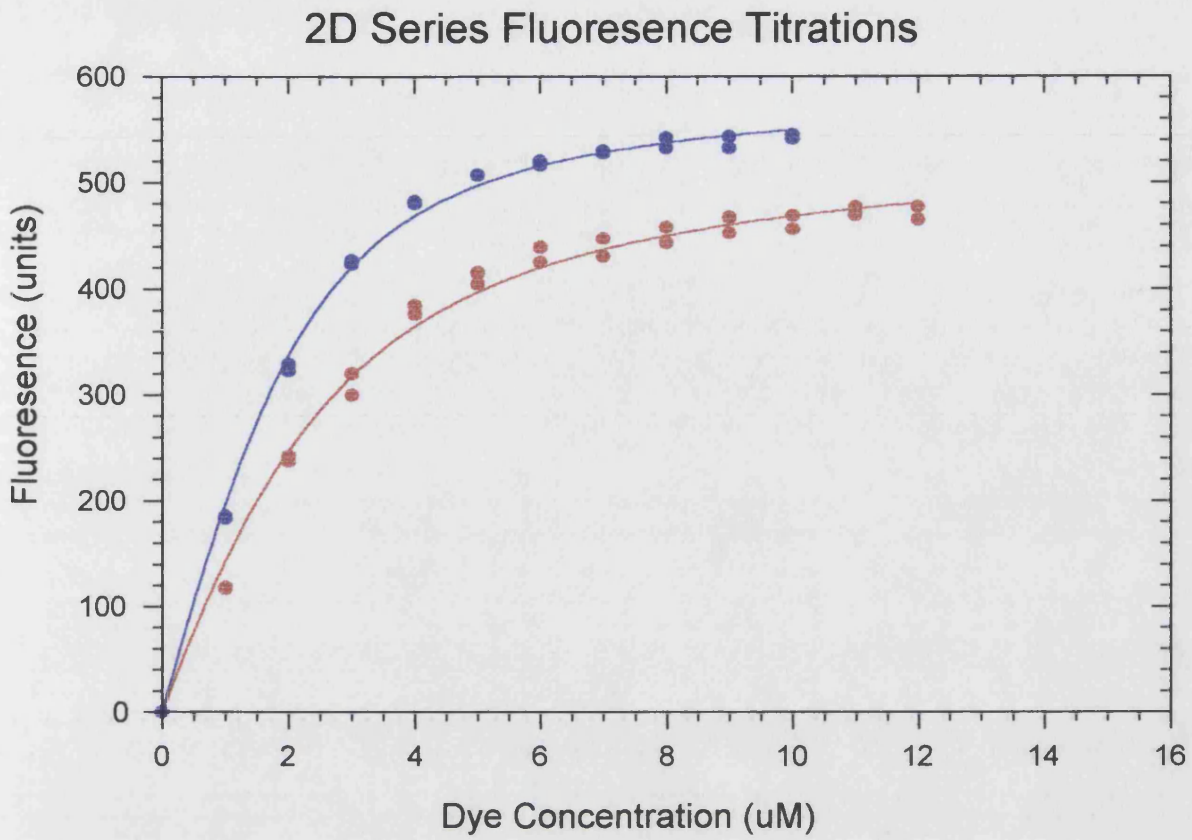

Figure 3.78 : Fluorescence titrations for the 2D dye-dextran series. Titrations measured quenching of 2.05 uM LDH by the addition of small volumes of 200 uM (dye concentration) stock solution. The quenching curve was corrected for the inner filter effect of the dye and shown as a difference curve from the initial value. Datasets shown are for 2D4 (red) and 2D9 (blue)

3.12 Fluorescence Titration with Thermophyllic Glucose Dehydrogenase

The unexpectedly fast and initially unobservable binding kinetics observed for the interaction of dye and dye-dextran conjugates with LDH and ADH showed that these proteins were not ideal models for studying the interaction of dye ligands with proteins. A possible source of an alternative dehydrogenase, Glucose Dehydrogenase from *Thermoplasma Acidophilum* available. This was attractive as a possible model protein as being a thermophyllic enzyme it would be expected to be less functional at 25 C than a comparable mesophyllic enzyme, hopefully producing measurable dye-binding kinetics at this temperature.

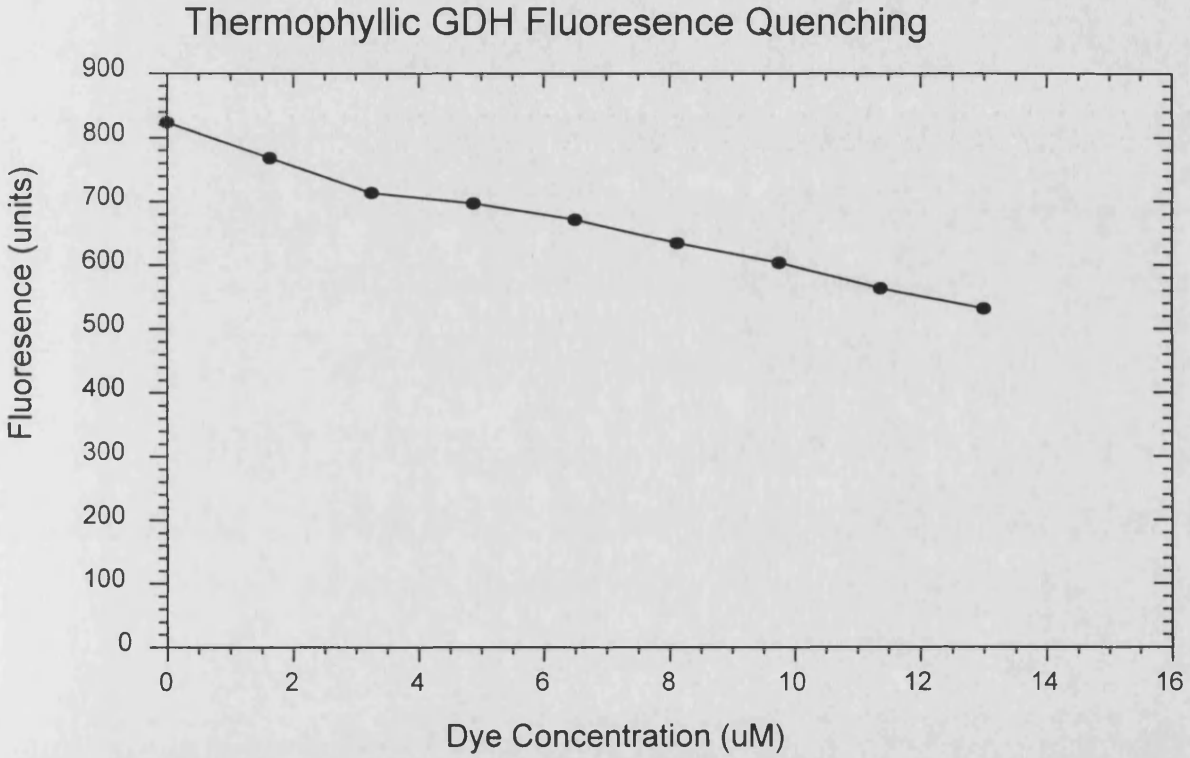

Figure 3.79 : Fluorescence titration for thermophyllic GDH with free dye. Titrations measured quenching of 3.0 uM GDH by the addition of small volumes of 325 uM stock dye solution. The quenching curve can be accounted for purely by the inner filter effect of the dye and the dilution effect of the additions.

Due to the comparatively small quantities of protein initially available a fluorescence quenching experiment was used to determine the suitability of the protein for further studies. The results of a fluorescence titration with free Cibacron Blue F3-GA are shown in **Figure**

3.79. The protein does not appear to bind dye in a manner producing any quenching of fluorescence, the apparent quenching being accountable purely by the inner filter effect due to the absorbance of the dye added and the dilution effect of the additions.

3.13 Dye - Dextran Rapid Spectral Kinetics with LDH

The kinetics of binding of dye-dextran conjugates to dye and dye-dextrans to LDH were initially measured under conditions similar to those used for the equilibrium spectral titrations. Measurements were made using a Hi-Tech Scientific SF-61 Stop-Flow machine set up using the diode array option for spectral scanning, allowing the monitoring of multiple wavelengths.

From the equilibrium experiments it was expected to see a hyperchromic shift with a maximum at around 660 nm for the free dye with a small hypochromic shift at around 550 nm, and a hyperchromic shift at around 660 nm with no hypochromic shift for the dye-dextrans.

Initial conditions were determined to give final concentrations in the observation cell of 25 uM dye and 120 uM sub-unit concentration of LDH (approx. 4 mg/ml) in 50 mM sodium phosphate buffer pH 7.9 at 25 C. With an effective excess of LDH by a factor of at least 5 (assuming 100 percent dye availability), this should approximate roughly to a pseudo first order reaction with respect to dye.

The initial experiments with free dye showed no detectable change in the observed absorbance at the expected wavelengths. It was thought that this was probably due to the free dye binding reaching completion within the dead time of the stop flow.

In an attempt to reduce the rate of reaction and hence produce observable kinetics the concentration of both reactants was reduced. The limiting factor in reducing the concentration is the fact that the absorbance changes being measured are not large (in the region of 0.03 - 0.06 absorbance units). Thus there is little scope for lowering the concentration of reactants before the absorbance change produced will be reduced below the detection limits of the apparatus. Halving the concentration of dye and reducing the concentration of LDH by a

factor of ten should produce a reduction in rate of just over an order of magnitude , presuming a reaction which is first order in relation to both reactants. These conditions should still produce an absorbance change of around half the magnitude initially expected, which would still be detectable. Stop-flow experiments using these revised conditions still showed no detectable change in absorbance, the reaction still apparently reaching completion within the dead time of the instrument and too fast to yield measurable kinetics.

Similar experiments were then repeated with the T40.20 dye dextran conjugate.The results of these experiments again showed that there was no measurable spectral change upon mixing indicating that the reaction was reaching completion within the dead time of the instrument (approximately 1.5 ms). The use of a lower pH (6.5) which might be less favourable for binding also failed to reduce the rate to observable levels.

A trial using horse liver ADH in place of LDH under similar conditions as those used initially for LDH showed that this too did not yield any measurable spectral changes upon mixing.

It was then discovered that by reducing the temperature to 4 C the reaction rate was lowered sufficiently to yield measurable kinetics. The difference spectrum produced by the binding of LDH (96 uM subunits) to dye-dextran conjugate T40.20 (25 uM) is shown in **Figure 3.80**. This difference spectrum is produced by subtracting the initial scan from all the subsequent scans in the same manner as for the lysozyme rapid kinetic datasets shown in **Figures 3.33, 3.34**. Comparison of the shape of the spectrum with that shown in **Figure 3.56** for the equilibrium titration shows that the spectrum appears essentially identical to the kinetically produced difference spectra.

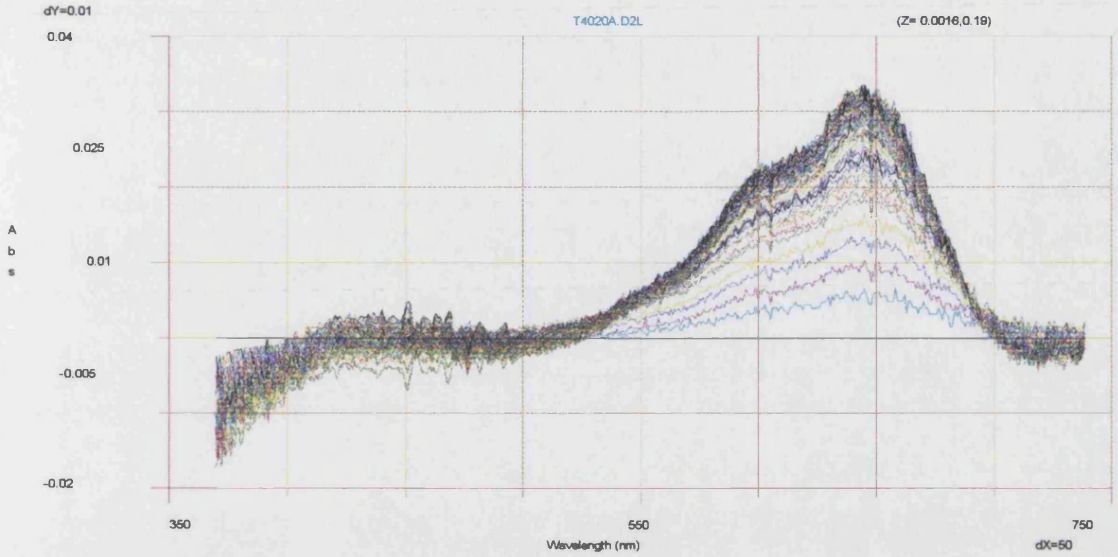

Figure 3.80 : Multiple wavelength kinetics of T40.20 binding to LDH. Final concentrations are 25 uM T40.20 dye-dextran and 96 uM LDH (subunits).The spectra shown are difference spectra produced by subtracting the initial spectrum taken from the rest.

Rapid kinetic measurements were then recorded over a range of differing concentrations of LDH at the same dye concentration for a range of dye-dextrans. For these kinetic measurements datasets were recorded at a single wavelength of 650 nm, corresponding to the maximum in the difference spectrum. Single wavelength measurements using a photomultiplier have several advantages over the usage of the diode array both in terms of the number of data points collected, the resolution and the signal to noise ratio.

The data were transformed into the absolute difference from the starting point and are shown in **Figure 3.81-3.86**. Each figure shows kinetic data taken at four LDH concentrations (6, 12, 24 and 48 uM) for a single dye-dextran conjugate at 20 uM.

Even at 4 C and the lowest concentrations of LDH and free Cibracon Blue F3-GA no observable difference in absorbance could be kinetically measured, the reaction having reached completion within the mixing time (approx. 1 ms) of the stop-flow.

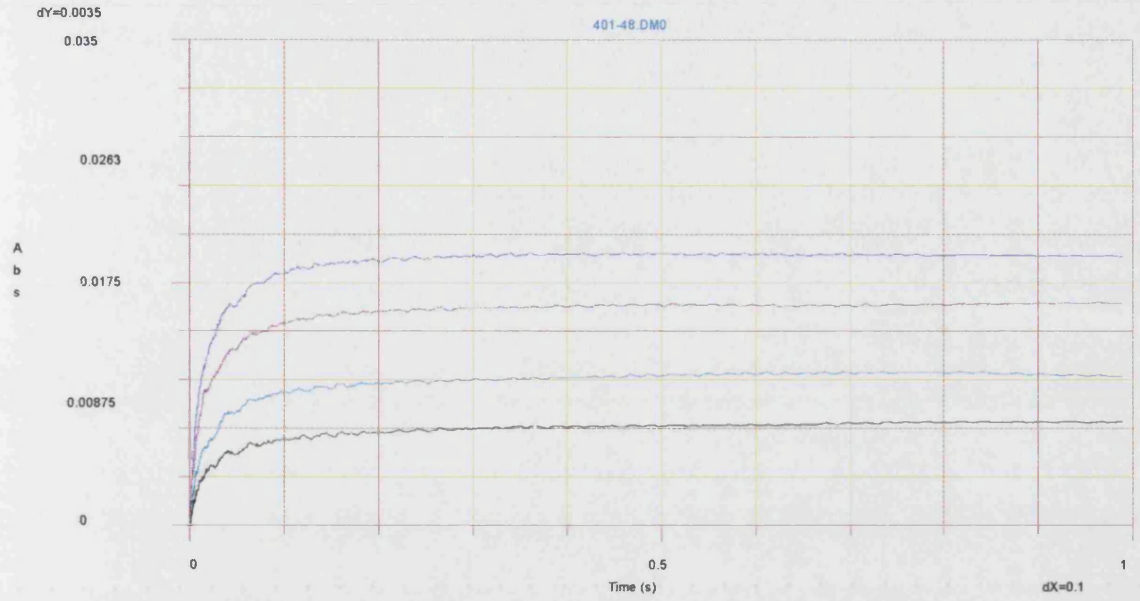

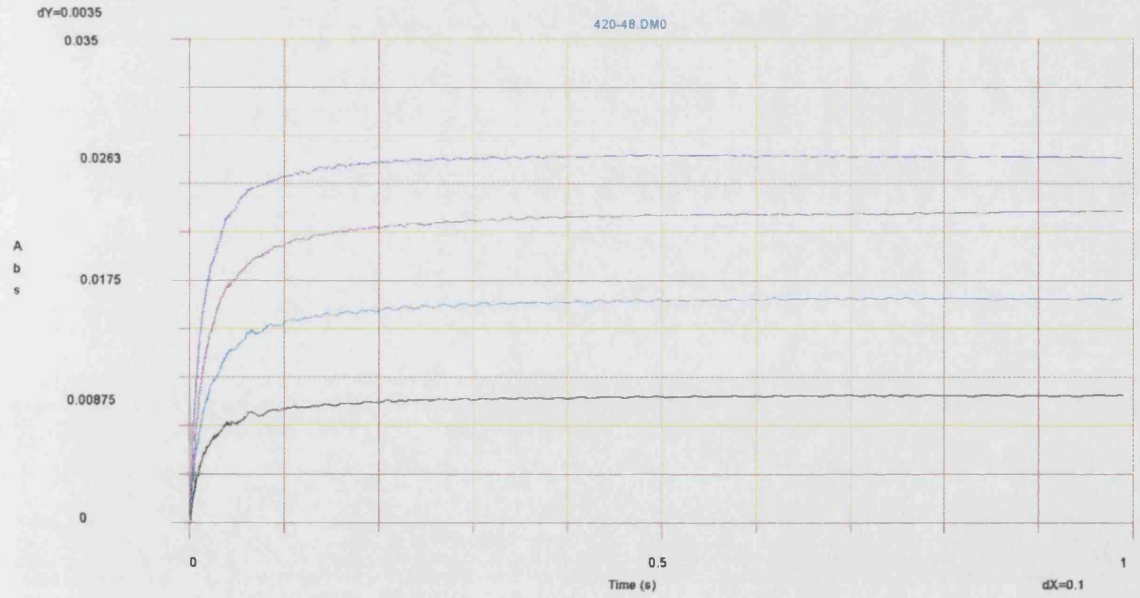

Figures 3.81, 3.82 : Kinetic binding curves for the dye-dextran conjugates T40.1 (top) and T40.20 (bottom). All the curves have been transformed into difference curves from the starting absorbance. Concentrations of dye-dextrans was 20 uM for all experiments. Curves for four LDH concentrations are shown, 6 uM (black), 12 uM (cyan), 24 uM (red) and 48 uM (blue).

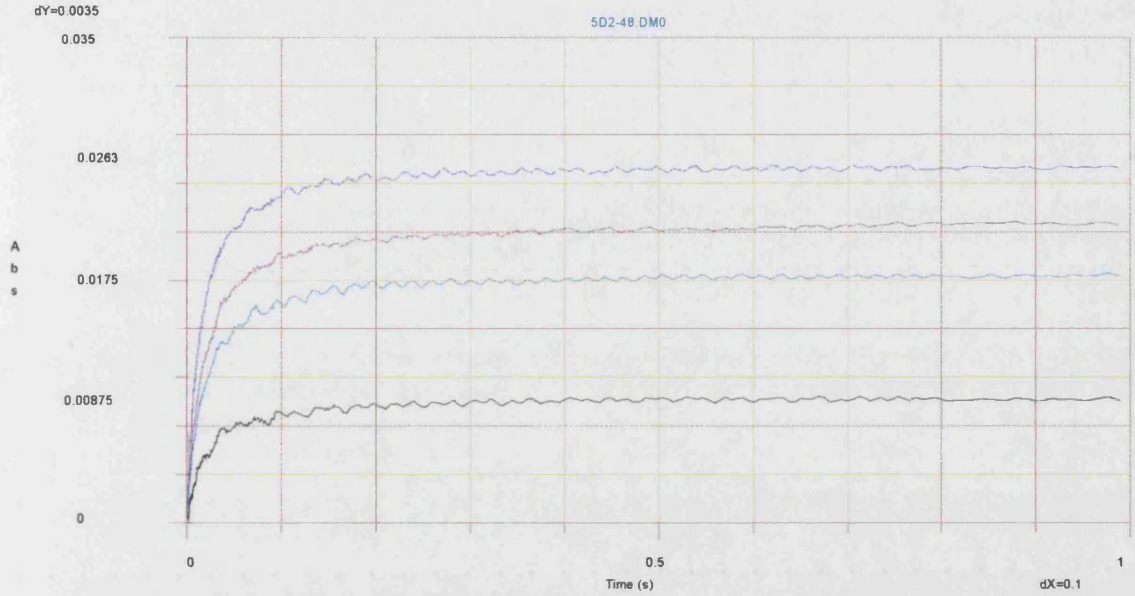

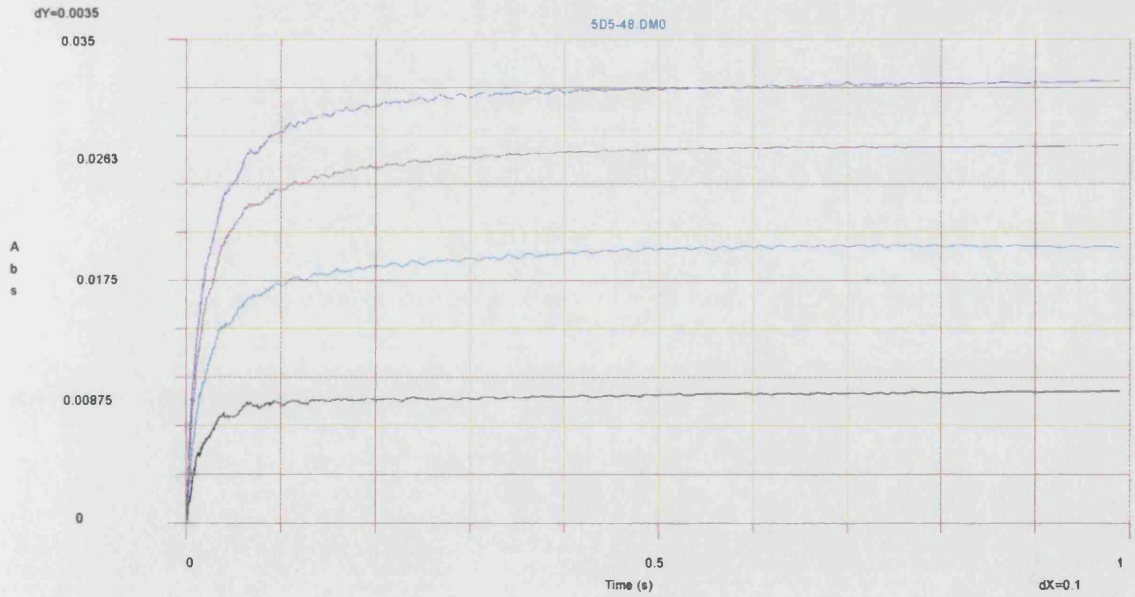

Figures 3.83, 3.84 : Kinetic binding curves for the dye-dextran conjugates 5d2 (top) and 5d5 (bottom). All the curves have been transformed into difference curves from the starting absorbance. Concentrations of dye-dextrans was 20 uM for all experiments. Curves for four LDH concentrations are shown, 6 uM (black), 12 uM (cyan), 24 uM (red) and 48 uM (blue).

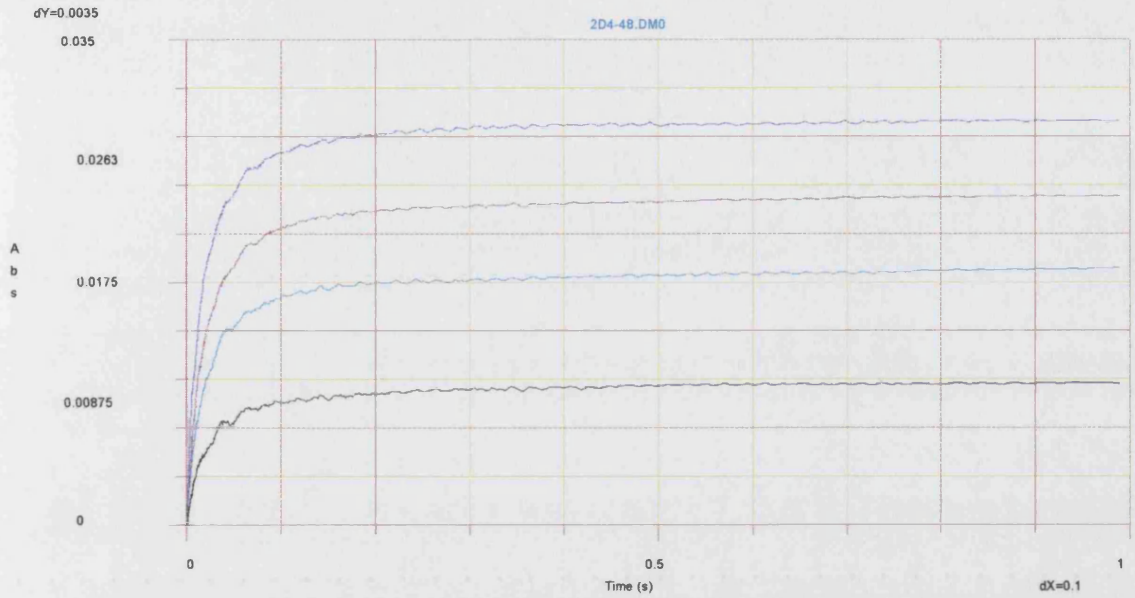

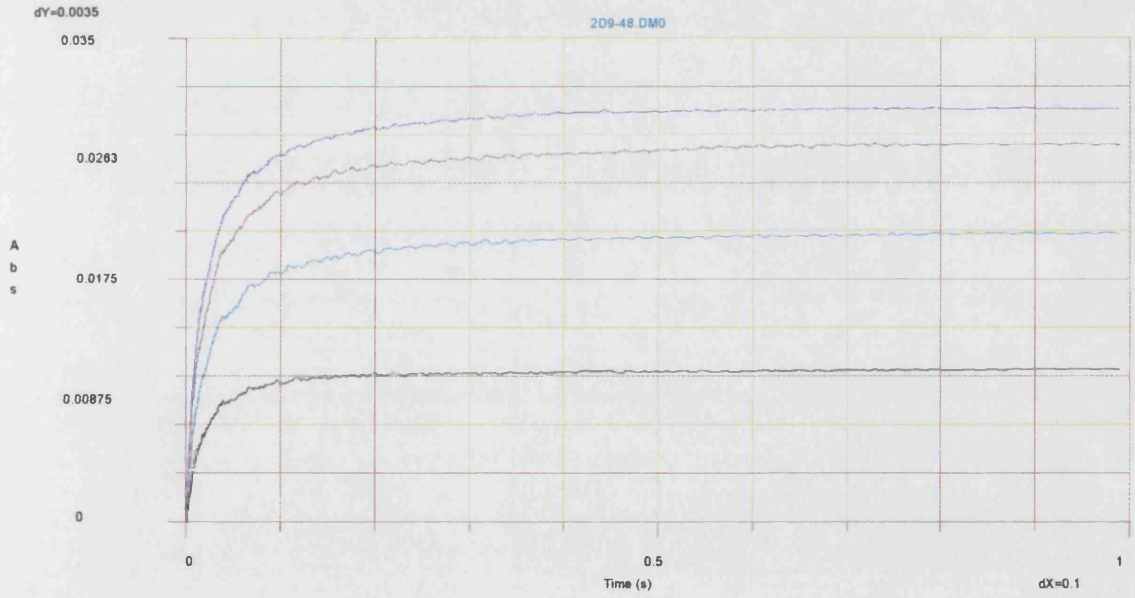

Figures 3.85, 3.86 : Kinetic binding curves for the dye-dextran conjugates 2d4 (top) and 2d9 (bottom). All the curves have been transformed into difference curves from the starting absorbance. Concentrations of dye-dextrans was 20 uM for all experiments. Curves for four LDH concentrations are shown, 6 uM (black), 12 uM (cyan), 24 uM (red) and 48 uM (blue).

3.14 Rapid Fluorimetric Kinetics with LDH

The kinetics of the binding of dye and dye-dextrans to LDH were also measured using the fluorescence quenching of the intrinsic LDH fluorescence upon dye binding. The greater sensitivity of fluorimetric methods allowed the use of lower LDH and dye concentrations which should lower the rate further still. This was however partially negated by the usage of a second monochromator on the emitted light with the resultant losses this entailed.

Figure 3.87 shows the first visible binding kinetics of free Cibracon Blue F3-GA to LDH, although it can be seen that this is still at the limit of what can be measured using this equipment as only the end of the reaction is visible, most still taking place within the dead time of the instrument. Quenching curves for dye-dextrans of the T40 and 2D series are then shown in **Figures 3.88, 3.89**.

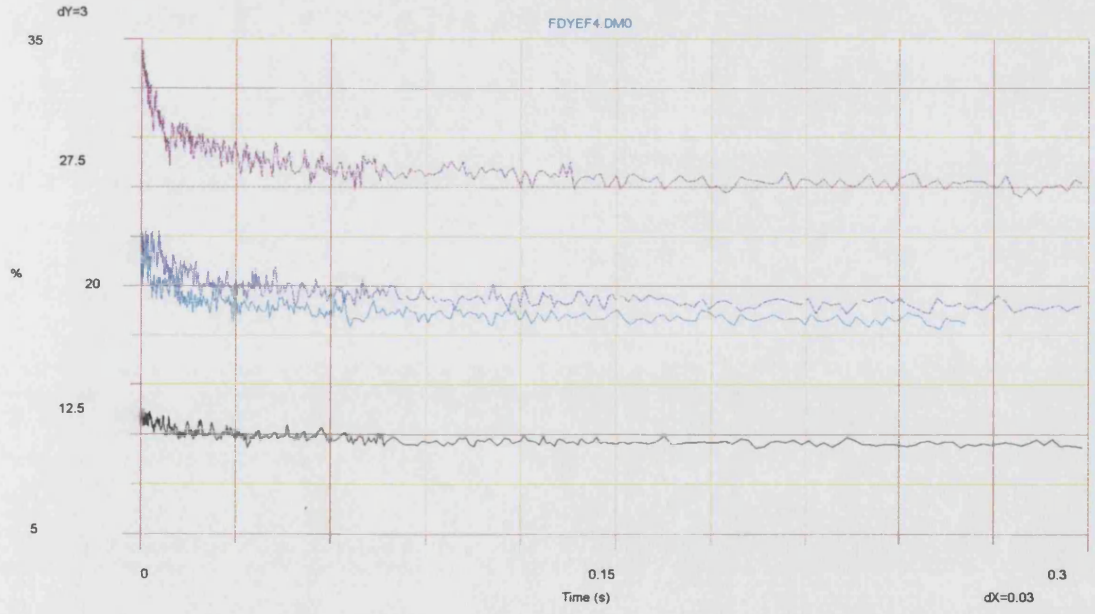

Figure 3.87 : Fluorescence quenching curves for free dye at 2 uM LDH, 25 uM (black) and 10 uM (cyan) free dye: 1 uM LDH, 10 uM (red) and 5 uM (blue) free dye.

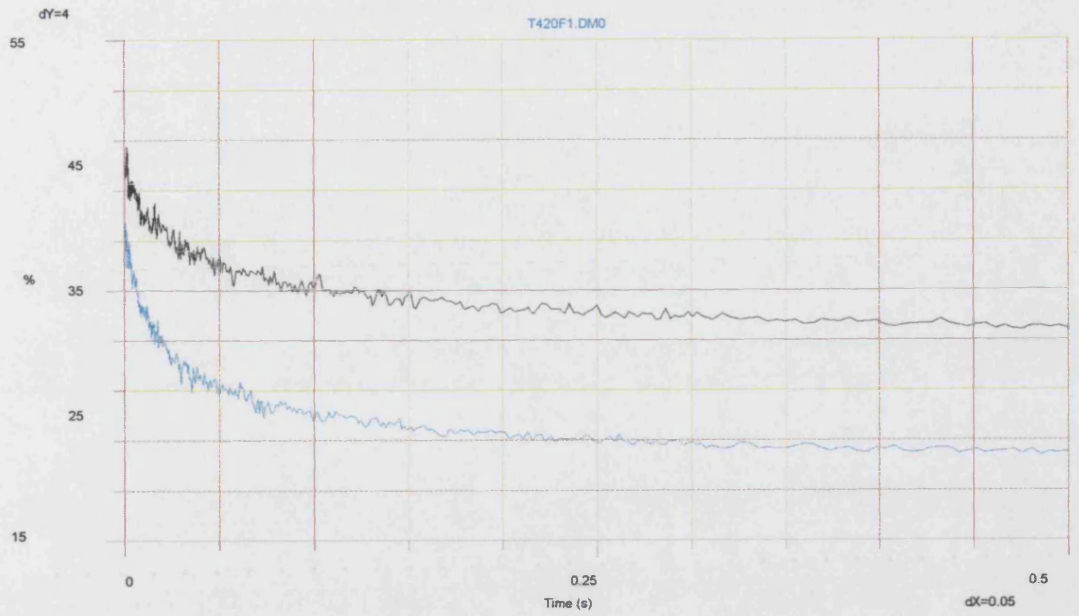

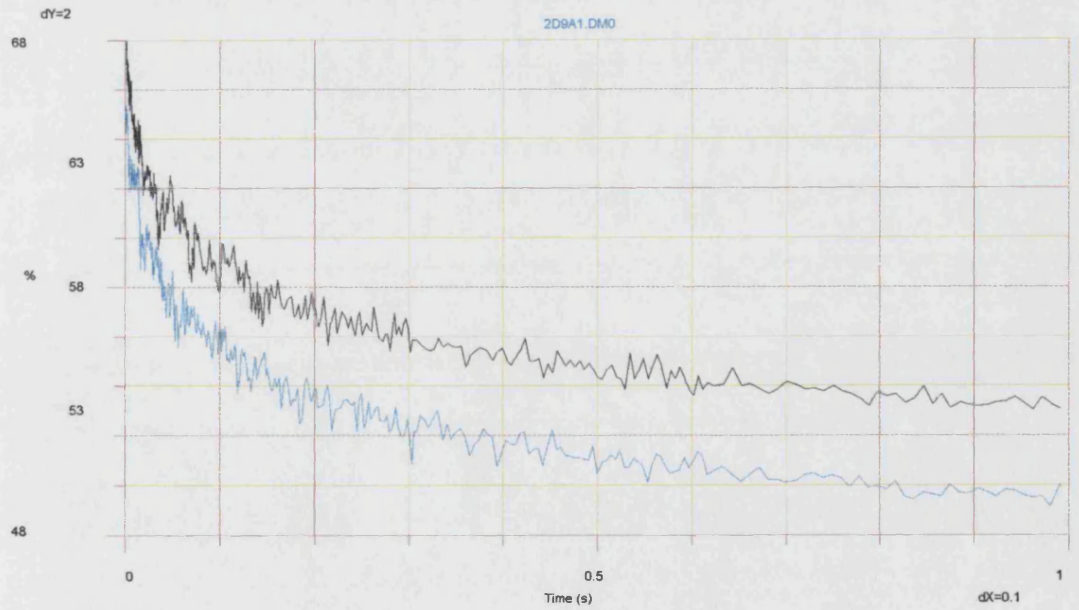

Figures 3.88, 3.89 : Fluorescence quenching for 2 uM LDH with 10 uM of (top) dye-dextrans T40.1 (black) and T40.20 (cyan) and (bottom) dye-dextrans 2D4 (black) and 2D9 (cyan).

3.14 Spectral Titration with Equine ADH

Spectral titrations of equine ADH against free Cibracon Blue F3-GA and the dye-dextran conjugate T40.20 are shown in **Figure 3.90** and **Figure 3.91** respectively. Unlike the spectral titrations with LDH there are very large differences in the difference spectra produced by the addition of free and conjugated dye. This indicates that the linkage to the dextran backbone has a greater influence on binding to ADH than it does to binding to LDH.

The differences in the spectra are quite extensive, the maximum of the hyperchromic peak with free dye occurring at 770 nm as opposed to 750 nm for the conjugate. The large hypochromic trough at 580 nm is entirely absent from the conjugate difference spectrum as is the small hypochromic shift at 705 nm in the conjugate binding spectrum absent from that of the free dye. Overall the difference spectrum produced by binding of the free Cibracon Blue F3-GA is similar to that observed with lysozyme (**Figure 3.34**), whilst that of the dye-dextran conjugate is close to that seen with LDH binding to dye-dextran conjugates (**Figure 3.56**).

Although the comparative magnitude of the difference spectrum is less than half the size of that seen with the free dye, this can be accounted for by the fact that only around one third of the dye in a dye-conjugate is expected to be available for binding.

Fits using the mutual depletion model to the magnitude of the difference spectra are shown in **Figures 3.92, 3.93.** The magnitude of the spectra for free dye binding is taken from the difference between the hypochromic trough at 580 nm and the hyperchromic peak at 670 nm. This has the advantage of producing a measurement of a greater magnitude and also automatically compensating for and inconsistencies in the baseline. For the dye- conjugate only the magnitude of the peak at 650 nm is taken as the small hypochromic trough is not clearly defined. The constants determined for the fits are shown in **Table 3.15.**

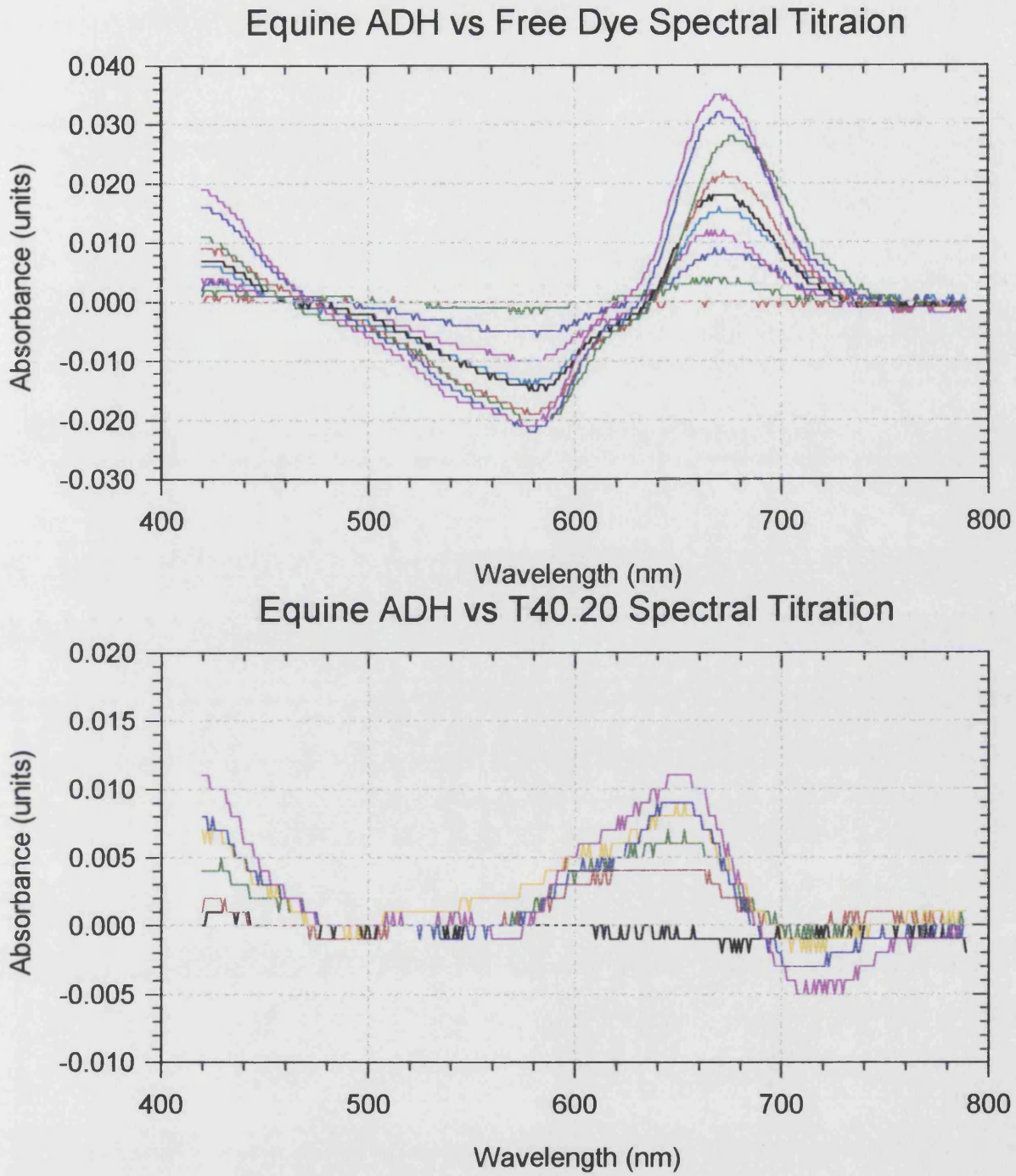

Figures 3.90, 3.91 : Spectral titrations of Equine ADH against 10 uM free Cibracon Blue F3-GA (top) and 10 uM T40.20 dye-dextran conjugate (bottom). Sequential additions of varying quantities of a 1 mM (subunit) stock solution of ADH were made and the difference spectrum recorded after each addition.

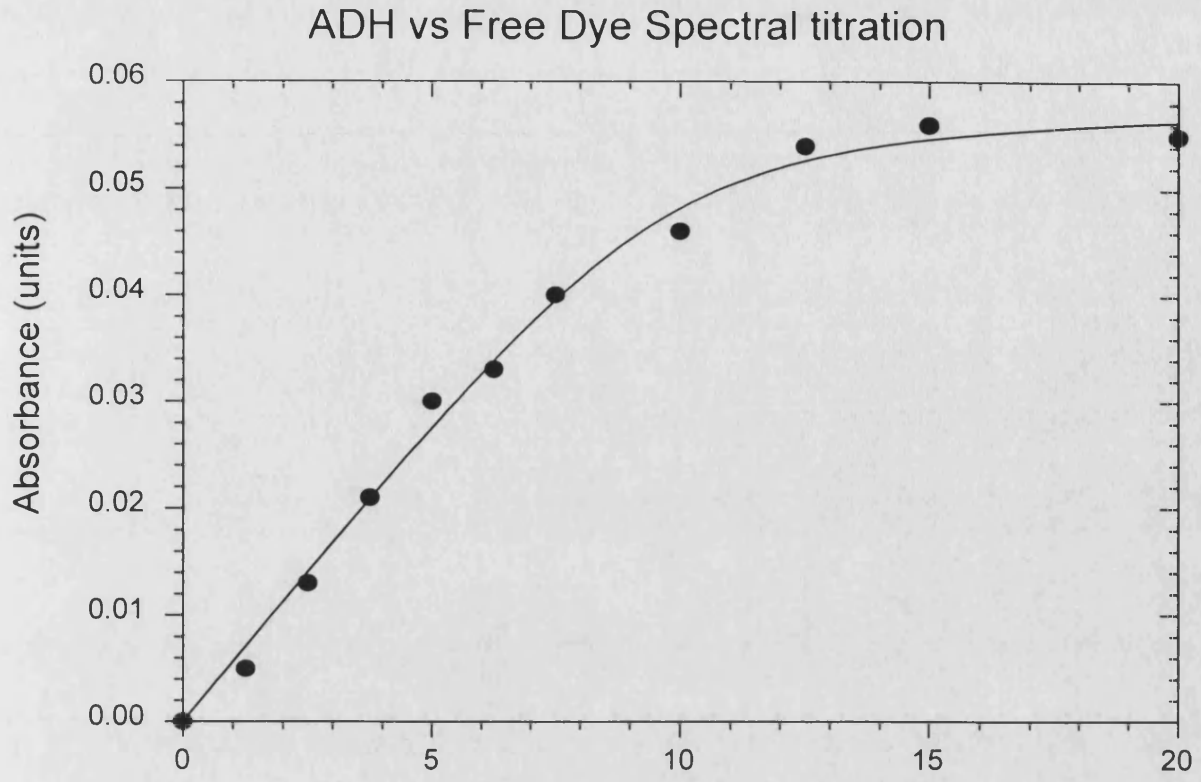

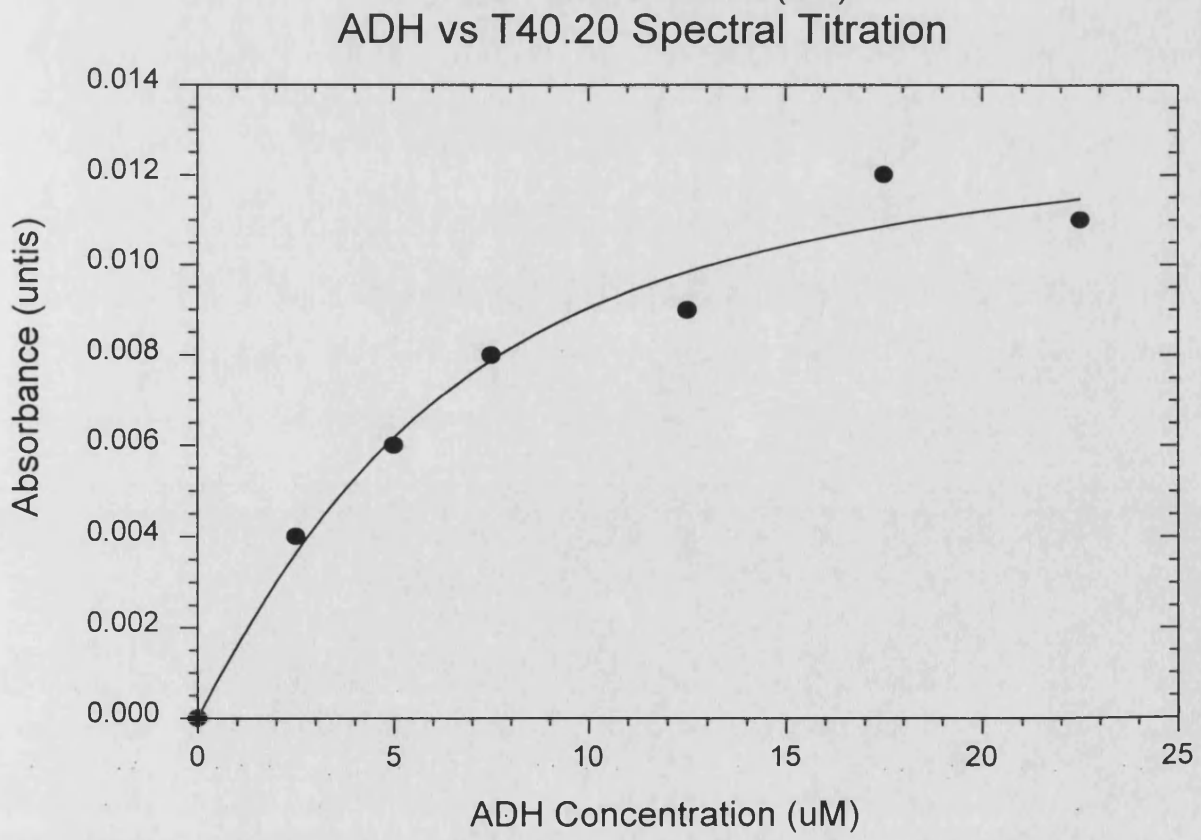

Figures 3.92, 3.93 : Difference binding curves produced from the spectral titrations shown in the previous two figures. For free dye the difference between the maxima at 670 nm and the minima at 580 nm was taken, whilst for the dye-dextran conjugate T40.20 purely the maxima at 650 nm was used.

Table 3.15 : Constants used for the fits for ADH spectral titrations

	Lt (uM)	**Kd** (uM)	**ΔE** ($uM^{-1}cm^{-1}$)
Free Dye	9.87	0.40	0.0059
T40.20	4.55	3.57	0.0030

The dataset for the T40.20 spectral titration shown in **Figure 3.93** is not good enough to produce a reasonable fit by allowing all values to float. The value for the difference in extinction coefficients was therefore fixed at a value approximately half that for the free dye fit in which corresponds to the change expected from the free dye maxima alone (the trough and peak being of approximately equal magnitude). This assumption yields reasonable values for the available ligand and the dissociation constant and an apparently good fit to the dataset.

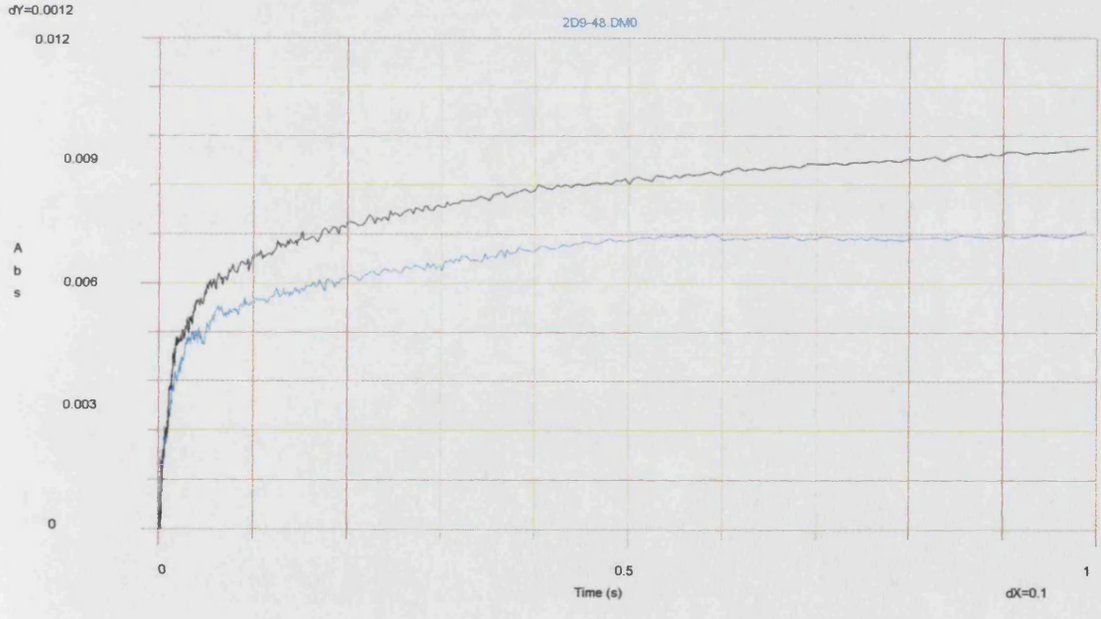

Figure 3.94 : Kinetic binding curves for binding of 20 uM dye-dextran conjugates 5D5 (black) and 2D9 (cyan) to ADH. ADH concentrations were 125 uM for 5D5 and 50 uM for 2D9. Absorbance measurements were transformed into an absolute difference from the starting value.

Figure 3.94 shows kinetic difference spectra at 650 nm for the 5D5 and 2D9 conjugates. The shape of these binding curves can be seen to be similar to those shown previous for dye-dextran conjugates with LDH.

Fluorescence quenching curves for ADH with free dye and with dye-dextran conjugates from the T40 and 2D series are shown in **Figures 3.95-3.97**.

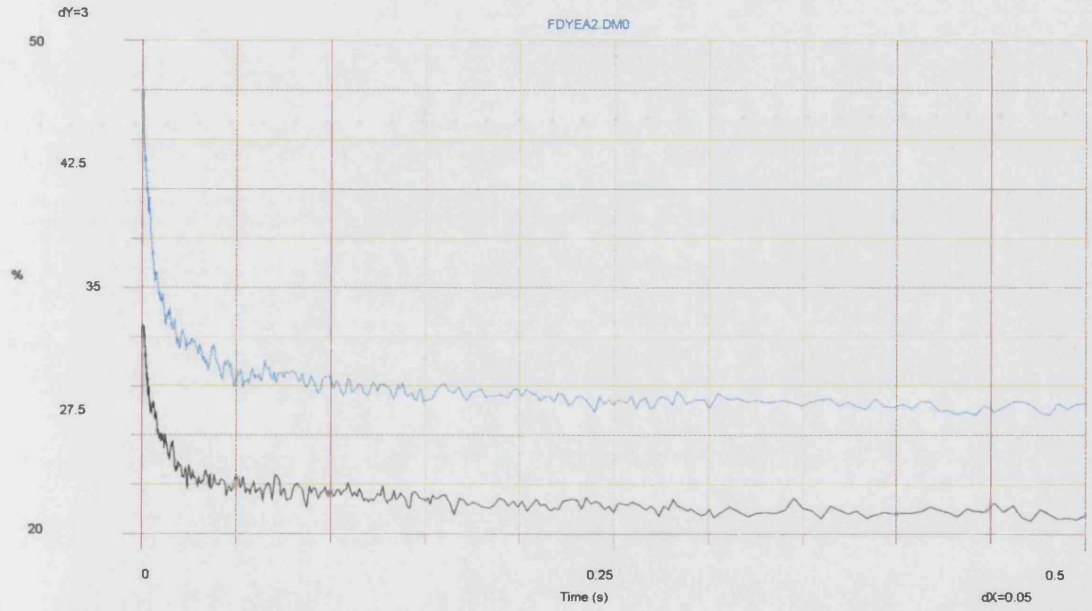

Figures 3.95 : Fluorescence quenching curves at 2 uM ADH with 10 uM (black) and 5 uM (cyan) free dye.

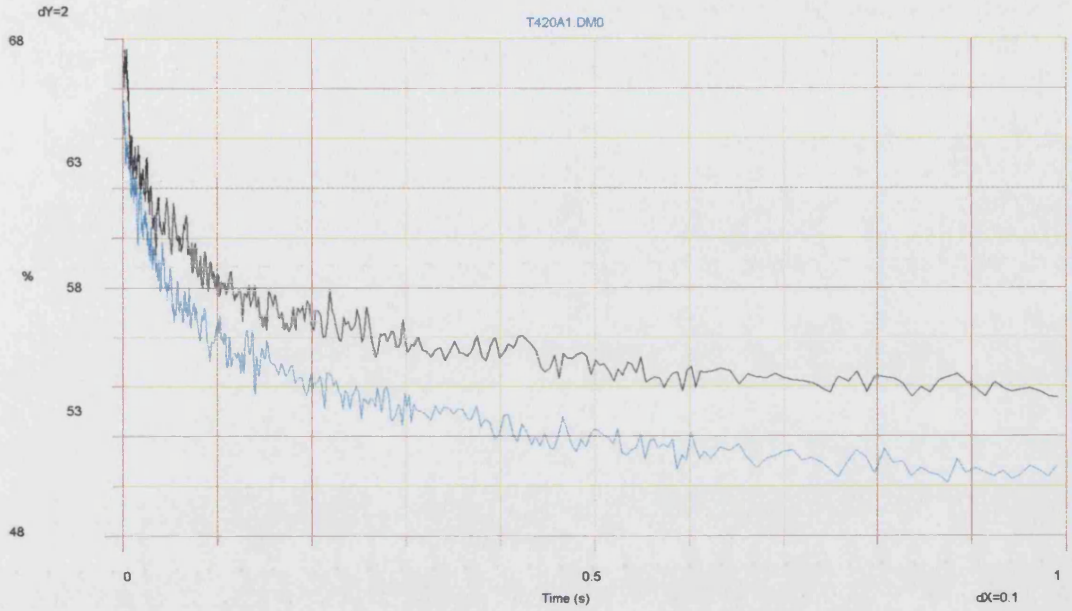

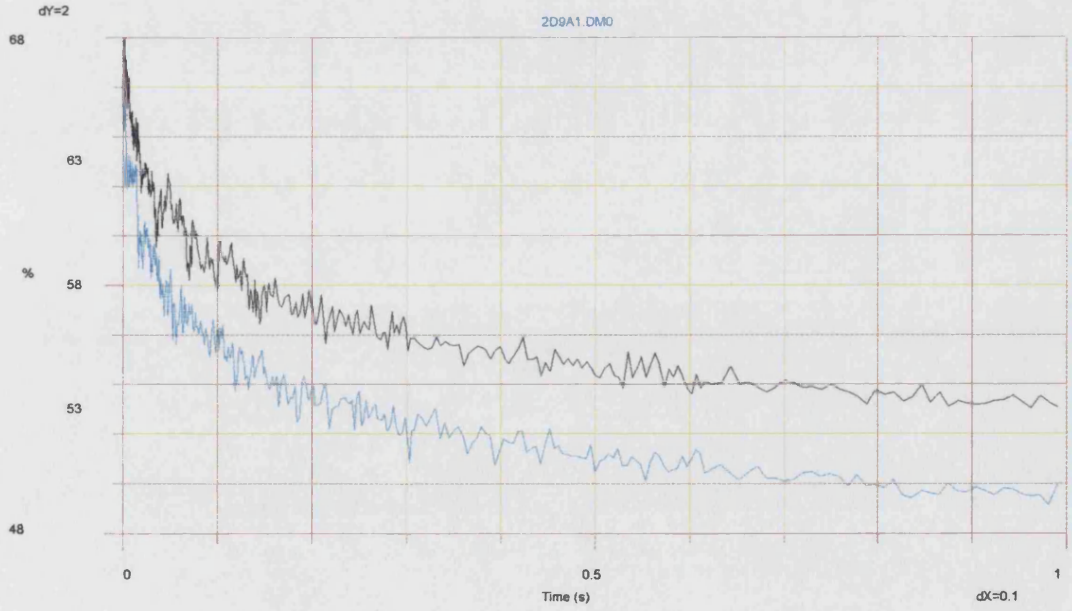

Figure 3.96, 3.97 : Fluorescence quenching for 2 uM ADH with 10 uM of dye-dextrans (top) T40.1 (black) and T40.20 (cyan) and (bottom) with 10 uM of dye-dextrans 2D4 (black) and 2D9 (cyan).

3.16 Spectral Titration with Saccharopine Dehydrogenase

Yeast saccharopine dehydrogenase (Sigma) was used for a spectral titration with the T40.20 dye dextran conjugate. **Figure 3.98** shows an absorption spectrum of the protein in 50 mM sodium phosphate buffer pH 7.9 from 190 - 800 nm. As well as the expected protein absorbance there is also apparently a minor absorbing contaminant present producing a peak of absorbance at 414 nm. The nature of this is unknown, but it is presumed to be something carried over from the purification procedure.

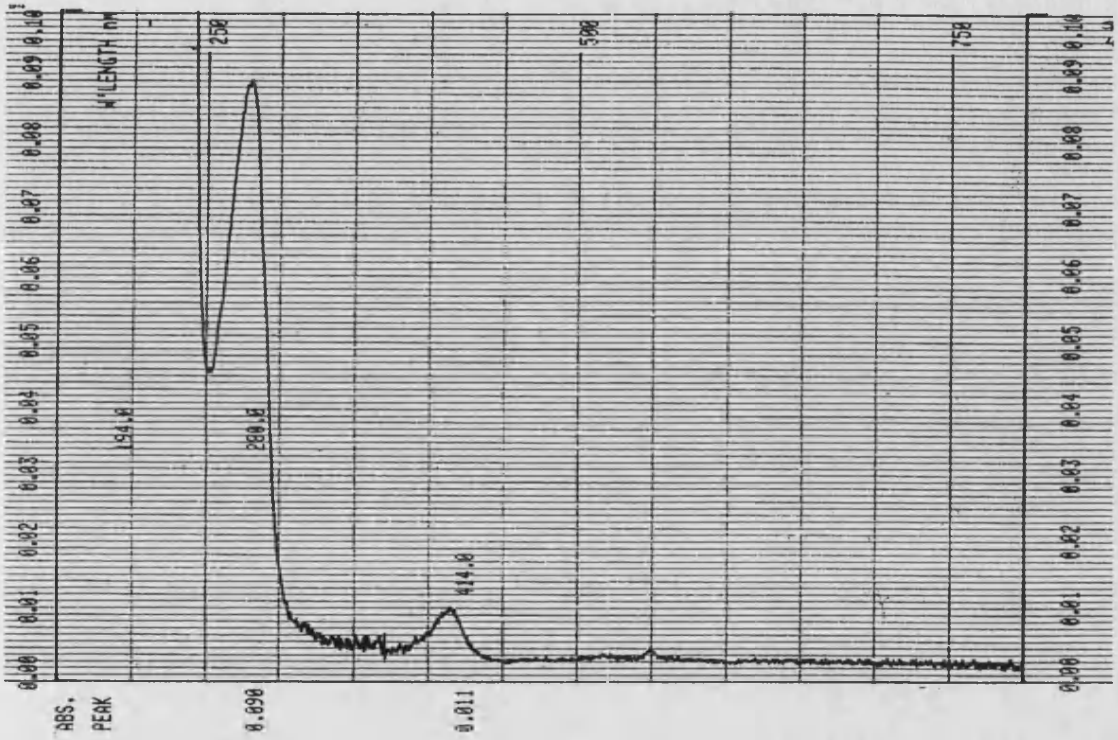

Figure 3.98 : Scanned absorbance spectrum of Yeast saccharopine dehydrogenase as supplied by Sigma. 10 ul of stock solution was diluted into 1 ml 50 mM sodium phosphate pH 7.9. In addition to the expected aromatic absorption peak at 280 nm there was an additional smaller peak at 414 nm. This peak was presumed to be due to a contaminant from the purification procedure used in the preparation of the enzyme.

The spectral titration is shown in **Figure 3.99.** From this it can be seen that there is no detectable spectral change on addition of saccharopine dehydrogenase to the T40.20 dye-dextran conjugate. Even further additions of another 20 ul of stock solution (data not shown) failed to produce any difference spectrum. It therefore seems that saccharopine dehydrogenase does not interact with Cibracon Blue F3-GA.

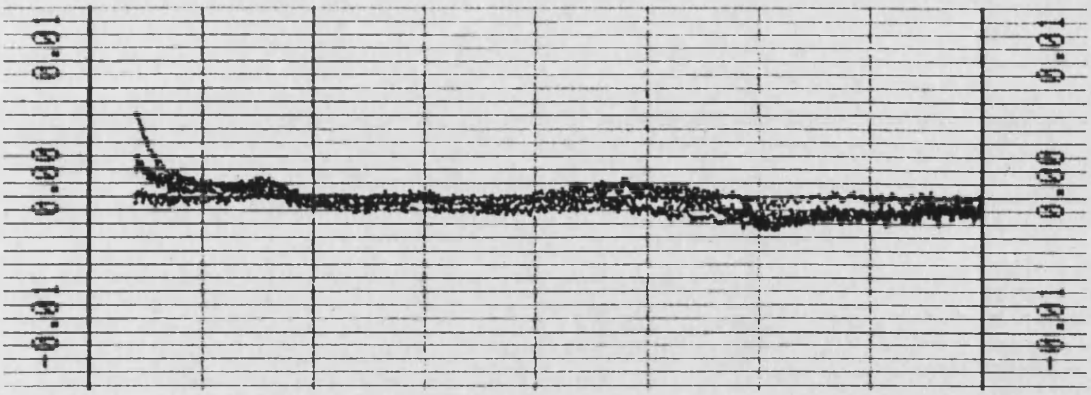

Figure 3.99 : Spectral titration of dye-dextran conjugate T40.20 with saccharopine dehydrogenase. Additions of 2 x 2.5 ul, 1 x 5 ul and 1 x 10 ul of the saccharopine dehydrogenase stock were added to a 25 uM solution of T40.20. The scans show that no difference spectrum was measured indicating that there was no binding. The difference at around 420 nm is due to the absorbing impurity in the stock shown in the previous figure.

3.17 Spectral Titration with Billiverdin Reductase

Billiverdin reductase (BVR) was spectrally titrated against free dye (data not shown) and two dye-dextran conjugates T40.20 and 2D9 shown in **Figures 3.100, 3.101**. The spectral titration with T40.20 shows a difference spectrum with a hyperchromic shift centred at 520 nm. However in comparison there is no apparent difference spectrum shown for the titration with the 2D9 dye-dextran conjugate or with free dye (which gave similar results to that shown for 2D9). This is possibly due to the small magnitude of the changes involved which are at the limits of resolution of the equipment making it possible to lose the signal within the background noise.

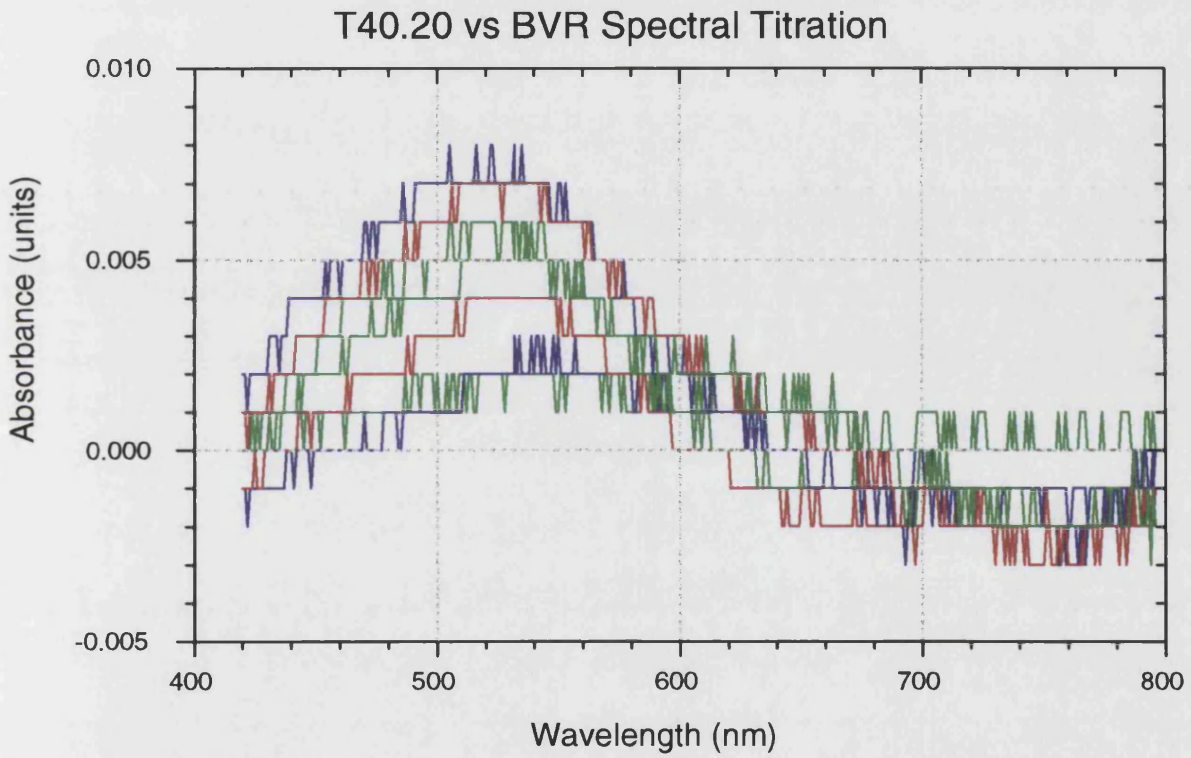

Figure 3.100 : Spectral titration of 17.5 uM dye-dextran T40.20 with BVR. Sequential additions of a 0.45 mM stock solution of BVR were made with the difference spectra between 420 nm and 800 nm being recorded after each addition.

Figure 3.102 shows the difference spectrum produced on rapid mixing of dye-dextran T40.20 with BVR. There is no observable difference spectrum produced, showing that any reaction has already reached completion within the dead time of the instrument.

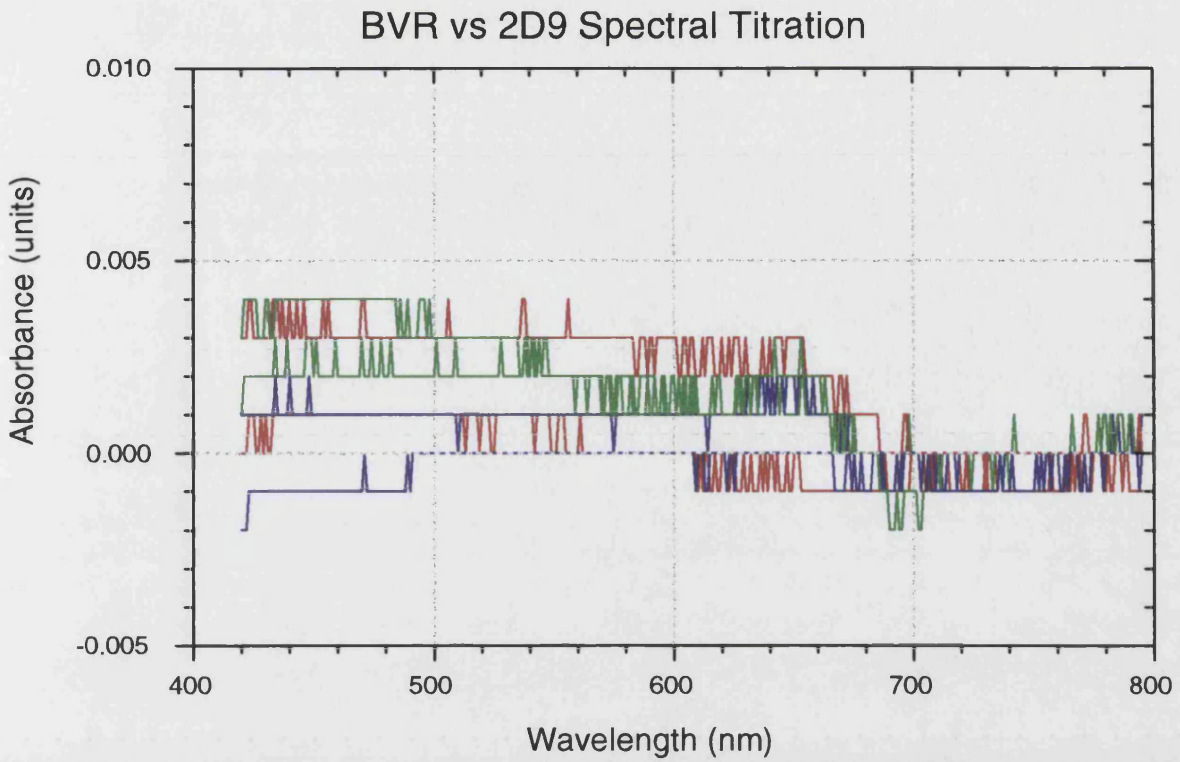

Figure 3.101 : Spectral titration of 17.5 uM dye-dextran 2D9 with BVR. Additions of BVR were made and the difference spectra recorded as for the previous figure.

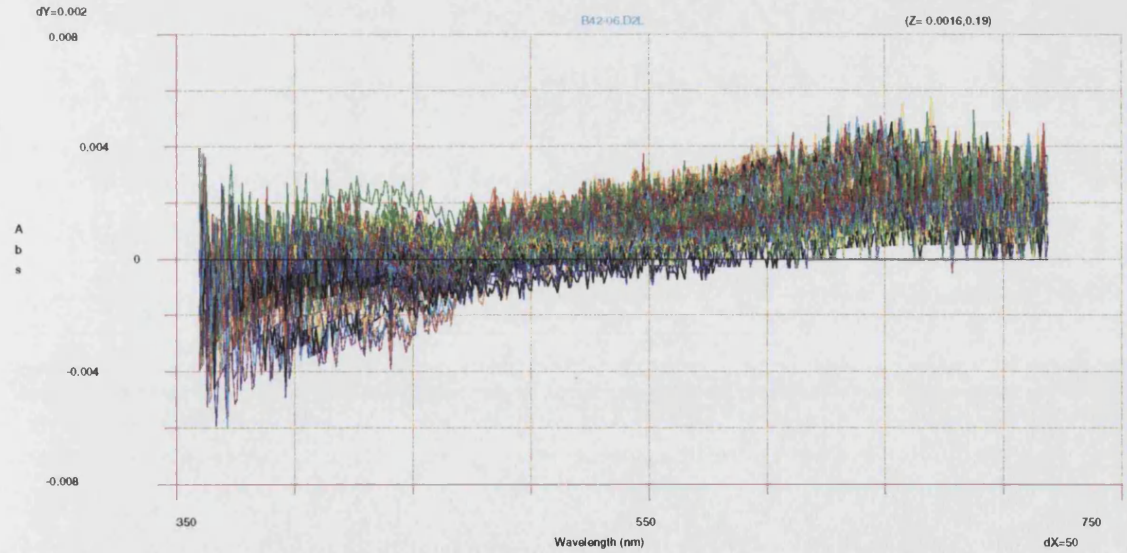

Figure 3.102 : Difference spectra produced on mixing 20 uM T40.20 with 50 uM BVR. The difference spectra were produced by subtracting the inital spectrum from all the subsequent ones. It can be seen that there is no visible difference, the spread of spectra being purely the background noise of the instrument.

3.16 Dye destacking kinetics

It is known that aromatic dyes such as Cibracon Blue F3-GA associate together through interactions between the planar aromatic rings present, notably for Cibracon Blue F3-GA, the anthroquinone chromophore present in the structure. As shown in **Figure 3.12b** these 'stacking' interactions alter the absorbance of the dye in a concentration dependent manner.

This dye stacking interaction has been used as a possible explanation for the complex binding kinetics seen for the interaction of dye-dextran conjugates with proteins[48]. To test this hypothesis kinetic measurements were made of the rapid dilution of both Cibracon Blue F3-GA and a range of other similar dyes.

The spectra measured upon rapid dilution of 40 uM Cibracon Blue F3-GA in 50 mM sodium phosphate pH 7.9 with an equal volume of buffer are shown in **Figure 3.103**, recorded over a timecourse of 0.192 seconds after mixing. This is transformed into difference spectra from the initial spectrum taken in **Figure 3.104**. It can be seen that no spectral change is observable over the timecourse taken. Therefore any destacking caused by the dilution had already reached completion within the dead time of the instrument.

Likewise dilution spectra were recorded in the same manner for 0.125 mg / ml solutions of Procion Blue MX-3G (**Figure 3.105**) and Procion Red MX-5B (**Figure 3.106**). In both of these cases, as for that with Cibracon Blue F3-GA, no observable changes in absorbance could be seen over the timecourse recorded.

The dilution spectra and difference spectra produced from them are shown for the dyes Procion Orange MX-G in **Figures 3.107, 3.108** and for Procion Yellow MX-R in **Figures 3.109, 3.110**. In these cases dilution of the dye-containing solution yields a difference spectrum produced presumably by the relaxation of the dye stacking equilibria into a different position as the dye is diluted.

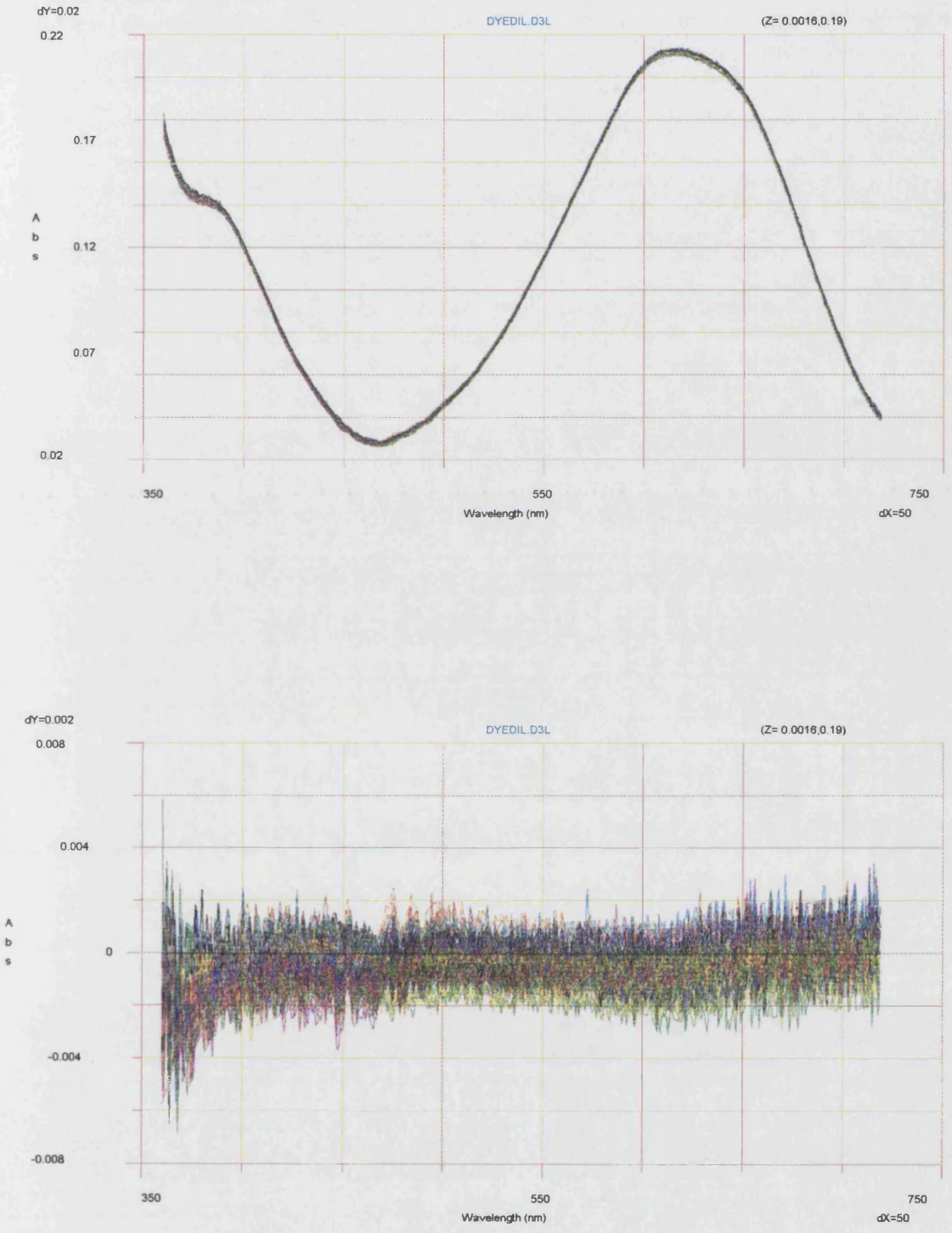

Figures 3.103, 3.104 : Spectra (top) and difference spectra (bottom) taken over a timecourse of 0.192 seconds on rapid dilution of 40 uM Cibracon Blue F3-GA to 20 uM. This shows that there is no observable difference spectrum produced on dilution of Cibracon Blue F3-GA.

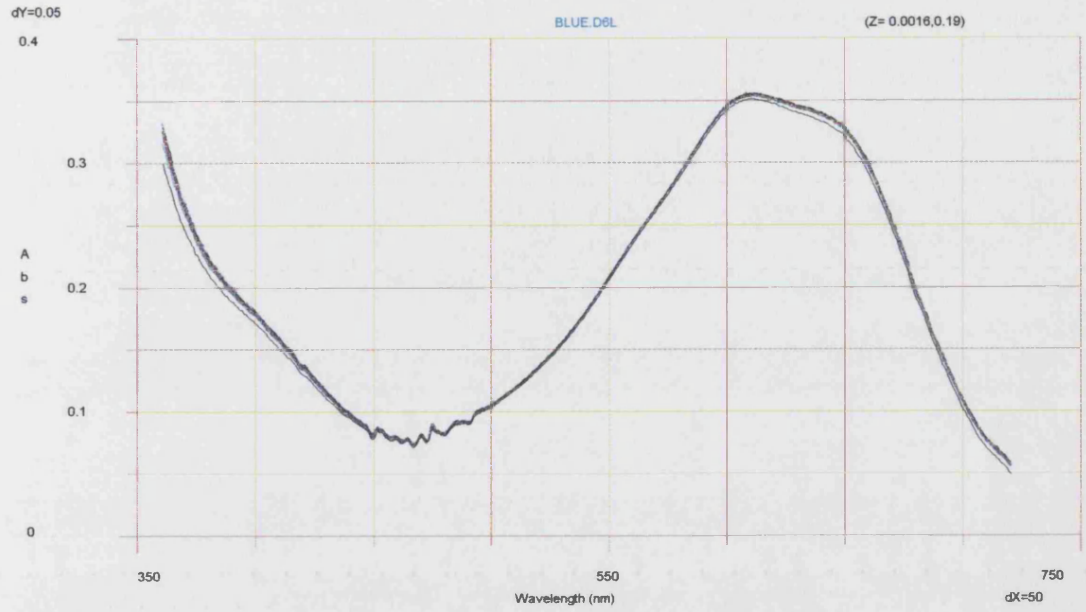

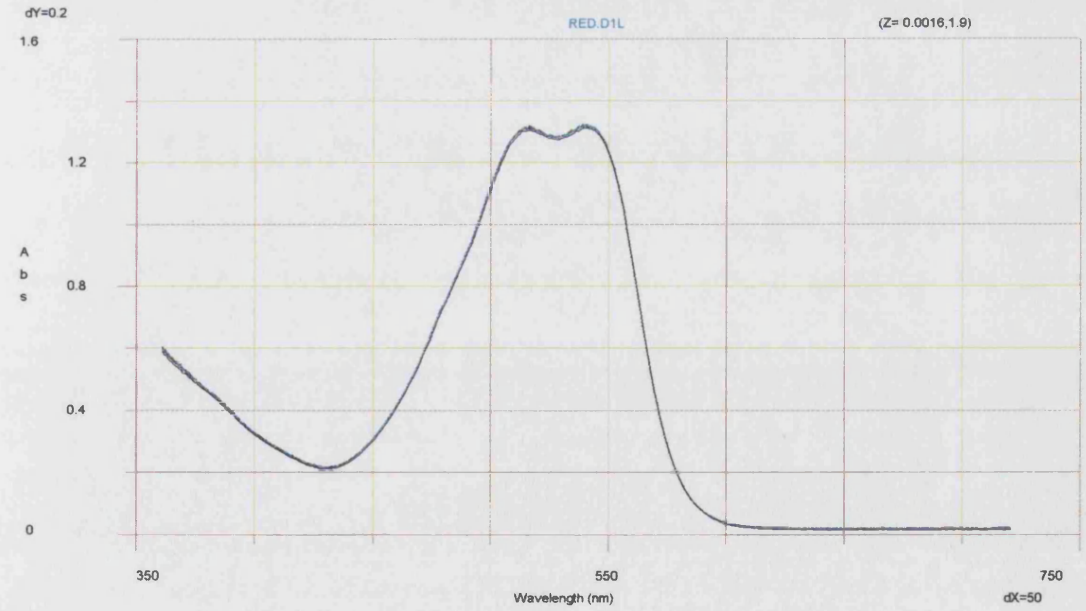

Figures 3.105, 3.106 : Spectra taken over a timecourse of 0.192 seconds on rapid dilution by a factor of two of 0.125 mg/ml Procion Blue MX-3G (top) and Procion Red MX-3G (bottom). Neither shows any observable difference spectrum upon dilution.

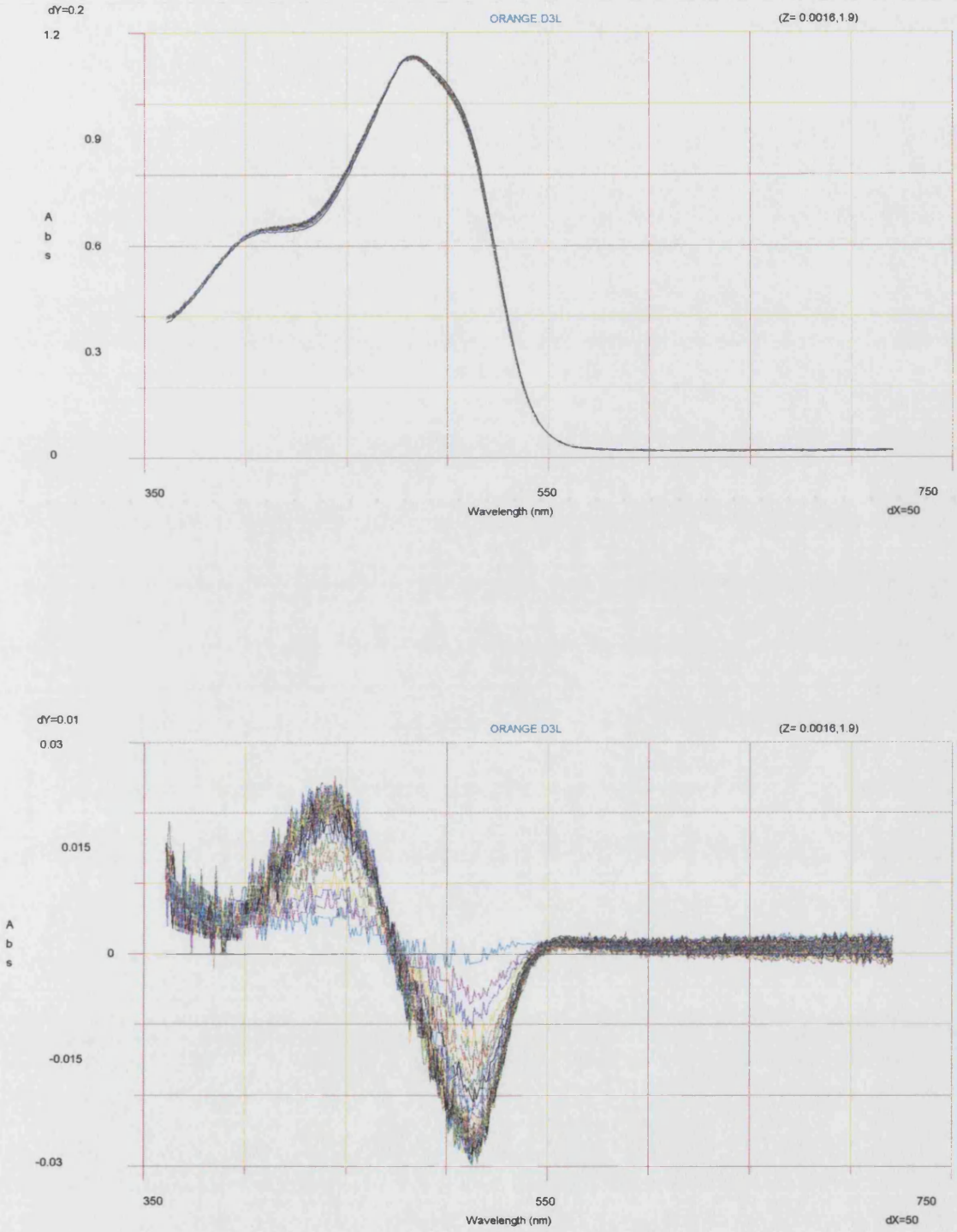

Figures 3.107, 3.108 : Spectra (top) and the difference spectrum (bottom) produced on rapid dilution by a factor of two of 0.125 mg/ml Procion Orange MX-G taken over a timecourse of 0.192 seconds. The difference spectrum produced upon dilution shows the destacking of dye-molecules.

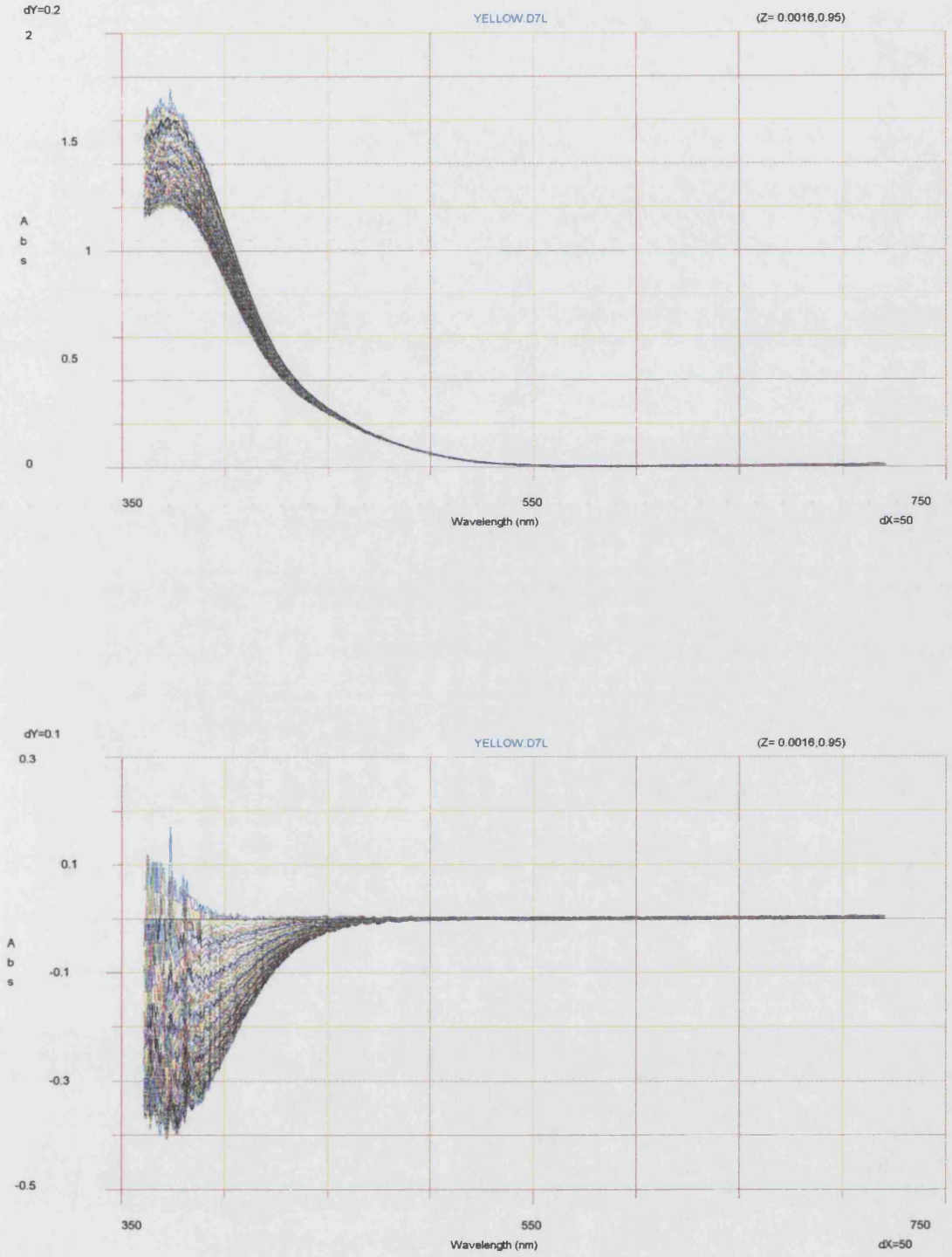

Figures 3.109, 3.110 : Spectra (top) and the difference spectrum (bottom) produced on rapid dilution by a factor of two of 0.125 mg/ml Procion Yellow MX-R taken over a timecourse of 0.192 seconds. The difference spectrum produced upon dilution shows the destacking of dye-molecules.

Discussion

4.1 Synthesis of Dye-Dextran Conjugates

The results of the synthesis of dye-dextran conjugates agree in general principle in those previously shown for the reaction of Cibracon Blue F3-GA with high molecular weight dextrans. Mayes et al.[25] produced a timecourse for the reaction and suggested that the degree of substitution reached for a dye-dextran conjugate was lower than that expected from the quantity of dye added due to the competing reaction of 'active' chloro-dye with free hydroxyl ions in solution to produce 'inactive' hydroxyl-dye.

Presuming that the two competing reactions with the active dye can be described as pseudo first order as both the available free hydroxyl concentration on the dextran backbone and that in solution are both in large excess to the dye concentration then the final concentration of dye coupled to the dextran should be in direct proportion to the quantity of dye added.

For example the reaction to produce the T40.10 conjugate 1.31g dye was added to 2.0 g dextran in a volume of 100 mls at a pH of approximately 13 (2g Na_2CO_3).

This gives a concentration of active dye (assuming 60 percent present in the stock) of :-

$$\frac{1.31 * 0.6 * 10}{774.2} = 16.9\,mM$$

Of free dextran hydroxyls (presuming average 3 per glucose with Mwt of 163) of :-

$$\frac{2.0 * 3 * 10}{163} = 370\,mM$$

Free hydroxyls in solution at pH 13 = 100 mM [OH^-]

Thus both the free and dextran bound hydroxyl concentrations are in large excess of the dye concentration and the reaction can be considered as pseudo first order with respect to both these components.

The competing reactions can then be described as :-

$$Dye-OH \xleftarrow[K_1]{OH^-} Dye-Cl \xrightarrow[K_2]{Glucose} Dye-Glucose$$

With the rates of the two reactions as K_1 and K_2 respectively.

And the reaction described (where S is the starting active dye concentration) by :-

$$\frac{dS}{dt} = -K_1[S] - K_2[S], \quad \frac{dD^{OH}}{dt} = K_1[S], \quad \frac{dD^{Glucose}}{dt} = K_2[S]$$

Thus at the endpoint the ratio of products is equal to the ratio of the reaction rates i.e.

$$\frac{[D^{OH}]}{[D^{Glucose}]} = \frac{K_1}{K_2}$$

Which is independent of the starting concentration of active dye.

This shows that if the above assumptions are true then the degree of substitution of the dye-glucose conjugate produced should be directly proportional to the starting concentration of dye used.

However it was shown that the this is not the case and that instead the degree of substitution produced versus starting concentration of dye appear to follow a saturable curve, with a limit of the degree of substitution capable of being produced in a single step. Thus at high dye concentrations there is another limiting factor preventing further reaction of dye with the dextran. This however does not limit the ultimate loading of a dye dextran conjugate as the dye-dextran conjugate produced can be further reacted with fresh dye to produce higher loadings than those obtainable in a single step as shown by Mayes et. al.[25].

This effect is possibly explained by the phenominum of dye 'stacking' in which dye molecules in solution apparently aggregate through interactions between the planar aromatic rings present. This aggregation has been shown to alter the absorption spectrum of the dye, the effect being minor at low concentrations, but increasing rapidly as the concentration is raised[38] as would be expected for a bimolecular or greater reaction. If stacked molecules are precluded from reacting with the dextran due to steric effects then this would effectively sequester a population of dye unavailable for reaction. This effect would persist throughout the reaction as stacking could be expected to take place between both the 'active' chloro-triazine dye molecules and the 'inactive' hydroxy-triazine dye molecules as the substitution of the hydroxyl group for the chloride should have little influence on the anthroquinone ring primarily implicated in stacking effects.

Dye stacking also has implications for the distribution of dye molecules linked to a single dextran backbone. It is possible that after one dye has been covalently attached to a dextran then this might act as a 'nucleation' site for attachment of further dye molecules due to the possibility of dye stacking between the attached dye and free dye molecules increasing the local concentration around the attachment site and thus increasing the likelihood of further dye being attached close to the original dye. This effect would be expected to be increased under the high salt conditions commonly used to promote the attachment of dye to solid supports[55,65,66], which have also been shown to promote dye stacking and ion-pair formation[38]. These synthesis protocols have their origin in the procedures used for dying textiles in which salt is added to promote the interaction between the dye and the textile to increase the efficiency of dying. Although this may be advantageous for the commercial dying of textiles in which dye distribution is not important, it may well be disadvantageous in biochemical systems. High local concentrations of dye molecules on a support may well be

less effective than an even distribution due to the increased likelihood of steric hindrance of protein binding to clusters of attached dyes.

4.2 Dye Purification

Cibracon Blue F3-GA is generally supplied as what is basically an industrial grade dye. This means that it contains a variety of impurities, possibly including preservatives and bulking agents. It has also been shown to be supplied from different sources as any of the varying sulphonate isomers (*ortho-*, and mixtures of *meta-* / *para-*) and of the precursors in the synthesis of these final compounds[67]. There have been various paper and thin layer techniques used to assess the purity of commercial preparations of Cibracon Blue F3-GA [55,67,68,69,70,71]. While some of these have shown only one species to be present, others [67,68,70] have shown as many as 15 coloured components, with different sources containing different components. In cases where no polydispersity of coloured compounds within the sample were noted, it is possible that the solvent systems used, e.g. pure methanol[72], would not be capable of resolving similar chromophores. The dye itself is also present in both active and inactive forms - depending upon the presence of a chlorine (active) or hydroxide group (inactive) on the triazine ring.

Cibracon Blue F3-GA dye as supplied by Sigma is described as being the *ortho-* isomer. TLC of the dye as supplied by Sigma showed that it consisted of three significant coloured compounds. The major two being identified as the chloro and hydroxy forms of the *ortho-* isomer as shown by their interconversion under hydrolysing conditions. The third component remained unidentified, although is an apparently non-hydrolysable intermediate as its r.f. remained constant under the alkaline hydrolysis conditions which caused the interconversion of the other two components. If this component was the direct dichloro-triazine precursor in

the synthesis reaction then it would be expected to have undergone hydrolysis to a dihydroxy form which would be expected to have a different r.f. . Thus it must be presumed to be a non-hydrolysable precursor, possibly 1-Amino-4[(4-amino-3-sulphophenyl)amino]anthroquinone-2-sulphonic acid (ASSO) which is the direct precursor before the dicholorotriazine derivative. The chloro- ('active') form of the dye has been shown to be capable of reaction with proteins to form irreversibly bound conjugates[73]. It was therefore necessary to produce the pure 'inactive' hydroxy form of the protein by hydrolysis of the 'active' chloro dye to form the hydroxy form and then its subsequent purification by lipophillic column chromatography using Sephadex LH-20 to remove any remaining unreacted dye and impurities.

The purification with Sephadex LH-20 initially produced a relatively poor separation of the three major components in the dye sample. It was subsequently found that by alkalinising the solvent by the addition of a small volume of sodium hydroxide the separation on the column was dramatically improved with both the retention times and the differences between them being increased. This is obviously due to changes in the ionisation of the charged groups present in the dye molecules as the effective pH of the solvent is changed.

It had previously been noted that the media of the TLC plates could apparently catalyse the breakdown of the dye in certain solvent systems so that a far greater number of components were visualised by TLC than were actually present in the source material as determined by HPLC. No evidence of this was seen with the solvent system and TLC plates used.

4.3 Dye - Glucose Preparation

The production of a dye-glucose moiety would allow assessment of the effect of the coupling of the dye to a glucose molecule would have upon the interaction between the dye and model proteins. Direct reaction of dye with glucose would allow coupling of the dye to take place

with any of the free hydroxyl groups of the glucose. This would form dye-glucose conjugates with the dye attached at any of the 5 different free hydroxyls as well as the possibility of the attachment of more than one dye molecule to a single glucose. It is possible that dye-glucose molecules with the dye attached at differing carbons of the glucose could have different binding affinities. Thus the production of a non-homogeneous sample by simple reaction of dye with glucose could produce a mixture of different compounds with different affinities which would complicate the analysis of the results from any subsequent binding experiments performed.

It was therefore advantageous to produce a dye-glucose conjugate with the dye coupled to the glucose at a known position. This was achieved through the use of a protected glucose (diacetone glucose) in the synthesis which had only a single free hydroxyl group available for reaction.

The reaction of the diacetone glucose with the dye to form the intermediate product of a diacetone glucose - dye conjugate was shown to be successful by the production of a new compound visualised by TLC after the reaction. The subsequent alkaline hydrolysis of the reaction mixture to produce the desired product of diacetone glucose showed the disappearance of the band presumed to be the diacetone glucose - dye conjugate but the presumed product of dye-glucose appeared to run with a virtually identical r.f. to that of the hydroxyl dye also present in the mixture. This meant that it was necessary to purify the diacetone glucose - dye conjugate from the reaction mixture before deprotection to allow separation from the other components of the reaction mixture.

The diacetone glucose - dye conjugate was therefore purified by column chromatography to produce pure product. This was then hydrolysed under alkaline conditions to yield the desired product of dye - glucose. However it was shown by TLC that an additional purification step

was then needed as although the deprotection reaction showed complete hydrolysis of the diacetone glucose, some other dye containing species presumed mainly to be hydroxyl dye were also present. This was despite the fact that the ether linkage between the dye and glucose should be stable under the mild alkaline hydrolysis conditions used. A further column chromatography step was therefore used to produce the desired product of pure diacetone glucose which was confirmed by TLC.

4.4 Dye Stacking / Deviation from Beer's Law

It has been previously observed that aqueous solutions of Cibacron Blue F3-GA deviate from Beer's Law[38,74,75]. This has been explained by a combination of 'stacking' effects due to the interaction of the planar aromatic rings of the dyes and ion-pair formation between dye molecules in solution. Both of these effects alter the electronic environment of the chromaphoric anthroquinone ring causing hypochromic and hyperchromic shifts in the absorbance spectrum of the dye as its concentration is increased. It was also noted that although there is a hypochromic effect at the absorbance maximum of the dye at 610 nm, the overall changes did not shift the wavelength of the maxima as had been observed with other dye molecules such as Acridine Orange[76]. As dye stacking has been used as an explanation of both the deviation of absorbance of dye containing solutions and of the complex binding kinetics observed for the interaction of dye with a model protein[39,48] it is obviously of interest to attempt to model the stacking interaction. A simplistic model assumes that the stacking interaction is represented as a equilibrium between stacked and unstacked dye with the stacked dye complex consisting of a pair of interacting dye molecules (**Eqn. 1**). The absorbance of a solution containing dye can then be modelled by the following equations in terms of the measured absorbance (**A**), the concentrations of free dye (**Df**), stacked dye ($\mathbf{Df_2}$)

and total dye ($\mathbf{D_0}$), and the extinction coefficients of the free dye ($\mathbf{E_f}$) and the stacked dye complex ($\mathbf{E_s}$).

1) $2Df \Leftrightarrow Df_2$

2) $D_o = [Df] + 2[Df_2]$

3) $A = E_f[Df] + E_s[Df_2]$

Hence from equations 1,2 & 3 the absorbance of a solution is given by :

4) $A = E_f([D_o] - 2[Df_2]) + E_s[Df_2]$

The equilibrium constant (K_s) between stacked and free dye is given by :

5) $$K_s = \frac{Df_2}{(D_o - 2Df_2)^2}$$

Solving 4 & 5 quadratically for absorbance gives:

6) $$A = E_f\left[D_o - \frac{\left(\left(4D_o + K_s - \sqrt{K_s(8D_o + K_s)}\right)\right)}{4}\right] + E_s\frac{\left(4D_o + K_s - \sqrt{K_s(8D_o + K_s)}\right)}{8}$$

This model was then used to produce a fit to absorbance versus concentration data generated by addition of successive aliquots of concentrated dye solution to a cuvette. Once corrected for the dilution effect of the additions the data showed the expected negative deviation from Beer's Law and the data were fitted to **Eqn. 6** to give an equilibrium constant for the stacking interaction and an extinction coefficient for the stacked dye. The extinction coefficient of the dye ($\mathbf{E_f}$) has a value of 13,600 M^{-1} cm^{-1}. at 610 nm[77]. Fixing this value then allows the equation to be solved for the two unknowns $\mathbf{E_S}$ and $\mathbf{K_S}$ as the total dye concentration $\mathbf{D_0}$ is

known. The extinction coefficient determined by the curve fit for the stacked dye represents that of the complex of a pair of stacked dye molecules. Thus the extinction coefficient of a single dye molecule under stacked conditions will be half this, a value determined to be 11,070 M^{-1} cm^{-1} with the dissociation constant for stacked dye, $\mathbf{K_S}$ as 8.76 x 10^{-5} M^{-1}.

Even though data for free dye stacking have appeared in the literature there appears to have been no attempt to model the observed data for the stacking interaction. The observed results for the spectral changes involved in dye stacking are in agreement with those previously shown by Federici et. al.[78]. The simple model used to describe the dye stacking provides a good fit to these data. The bimolecular dependence upon dye concentration explains the observation that at concentrations of less than 5 uM the stacking interaction is negligible and the dye can be presume to exist mainly as unstacked molecules.

Values for dye stacking have however been previously estimated as part of the model proposed by Hubble et. al.[48] to describe the binding of dye and dye-dextran conjugates to lysozyme. Although the value of the stacking constant $\mathbf{K_S}$ is in the same region as those previously determined (10^{-4} - 10^{-6} M^{-1}), the extinction coefficient determined for the stacked dye is considerably greater than the values estimated (2,000 - 9,000) in the fits to the lysozyme binding data. This may in part be explained by differences in the stacking effect between free dye and that linked to a dextran backbone.

4.5 Purification of Yeast Saccharopine Dehydrogenase

Yeast (*Saccharomyces Cerravisiae*) Saccharopine Dehydrogenase was potentially useful as a model enzyme for evaluating dye binding interactions. It is a monomeric NADH utilising dehydrogenase with a molecular weight of approximately 39 k Daltons. This gives it a similar subunit size to that of horse liver ADH and rabbit muscle LDH, both of which have been

extensively used for studies of dye-protein interactions. Although both the aforementioned dehydrogenases are readily available from standard sources (Sigma) in the milligram quantities needed for spectrophotometric binding studies, both saccharopine dehydrogenase and scallop octapine dehydrogenase (which has been previously used for studying dye-protein interactions) are not available in the quantity and purity required at reasonable cost. It was therefore decided to purify the enzyme from yeast.

The purification protocol used was based upon a previously published one[60], using an autolysis of dried yeast powder followed by ammonium sulphate fractionation to yield a partially purified ammonium sulphate precipitate which could be stored at 4 C and used as a stock for further purification. A single step affinity purification from the crude extract was attempted using Cibracon Blue F3-GA Sepharose media with both single step and gradient salt elutions being trialed. The single step elution showed that only a small proportion of the activity bound to the column. However, as the rates were not corrected for background NADH oxidase activity, which had shown to be present as almost half the total level of activity in the crude extract, it was not clear if the bound activity was specific saccharopine dehydrogenase activity.

A single step elution using a 1 M KCl wash would be expected to elute all material bound to the column in a single peak including both the desired protein as well as contaminating ones. A more specific elution should yield a higher purity product with better specific activity. However, the gradient elution showed no improvement in the resolution of the bound activity as the protein eluted in a single tailed peak, rather than multiple peaks which might be expected if different proteins were being specifically eluted from the column as the salt concentration was increased.

The other portion of the ammonium sulphate precipitate was used for the next step of the purification procedure according to the original protocol which used a CM-Sephadex ion-exchange column. Analysis of the eluted material from this column using SDS-PAGE showed the presence of an approximately 40 kDa. protein band eluted within the peak which would correspond with the expected size of saccharopine dehydrogenase. The protein at this stage was still far from pure, with the fractions containing numerous other contaminating proteins.

At this point a small quantity of pure saccharopine dehydrogenase which had been ordered from Sigma arrived and was used for a trial spectral titration using the T40.20 dye-dextran conjugate. The results of the spectral titration showed that no detectable difference spectrum was produced upon addition of saccharopine dehydrogenase to the dye-dextran conjugate. This indicates that there is no specific interaction between the dextran bound Cibracon Blue F3-GA and the protein, making it unsuitable for use as a model protein for studying dye-protein interactions in this system. There is however some question over the enzyme as supplied by Sigma due to the presence of a absorbing impurity within the protein sample. The possibility cannot be ruled out that the presence of this might have been inhibiting the binding of Cibracon Blue F3-GA to the protein. The small quantities apparently present make this unlikely. It would have been advantageous to dialyse the protein to remove any such impurities which might prevent binding to the dye. However with the small volume and quantity of protein available, the losses involved in dialysis were prohibitive and the quantity of possible contaminants presumed to be low enough to ignore.

The lack of binding to the dye-dextran conjugate also provides an explanation for the lack of efficacy of the affinity chromatography step. If saccharopine dehydrogenase does not interact with the dye-dextran then it is unlikely to interact specifically with the affinity matrix. The

binding of some activity to the column can be explained by a combination of binding of other proteins with NADH oxidase activity and binding of some of the saccharopine dehydrogenase due to non-specific hydrophobic and ion-exchange interactions with matrix bound dyes. This is supported by the fact that a gradient elution failed to resolve a peak of activity from the column which might be expected if a specifically bound protein was being eluted.

4.6 Purification of Scallop Octopine Dehydrogenase

This dehydrogenase plays a similar metabolic roll in molluscs, nemerteans, sipunculids and coelenterates as lactate dehydrogenase does in mammals[79]. As mentioned previously it fulfils both basic criteria required for a model protein for the experimental system by being both an NAD dependant dehydrogenase and monomeric, with a molecular weight of around 40 k Daltons.

The basic preparation of the crude extract from the Scallop tissue was more complex and time consuming than for the comparative step in the purification of the yeast octapine dehydrogenase, which had been one of the considerations in first attempting the purification of the yeast protein. Notably considerable effort was involved in dissecting the reproductive organs from the frozen Scallops and slicing the frozen tissue prior to blending to aid in homogenisation of the tissue.

Initially a small quantity of Scallop tissue was prepared and used to check that enzyme activity was present in the extract and the first steps of the published purification protocol. Comparison of the rates of the activity assay with and without the substrates for octapine dehydrogenase showed that the background activity in the crude extract was very low (less than 1/20th of the total activity) and that the crude extract had a specific activity comparable with those previously published showing that the frozen scallops obtained were suitable as a

source material. In contrast previous procedures had used either fresh tissue, or adductor muscles dissected and frozen directly from fresh Scallops.

The dialysed ammonium sulphate fraction from the first trial was split into two portions which were used to test the first ion exchange step from the original protocol and a dye-affinity purification step. It was found that the DEAE Sephacel ion-exchange media used in the first published purification protocol[62] was difficult to handle due large changes in its bed volume as the ionic strength was changed. Dye affinity chromatography purifications were trialed with material both directly after the ammonium sulphate fractionation and also after the ion exchange step. Neither of these two affinity chromatography trails were successful in binding significant activity to the column.

Due to the physical problems encountered with the use of the DEAE Sephacel media it was substituted for DE-52 cellulose. This was shown to have similar ion-exchange properties in terms of binding and elution of octapine dehydrogenase without the physical problems encountered with the DEAE Sephacel media. This was then successfully upscaled and used to prepare a large quantity of protein for the subsequent gel filtration step. After the gel filtration step the purified protein was assayed by densitometry of a colloidal Coomassie Blue stained SDS-PAGE gel. This showed that the protein was only approximately 25 percent pure. This is substantially lower than those reported at a similar point in the other previously published procedures which vary from 45 percent to apparently near homogeneity. The significant difference seeming to be the apparent purity after the ion exchange step. This is possibly linked to the use of different ion-exchange media for example DEAE Sepharose which may have some size fractionation as well as ion exchange properties.

As a final purification step dye-affinity chromatography was attempted using a Cibracon Blue F3-GA Sepharose column. Surprisingly even at this stage the column did not appear to bind

any significant quantity of octapine dehydrogenase. This is direct contrast to other studies by other investigators which have used octapine dehydrogenase as a model protein to study protein interactions with Cibracon Blue F3-GA columns[80]. It must be noted however that these authors have previously cited Cibracon Blue F3-GA as being the *meta- /para-* isomers of the dye rather than the *ortho-* isomer as supplied by Sigma and used in these studies. As has been discussed earlier there can be significant differences in the binding between the various isomers of the dye which my well explain these anomalous results.

Due to the lack of success with the Cibracon Blue F3-GA affinity column it was decided to synthesise and use a Reactive Green 19 affinity column as this had been used previously in an octapine dehydrogenase purification at this point[64]. The column was loaded and eluted in accordance with the published protocol. However, in contrast to the original paper in which all activity was reported to be eluted in the 150 mM NaCl elution step, little was present in this step. The reason for this is unclear, but there is the possibility that this might be due to slight structural differences between the dye as used in the original paper and soured from ICI Chemicals as Procion Green H-E4-BD and the equivalent compound, Reactive Green 19, obtained from Sigma for the synthesis of the affinity matrix. It is not unknown for there to be structural differences between some 'equivalent' triazine dye compounds depending on the original source as exemplified by the known misnaming and confusion in structures between compounds referred to as Reactive Blue 2 / Cibracon Blue F3-GA[81,82].

At this stage the protein was not pure enough to use for binding studies and there was also some evidence from the dye-affinity chromatography trials that it might in fact not interact at all with the isomer of Cibracon Blue which was being used. As an alternative monomeric NADH utilising enzyme, billiverdin reductase, had become available in a pure form the octapine dehydrogenase purification was left at this point.

4.7 Spectral Titrations using Lysozyme

The mutual depletion model models the equilibrium between bound dye and dye in solution by taking into account the difference between the absorbance spectra for free dye and bound dye. Thus for a solution containing bound and unbound dye the overall absorbance A of the system at a specific wavelength can be described as follows ;

1) $$A = Ef[Df] + Eb[Db]$$

Where ***Ef*** and ***Eb*** are respectively the extinction coefficients for the free and bound dye at the chosen wavelength and ***Df*** and ***Db*** are their concentrations.

When measuring the difference spectrum between solutions of equal dye concentration, only one of which contains protein, then the change in absorbance between the two solutions is given as follows ;

2) $$\Delta A = [Db](Eb - Ef)$$

The concentration of ***Db*** can then be calculated from the equilibrium between free and bound species. The equilibrium constant ***Kd*** is described by the following equation.

3) $$Kd = \frac{([Dt] - [Db])([Et] - [Db])}{[Db]}$$

where ***Lt*** is the total concentration of ligand binding sites, ***Dt*** the total dye concentration and ***Kd*** the dissociation constant.

Solving equation 3 for ***Db*** gives the physically significant root

4) $$Db = \frac{([Df] + Kd + [Lt]) - \sqrt{([Df] + Kd + [Lt])^2 - 4[Df][Lt]}}{2}$$

By substituting this into equation 2 the absorbance change can be related to ***Kd***, ***Df*** and ***Et***.

5) $$\Delta A = (Eb - Ef)\frac{([Df] + Kd + [Lt]) - \sqrt{([Df] + Kd + [Lt])^2 - 4[Df][Lt]}}{2}$$

For a difference titration the $(Eb - Ef)$ term can be replaced by a term ΔE which represents the difference between the extinction coefficients of the free and bound dye.

It has been shown by Mayes et al.[25,39] that only around 30 percent of the dye bound to dextran is available for binding to lysozyme in their model system. In spectral titrations using a fixed dye concentration, ***Dt*** in the above equation can be allowed to float. As the actual concentration of dye is determined separately, the quantity of dye available for binding can be calculated by comparing the actual value ***Dt*** (determined spectrophotimetrically) with the apparent value ***Da*** determined from the curve fit of the equation fit to the data. Thus the fractional availability of dye for binding is given by ;

$$6) \qquad Fa = \frac{Da}{Dt}$$

In the case of the reverse spectral titration experiment with fixed enzyme concentration and a varying dye concentration then this term must be introduced into the fit, thus by substituting **[*Dt*]** in equation 5 by **(*Fa* [*Dt*])** then can be fitted for ***Dt***, ***Fa***, ***Lt*** and ***Et***.

An alternative more complex model involving dye stacking has been proposed by Hubble et. al.[48] This assumes that the dye available for binding is also available for a competing stacking interaction. Thus the equilibrium between the various forms of the dye is shown as :-

$$Ds \xleftrightarrow[Ks]{Df} Df \xleftrightarrow[Kd]{Li} Db$$

Where ***Ds*** is the stacked complex Df_2 and ***Db*** the bound dye complex ***Df.Lt***.

The dye stacking model is less trivial to solve due to the introduction into the model of a third dye specie which has an effect upon both the dye availability and the absorbance of the solution. This results in a cubic expression for ***Db*** which is no longer capable of being solved

by a simple algebraic expression. A complete account of the reasoning and derivation of this is given by Hubble et al.[48]

The stacking model is unnecessary to model the equilibrium spectral titration results. It can be seen that good fits to the data from the equilibrium titration experiments are obtained using the simple binding model. This can be attributed to the fact that the concentration of dye used in the experiments (20 - 25 uM) is in the region where the level of stacking is comparatively low. In combination with the low number and limited resolution of the datapoints recorded this makes it difficult to distinguish between simple and more complex models in terms of goodness of fit. .

4.8 Dye -Lysozyme Rapid Kinetics

The binding kinetics between dye-dextran conjugates and lysozyme have been shown to deviate markedly from those described by a simple model although those for free dye appear to deviate less significantly[39]. As noted previously it can be difficult to differentiate between different models on the basis of equilibrium titration data due to the fact that one is observing only the end point of a perturbation in the equilibrium of the system in which all kinetic processes involved are invisible. By recording kinetic data it is possible to differentiate between different kinetic processes involved in a system providing they fall within the range of measurement of the instrument.

The spectral data recorded using the diode array from dye and dye-dextran binding to lysozyme show the spectra appear to have reasonably clean isosbestic points which is indicative of the interconversion of two absorbing species. From this there is no clear evidence of the presence of other spectral intermediates when the experiments are performed with an excess of lysozyme.

The experiments with free dye over a range of lysozyme concentrations (31.25 - 250 uM) show the unexpected result that as the concentration of lysozyme is increased the rate of precipitation in the samples decreases. In fact at the two highest concentrations used there is no evidence of precipitation. This can be explained if the precipitation and binding reactions are competitive such that when there is a large excess of lysozyme the specific binding interaction competes out the non-specific interactions presumed to cause precipitation. From this it is inferred that lysozyme has both a high affinity and a low affinity interaction with Cibracon Blue F3-GA and that it is the low affinity 'non-specific' interaction that mediates precipitation.

This is in agreement with the results reported for the interaction with the dye using a gel permeation technique based on the Hummel and Dreyer approach[83] which had shown evidence for both a high affinity and a low affinity interaction with the dye-dextran conjugates[25] It has been previously demonstrated that the dye mediated precipitation of serum proteins is mediated similarly by the non-specific binding of a large number of dye molecules which cause precipitation through a combination of hydrophobic and electrostatic interactions[84]. The lack of precipitation observed with the conjugates can be explained by the following hypothesis. With the free dye as one or more dyes bind to the protein through low affinity ion-exchange effects, the charge and hydrophobicity of the protein is altered allowing the protein / dye complexes to aggregate. In the conjugates the dye is bound to a soluble hydrophilic polymer backbone which will both tend to increase the solubility of the complexes formed and also distribute them spatially, sterically hindering the approach of other conjugates. However if the loading of dye on the backbone is increased the hydrophilicity and propensity for non-specific interactions is increased allowing precipitation to again take place.

The spectral binding data of free dye (250 uM) to lysozyme (25 uM) was globally fitted using the program Specfit (R.Binstead). The fit uses a simple binding model and produces a good fit with low residuals. This shows that under these conditions the data collected for the binding kinetics do not appear to deviate markedly from a simple binding model as previously shown at a single wavelength[39]. There is some initial offset of the first spectrum recorded in comparison to the remainder. This is accountable for by an artefact created by the photodiode array. When the stop flow is awaiting a trigger signal to start data collection information is not scanned from the diode array allowing it to saturate with light. Upon the trigger signal to start data collection a clearing pulse is sent to the diode array, however due to the previous saturation of the array the first scan can be distorted due to a 'photodiode blooming' effect. This effect results in incomplete clearing of the array, leaving some residual charge in the photodiodes slightly distorting the first dataset taken from it. For subsequent datasets scanned from the array, the array has not been saturated and this is no longer a consideration. Having noted this effect with the manufacturers of the system a 'fix' was later introduced into the stop flow system such that an additional clearing pulse was sent to the diode array shortly before data collection began. This successfully reduced any 'blooming' effects to almost within the noise levels of the equipment.

Although the data from the free dye binding experiments can be successfully modelled by a simple binding model, those for the dye-dextran conjugate show the more complex behaviour previously noted. From the example fit to a cross section through a dataset at the major hypochromic trough at 595 nm it can be seen that this does not adequately describe the shape of the binding curve seen. Comparison of cross sections through the binding curves generated over a 8 fold range (31.25 - 250 uM) of lysozyme concentrations at two different dye-dextran concentrations (22 uM, 44 uM) shows that there appears to be little difference in the binding

curves produced except at the concentrations where lysozyme is no longer in excess. This suggests that when there is an excess of binding sites available then the binding kinetics are zero order with respect to site concentration.

4.9 Spectral Titration with LDH

Initially spectral titrations measuring dye binding to LDH were performed by additions of equal quantities of dye or dye-dextran to sample and reference cuvettes, with the sample cuvette containing a known concentration of LDH. This produced difference spectra which appeared to have large variations in the baseline between additions such that the isosbestic points normally visible in such titrations were unclear and it was difficult to make accurate determinations of the magnitude of the spectra. This problem with variation in the apparent baseline is inherent in the design of this experimental method for at least two reasons. Firstly it involves the measurement of the difference spectrum at the same time that quantities of absorbing material were being added to both sample and reference cuvettes. Any small difference in the quantity of dye added to each cuvette would effect the difference in absorbance between the two cuvettes, and hence the results produced. This was exasperated in the case of the addition of the dye-dextran conjugates, which have a higher viscosity and are thus more difficult to pipette accurately with an air displacement pipette. Pipetting errors were reduced by using a positive displacement pipette for the addition of all dextran containing solutions. The second problem is also related to the fact that the concentration of dye is being altered thoughout the experiment. As the concentration of dye is increased in both the cuvettes the proportions of both free and stacked dye will also be varying between the cuvettes due to the presence of LDH bound dye in one of the cuvettes. This will be accentuated at the lower dye concentrations where a significant proportion of the available

dye in the sample cuvette will be bound to LDH. This will reduce the effective concentration of free dye in the sample cuvette to concentrations where little of the unbound dye will be stacked. In comparison the dye in the reference cuvette will be present mainly in the stacked form. Thus the difference spectra measured between the two cuvettes will be due not only to the LDH bound dye, but also to the difference in the stacked dye concentrations.

The reverse experiment, as performed by Mayes et al.[39], in which enzyme is added to dye solutions has fewer problems inherent in its methology. The enzyme does not absorb in the visible light region where the difference spectrum is being measured, and hence there is no direct effect on the baseline absorbance. The are possible differences due to a dilution effect if slightly different volumes are added to each cuvette, but the magnitude of any such effect is negligible due to the small volumes being added and this is common to both methods. Also any stacking effects will have greater significance only towards the end of a titration where the concentration of free dye is being lowered to concentrations where the ratio of stacked to free dye is being appreciably effected. In this range the spectral changes being measured are small and will have less effect on the shape of the binding curve.

One of the reasons for not initially using the later method was that with the previous experiments using lysozyme it had involved the use of enzyme solution at a high (5 mM) concentration, which in the case of LDH was prohibitive due to both cost and the limiting solubility of LDH. However, data from the initial experiments titrating dye against LDH indicated that the affinity was at least an order of magnitude higher. Due to this and a larger difference in the extinction coefficient of the bound and free dye measurement was possible using a stock solution of lower absolute concentration (1 mM subunit concentration). Therefore after the initial titrations against a fixed LDH concentration all subsequent titrations were of protein against a fixed concentration of dye.

Comparison of the results for the titration of free and the dye dextran conjugates which were titrated using both methods shows some variation between the determined values for the difference between the extinction coefficients of free and bound dye (ΔE), the dissociation constants (***Kd***) and the fractional availability of the dye for the dye-dextran conjugates. As has been alluded to previously one of the problems with curve fits to these sorts of datasets is that the limited number of datapoints and resolution limits the accuracy of a fit and its sensitivity to variation in the parameters. With several interdependent parameters it is possible to accommodate significant variations in individual parameters without having a large effect on the apparent goodness of fit to the data. This problem is especially acute with datasets such as those for the titrations against a fixed LDH concentration in which the experimental error is large in comparison to the values determined. This is also a factor that must be borne in mind in terms of modelling the data. As mentioned previously there is strong evidence that dye stacking may have some effect on the measurements of these interactions. However in terms of equilibrium binding data the weaker stacking interaction will not have a major effect on the apparent dissociation constant.

The determined values for free dye and dye-dextran affinity to LDH are similar to those previously published and the trend of decreasing Kd as dye loading is increased for the dye-dextran conjugates follows that previously observed with lysozyme and for the affinity partitioning of LDH with Procion Yellow HE-3G, another triazine dye[85].

Comparison of the determined constants for the binding of the T40.1 and T40.20 dye-dextran conjugates at 25 C and 4 C shows similar values for the determined Kd (1.81 and 1.10 uM respectively at 25 C compared to 2.33 and 1.18 uM at 4 C) for both conjugates at both temperatures. The position of the binding equilibrium seeming relatively insensitive to

temperature changes despite the large changes in the kinetic constants seen at the lower temperatures (q.q.v.).

The fractional availability of the dye-dextran conjugates in general seems higher at around 0.5-0.6 than that previously measured (0.3) for the interaction between lysozyme and dye-dextrans. This could be linked to the considerably higher affinity of dye to LDH than to lysozyme which might compete more effectively with the effects reducing dye availability. It has been shown that salt concentration can have a significant effect of apparent dye availability on Sephaorse supports[86]. This was explained by the reduced availability of dye not being due to true steric hinderance, but interaction between the dye molecule and the support matrix, which has essential the same structure as the dextrans used in this work. By altering the solvent conditions the interaction with the matrix was reduced and the dye availability increased. Thus a stronger interaction between the dye and the ligand binding site might increase the dye availability.

The titration of the dye-glucose conjugate formed as a model compound for the dye-dextran interaction produces a difference spectrum upon binding to LDH that appears almost identical to that seen with the free dye rather than that observed with dye-dextrans. In this respect it retains the noticeable hypochromic shift with a minimum at 545 nm. The binding constant determined using a fit to the mutual depletion model for the dye-glucose (2.17 uM) is comparable to those determined for free dye by spectral titrations (1.68, 1.23 uM). In combination with the kinetic data it appears that dye-glucose behaves in a manner more similar to that of free dye to that of a dye-dextran conjugate.

4.10 Fluorescence Titrations

Fluorescence titration has the advantage over spectral titration in the fact that a specific interaction between the protein and dye which allows quenching of the proteins intrinsic fluorescence is being measured. The model needed to represent the system is therefore simplified even if processes such as dye stacking are taken into account, as although stacking may have some effect on dye availability it will have no direct effect on the fluorescence of the system. It is also unlikely that the fluorescence quenching could be caused by non-specific interactions with the protein. In contrast the spectral perturbation of the dye ligand could be due not just to a single specific interaction, but a mixture including more general interactions. The fluorescence techniques therefore provide an alternative method of validating the results from the those using the spectral methods.

However some care must be taken in the treatment of the data as solutions containing dye have a considerable absorbance in the UV region where the protein fluorescence is monitored. This absorbance will produce an 'inner filter' effect reducing the effective illumination of the sample and also the yield of fluorescent light from it. The protein itself will also have an inner filter effect but this is less significant as its absorbance only effects the excitation wavelength (280 nm) and the magnitude is both small (approx. 0.080) and constant throughout the experiment.

A simple method for the correction of the inner filter effect involves the use of a graphic extrapolation method[87]. It was shown that under certain conditions the fluorescence of the system could be described by :

$$\ln F_{obs} = \ln F_o - \varepsilon L[X_T]$$

Where ε is the molar extinction coefficient of the ligand, L is the path length through which the light must travel. Thus a plot of $\ln F_{obs}$ vs X_T should be linear if the change in

fluorescence is purely due to the inner filter effect. Therefore at saturating concentrations of ligand this linear relationship should apply and the plot should become a straight line. Calculation of this line gives an empirical determination of the value of εL which can be used to correct the data.

This is a simplification of the actual phenominum which has been treated in greater depth by Parker[88] and Holland et al.[89] who derived the following equation describing the correction for the inner filter effect on fluorescence at the excitation wavelength :

$$\frac{F}{F_{obs}} = C = \frac{2.303A(x_1 - x_2)}{10^{-Ax_1} - 10^{-Ax_2}}$$

This includes a correction for the exponential reduction in illuminating intensity across the cell path, where $\mathbf{x_1}$ and $\mathbf{x_2}$ are the positions of the slit window relative to the cell and **A** is the molar absorbance of the sample at the excitation wavelength. This assumes that the efficiency of detection of the fluoresced light is uniform across the observation window. This correction was shown to hold true up to an absorbance of 2 with the instrument set-up used. Although this equation only compensates for the inner filter effect at the excitation wavelength it can also be applied in a similar manner to inner filter effects occurring at the emission wavelength.

The use of a small pathlength cell (4 x 4 mm) for the fluorescence experiments reduces the error in the simple correction as the illumination is closer to the approximation of a point source, as well as reducing the overall pathlength and thus the magnitude of the inner filter effect.. This is different to the rapid kinetic experiments in the stop-flow which has an observation cell of 10 x 2.5 mm with the illumination across the longer dimension.

Using the same principles as outlined for the simple correction Latzowicz[90] stated that the corrected fluorescence intensity for a sample adsorbing at both the excitation and emission wavelengths is given by :

$$F = F_{obs} 10^{\left(\frac{A_{ex}+A_{em}}{2}\right)}$$

From examination of the form of these equations it can be seen that for a titration with inner filter effects at both excitation and emission wavelengths the same principles for the empirical graphical determination of a correcting factor still hold. Thus by linear regression analysis of the linear end point region of the titrations on a semi-logarithmic plot a correcting factor can be determined that should be common for all the titrations using the same protein and dye-ligand. Thus :

$$F = F_{obs} 10^{C[X_T]}$$

Where ***C*** is the correcting factor determined by linear regression and is approximately equal to the average optical density of the sample at the excitation and emission wavelengths.

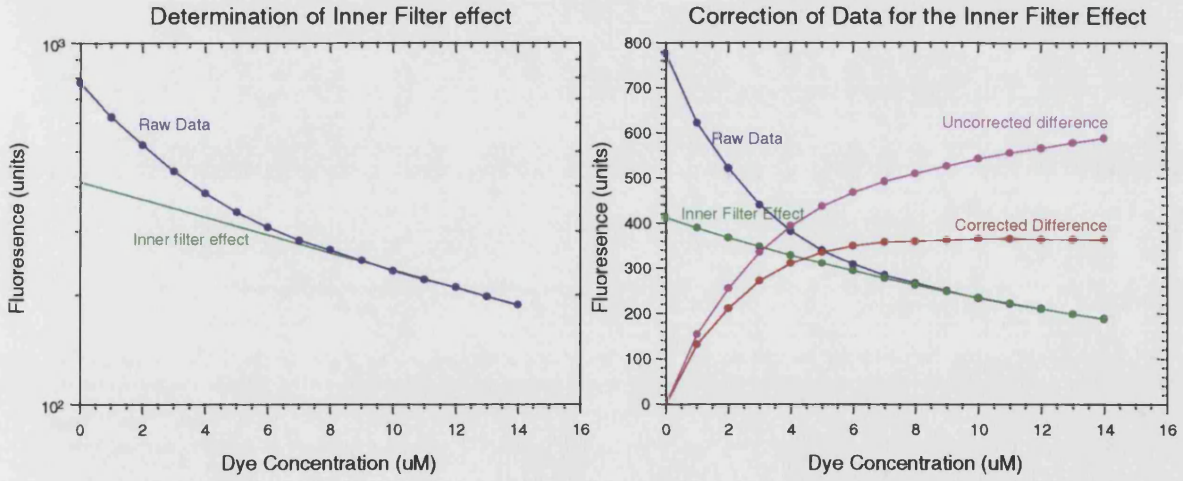

Figures D1a,D1b : Figure D1a shows a semi logarithmic plot of a fluorescence binding curve from which the quenching constant for the inner filter effect is determined by linear regression to the later portion of the curve. Figure D1b then shows the same dataset on a normal plot along with the difference spectrum produced after compensation for the inner filter effect.

The application of this graphical approach for the determination of the compensation factor for the inner filter effect is shown in **Figures D1a, D1b**. These show the semi-logarithmic plot used to determine the constant used to compensate for the inner filter effect and the subsequent transformation of the data into a corrected difference curve. The importance of the correction can be seen by comparison of the uncorrected binding curve to that produced when the inner filter effect is taken into consideration. Once the titration data have been corrected for the inner filter effect then they are fitted using the mutual depletion model as previously explained.

The determined values from the fits are in broad agreement with those from the spectral titrations showing the validity of both the methods for measuring the dye-protein interaction. As seen previously with the spectral titrations the dissociation constant (**Kd**) decreases as the ligand loading increases for each backbone size. There also seems to be some increase in the affinity as the absolute loading of the backbone is increased i.e. dye-dextrans with the same relative loadings but increasing backbone size. However there does not seem to be any real evidence for a true co-operative binding effect as might have been expected with the large dextran backbones and higher loadings. As the size and loading of the dextran backbone is increased it might be expected that this would allow and promote the interactions of multiple dye molecules attached to a single dextran backbone with more than one of the four sites available for specific binding with the tetrameric LDH. The size of even the smallest dextran (40 kDa.) would give a length of around 500 Å compared to LDH which has an equivalent spherical diameter of 70 Å. Thus for the larger dextrans it would be expected that their size should be more than adequate to allow wrapping around the molecule. Measurements by Johansson and Joelsson[85] of the competitive inhibition of the enzymic activity of LDH with Procion Yellow - dextran conjugates appeared to indicate increasingly co-operative binding

as the average dye loading was increased from 1.3 to 8.3 dyes per dextran molecule (73 kDa.). However they saw no evidence of the expected steeper extraction profiles in two phase partitioning experiments that would be expected from these results. The range of loadings of dye-dextrans used for this work covers a similar range (absolute loadings of 1.2 - 5.1 for T70 series using the same size dextran) and the spectral and fluorescence titrations show only a small increase in affinity as the loading is increased.

4.11 Dye - Dextran Rapid Spectral Kinetics with LDH

The equilibrium titrations of dye-dextran conjugates to LDH showed that the binding interaction could be measured using both spectral and fluorescence techniques. The results of these experiments producing binding curves that appeared to give a reasonable fit to a simple binding model. However the kinetic measurements of the interaction with lysozyme had shown that the binding kinetics were more complex than could be represented by this simple mutual depletion model. Kinetic binding measurements were then attempted with LDH to validate some of the deductions made from the previous work using lysozyme as a model protein.

Initial experiments with free dye and LDH at 25 C showed no measurable spectral changes using a similar dye concentration to that used for the titrations. This indicated that the reaction had reached completion within the mixing time of the stop-flow (approximately 1.5 milliseconds). Similar experiments were then repeated using the T40.20 dye dextran conjugate as this might be expected to produce slower kinetics due to the additional steric constraints placed upon the dye molecule when connected to a dextran backbone. This too produced no measurable change upon mixing. Experiments using equine ADH also showed no detectable kinetics with the dye-dextran conjugate. It was then found that by lowering the

reaction temperature to 4 C the reaction was slowed to the extent that the binding kinetics of the dye-dextran conjugates could be observed, but that of the free dye was still too fast to be observed. The temperature dependence of biological reactions is normally referred to by the term Q_{10}, which is the change in rate of reaction on an alteration of 10 C in temperature. This value is related to the activation energy (E) of the reaction by the Arrhenius equation[91] which (in its modern form) gives the velocity of the reaction as :

$$v = Ae^{(-E/RT)}$$

Where R is the gas constant, T the absolute temperature and A the pre-exponential factor. Most biological interactions have a Q_{10} of around 2 which relates at 20 C (293 K) to an activation energy of around 49 $KJmol^{-1}$. By examination of the kinetic data recorded for the binding of the T40.20 conjugate, a detectable change still occurs in the 50-200 ms region. Thus for no change to be detectable at 25 C the reaction must have reached at least this point in the 1-2 ms dead time of the instrument. This gives a Q_{10} for the reaction in the region of at least 10 which is considerably higher than would be expected. Values of larger than 2 are usually indicative of structural rearrangements involving entropic effects[92].

Although at 4 C the binding kinetics of the dye-dextrans are slow enough to be measurable, those with free-dye are still to fast to measure. This indicates that the rate limiting step is not the same in the binding processes for the free and the conjugated dye-dextrans. Examination of the binding curves measured for conjugates with backbone sizes from 40 kDa to 2,000 kDa shows that qualitatively there appear to be few differences between them, all producing curves which by inspection have similar rates and shapes. Thus although the binding of the dye to a dextran backbone appears to have a fundamental effect on the binding process there does not appear to be any further effect on this as the size of the dextran is increased. The dye-glucose conjugate produced appears to behave in a similar manner to free dye rather than

that of a dye-dextran both in terms of the difference spectrum produced upon titration with LDH and its binding kinetics which are also too fast to be detectable. This shows that the differences in the behaviour of free dye to that of a dye-dextran are not due to the coupling to and presence of the immediately adjacent glucose molecule.

Visual inspection of the shape of the binding curves showed that they appeared to be more complex in form than could be described by a simple binding model. This is clearly demonstrated by the example curve fit to a kinetic version of a simple binding model shown in **Figure 4:2.** The model is described as follows :

1) $$La + Da \underset{k_2}{\overset{k_1}{\leftrightarrow}} La.Da$$

Where ***La*** represents the concentration of available ligand binding sites, ***Da*** the concentration of free dye and ***La.Da*** the complex formed between the two. The dissociation constant ***Kd*** is given by the ratio of k_1 the rate constant for the forward association reaction to k_2 that for the reverse dissociation reaction.

2) $$Kd = \frac{k_1}{k_2}$$

The reaction can therefore be described as the set of differential equations :

3) $$Da' = k_2[La.Da] - k_1[La][Da]$$

4) $$La' = k_2[La.Da] - k_1[La][Da]$$

5) $$La.Da' = k_1[La][Da] - k_2[La.Da]$$

As for the equilibrium titrations the absorbance of a dye containing solution is given by :

6) $$A = Ef[Da] + Eb[Db]$$

Where ***Db*** is the concentration of the dye-protein complex ***La.Da***. At the starting point of the reaction the concentration of bound dye is zero. Therefore if the difference from the starting absorbance is measured then the equation is simplified to :

7) $\Delta A = \Delta E[Db]$

Where ΔE is the difference in the extinction coefficients between bound and free dye.

The set of differential equations (**Eqn. 3-5**) can be used directly in the Scientist package which along with equations 2 and 7 allow the reaction to be described in terms of the starting concentrations of dye and ligand binding sites, ***Da*** and ***La***, the equilibrium constant for the reaction (***Kd***) and difference between the extinction coefficients (ΔE) (both previously estimated by titrations) and the forward rate constant for the reaction, k_1. Known values can be set as constants and the unknowns fitted itteritively using a Marquadt least squares procedure.

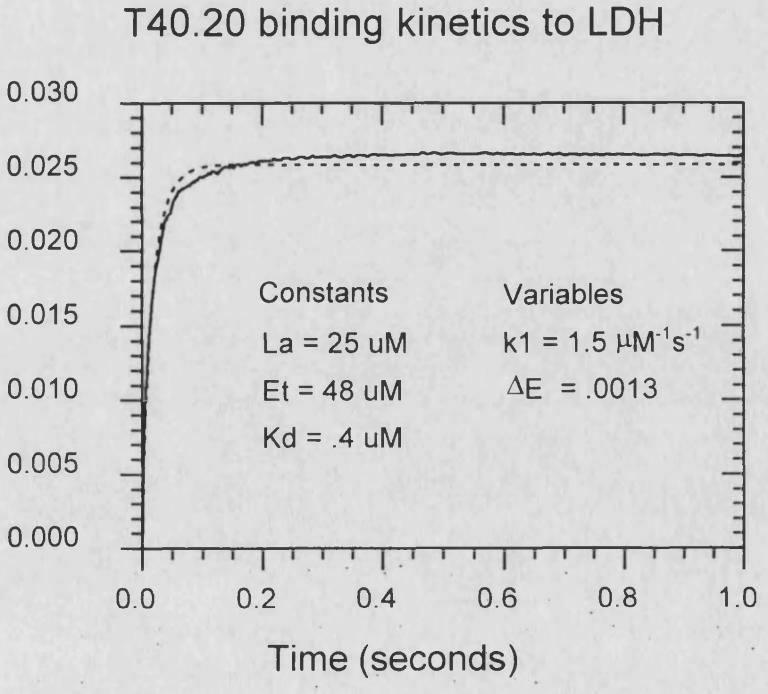

Figure 4.2 : Curve fit of T40.20 / LDH binding curve to a simple binding model.

The complex binding curves seen previously for dye binding to lysozyme had previously been more successfully modelled using a model involving the dye stacking interaction[48]. This produced a biphasic curve in which initially binding to free unstacked dye was rapid, followed by a second slower phase limited by the rate of dye destacking. The first problem in the application of this model to the LDH binding curves is the fact that the timescales of the reactions are completely different. If the rate of dye destacking provides the slower phase in the lysozyme binding reaction then there should be a similar slow phase visible in the LDH binding reaction. As the LDH binding reaction appears to have reached completion within the dead time of the instrument at 25 C, it seems unlikely that the same processes are involved in the rate limiting step for both reactions. However modelling of the stacking interaction shows that in the range of concentrations of dye used a considerable proportion of the free dye present will be in the stacked form. As previously mentioned, the values for the dissociation constant for stacked dye previously determined from fits to lysozyme binding data are in general agreement with that determined for free dye stacking (8.76×10^{-5} M).

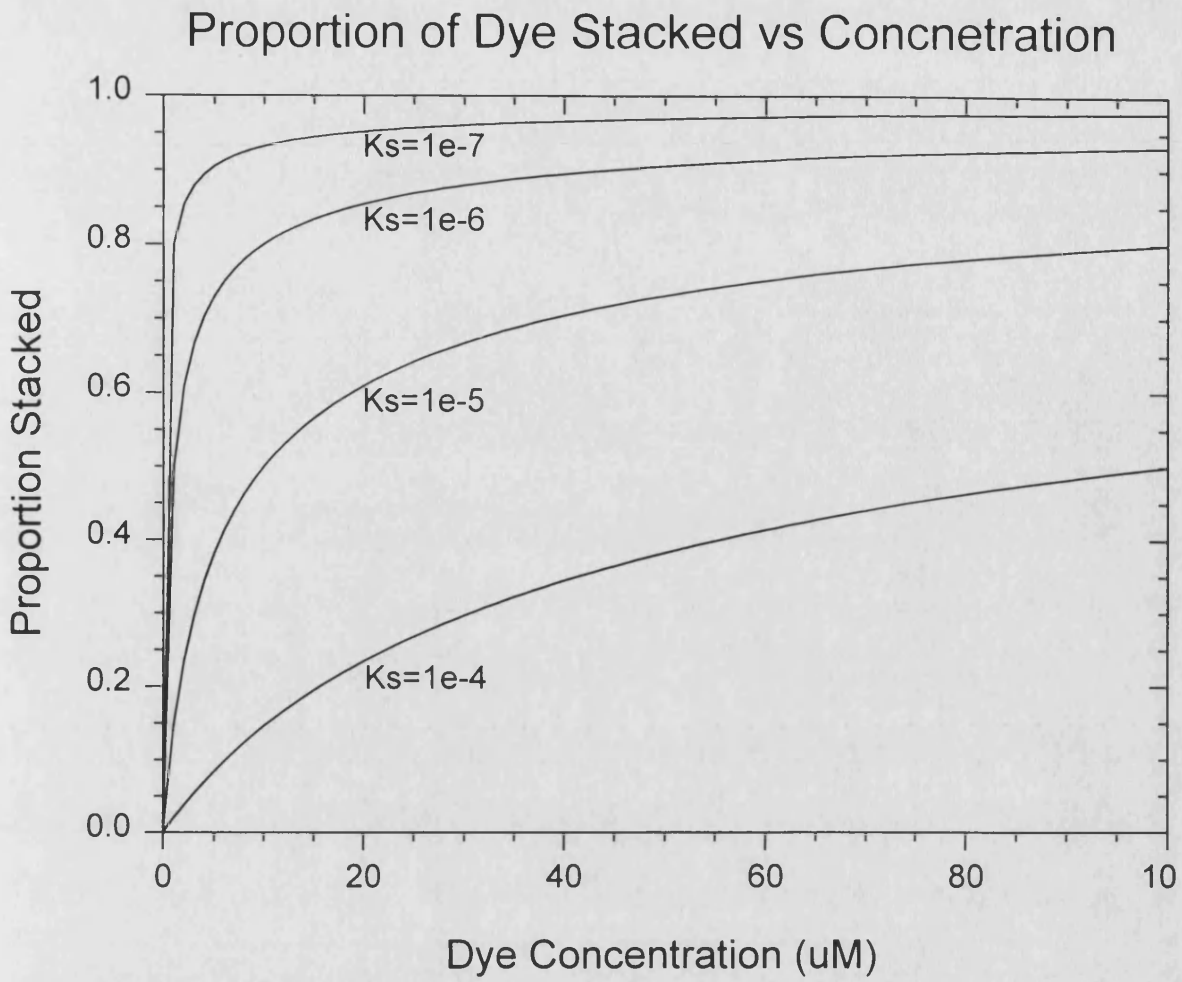

Figure 4.3 : Curves showing the proportion of dye stacked against dye concentration for a range of dissociation constants for the stacking interaction from 10^{-4} - 10^{-7} M.

Figure 4.3 shows curves representing the proportion of dye present in stacked form in the concentration range of 0 - 100 uM with a range of dissociation constants for the stacking interaction from 10^{-4} - 10^{-7} M. It can be seen that the proportion of dye stacked will vary considerably in the concentration range used (0 - 50 uM) in these experiments. However the significance of this in terms of the kinetics of the dye - protein interactions is questionable. This is shown by the fact that no observable change can be seen on the rapid dilution of a 50 uM Cibracon Blue F3-GA solution to 25 uM in the stop-flow. This rapid dilution should result in the perturbation of the dye-stacking equilibrium as the concentration of stacked dye will be higher at 50 uM than at 25 uM. Thus if the rate constant for dye stacking is slow

enough then there should be an observable change in the absorbance as the equilibrium relaxes into its new position. As no change is observable then it can be deduced that the stacking interaction for free dye is a rapid equilibrium and will therefore have no significance to the binding kinetics. This however does not rule out the possibility that stacking interactions may still play a significant role in the kinetics of dye-dextran conjugate interactions. In the case of dye-dextrans there will be stacking interactions between both dye molecules attached to different dextran backbones and those taking place between dyes attached to the same backbone. Whilst the intermolecular interactions will be concentration dependent as for those involving free dye, the intramolecular interactions between dyes attached to the same backbone will not as the effective local concentration of dye molecules will still be the same. There is clear evidence for intramolecular stacking from photon correlation spectroscopy measurements made by Hubble et al.[48] of dye - dextrans in solution. These showed that as the degree of loading on a backbone was increased the apparent molecular weight of the dextran (measured by its effective diffusion coefficient) decreased. This is explained by dye stacking interactions causing the dye-dextrans to fold up on themselves leading to a compaction of the molecule and hence an increase in its measured diffusional coefficient. The kinetics of intramolecular dye stacking could be expected to behave in a different manner in dye-dextrans as any movement of the dye molecules must be accompanied by movements within the dextran backbone. Unlike the intermolecular interactions there also does not appear to be a simple way of kinetically quantifying the interactions. Thus although intermolecular stacking can be ruled out as a kinetically significant process in the case of Cibracon Blue F3-GA, intramolecular interactions may well have some effect.

Intramolecular interactions should depend on both the dye loading and also the size of the backbone. Thus if these interactions are having a significant role in the kinetics of dye binding it would be expected that there should be noticeable differences in the binding kinetics of a dye-dextran with an average backbone size of 40 kDa with an average of around 1 dye molecule attached per dextran (T40.1) and one with a 2,000 kDa backbone with 196 dyes attached (2D9). However this is not the case. Thus although there does appear to be some fundamental effect on the binding kinetics due to the attachment of the dye to a dextran backbone, it does not seem to have any significant dependence on either dye loading or backbone size within the range studied.

In an attempt to gain further insight into the type of processes that might be involved in the binding kinetics the binding curves were analysed by a process of exponential peeling.

In this method a curve is analysed by fitting and subtraction of successive single exponential curves from the original data. The fit is based upon the final 10 - 20 percent of the magnitude of the curve which is used to derive a rate and magnitude for the single exponential. This curve is then subtracted from the original data to produce a 'processed' curve. The fit is then repeated in a similar manner to this curve and the parameters for the next single exponential determined. This process is repeated until the last fit is to the entire residual data.

An example of the stripping procedure is shown in **Figure 4.4**. It can be seen that the original dataset is represented as a total of three exponentials which have been sequentially fitted and subtracted from it. This process was repeated for all the binding curves and the results are shown in **Table 4.1**.

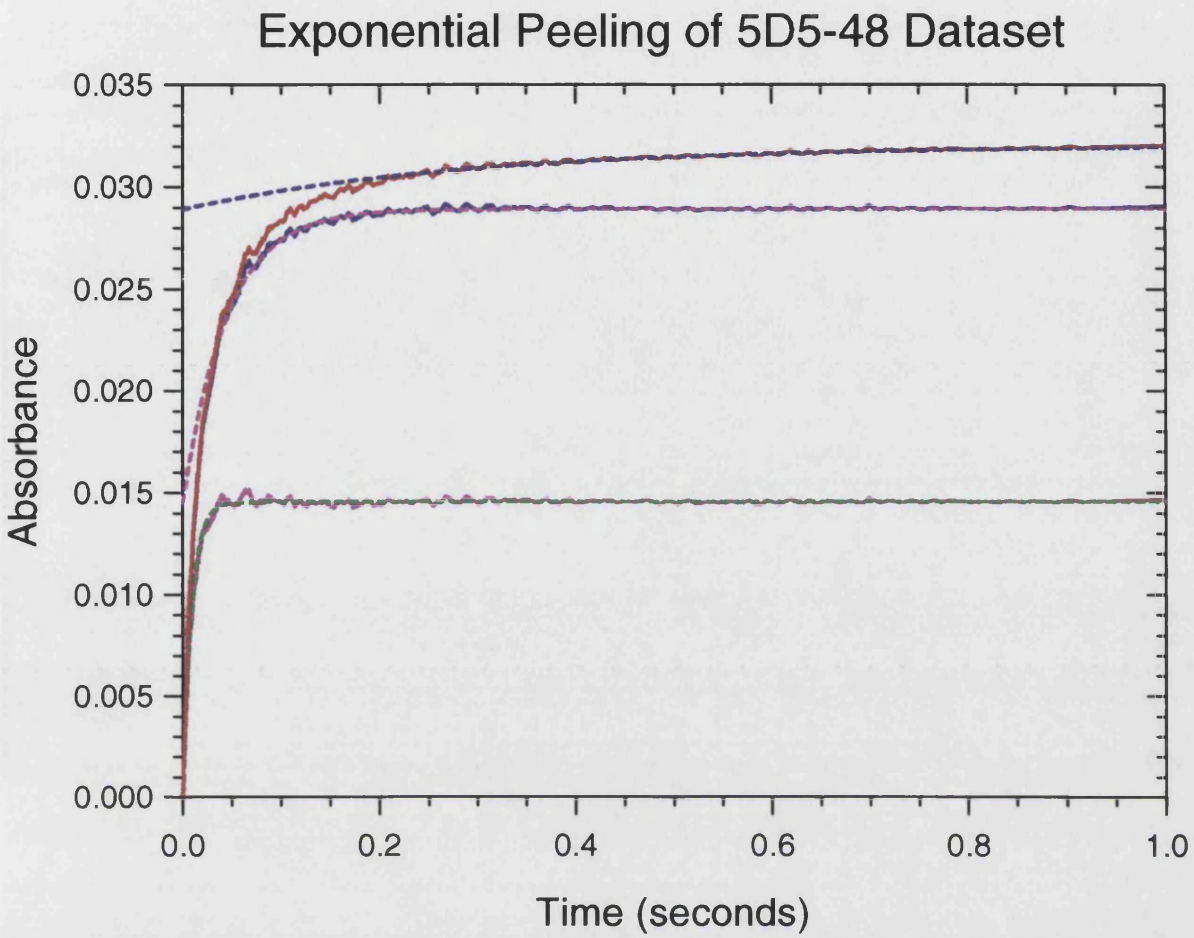

Figure 4.4 : Exponential stripping of kinetic dataset 5D5-48 (originally shown in **Figure 3.84**). Fitted curves are shown as dotted lines, processed data as solid lines. The original dataset is shown in red with subsequent processed data in blue and magenta.

It was found that all the curves could be represented by the sum of 3 exponentials. The table contains values for each of the exponential constant (in bold) followed by the magnitude of the exponential and the overall magnitude of the data to which the curve was being fitted. Thus for the final exponential the magnitude of the data is the same as that of the fitted curve and is therefore not shown.

Table 4.1 : Determined values for exponential peeling of LDH binding curves

		6 uM			12 uM			24 uM			48 uM	
T40.1	**2.877**	**23.1**	**177.69**	**2.945**	**24.64**	**105.55**	**6.79**	**28.95**	**179.7**	**10.93**	**39.79**	**207.7**
	0.00137	0.0033	0.0029	0.00181	0.00394	0.0055	0.002	0.0067	0.00718	0.00379	0.00824	0.0075
	0.00757	0.00618		0.01125	0.00945		0.016	0.0139		0.0196	0.0158	
T40.20	**5.81**	**36.67**	**185.33**	**6.6**	**37.7**	**103.74**	**5.84**	**29.4**	**231.94**	**10.9**	**47.11**	**244.45**
	0.0015	0.0045	0.00321	0.0031	0.0061	0.00694	0.0034	0.0069	0.00632	0.0045	0.01635	0.0073
	0.0092	0.0077		0.0162	0.0131		0.0224	0.0139		0.02655	0.0237	
5D2	**8.5**	**77.51**	**xxx**	**5.09**	**24.2**	**126.57**	**4.82**	**29.15**	**120.14**	**6.38**	**27.8**	**128.01**
	0.0029	0.00606	xxx	0.0021	0.0083	0.00754	0.0031	0.0098	0.0087	0.0026	0.0105	0.0126
	0.00895	xxx		0.0179	0.0158		0.0216	0.0185		0.0256	0.0231	
5D5	**1.95**	**35.9**	**117.2**	**4.73**	**32.7**	**120.95**	**6.33**	**36.8**	**131.03**	**3.47**	**22.6**	**113.6**
	0.0011	0.0041	0.00447	0.0042	0.0095	0.0065	0.0053	0.0126	0.00936	0.0031	0.0144	0.0145
	0.0097	0.0086		0.0202	0.016		0.0273	0.022		0.032	0.0289	
2D4	**5.13**	**33.5**	**113.36**	**2.56**	**25.6**	**101.2**	**2.54**	**26.7**	**118.18**	**5.98**	**29.1**	**122.13**
	0.0021	0.0044	0.00373	0.002	0.0088	0.00788	0.002	0.0128	0.00917	0.0028	0.012	0.01426
	0.0102	0.0081		0.0186	0.0167		0.0239	0.0219		0.0291	0.0263	
2D9	**3.83**	**28**	**117**	**5.05**	**21.7**	**93.97**	**4.06**	**26.5**	**161.13**	**7.17**	**24.9**	**114.4**
	0.0009	0.0054	0.0047	0.0032	0.0074	0.01018	0.0039	0.0143	0.0093	0.0062	0.0132	0.01318
	0.011	0.0101		0.0208	0.0176		0.0274	0.0236		0.0299	0.0264	

This table shows values determined by exponential stripping of the LDH binding datasets shown in **Figures 3.81-3.86**. Datasets for each dye-dextran conjugates was collected at each of the four concentrations shown (6,12,24 and 48 uM). Each fit is the sum of three exponentials (shown in **bold** under each concentration). Under each of these exponential values are two futher values giving first the magnitude of the exponential and then the magnitude for the curve that it was fitted to. Thus for the thrid exponential this value is not given as it is the same as the magnitude of the third exponential.

Examination of the determined values for the exponentials shows that all of the binding curves seem to be represented as three exponentials of roughly similar magnitude and rate there are no clear trends present either as the concentration of LDH is increased or as the loading and size of the backbone is increased. This shows that the binding reaction is probably not the sum of simultaneous exponential processes, but a more complex sequential system.

4.12 Rapid Fluorimetric Kinetics with LDH

The greater sensitivity of the fluorimetric methods for measuring the dye-protein interactions allows the use of significantly lower concentrations than those used for the spectral studies. Initial studies used monochromated excitation at 280 nm with a 320 nm cut-off filter being used for the emitted light. This had the advantage of increased sensitivity over the dual monochromated fluorimeter used for the equilibrium titrations as all emitted light above 320 nm was collected. However when the emission spectrums for the native and quenched protein were compared it could be seen that quenching also seemed to be accompanied by a slight red shift of the emission spectrum. This could be explained by binding of the dye being accompanied by a change in the environment of the quenched tryptophan residues.

This makes interpretation of the quenching curves produced very difficult as the absorbance of the dye and hence its inner filter effect is also varying in this region. Therefore the correction for the inner filter effect will vary according to the amount of dye bound.

This is simplified by the use of a second monochromator for the emitted light. By selecting a specific wavelength this reduces the effect of integrating all of the emitted light above the wavelength of the cut-off filter where both emission and absorbance is varying to a single wavelength which will have a constant ratio.

The use of lower concentrations allowed by the fluorescence technique allows the concentrations to be reduced to the extent that some of the free dye binding curve could be visualised. However from the information determined from the fluorescence titrations it can be determined that the entire quenching curve should show a change which is approximately 200 percent of the value of the endpoint. By comparison of the quenching curves it can be seen that the changes seen are far less than this. Also the magnitude of the curves increases as both the dye and protein concentrations are reduced. This is due to the fact that a large

proportion of the reaction is still taking place within the dead time of the instrument. Without being able to visualise the entire binding curve it is difficult to meaningfully interpret them.

The curves for the fluorescence quenching of the dye-dextran conjugates show a similar complex shape to the absorbance difference curves produced. This confirms that both the spectral and fluorescence techniques appear to be measuring the same interaction. Comparison with the absorbance curves shows that the signal to noise ratio appears far worse with the fluorescence technique despite the fact that for the titrations the fluorescence technique seems to have far better reproducibility than the spectral one.

4.13 Experiments with Equine ADH

One of the possible factors involving in the complex binding kinetics seen with LDH is the fact that LDH is a tetrametric enzyme and although ligand binding to it is not co-operative, the multiple ligand binding sites allow the possibility of more complex interactions with a multivalent ligand such as a dye-dextran. Equine ADH is a dimeric dehydrogenase of around 70 kDa. known to bind Cibracon Blue F3-GA at its NADH binding site. It is also readily available in the quantities necessary for use in dye binding experiments.

The difference spectra produced by spectral titrations with ADH show considerably more difference between free dye and dye-dextran than that previously seen with LDH. The difference spectrum for free dye binding shows a large hypochromic shift at 580 nm followed by a large hyperchromic shift at 670 nm. This is more similar to the difference spectrum seen on dye-dextran binding to lysozyme to that seen between free dye and LDH. In contrast the dye-dextran binding curve shows a hyperchromic peak at 650 nm followed by a minor hypochromic trough at 720 nm which is similar to the dye-dextran binding curve to LDH.

Curve fits to cross sections through the hypochromic peaks of the binding data using the mutual depletion model give Kds of 0.40 uM and 3.57 uM for free dye and the T40.20 conjugates respectively. This is a far greater difference in affinities than those measured for binding to LDH (1.23 and 1.81 uM), which together with the large differences seen between the difference spectra indicate that the presence of the dextran backbone appears to be having a larger effect on the binding interaction.

However the absorbance difference kinetic binding curves again show a similar shape to those previously seen for binding to LDH, although at a slightly slower rate. Again a fit to a simple kinetic model shows that the binding kinetics are more complex than can be described by such a model. Along with the similarity of shape of the curve, this indicates that an alteration of the number of binding sites per protein does not seem to have a large effect on the binding kinetics.

The free dye fluorescence quenching curves show the binding reaction with free dye does seem to be slower than that seen with LDH allowing more of the reaction to be visualised. However the magnitude of the curve for the higher concentration of dye used is still larger than that seen for the lower concentration indicating that a considerable proportion of the reaction is still occurring within the mixing time of the stop-flow.

4.14 Binding Measurements with other Proteins

As the initial experiments with rabbit muscle LDH and equine ADH had not produced measurable kinetics at 25 C the possibility of using a thermophyllic enzyme which might have poor and hence measurable specific dye binding had been attempted. Due to the small quantities of protein available it was only feasible to attempt to use the more sensitive fluorescence techniques The trial fluorescence titration with *Thermoplasma acidifolium* GDH showed that

there did not appear to be any specific protein fluorescence quenching on addition of Cibracon Blue F3-GA. This could be due to either the protein not binding the dye or dye binding not causing any quenching of the intrinsic protein fluorescence. In either case this made the protein unsuitable for use for binding studies.

Having shown that both spectral and fluorescence techniques could be used to study dye interactions with both the tetrameric LDH and the dimeric ADH it was desirable to also have a monomeric protein for comparison. Two possible candidates for this were saccharopine dehydrogenase from *Saccharomyces ceravisiae* and scallop octopine dehydrogenase. Spectral titrations with saccharopine dehydrogenase sourced from Sigma showed no visible difference spectrum on addition to a dye-dextran indicating that the protein did not interact specifically with Cibracon Blue F3-GA and was therefore also unsuitable as a model protein.

Octapine dehydrogenase was then purified form scallops. Using a protocol based around those previously published to around 25 percent purity but did not bind to a Cibracon Blue affinity column, which as discussed previously meant that it was unlikely to be useful for binding studies.

A alternative monomeric NADH requiring enzyme, billiverdin reductase was then used for trial spectral titrations. Although this did appear to produce a weak difference spectrum with the T40.20 dye-dextran conjugate, measurements with the 2D9 conjugate were not successful. The small magnitude of the observed changes may be responsible for the problems with the later spectral titration and prevented any meaningful interpretation of the former. Kinetic spectral measurements of T40.20 with BVR showed no measurable difference spectrum, indicating that either the interaction may be too fast to measure even at 4 C, or that considerably higher concentrations would be need to increase the signal to noise ratio sufficiently to visualise the interaction.

4.15 Dye destacking kinetics

The interaction between dye molecules in solution, mediated through interactions between their planar aromatic rings may have a significant effect on the availability and binding of both free and conjugated dye molecules. To assess the kinetic significance of the dye stacking interaction several different dyes were rapidly diluted in the stop flow and spectra recorded.

From these experiments the stacking interaction for Cibracon Blue F3-GA appears to be a rapid equilibrium and will not have any significant role in the observed kinetics for dye - protein interactions. However observable destacking kinetics were visible with both Procion Orange MX-G and Procion Yellow MX-R.

This indicates that depending on the nature of the dye-ligand used the stacking process may well be a rate limiting factor in the binding process. For example the rate limiting step in the binding kinetics of Cibracon Blue F3-GA to LDH and ADH is only slow enough to measure when the temperature is reduced to 4 C and is too fast to measure at 25 C. These dilution experiments at 25 C show that the rate of destacking of some of the dyes is slower than the current limiting step in dye binding to these proteins. Thus for these dyes destacking would probably become a kinetically significant process in the binding interaction as it would limit free dye availability.

Conclusions and Future Work

In extension to the previous work by Mayes et al. on the binding interaction of dye-dextran conjugates to lysozyme the spectral kinetic studies of the binding interaction in this work have provided further evidence of a specific high affinity interaction between lysozyme and Cibracon Blue F3-GA. Global analysis of spectral datasets confirmed that although free-dye binding appears to deviate only slightly from a simple binding model, binding of dye-dextran conjugates shows significant deviations. However no evidence of additional spectral intermediates which might account for such deviations were seen in any of the spectral binding curves, with clear isobestics being present at several wavelenghths.

Measurements were made using both spectral and fluorimetric techniques of the kinetics and thermodynamics of the interaction of a range of dye-dextran conjugates of differing sizes and loadings with a range of model proteins. To counter one of the criticisms of the earlier work with lysozyme as a model protein these proteins were selected based upon their possesion of better defined specific binding sites for the dye, usually that of their nucleotide co-factor. It was shown that both spectral and fluorimetric techniques appear to be measuring the same interaction and give similar values for the dissociation constants and similarly shaped binding curves.

Kinetic measurements indicate that the kinetics of the dye-protein interactions appear to be highly temperature dependant, with the rate of binding decreasing far more rapidly than would have been expected as the temperature is lowered. This however does not appear to effect the position of the binding equilibrium. Such highly temperature dependant kinetics are usually indicative of structural rearrangements involving entropic effects. To test if the complex kinetics observed for the binding of the dye-dextran conjugates was due to an immediate steric

effect of coupling to the glucose backbone of the dextrans a dye-glucose conjugate was synthesised, purified and used for binding measurements. The dye-glucose conjugate produced showed behaviour similar to that of the free dye and not the dye-dextran conjugates, showing that the presence of the immediatly adjuacent glucose did not appear to be responsible for the differences in binding between free dye and the dye dextrqan conjugates.

The rate of dye-dextran binding was found to be considerably slower than that of free-dye, indicating that the dextran backbone is having a considerable effect on the binding kinetics. It had previously been postualated that this could be explained by the stacking interactions taking place between the aromatic rings of the dyes. Studies were therefore made of the dye-stacking interaction and the significance of intermolecular stacking as a kinetically significant process in the binding of Cibracon Blue F3-GA was ruled out. Intramolecular stacking in dye-dextran conjugates is difficult to quantify and may still have considerable effects. However the binding kinetics do not seem to be especially sensitive to large changes in the dye-loading and size of the backbone which would be expected to effect intramolecular stacking, providing some evidence that intramolecular stacking may not be a kinetically signifcant process in the case of Cibracon Blue F3-GA.

Attempts to find a suitable monomeric enzyme for use as a model system were hampered by apparent lack of binding to the dye of both saccharopine dehydrogenase and octapine dehydrogenase and problems with obtaining suitable data with biliverdin reductase.

Dye destacking kinetics were also studied for a range of dyes, some of which were shown to have destacking kinetics that might have a significant role in the kinetics of their their binding to proteins.

An extensive range of measurements with several proteins has shown that binding processes involving dye conjugates are not simple interactions. It seems unlikely that the previously proposed dye-stacking model provides an appropriate description of the processes involved, but no alternative model has yet been developed which does suitably describe the results seen. One of the fundamental problems with the kinetic work has been the lack of good binding data for the interaction with free dye. This would help confirm if the complexity seen is due to multiple steps in the binding process itself or limits on the effective availability of dye for binding. Further careful investigation of the temperature dependence of the kinetics might yield useful information about the number and nature of the steps in the ligand binding process. A further possibility for investigation would be the use of solutions containing ethylene glycol which may well both slow the reaction further and also allow the use of lower temperatures which alleviate some of the problems encountered.

References

[1] Hammond, P.M. and Scawen, M.D. (1989) *J. Biotechnol.*, **11**, 119-134.

[2] Spalding, B.J. (1991) *Biotechnology*, **9**, 229-233.

[3] Lowe, C.R. and Dean, P.D.G. in "Affinity Chromatography", Wiley, New York, 1974.

[4] Lowe. C.R. (1984) *J. Biotechnol,.* **1**, 3-12.

[5] Liu, Y.C:, Ledger, R. and Stellwagen E. (1984) *J.Biol. Chem.,* 259, 6, 3796-3799.

[6] Chase, H.A. (1984) *J. Chromatogr.*, **297**, 179-201.

[7] Anspach, F.B., Jonston, A., Wirth, H.J., Unger, K.K. and Hearn M.T.W. (1989) *J. Chromatogr.*, **476**, 205-225.

[8] Muller, W. (1990) J. Chromatogr. 510, 133-140.

[9] Tsuneda, S., Shinano, H., Saito, K., Furusaki, S. and Sugo, T. (1994) Biotechnol. Prog. 10, 76-81.

[10] Hansson, H. and Kagedal, L.K. (1981) J. Chromatogr. 215, 333-339.

[11] Albertsson, P.A. in "Partion of Cell Particles and Macromolecules" Wiley, New York, 3 rd Ed., 1986.

[12] Matiasson B. and Larson M. (1985) *Biotech. & Gen. Eng. Rev.,* **3**, 137-174.

[13] Flanagan, S.D. and Barondes, S.H. (1975) *J. Biol. Chem,.* 250, **4**, 1484-1489

[14] Johansson G. and Shanbhag,(1975) *J. Chromatogr.*, **284**, 63.

[15] Takerkart G., Segard, E. and Monsigney, M. (1974) *FEBS Lett.*, **42**, 218.

[16] Kula, M.-R., Johansson, G., and Buckmann, A.F., (1979) *Biochem. Soc. Trans.*, **7**, 1.

[17] Chaabouni, A. and Dellacherie, E. (1979) *J.Chromatogr.*, **171**, 135.

[18] Kula, M.-R., Kroner, K.H. and Hustedt, H., (1982) *Adv. Biochem. Eng.*, **24**, 73.

[19] Flanagan, S.D., Barondes, S.H. and Taylor, P., (1976) *J. Biol. Chem.*, **251**, 858.

[20] Olde, B., and Johansson, G. (1985) *Neuroscience*, **15**, 1247.

[21] Johansson, G. and Andersson, (1984) M. *J.Chromatogr.*, **303**, 39.

[22] Johansson, G., Joelsson, M. and Akerlund, H.,-E., (1985) *J. Biotechnol.*, **2**, 225.

[23] Johansson, G., and Joelsson. M. (1987) *J. Chromatogr.*, **393**, 195.

[24] Fowell, S.L., and Chase. H.A., (1986) *J. Biotechnol.*, **4**, 335.

[25] Mayes, A.G., Moore, J.D., Eisenthal, R. and Hubble. J. (1990) *Biotech. Bioeng.*, **36**, 1090.

[26] Lowe. C.R., Burton, S.J., Burton, H.P., Stewart, D.J., Purvis, D.r., Pitfireld, I. and Eapen, S. (1990) *J. Mol. Recog.*, **3**, 117.

[27] McLoughlin, S.B. and Lowe, C.R. (1988) *Rev. Prog. Colouration.*, **18**, 247.

[28] Haeckel, R., Hess, B., Lauterborn, W. and Wuster, K-H. (1968) *Hoppe-Seyler's Z. Phys. Chem.*, **349**, 699.

[29] Thompson, S.T., Cass, K.H., and Stellwagen,E., (1975) *P.N.A.S.*,**72**, 669.

[30] Stellwagen, E. (1977) *Acc. Chem. Res.* **10**, 92.

[31] Bessiner, R.S., Quiocho, F.A., and Rudolph, F.B. (1979) *J. Mol. Biol.*,**134**, 847.

[32] Bohme, H.J., Kopperschlager, G., Schultz, J. and Hofmann E. (1972) *J.Chromatogr.*, **69**, 209-214.

[33] Biellmann, J-F., Samama, J-P., Branden C.I. and Eklund, H. (1979) *Eur. J. Biochem.*, **102**, 107-110.

[34] Lowe, C.R., Burton, S.J., Pearson, J.C., Clonis Y.D. and Stead, C.V. (1986) *J. Chromatogr.*, **376**, 121-130.

[35] Scopes, R.K. (1986) *J. Chromatogr.*, **376**, 131-140.

[36] Thompson, S.T., and Stellwagen E., (1976) *P.N.A.S.*, **73**, 361.

[37] Johansson, G., and Joelsson, M. (1991) *J.Chromatogr.*, **537**, 219.

[38] Subramanian, S. (1982) *Arch. Biochem. Biophys.*, **216**, 116.

[39] Mayes, A.G., Hubble, J. and Eisenthal, R. (1992) *Biotech. Bioeng.*, **40**, 1263.

[40] Lehrer, S.S., and Fasman, G.D. (1966) *Biochem. Biophys. Res. Commun.*, **23**, 133.

[41] Halfman, C.J., and Nishida, T. (1972) *Biochemistry*, **11**, 3493.

[42] Gutfreund, H. (1972) *Enzymes: Physical Principles*, Wiley-Interscience, London.

[43] Grove, T.H., Ishaque, A. and Levy, H.R. (1976) *Arch. Biochem. Biophys.*, **177**, 307.

[44] Haghigi, B. and Levy, H.R. (1982) *Biochemistry*, **21**, 6421.

[45] Alred, P.A., Johansson, G. and Tjerneld, F. (1992) *Anal. Biochem.*, **205**, 351.

[46] Velick, S.F. (1958) *J. Biol. Chem.*, **233**, 1455.

[47] Iwebio. I. and Weiner, H. (1972) *Biochemistry,* **11**, 1003.

[48] Hubble, J., Mayes, A.G. and Eisenthal R. (1993) *Anal. Chim. Acta*, **279**, 167.

[49] Kirchberger, J., Cadelis, F., Kopperschlager, G., and Vijayalakshmi, M.A. (1989) *J.Chromatogr.*, ??, 290.

[50] Mislovicova, D., Gemeiner, P., and Stratilova, E. (1990) *J. Chromatogr.*, **510**, 197.

[51] Wang, W.-H., Kuboi, R., and Komasawa, I. (1992) *Chemical Engineering Science*, **47**, 1, 113.

[52] Pearson, J.C, Burton, S.J., and Lowe, C.R. (1986) *Anal. Biochem.*, **158**, 382.

[53] Naumann, M. Reuter, R., Metz, P., and Kopperschlager, G. (1989) *J. Chromatogr.*, **466**, 319.

[54] Johansson, G., and Joelsson, M. (1987) *J. Chromatogr.*, **411**, 161.

[55] Bohme H.J., Kopperschlager,G., Schultz, J., and Hofmann E. (1972) *J. Chromatogr.* **69**, 209.

[56] Chambers G.K. (1977) *Anal. Biochem.* **83**, 551.

[57] Mayes, A. (1992) *PhD thesis*, University of Bath.

[58] Pearson, J.C., Burton, S.J. and Lowe C.R. (1986) *Anal. Biochem.* **158**, 382-389.

[59] Jaenicke, R. and Knof, S. (1968) *Eur. J. Biochem.*, **4**, 157.

[60] Ogawa, H. and Fujioka, M. (1978) *J. Biol. Chem* **253**, 3666-3670

[61] Fujioka,M and Nakatani, Y. (1974) *J. Biol. Chem.* **249**, 6886-6891.

[62] Thoai, N.V., Huc, C., Pho, D.B. and Olomucki, A. (1969) *Biochem. Biophys. Acta.* **191**, 46-57.

[63] Honneuse-Doublet, M-O., Lefebure, F., and Olomucki, A. (1980) *Eur. J. Biochem.* **108**, 261-269.

[64] Zettlmeissl, G., Teschner, W., Roudolph, R. Jaenicke, R. and Gade, G. (1984) *Eur. J. Biochem.* **143**, 401-407.

[65] Heynes, W. and Moor, P., (1974) *Biochem. Biophys. Acta.* **358**, 1.

[66] Barid, J.K. Sherwood, R.F., Carr, R.J.G. and Atkinson, A., (1976) *FEBS Lett.* **70**,61.

[67] Hanggi, D. and Carr, P. (1985) *Anal. Biochem.* **149**, 91

[68] Weber, B. H., Willeford, K., Moe, J.G. and Peizkiewicz, D. (1979) *Bichem. Biophys. Res. Commun.* **86**, 252.

[69] Issaly, I., Poiret, M., Tauc,P. Thiry, L., and Herve, G. (1982) *Biochemistry* **21**, 1612.

[70] Witt, J. J., and Roskoski , R.R. (1980) *Biochemistry* **19**, 143.

[71] Edwards, R.A., and Woody, R.W. (1977) *Biochem. Biophys. Res. Commun.* **79**, 470.

[72] Nahum, A., and Horvath, C. (1981) *J. Chromatogr.* **203**, 33.

[73] Puri, N.R. and Roskoski, R Jr. (1994) *Biochem. J.*, **300**, 91-97.

[74] Federici, M.M., Chock, P.B. and Stadtman E.R. (1985) *Biochem.* **24**, 647-660.

[75] Stellwagen, E. and Liu, Y-C. (1987) Quantitavtive Considerations of Chromatography using Immobilized Biomimetic Dyes, Ch. 4., in "Analytical Affinity Chromatography", Chaiken, I.M., CRC Press: Boca Raton.

[76] Robinson, B.H., Loffler, A., and Schwartz, G. (1973) *J.Chem Soc. Farady Trans.* **69**, 56-69.

[77] Thompson, S.T. and Stellwagen, E. (1976) *Proc. Nat Acad. Sci. USA* **73**, 361-365.

[78] Thoai, N.V., Huc, C., Pho, D.B. and Olomucki, A. (1969) *Biochem. Biophys. Acta.* **191**, 46-57.

[79] Liu, Y-C and Stellwagen, E. (1987) *J. Biol. Chem.* **262**, 2, 583-588.

[80] Hanggi, D. and Carr, P. (1985) *Anal. Biochem.* **149**, 91.

[81] Burton, S.J. et. al. (1988) *J. Chromatogr.* **435**, 127

[82] Hummel J.P. and Dreyer, W.J. (1962) *Biochem. Biophys. Acta.*, **63**, 530

[83] Birkenmeier, G. and Kopperschlager, G. (1991) *J. Biotech.* **21**, 93-108.

[84] Johansson, G and Joelsson, M., (1987) *J. Chrom.* **411**,161-166.

[85] Liu, Y-C. and Stellwagen E. (1987) *J. Biol. Chem.* **262**, 2, 583-588.

[86] Mertens M.L. and Kagi J.H.R., (1979) *Anal. Biochem.* **96**, 448.

[87] Parker C.A., "Photoluminesence of Solutions." Elsevier, Amsterdam, 1968.

[88] Holland J.F., R.E.Teets, P.M. Kelly, and A. Timmick, (1977) *Anal. Chem.* **49**, 709

[89] Latzowicz J.R., "Principles of Fluoresence Spectroscophy", Plenum, 1983.

[90] Arrhenius, S. (1889) *Zeitschrift fur physicalische Chemie*, **4**, 226-248.

[91] Gutfreund, H. (1995), "Kinetics for the Life Sciences" CRC Press, Cambridge.

Appendix 1

Computer controlled data acquisition from Cecil CE 6600

The following program was written by the author to control and acquire data from a Cecil CE 6600 series spectrophotometer using the built in RS232 serial interface and associated command set. The remote commands and communications protocol were obtained from Cecil Instruments Ltd. Manual D 5500 00 10 part 1. The program was originally written in Microsoft QBasic and run on a XT (8086) clone with an EGA graphics display. Some communications problems with the spectrophotometer were encountered due to the slow response of the interpreted BASIC running on this machine and the code was subsequently ported to Turbo Basic which allowed it to be compiled and run as a separate executable.

The program is written specifically for spectral scanning purposes and does not implement any of the additional functions normally available on the spectrophotometer by manual control. Once control of the spectrophotometer is placed under the control of the computer by selecting the 'Remote' option on the spectrophotometer the user is then requested for the range of wavelengths to be scanned and the scan rate. The spectrum is then scanned with real time graphical display and the data stored by the computer. This can then be saved as an ASCII datafile consisting of a small header containing information about the scan followed by a list of wavelength and absorption data. This ASCII file can then be read by virtually any spreadsheet program and used for the display and processing of the data.

As mentioned previously the program requires a minimal specification computer of an XT compatible with an EGA display. This allowed the use of otherwise 'redundant' equipment for the simple task of control and data acquisition.

A commented listing of the program follows:

```
REM Computer data acquisition for Cecil CE6600 Spectrophotometer.
REM (c) copyright R.M.Maytum 1994

REM Declaration of subroutines

DECLARE SUB axis ()
DECLARE SUB fwrite (ofname$)
DECLARE SUB fread (iname$)
DECLARE SUB rplot ()
DECLARE SUB csend (cs$)
REM Main Program
REM
DIM cp%(80)

REM Selection of EGA graphics mode and setup of graphics window

SCREEN 2
CLS
VIEW (10, 10)-(630, 150), , 1
VIEW (0, 152)-(639, 199)
REM Ask user to chose between input from file or spectrometer
REM
LOCATE 20, 1
INPUT "Read data from file or spec (f/s) "; an$
IF an$ = "f" OR an$ = "F" THEN INPUT "File name : "; iname$: CALL fread(iname$):
GOTO pl
CLS

REM If spectrophotometer selected ask parameters, start and finish wavelengths, scan rate
and scale for Y axis

LOCATE 20, 1
INPUT "Start scan wavelength : "; wls$
INPUT "End scan wavelength : "; wle$
INPUT "Scan rate (nm/sec : .5/1/2/5/10) : "; ssp$
INPUT "Y scale : "; ymin, ymax
CLS
ssp = VAL(ssp$)
wls = VAL(wls$)
wle = VAL(wle$)
ssize = wle - wls
np = 10
xmin = wls: xmax = wle

REM Determination of number of datapoints read per wavelength according to scan rate.

SELECT CASE ssp
    CASE 5
```

```
        np = 4
    CASE 10
        np = 2
END SELECT
dsize = ssize * np
LOCATE 20, 1: PRINT "Number of data points : "; dsize

REM Define array for storage of wavelength data and open serial communications with
spectrophotometer.

DIM dta(dsize, 2)
IF LEN(ssp$) = 1 THEN ssp$ = ssp$ + " "
OPEN "COM1:4800,E,7,1,BIN,RB2048" FOR RANDOM AS #1
FIELD #1, 1 AS ans$
FIELD #1, 1 AS ps$

REM Send check signal to see if spectrophotometer is ready.

PRINT "Initiating communications"
CALL csend("?RPS")
PRINT an$
PRINT MID$(an$, 3, 1)
INPUT dummy
IF MID$(an$, 3, 1) <> "R" THEN an$ = "": DO: INPUT dummy: la$ = an$: CALL
csend(CHR$(6)): LOOP UNTIL an$ = "21" AND la$ = "21"

REM Send parameters for scan (start and finish wavelengths and scan rate)

snd$ = "?WLS" + LEFT$(wls$, 3)
CALL csend(snd$)
snd$ = "?WLE" + LEFT$(wle$, 3)
CALL csend(snd$)
snd$ = "?SSP" + LEFT$(ssp$, 2)
CALL csend(snd$)

REM Ask user to start scan

INPUT "press return to scan"; dummy$
snd$ = "?SCR"
CALL csend(snd$)
IF an$ <> "6" THEN PRINT "Scan not accepted : Terminating program": END

REM Data read routine. Reads data from spectrophotometer and plots data on screen.

CALL axis
snd$ = ""
dp% = 0
FOR ll% = 0 TO ssize - 1
```

```
CALL csend(snd$)
IF an$ = "21" AND ll% < ssize - 1 THEN CALL csend("")
IF an$ = "-1" THEN CALL csend(CHR$(21))
PRINT an$
rpos = 2
dta(dp%, 0) = VAL(MID$(an$, rpos + 1, 5))
FOR l% = 1 TO np
rpos = rpos + 7
dta(dp%, 1) = VAL(MID$(an$, rpos, 6))
dta(dp% + 1, 0) = dta(dp%, 0) + (1 / np)
IF dp% = 0 THEN PSET (dta(0, 0), dta(0, 1)) ELSE LINE -(dta(l%, 0), dta(l%, 1))
dp% = dp% + 1
NEXT l%
snd$ = CHR$(6)
NEXT ll%
VIEW (0, 152)-(639, 199)
CLS

INPUT "Finished"; dummy
CLOSE #1
CLS

REM Draw routine - Allows rescaling of Y axis and replotting of data.

pl:
LOCATE 20, 1
INPUT "Rescale plot (y/n)"; rp$
IF rp$ = "y" OR rp$ = "Y" THEN INPUT "Y Scale : "; ymin, ymax: GOTO pl

REM Ask user if they wish to save data in a file.

INPUT "Output data file (y/n) "; rp$
IF rp$ = "y" OR rp$ = "Y" THEN INPUT "File name : "; ofname$: CALL fwrite(ofname$)
END

REM *** SERIAL PORT RESPONSE ERROR ***

tout:
an$ = "-1"
fl = 1
PRINT "No response from serial port"
RETURN

REM *** END OF MAIN PROGRAM ***

REM Subroutine for drawing axis for plotting data.

SUB axis
```

```
VIEW (10, 10)-(630, 160), , 1
WINDOW (xmin, ymin)-(xmax, ymax)
CLS
xstep = INT(ssize / 4)
LINE (xmin, 0)-(xmax, 0), 2
FOR l% = xmin TO xmax STEP xstep
LINE (l%, ymin)-(l%, ymax), 2
NEXT l%
END SUB

REM Subroutine for sending control codes to spectrophotometer.

SUB csend (cs$)
SHARED an$, fl, hp%, cp%(), ps$, ans$
ON TIMER(20) GOSUB tout
hp% = 0
an$ = ""
IF LEN(cs$) > 0 THEN PRINT #1, cs$ ELSE IF LEN(c$) = 1 THEN LSET ps$ = cs$: PUT
#1, 1
LOCATE 20, 1
CLS
PRINT cs$,
TIMER ON
fl = 0
DO
      GET #1, 1
      cp%(hp%) = ASC(ans$)
      IF cp%(hp%) = 3 OR cp%(hp%) = 6 OR cp%(hp%) = 7 OR cp%(hp%) = 21 THEN fl =
1: hp% = hp% - 1
      hp% = hp% + 1
LOOP WHILE fl = 0
TIMER OFF
IF hp% = 0 THEN
      SELECT CASE cp%(hp%)
            CASE 6
                  PRINT "ACK": an$ = "6"
            CASE 7
                  PRINT "BEL": an$ = "7"
            CASE 21
                  PRINT "NAK": an$ = "21"
            CASE ELSE
                  PRINT "unknown"
      END SELECT
END IF
FOR l% = 0 TO hp%
IF cp%(l%) > 31 THEN an$ = an$ + CHR$(cp%(l%))
NEXT l%
END SUB
```

```
REM Subroutine to read datafiles.

SUB fread (iname$)
SHARED xmin, xmax, ymin, ymax, dta(), ssize, np
OPEN iname$ FOR INPUT AS #2
INPUT #2, xmin, xmax, ymin, ymax, ssize, np
DIM dta(ssize * np, 1)
FOR l% = 0 TO ((ssize - 1) * np - 1)
INPUT #2, dta(l%, 0), dta(l%, 1)
NEXT l%
CLOSE #2
END SUB

REM Subroutine to write datafiles.

SUB fwrite (ofname$)
SHARED xmin, xmax, ymin, ymax, dta(), ssize, np
OPEN ofname$ FOR OUTPUT AS #2
PRINT #2, xmin, xmax, ymin, ymax, ssize, np
FOR l% = 0 TO ((ssize - 1) * np - 1)
PRINT #2, dta(l%, 0), dta(l%, 1)
NEXT l%
CLOSE #2
END SUB

REM Subroutine to replot dataset.

SUB rplot
SHARED xmin, xmax, ymin, ymax, dta(), ssize, np
CALL axis
PSET (dta(0, 0), dta(0, 1))
FOR l% = 1 TO ((ssize - 1) * np - 1)
LINE -(dta(l%, 0), dta(l%, 1))
NEXT l%
VIEW (0, 152)-(639, 199)
END SUB
```

Appendix 2

Biochemical Society Transactions (1996)

Interactions of proteins with dyes conjugated to soluble polymers

R. Maytum*, R. Eisenthal* and J. Hubble+
Biochemistry Deptartment* and School of Chemical Engineering+
University of Bath, BATH, BA2 7AY, U.K.

Conventional chromatographic media are normally based on either porous or non-porous supports. Porous supports are often limited on a process scale by pore diffusional kinetics and/or mass transfer phenomena, whereas non-porous supports have a relatively low capacity. A 'tentacle ligand' system in which the ligands are bound to a soluble polymer attached to a non-porous support should enable high ligand densities while retaining the mass transfer advantages and flow properties of non-porous supports.

Such a system has been produced using dextran, a soluble polysaccharide, as the carrier, and the traizine dye Cibracon Blue F3-GA as the ligand. Cibracon Blue is a biomimetic ligand binding many proteins specifically at their dinucleotide binding sites[1]. Triazine dyes are also highly useful for our purposes as their binding to proteins can be directly and non-invasivly measured through spectral methods[2].

In the synthesis of such a tentacle system it is possible to vary both the size of the carrier molecule and the number of ligands bound to it. This has implications for both the capacity and the kinetics of the system. It is therefore important to quantify the effects that coupling the dye to a carrier have on dye-protein interactions, especially in terms of the size of the carrier and number of ligands bounds to it.

Dye-dextran conjugates are freely soluble in aqueous solutions. This allows the study of binding interactions without the additional complications that binding to an insoluble support may produce. It seems reasonable that any model obtained to describe the binding characteristics of these conjugates in free solution will be the first step towards understanding of the complete tentacle system. A range of conjugates with varying backbone size and dye loading have therefore been synthesised using a further modification of the method of Mayes et al [3].

Dextran (2g) of varying molecular weights was allowed to react with varying quantities of Cibracon Blue F3-GA in 100 mls 2% w/v Na_2CO_3 @ 45 °C, 48 hrs. The conjugates were purified by repeated precipitation by addition of an equal volume of ethanol, centrifugation and

resuspension in distilled water. This was repeated until the supernatant after centrifugation was clear. The final precipitate was resuspended in 50 mls distilled water to which sodium azide was added to prevent microbial growth. This stock solution was characterised by measurement of the dry weight of a 1ml aliquot, and the dye concentration measured in 6M HCl at the isosbestic point at 541 nm allowing calculation of the average number of dye molecules per dextran molecule (dye-loading).

Dye binding to model proteins was measured by both difference spectral and fluorescence quenching methods which are applicable to both equilibrium titration and stop-flow kinetic studies.

Difference spectra were measured in a Cecil CE6000 twin beam spectrophotometer. Sample and reference cuvettes (10x10 mm) contained 2 mls, 25 μM dye or dye/dextran, 50 mM sodium phosphate pH 7.9. To this small volumes of protein solution were added to the sample cuvette and a corresponding amount of buffer to the reference. The difference spectra between the two was measured after each addition.

Kinetic measurements were performed in Hi-Tech SF61-MX stop-flow system. Solutions containing twice the final concentrations (as for the titrations) of dye and protein were placed respectively in the two mixing syringes. The reaction was then monitored either at a single wavelength using a photomultiplier or at multiple wavelengths using a diode array detector.

Fluorescence quenching titrations were carried out using a Perkin Elmer fluorimeter. Dye or dye/dextran was titrated in a 5x5 mm cuvette against .5 ml of a protein solution of known concentration. In the case of LDH a concentration of 2.05 μM yielded an initial fluorescence of approximately 780 units. The resulting fluorescence quenching curve produced is corrected for the internal filter effect of the dye and then transformed into an absolute difference from the initial value.

The results for the equilibrium titrations were fitted to a mutual depletion model based around the following binding equation :

$$E + L \Leftrightarrow EL$$

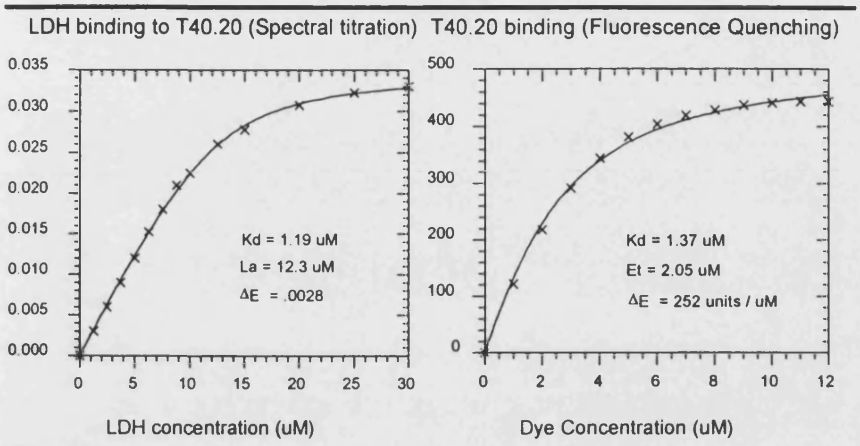

Figure 1.

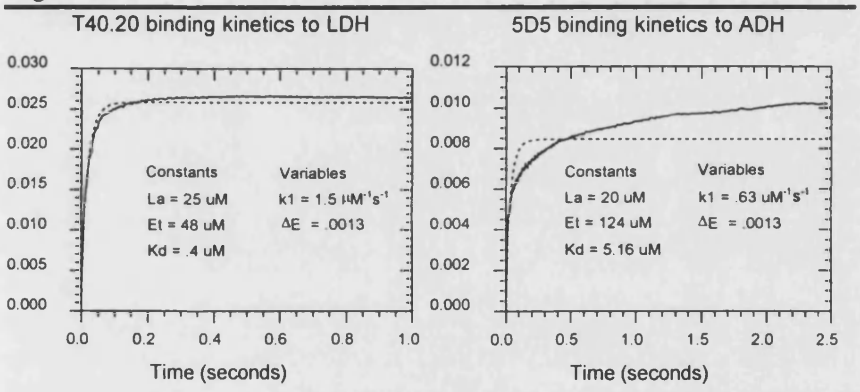

Figure 2.

Yielding a quadratic equation with the real solution of :

$$A = \Delta E \frac{(La + Kd + Et) - \sqrt{(La + Kd + Et)^2 - 4La\,Et}}{2}$$

Where A is the measured change, ΔE the change in extinction coefficient or fluorescence on binding, La the available ligand, Et the total protein added and Kd the dissociation constant. Kinetic data fits use an non-integrated form of the equation where $k1$ is the forward rate constant.

Curve fits to the binding data for LDH to the T40.20 dye-dextran conjugate are shown in Figure 1. T40.20 is a conjugate with a 40 kDa

dextran backbone and with an average dye loading of 4 dye molecules per dextran molecule. As can be seen there is good agreement between the values determined for the spectral titration and fluorescence quenching experiments. As fluorescence quenching is dependent upon a specific interaction between the dye and protein this indicates that the spectral measurements are also caused by the same specific interaction and are not greatly influenced by possible non-specific interactions which might also produce spectral perturbations. The fits to the model also appear good.

Single wavelength kinetic data for binding experiments using the dimeric equine ADH and tetrameric rabbit muscle LDH to dye-conjugates along with fits generated using the mutual depletion model are shown in Figure 2. Both traces appear similar in shape and deviate markedly from the mutual depleteion model. The previously proposed model based on the rate-limiting destacking of dye-ligands which had been used to describe the interaction of conjugates with lysozyme [4] was also inapplicable. Thus the data show that the both of the models used previously are inadequate to describe the kinetics of the dye - protein interactions, which is more complex than is apparent from equilibrium binding data.

A major problem with the development of a model is the lack of kinetic data for the free dye - protein interactions which are too fast to be observable spectrophotometrically. Fluorimetric stop-flow experiments, have a higher sensitivity and will allow the use of lower concentrations producing lower reaction rates, although analysis of the data is complicated by the inner filter effect of the dye mentioned previously.

R. Maytum was supported by an earmarked BBSRC studentship.

[1] Thompsom, S.T. and Stellwagen E., (1976) P.N.A.S., **73**, 361365.
[2] Subramaniam, S. (1982) Arch. Biochem. Biophys., **216**, 116-125.
[3] Mayes, A.G., Hubble, J. and Eisenthal, R. (1990) Biotech. Bioeng., **36**, 1090-1096.
[4] Mayes, A.G., Hubble, J. and Eisenthal, R. (1992) Biotech. Bioeng. **40**, 1263-1270.